Functional Interactions between Peroxisome Proliferator- Activated Receptor-Gamma and polipoprotein E Isoforms in the Regulation of Neural Functions in Models of Insulin Resistance-Relevance to Alzheimer's Disease

To, Alvina Wing Man

Awarding institution:
King's College London

Title: Functional Interactions between Peroxisome Proliferator- Activated Receptor-Gamma and polipoprotein E Isoforms in the Regulation of Neural Functions in Models of Insulin Resistance- Relevance to Alzheimer's Disease

Author: Alvina To

Functional Interactions between Peroxisome Proliferator-Activated Receptor-Gamma and Apolipoprotein E Isoforms in the Regulation of Neural Functions in Models of Insulin Resistance-Relevance to Alzheimer's Disease

Alvina To

A thesis submitted for the degree of Doctor of Philosophy at the Institute of Psychiatry, University of London

King's College London,

Institute of Psychiatry,

London

SE5 8AF

ABSTRACT

Insulin resistance, part of the metabolic syndrome, is associated with type 2 diabetes mellitus (T2DM) and increased risk for Alzheimer's disease (AD). The ε4 allele of APOE is the greatest genetic risk factor for sporadic, late onset AD, and is also associated with risk for T2DM. The thiazolidinediones (TZDs), PPARγ agonists, are peripheral insulin sensitisers used to treat T2DM and have been found to slow cognitive decline in mild to moderate AD patients. Since it is not yet clear how PPARγ affect insulin signalling processes in AD, I investigated the effects of the TZD, pioglitazone, on Aβ metabolism and tau phosphorylation in high fat diet (HFD)-induced insulin resistant mice carrying the human APOEε3 or APOEε4 genes.

HFD reduced tau phosphorylation at specific epitopes, independent of APOE genotype. Pioglitazone treatment reduced tau phosphorylation, in an APOE-dependent manner, with the APOEε3 mice being most responsive. Examination of HFD effects on the cortical transcriptome revealed increased expression of the ABCA1 gene in mice lacking APOE and the ADRA2A gene in APOEε4 mice. ABCA1 and apoE are associated with Aβ clearance in the brain, while ADRA2A suppresses insulin secretion and polymorphisms in this gene is associated with T2DM risk. Erk1/2, p38, JNK, and calcineurin were differentially expressed between APOEε3 and APOEε4 mice on HFD indicating these kinases and phosphatases may contribute to the increased risk for AD imparted by APOEε4.

I have identified APOE allele-dependent effects of PPARγ agonists on tau phosphorylation and have identified diet and APOE allele-dependent effects on gene expression that relate to AD. Further work is needed to validate current findings and to further elucidate the mechanism. A better understanding of the relative importance of brain and peripheral insulin resistance will greatly improve our understanding of the disease process and also aide the rational design of therapeutics to halt its progression.

ACKNOWLEDGEMENTS

First and foremost, I would like to thank my supervisors Simon Lovestone, Joern Schroeder and Diane Hanger for their invaluable guidance and support throughout my PhD.

I have been lucky in receiving help and inspiration from individuals within the department of Old Age Psychiatry, the Institute of Psychiatry in general, as well as collaborations outside the borders of this institute. As such, I would like to begin by expressing my gratitude to Richard Killick, Elena Ribe, Claudie Hooper, Abdul Hye, Mirsada Causevic and Michelle Lupton for generously sharing their expertise and research skills.

I would also like to thank Caroline Johnston, Katie Lunnon and Kuang Lin for their help and advice on the transcriptomics work presented in chapter 7.

Furthermore, I would like to extend my thanks to Judy Latcham, Michael Fullylove, Jason Smith and Sylvia Fung at GlaxoSmithKline for their excellent animal husbandry, which supported a vital part of the work presented in this thesis.

I am also greatful for the generous support of the BBSRC and GlaxoSmithKline in their funding of this studentship.

Last but not least, I would like to thank my family and friends for their support and encouragement throughout the four years of my PhD.

TABLE OF CONTENTS

LIST OF FIGURES AND TABLES

Figures

Tables

PUBLICATIONS ARISING FROM THIS WORK

To AWM, Ribe EM, Chuang TT, Schroeder JE, Lovestone S. (2011) The ε3 and ε4 Alleles of Human APOE Differentially Affect Tau Phosphorylation in Hyperinsulinemic and Pioglitazone Treated Mice. PLoS One 6; e16991.

ABBREVIATIONS

ABCA1	ATP-binding cassette, subfamily A, member 1
ABCG1	ATP-binding cassette, subfamily G, member 1
AD	Alzheimer's disease
ADAM	A disintegrin and metalloproteinase domain
ADRA2A	α-2A adrenergic receptor
AICD	APP intracellular domain
AMPA	Alpha-amino-3-hydroxy-5-methyl-4-isoxazole-propionate
AP1G2	Adaptor-related protein complex 1, γ2 subunit
APH1	Anterior pharynx defective 1
APLP1	Amyloid precursor-like protein 1
ApoE	Apolipoprotein E
APP	Amyloid precursor protein
APS	Ammonium persulphate
Arg	Arginine
Aβ	Amyloid beta
BACE	β-APP cleaving enzyme
BB/Wor	Bio-Breeding/Worcester
BBB	Blood brain barrier
BBZDR	Bio-Breeding Zucker diabetic rat
Ca^{2+}	Calcium
CaMKII	Ca^{2+}/Calmodulin-dependent protein kinase II
Cdk5	Cyclin-dependent kinase 5
cDNA	Complementary DNA
CHO	Chinese hamster ovary

CK1	Casein kinase 1
CM	Conditioned media
Cnpase	2', 3'-cyclic nucleotide 3' phosphodiesterase
CNS	Central nervous system
CSF	Cerebrospinal fluid
CTF	C-terminal fragment
Cys	Cysteine
DHCR7	7-dehydrocholesterol reductase
DM	Diabetes mellitus
DNA	Deoxyribonucleic acid
DYRK1A	Dual-specificity tyrosine phosphorylation regulated kinase 1A
EDTA	Ethylenediaminetetraacetic acid
EGFP	Enhanced green fluorescent protein
EGFR	Epidermal growth factor receptor
EGTA	Ethylene glycol tetraacetic acid
ELISA	Enzyme-linked immunosorbent assay
EthD-III	Ethidium homodimer III
FAD	Familial early onset Alzheimer's disease
FDR	False discovery rate
FTDP-17	Frontotemporal dementia with parkinsonism linked to chromosome 17
GABA	Gamma aminobutyric acid
GFAP	Glial fibrillary acidic protein
GO	Gene Ontology
Glu	Glutamine
GSK-3	Glycogen synthase kinase-3

HDL	High-density lipoprotein
HFD	High fat diet
HMG-CoA	3-hydroxy-methyglutaryl-CoA
HMGCR	3-hydroxy-3-methylglutaryl coenzyme A reductase
HOMA-IR	Homeostatic model assessment of insulin resistance
ICV	Intracerebroventricular
IDE	Insulin degrading enzyme
Igf1	Insulin-like growth factor 1
IPA	Ingenuity Pathway Analysis
IRS	Insulin receptor substrate
JNK	c-Jun N-terminal kinase
kDa	Kilodalton
KO	Knockout
KPI	Kunitz protease inhibitor
LDL	Low-density lipoprotein
Leu	Leucine
LFD	Low fat diet
LOAD	Late onset Alzheimer's disease
LRP1	Low density lipoprotein receptor-related protein 1
LSS	Lanosterol synthase
LTD	Long-term depression
LTP	Long-term potentiation
MAP	Microtubule-associated protein
MAPK	Mitogen-activated protein kinase
Met	Methionine

mRNA	Messenger RNA
MVD	Mevalonate decarboxylase
Neo	Neomycin
NFT	Neurofibrillary tangle
NIRKO	Neuronal insulin receptor knockout
NMDA	N-Methyl-D-aspartate
NPY2R	Neuropeptide Y receptor Y2
NSE	Neuron-specific enolase
NUDT19	Nudix nucleoside diphosphate linked moiety X-type motif 19
OGTT	Oral glucose tolerance test
PBS	Phosphate buffered saline
PCR	Polymerase chain reaction
PDK-1	Phosphate dependent kinase-1
PDPK	Proline-directed protein kinase
PHF	Paired helical filaments
PI3K	Phosphoinositide 3-kinase
PIP_2	Phosphatidylinositol 4,5-bisphosphate
PIP_3	Phosphatidylinositol 3,4,5-triphosphate
PKA	Protein kinase A
PMSF	Phenylmethylsulphonyl fluoride
PP2A	Protein phosphatase 2A
PPAR	Peroxisome proliferator-activated receptor
PPRE	Peroxisome proliferator response element
PS1	Presenilin 1
PS2	Presenilin 2

PSENEN-2	Presenilin enhancer 2
qRT-PCR	Quantitative real time polymerase chain reaction
RAGE	Receptor for advanced glycation end products
RGC	Retinal ganglion cell
RNA	Ribonucleic acid
ROS	Reactive oxygen species
RXR	Retinoid X receptor
sAPP	Soluble APP
SDS-PAGE	Sodium dodecyl sulphate-polyacrylamide gel electrophoresis
SNP	Small nucleotide polymorphism
STX7	Syntaxin 7
STZ	Streptozotocin
T1DM	Type 1 Diabetes Mellitus
T2DM	Type 2 Diabetes Mellitus
TGN	Trans-Golgi network
Thr	Threonine
TK	Thymidine kinase
TNF	Tumor necrosis factor
TRFR2	Transferrin receptor 2
TUBB4	Tubulin, beta 4
Tyr	Tyrosine
TZD	Thiazolidinedione
VLDL	Very low-density lipoprotein
WDFY1	WD repeat and FYVE domain containing 1
WT	Wild type

CHAPTER 1

Introduction

1.1 Alzheimer's disease

Alzheimer's disease (AD) was first described in 1906, by Alois Alzheimer, a German psychiatrist and neuropathologist. Alzheimer's findings were based on a female patient, Auguste Deter who suffered behavioural symptoms and progressive memory loss at the age of 51, who subsequently died aged 55 years. Alzheimer correlated her behavioural features with 'miliary foci' and neurofibrillary tangles (NFTs) in the cerebral cortex.

Today AD is the most common form of dementia, affecting 10% of the population who are 65 years of age and 50% of those who are over 85 years of age. It has been described as the pandemic of the 21st century (Jellinger, 2006). Currently it is estimated that 35.6 million individuals worldwide are affected with dementia, with 820,000 in the UK alone, a figure expected to triple by 2050 (Alzheimer's disease International (2010) Alzheimer's report).

Clinically, AD manifests initially as cognitive decline which spreads to changes in behaviour and as the disease progresses into full dementia, daily activities become impossible. Macroscopically, there is gross atrophy of the brain. Microscopically, amyloid beta (Aβ) plaques and NFTs, characteristic hallmarks of AD, are visible with extensive neuronal loss (Figure 1.1). These neuropathological hallmarks are observed in both familial early onset form of AD (FAD) and the late onset or sporadic form (LOAD), and begin many years before onset of clinical symptoms. Both genetic and environmental factors are implicated in the complex etiology of AD, with age considered the most important risk factor. FAD arises as a result of mutations in either of three genes; the amyloid precursor protein (APP), presenilin 1 (PS1) or presenilin 2 (PS2). For LOAD, the cause is unknown, although there is a strong linkage in APOEε4 carriers (Strittmatter et al., 1993).

Figure 1.1 Brain atrophy, amyloid plaques and neurofibrillary tangles

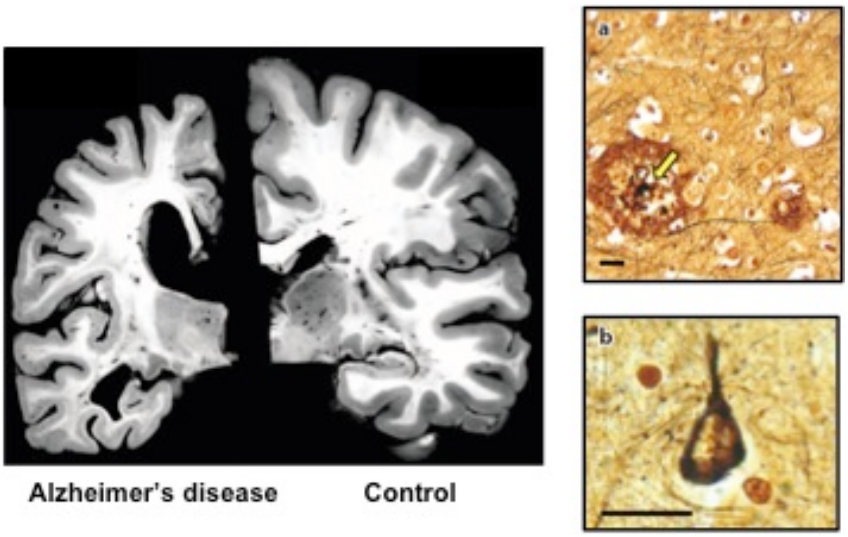

Post-mortem brain sections reveal severe brain atrophy in AD (left) compared with a cognitively normal individual (right). Image was taken from (Holtzman et al., 2011). The neuronal lesions of AD are stained by Bielschowsky Silver Stain (a, b). Neuritic plaques (a) consists of Aβ protein, surrounded by dystrophic neurites (dark black material, indicated by yellow arrow). A neurofibrillary tangle is shown in (b). This image was taken from (O'Brien and Wong, 2011). Bar, 40 μM.

1.1.1 Amyloid beta (Aβ) pathology and the discovery of amyloid precursor protein (APP)

Aβ plaques are extracellular, compacted spherical deposits of fibrils of Aβ peptides with sizes varying between 10-100μm. Aβ peptides consisting of 38 to 43 amino acids in length, are derived from proteolytic cleavage of the APP protein and can aggregate into fibrils as well as oligomers to form plaques. Aggregations of Aβ in a non-β sheet (non-fibrillar) conformation are deposited to form diffuse plaques and are detected by immunohistochemistry techniques. Aggregation of Aβ into a β sheet conformation in the extracellular space forms fibrillar deposits and can be detected

using stains such as Congo red and Thioflavin-S/T. Plaques are accompanied by degenerating neurites and gliosis, proliferation of astrocytes and reactive microglia in response to an inflammatory response (Holtzman et al., 2011) (for review).

Aβ was first identified as the major component of Aβ plaques in the mid 1980s (Glenner and Wong, 1984; Masters et al., 1985). The amino acid sequencing of Aβ shortly after, led to the discovery of the gene encoding APP localised on chromosome 21 (Kang et al., 1987). These findings complemented the observation that individuals with Down's syndrome (or trisomy 21) inevitably develop FAD because they have an extra copy of the chromosome 21 gene and immediately led to the suggestion that overproduction of APP or its cleavage products was central to AD pathogenesis.

1.1.1.1 The proteolytic processing of APP and the production of Aβ

The APP gene encodes a type I transmembrane protein in which alternative splicing gives rise to three major isoforms APP695, APP751 and APP770 (containing 695, 751 and 770 amino acids respectively) (Zhang et al., 2011b). These three major isoforms are found in human, rodents and all other mammalian species examined. The APP751 and APP770 isoforms contain a 56 amino acid Kunitz protease inhibitor (KPI) domain and are expressed in most tissues. On the other hand, the KPI domain is absent in the APP695 isoform which is primarily expressed in neurons within the central nervous system (CNS) (Kang and Muller-Hill, 1990; Rohan de Silva et al., 1997). In AD post-mortem brain tissue, the protein and mRNA levels of KPI-containing APP isoforms are elevated and are associated with an increase in Aβ deposition, suggesting they may have an amyloidogenic potential (Menendez-Gonzalez et al., 2005). Interestingly, the prolonged activation of extrasynaptic N-Methyl-D-aspartate (NMDA) receptors in neuronal cultures can shift the neuronal expression of APP695 to the expression of KPI-containing APP isoforms which was accompanied with an increase of $A\beta_{42}$ production (Bordji et al., 2010).

Full length APP is synthesised in the endoplasmic reticulum and is transported to the cell surface through the Golgi apparatus and trans-Golgi network (TGN). In neurons, the TGN contains the highest concentration of APP at steady state and from here APP is transported to the cell surface via TGN derived secretory vesicles. APP can undergo sequential proteolysis by enzymes via two competing pathways; the non-amyloidogenic pathway and the amyloidogenic pathway (Figure 1.2).

Figure 1.2 The proteolytic processing of APP

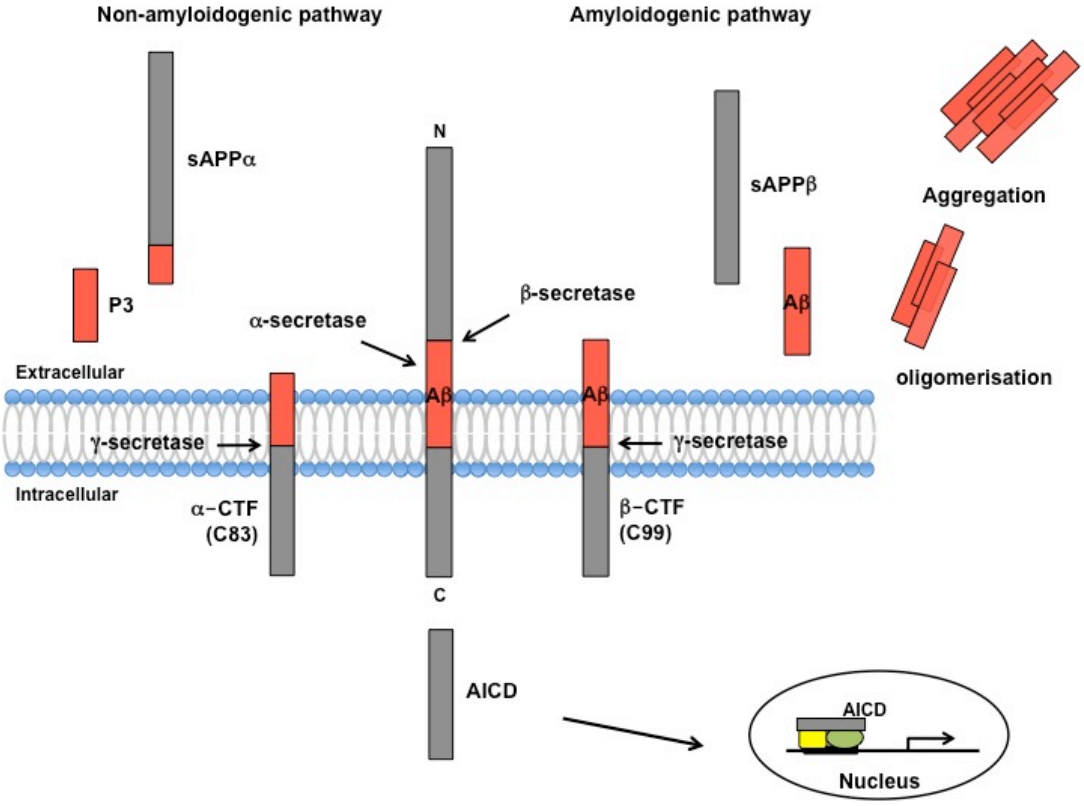

APP is processed via two pathways. In the non-amyloidogenic pathway α-secretase first cleaves APP to generate the soluble sAPPα fragment and the membrane bound C-terminal fragment, α-CTF or C83. In the amyloidogenic pathway, APP is cleaved by β-secretase (BACE) at the N-terminus of the Aβ sequence, generating sAPPβ and the membrane bound β-CTF or C99. Both α-CTF and β-CTF are subsequently cleaved by γ-secretase, giving rise to the p3 and neurotoxic Aβ peptides respectively and the APP intracellular domain (AICD). Aβ peptides associate to form oligomers and aggregate, ultimately forming Aβ plaques. The AICD has been proposed to migrate from the

cytosol into the nucleus and participates in the regulation of gene transcription. This figure is adapted from (Sastre et al., 2008).

In the non-amyloidogenic pathway, α-secretase cleaves APP within the Aβ domain, thus precluding the formation of Aβ and creates a neuroprotective sAPPα fragment (Goodman and Mattson, 1994) and a membrane bound C-terminal fragment (CTF), α-CTF or C83. α-secretase is a zinc metalloproteinase, member of the ADAM (a disintegrin and metalloproteinase) family. There is more than one enzyme from the ADAM family that mediates α-secretase activity and the most likely candidates include ADAM 9, 10, 17, 19 (Asai et al., 2003; Fahrenholz et al., 2000; Tanabe et al., 2007). The neuroprotective roles of sAPPα include neuronal plasticity, protection against excitotoxicity (Furukawa et al., 1996) and the regulation of neural stem cell proliferation (Caille et al., 2004; Ohsawa et al., 1999).

In the amyloidogenic pathway, APP is first cleaved at the N-terminal of the Aβ peptide sequence by β-secretase (or β-APP cleaving enzyme (BACE)). BACE is a membrane-bound aspartyl protease and is thought to be the limiting factor in the generation of Aβ from APP (Sinha et al., 1999; Vassar et al., 1999; Yan et al., 1999). This generates soluble APPβ (sAPPβ) and a membrane-bound β-CTF or C99. Interestingly, BACE2, a homolog to BACE1 is expressed in lower amounts in neurons (Bennett et al., 2000) and has been suggested to have a redundant role as BACE2 knockout mice are healthy whilst knockout of both BACE1 and BACE2 are lethal (Dominguez et al., 2005). Additionally, although sAPPβ differs from sAPPα by the absence of $A\beta_{1-16}$ region, sAPPβ has been reported to act as a death receptor 6 ligand and mediate axonal pruning and neuronal cell death (Nikolaev et al., 2009).

Both α-CTF and β-CTF are subject to subsequent cleavage by γ-secretase, giving rise to the p3 peptide or neurotoxic Aβ peptides respectively. The p3 peptide

($A\beta_{17-40}$, or $A\beta_{17-42}$) possesses no identified function and is rapidly degraded. In contrast, γ cleavage of β-CTF within the $A\beta$ domain is non-sequence specific, generating $A\beta$ peptides of various lengths ($A\beta_{38}$, $A\beta_{39}$, $A\beta_{40}$, $A\beta_{42}$ and $A\beta_{43}$) and the concomitant release of APP intracellular domain (AICD). $A\beta_{40}$ is the major species generated whilst $A\beta_{42}$ is the more amyloidogenic form. AICD has been proposed to migrate from the cytosol to the nucleus and participate in gene transcription events (Cao and Sudhof, 2001). These targets of AICD include: APP, GSK-3β, neprilysin, BACE1, EGFR (epidermal growth factor), TIP60, KAI1, LRP1 (Low density lipoprotein receptor-related protein 1) (Kim et al., 2003; Liu et al., 2007; Pardossi-Piquard et al., 2005; von Rotz et al., 2004; Zhang et al., 2007). γ-secretase is a multi-subunit catalytic complex. The subunits include PS1 or PS2, nicastrin, anterior pharynx defective 1 (APH1) and presenilin enhancer-2 (PSENEN-2) (Kimberly et al., 2003). PS1 and PS2 are the catalytic components of γ-secretase, these contain two critically conserved aspartate residues indispencible for γ-secretase activity (Li et al., 2000; Wolfe et al., 1999). Nicastrin and APH1 act as scaffolding proteins for the complex whilst PSENEN-2 regulates PS1 endoproteolysis to generate the active form of γ-secretase (Ahn et al., 2010). Under physiological conditions, non-amyloidogenic processing accounts for 95% of all APP processing. Thus, although to a lesser extent, amyloidogenic APP processing takes place naturally in every human being along their life span.

FAD is caused by the mutations in any of the three genes; APP, PS1 and PS2. APP mutations that cluster close to the γ-secretase site in the C-terminus $A\beta$ region promotes the generation of the more amyloidogenic $A\beta$ species, $A\beta_{42}$ (Haass et al., 1994; Suzuki et al., 1994). Furthermore, mutations internal to the $A\beta$ sequence, C-terminal to the α-cleavage site do not elevate the $A\beta_{42}$ to $A\beta_{40}$ ratio but change the sequence of $A\beta$ production with a tendency to oligomerise, fibrillise and promote deposition (Grabowski et al., 2001; Nilsberth et al., 2001; Van Nostrand et al., 2001). $A\beta$ deposition occurs during normal aging to some degree but this process is dramatically enhanced in AD. However, mice do not normally develop $A\beta$ plaques with

aging, unless they have been genetically modified. The amino acid sequence of APP between human and mice have a high degree of homology, 96.8% (Yamada et al., 1987). Within Aβ region of mouse APP, there is a three amino acid difference compared to human APP and this may account for the absence of Aβ plaque formation in mice (Yamada et al., 1987).

PS1 and PS2 are the products of the second (PSEN1) and third (PSEN2) genes located on chromosome 14 and chromosome 1 respectively. PS1 forms the catalytic component of γ-secretase which modulates the final cleavage of APP whilst PS2 is a homologue of PS1 (Levy-Lahad et al., 1995). Like APP mutations, mutations in PS1 and PS2 also increase the generation of $A\beta_{42}$. So far, at least 185 PSEN1 mutations and 13 PSEN2 mutations have been identified (http://www.molgen.ua.ac.be/ADMutations).

1.1.1.2 Intracellular Aβ

Extracellular Aβ plaques are thought to be pathogenic by inducing neuronal cell death, this can be via a range of mechanisms such as tau hyperphosphorylation (Ghribi et al., 2003), alteration of calcium influx (Ho et al., 2001), induction of inflammatory responses and activation of microglia (Eikelenboom et al., 2002; Gasic-Milenkovic et al., 2003). However in 1993, a report by Lee and Trojanowski's group provided the first biochemical evidence of endogenous intracellular Aβ (Wertkin et al., 1993). Subsequent research indicated increased levels of this intracellular pool of Aβ in a neuronal cell line upon neuronal maturation and with time (Skovronsky et al., 1998; Turner et al., 1996). Further studies on postmortem Down syndrome brain tissue (Busciglio et al., 2002; Gouras et al., 2000; Mori et al., 2002; Wertkin et al., 1993) and in APP transgenic mouse brains (Wirths et al., 2001) indicated that $A\beta_{42}$ immunoreactivity increased intraneuronally with aging. Additionally, in MCI patients Aβ immunoreactivity was reported to be more apparent in the entorhinal cortex and

hippocampus (Gouras et al., 2000), two brain regions primarily affected by AD pathology. Intracellular Aβ was also shown to precede the formation of extracellular Aβ deposits in post-mortem brain tissue of Down syndrome patients (Gyure et al., 2001; Mori et al., 2002), which suggests the accumulation of intracellular Aβ is an early event (Gouras et al., 2000).

The importance of intracellular Aβ accumulation of was strengthened by the evidence that intracellular Aβ can cause neurotoxicity. Neurotoxicity was evident by the use of triple labelling of Aβ, TUNEL and Hoechst in post-mortem AD brain tissue (Chui et al., 2001). Similarly, neuronal expression of Aβ in mice (LaFerla et al., 1995) and the expression of intracellular human Aβ in cortical neuronal cultures from rats (Kienlen-Campard et al., 2002) induces neuronal apoptosis. Zhang *et al* also demonstrated that microinjections of the $A\beta_{42}$ peptide into cultures induced significant cell death, specifically in human primary neurons as oppose to human primary astrocytes, neuronal and non-neuronal cell lines (Zhang et al., 2002). The mechanism of intracellular Aβ toxicity is unknown however, intracellular $A\beta_{40}$ and $A\beta_{42}$ has been demonstrated to directly activate the p53 promoter thereby initiating p53 dependent apoptosis (Ohyagi et al., 2005). This was apparent in guinea pig primary neurons after oxidative DNA damage, when $A\beta_{42}$ was localised in the nucleus with increased p53 mRNA levels. Elevation of p53 mRNA was also found in post-mortem brain tissue of sporadic AD patients and in Tg2576 mice (Ohyagi et al., 2005).

Although nowadays there is no doubt about the existence of intracellular Aβ, a key question with no answer is whether part of the Aβ generated intracellularly is not secreted or if part of the secreted peptide is taken up by the cell and contribute towards the formation of intracellular Aβ pools. Some possibilities include a) retention of APP and production of $A\beta_{42}$ in the ER lumen, b) the inability of Aβ to be secreted because Aβ may be passively leaked along any component of the secretory pathway, c) secreted Aβ is internalised into endosomes (Selkoe et al., 1996) or lysosomes (Yang et

al., 1998) causing increased lysosomal membrane permeability and leak into the cytosol, d) secreted extracellular Aβ can be internalised via passive diffusion across the plasma membrane into the cytosol or via binding to cell surface receptors such as the α7 nicotinic acetylcholine receptor (Nagele et al., 2002), LRP (Bu et al., 2006; Zerbinatti et al., 2006) and the scavenger receptor for advanced glycation end products (RAGE) (Deane et al., 2003; Sasaki et al., 2001; Yan et al., 1996).

Some studies have indicated a relationship between extracellular and intracellular Aβ. Observations in various transgenic mouse models of AD supports this theory; the accumulation of intracellular Aβ occurs before the appearance of extracellular Aβ deposits (Chui et al., 1999; Li et al., 1999b; Lord et al., 2006; Oakley et al., 2006; Wirths et al., 2001) and the accumulation of intracellular Aβ correlated with cognitive deficits (Oddo et al., 2003). Furthermore, Oddo *et al* identified an inverse relationship between the intracellular and extracellular pools of Aβ in a triple transgenic AD model (Oddo et al., 2006a). These provide evidence that the formation of extracellular Aβ plaques may originate from a source of intracellular Aβ. A paper by D'Andrea *et al* demonstrated by immunohistochemistry and digital image analysis in post-mortem AD brain samples, that excessive accumulation of intracellular Aβ led to neuronal lysis and dispersion of intracellular Aβ content into the extracellular matrix (D'Andrea et al., 2001). Other studies using mouse models have demonstrated that clearance of extracellular Aβ plaques using immunotherapy can also reduce intracellular Aβ (Oddo et al., 2004) and improve cognition (Janus et al., 2000; Morgan et al., 2000).

1.1.1.3 The amyloid cascade hypothesis

The amyloid cascade hypothesis proposed by Hardy and Allsop in 1991 (Hardy and Allsop, 1991), has become the dominant theory in the AD field. This hypothesis states that the aberrant processing of APP leads to the build-up and deposition of $A\beta_{40}$ and $A\beta_{42}$ peptides, especially the more amyloidogenic form, $A\beta_{42}$, and is thought to initiate a cascade of events leading to the formation of amyloid plaques, NFTs and consequently synaptic degeneration, neuronal death and eventually cognitive decline observed in patients with AD.

Since the identification of Aβ as the main component of extracellular Aβ plaques by Glenner and Wong, a substantial amount of studies has supported the amyloid cascade hypothesis. Genetic data from FAD has provided the strongest evidence; mutations in either of the APP, PS1 and PS2 genes increase the generation of Aβ or the production of $A\beta_{42}$ in many studies. Mutations in the PS1 gene causes increased production of the $A\beta_{42}$ species, which is accompanied by a reduction in levels of $A\beta_{40}$. This observation has led to the proposal that the ratio $A\beta_{42}/A\beta_{40}$ is a more important factor than the absolute levels of $A\beta_{42}$ species and the $A\beta_{42}/A\beta_{40}$ ratio is inversely associated with age of AD onset. Further support for the amyloid cascade hypothesis comes from transgenic mice models of AD. APP transgenic mice expressing mutant human APP have time-dependent increase in extracellular Aβ that appears to correlate with behavioural changes, similar to AD (Hsiao, 1998). In double transgenic mice, expression of mutant APP and mutant tau show that the formation of NFTs is enhanced under the influence of Aβ (Lewis et al., 2001; Terwel et al., 2008). Similarly, injection of synthetic Aβ into the brains of tau transgenic mice or double transgenic mice (expressing mutant APP and mutant tau) induces the hyperphosphorylation of tau and NFT formation, therefore pointing out the role of Aβ upstream of tau (Gotz et al., 2001; Lewis et al., 2001; Oddo et al., 2003; Santacruz et al., 2005). These transgenic models have been useful in the investigation of Aβ immunotherapies. In triple

transgenic mice displaying Aβ plaque and NFT pathology, Aβ immunisation not only reduced extracellular and intracellular Aβ accumulation but also early tau pathology (Oddo et al., 2004). Other amyloidogenic proteins such as Dan-amyloid which deposits in the brain of patients with familial Danish dementia promotes NFT lesions when Dan-amyloid is expressed in tau transgenic mice (Coomaraswamy et al., 2010). This study further suggests amyloidogenic peptides drive similar pathogenic pathways.

Even though a vast amount of data supports the amyloid cascade hypothesis, the original idea that the deposition of extracellular Aβ plaques consisting of Aβ fibrils are pathogenic, has been challenged and modified over time. The amyloid cascade is currently still the leading hypothesis, however it is believed that fibrillar Aβ is no longer triggering secondary events that will lead to neurodegeneration but instead it is caused by the presence of soluble and oligomeric Aβ species. Firstly, advance development of imaging techniques that allows the imaging of Aβ plaques *in vivo* using Pittsburgh compound B have shown the presence of Aβ plaques in AD patients as well as in cognitively normal individuals. This data suggests that insoluble Aβ plaques may not actually trigger pathological events as thought but instead may be neuroprotective (Caughey and Lansbury, 2003). Secondly, work by Braak and Braak indicates that NFTs precede the appearance of Aβ plaques in the AD brain and is also a better measure of disease severity (Braak et al., 2006) (discussed in section 1.1.2). Thirdly, transgenic mouse models have provided further insight; mice expressing mutant human APP develop memory deficits prior to the onset of Aβ plaque deposition. Another group demonstrated in the PDAPP mice model, that insertion of a C-terminal cleavage site (Asp664) in APP which normally causes production of a toxic fragment C-31, prevented and improved memory deficits whilst Aβ production was unaltered (Galvan et al., 2006). Additionally in Tg2576 mice, despite the development of Aβ plaques in the brain, these mice continued to have normal memory function (Lesne et al., 2008). Also, in a recent clinical trial, long-term $A\beta_{42}$ immunisation for the removal of Aβ plaques did not improve memory and cognition (Holmes et al., 2008). Thus, these

data suggests that Aβ plaques are not the root cause of disease and recent research has largely focused on the connection between Aβ neurotoxicity and soluble, non-fibrillar Aβ oligomers.

Aβ is present in multiple forms. Aβ is produced as a monomer and these can aggregate to form oligomers consisting of dimers and trimers. The most toxic form of Aβ is thought to be oligomers which have been shown to correlate with synaptic dysfunctions and disruption of learning and memory, and long-term potentiation (LTP) in animals (Cleary et al., 2005; Walsh et al., 2002). The formation of Aβ oligomers is thought to occur intracellularly (Oddo et al., 2006b; Takahashi et al., 2004; Walsh et al., 2000), specifically within lipid rafts (Kawarabayashi et al., 2004; Kim et al., 2006). In soluble fractions of the human brain and Aβ plaque extracts, SDS-stable low molecular weight Aβ oligomers, dimers and trimers, have be detected and suggests that they could act as basic building blocks for larger oligomers and fibrils (Podlisny et al., 1995; Walsh et al., 2000). These Aβ oligomers have been shown to inhibit LTP *in vivo* (Cleary et al., 2005; Klyubin et al., 2005; Lesne et al., 2006; Trommer et al., 2005; Walsh et al., 2002). Their high toxicity has also been supported by *in vitro* data, showing that dimers and tetramers are 3-fold and 13-fold more toxic than monomers, respectively (Ono et al., 2009). Furthermore, Lesne *et al* detected the accumulation of the Aβ*56 form of soluble Aβ in Tg2576 mice, which consists of SDS-stable nonamers and dodecamers (Lesne et al., 2006). Purification of Aβ*56 from memory impaired Tg2576 mice and subsequent administration into wild type rats induced significant memory impairment in spatial memory performance. Another study also demonstrated that Aβ*56 levels correlated with the cognitive decline in an APP23 mouse model (Lefterov et al., 2009).

The amyloid cascade hypothesis is widely accepted and drives much of AD research however a growing consensus is that tau might actually be part of the pathway; tau is not just a passive target but an active component early on in the cascade. In hippocampal cultures obtained from wild type, tau knockout and human tau

transgenic mice, treatment of fibrillar Aβ caused neuronal degeneration in wild type and human tau only whilst cell death was prevented in tau knockout neurons (Rapoport et al., 2002). Recently an *in vivo* study reported that dendritic function of tau mediates Aβ toxicity as mice lacking or expressing truncated tau was protected from Aβ-induced toxicity and memory deficits (Ittner et al., 2010). Tau is associated with postsynaptic targeting of the Src kinase, Fyn, that mediates an interaction between NMDA receptors and postsynaptic density protein 95 (PSD95). This interaction is required for Aβ toxicity. Furthermore, these observations could be recapitulated by using a peptide that uncouples Fyn mediated interaction of NMDA and PSD95 *in vivo*. Thus, these data suggest tau has an important role in mediating Aβ toxicity.

1.1.2 Tau pathology

In addition to Aβ plaques, the second characteristic pathological hallmark of AD are NFTs. NFTs appear in nerve cell bodies whilst neurophil threads are present in neuronal processes. NFTs are aggregates of paired helical filaments (PHFs) (Kidd, 1963), themselves composed predominately of hyperphosphorylated forms of the microtubule associated protein, tau (Grundke-Iqbal et al., 1986). Both Aβ plaques and NFTs are abundant in the AD brain. However, in contrast to Aβ plaques, NFTs appear to be distributed, and to appear, in a predictable pattern. NFTs originate from the layer II neurons of the entorhinal cortex and spread to the outer molecular layer of the dentate gyrus (Braak and Braak, 1991). Studies have shown that the extent and distribution of NFT in AD correlate to the degree of dementia and the progressive cognitive decline (Arriagada et al., 1992) and also serves as a useful post-mortem diagnostic marker (Braak et al., 2006).

1.1.2.1 Tau structure, isoforms and function

Tau was first identified in 1975 (Weingarten et al., 1975). It is a highly soluble microtubule-associated protein (MAP) and with two other MAPs; MAP1 and MAP2, is mainly expressed in neurons, being predominately found within axons. All MAPs are involved in microtubule stabilisation to help maintain the complex neuronal morphology and help facilitate axonal transport along microtubules.

Tau is preferentially expressed in the human brain and alternative splicing of the single gene (MAPT) on chromosome 17 (Himmler, 1989) generates the six major isoforms of tau (Goedert et al., 1989). The protein isoforms range from 352 to 441 amino acids in length with molecular weights of between 45-65 kDa. They are distinguished by the number of microtubule binding domain repeats (R) in the C-terminal (3 or 4 repeats) and by the presence or absence of 2 N-terminal insertions (N). The presence or absence of exon 10 generates the 3R or 4R isoforms respectively and the inclusion of exons 2 and 3 generates the zero, one or two N-terminal insertions, the 0N, 1N or 2N isoforms. Thus, alternative splicing gives rise to three 3R isoforms of tau (3R0N, 3R1N and 3R2N) and three 4R isoforms (4R0N, 4R1N and 4R2N) (Figure 1.3). The repeat domain is known to be important for the stabilisation of microtubules and also in forming the core of PHFs (Wischik et al., 1988). Therefore, 4R tau isoforms are more efficient in promoting microtubule assembly than 3R tau isoforms (Alonso et al., 2001b). Tau splicing is developmentally regulated; the smallest isoform, 0N3R tau is the only form expressed in foetal brain. By contrast all 6 isoforms are expressed in the mature brain. Additionally, foetal tau is highly phosphorylated compared to adult tau. Phosphorylation is thought to reduce the affinity of tau binding to microtubules. The reduced affinity of foetal tau for microtubules is thought to be required for the high level of plasticity occurring during early brain development. In disease, the reduced affinity of phosphorylated tau abolishes microtubule binding and can lead to destabilisation of the cytoskeleton (Drewes et al., 1995; Sengupta et al., 1998), which can impair tau-

dependent cellular functions such as axonal growth, axonal transport and the correct propagation of electrical signals needed for synaptic transmission.

Figure 1.3 Schematic representation of the tau isoforms in the human brain

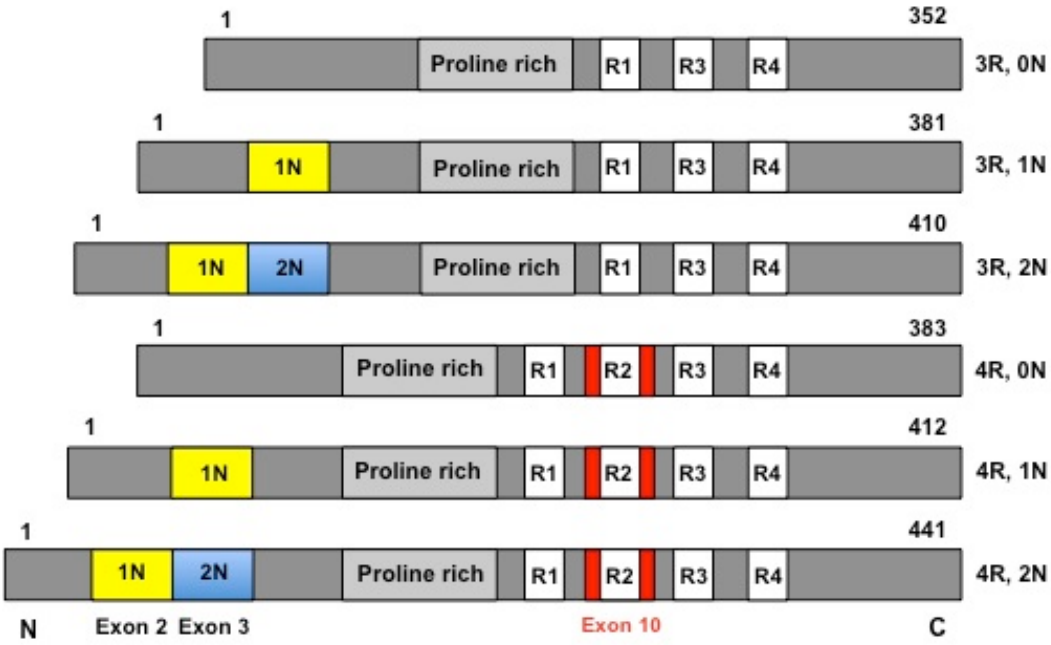

Alternative splicing of a single gene generates the six isoforms of human tau. Exons 2 and 3 encodes the two N-terminal inserts, 1N and 2N, respectively. These give rise to the 1N or 2N tau isoforms whilst the absence of exons 2 and 3 gives rise to the 0N tau isoforms. Exon 10 encodes the microtubule binding repeat R2 and its presence or absence yields the 4R or 3R tau isoforms respectively. The microtubule binding repeats form the binding region for tau and the proline rich region has been proposed to increase the interaction between tau and microtubules. The number of amino acid is indicated above each tau isoform. This figure is adapted from (Hanger and Noble, 2011).

1.1.2.2 Tau phosphorylation

All six tau isoforms are subject to phosphorylation by the addition of phosphate groups on three receptor amino acids; serines (Ser), threonines (Thr) and tyrosines (Tyr). Phosphorylation sites have been identified *in vivo* by a range of techniques such as mass spectrometry, Edman degradation and the use of phospho-specific tau antibodies. There are 85 putative phosphorylation sites on tau; 45 serines, 35 threonines and 5 tyrosines (Martin et al., 2011) (for review), which may be subjected to phosphorylation by one or more kinases. To date, approximately 20% have been identified as being phosphorylated in normal brain tissue (Hanger and Noble, 2011). These sites are substrates for three classes of tau kinases: proline-directed protein kinases (PDPK), non-proline-directed protein kinases (non-PDPK) and tyrosine specific kinases. Amongst the PDPK are glycogen synthase kinase-3 (GSK-3) (Mandelkow et al., 1993), cyclin-dependent kinase 5 (Cdk5) (Baumann et al., 1993) and the mitogen-activated protein kinases (MAPKs): c-Jun N-terminal kinase (JNK), p38 MAPK and Erk1/2 (Goedert et al., 1997; Hyman et al., 1994; Mandelkow et al., 1993; Reynolds et al., 1997b). These have been identified in NFTs in post-mortem AD brain tissue and related pathologies and have also demonstrated the ability to phosphorylate tau *in vitro* (Mandelkow et al., 1993). Non-PDPK target serine or threonine residues not preceded by a proline and these include casein kinase 1 (CK1), protein kinase A (PKA), Ca^{2+}/Calmodulin-dependent protein kinase II (CaMKII) and dual-specificity tyrosine phosphorylation regulated kinase 1A (DYRK1A) (Lee, 2005; Sergeant et al., 2008). Tyrosine kinases include the Src family kinases, Src (Lee, 2005), Lck (Williamson et al., 2002), Syk (Lebouvier et al., 2008), Fyn (Lee et al., 2004) and c-Abl (Derkinderen et al., 2005).

GSK-3 and Cdk5 are highly expressed in the brain (Anderton et al., 2001; Liu et al., 2006; Wang et al., 1998). Both can target a large combination of common phosphorylation sites (Lew et al., 1994; Tsai et al., 1993; Woodgett, 1990) and have been shown to be associated with all stages of NFT pathology in AD (Pei et al., 1999;

Pei et al., 1998). GSK-3 exists as two isoforms, α and β, sharing 85% sequence homology at the protein level and are encoded by genes on chromosome 19 and 3, respectively (Woodgett, 1990). A brain enriched splice variant of the GSK-3β isoform, GSK-3β2, has also been identified containing an additional exon encoding 13 amino acid (Mukai et al., 2002). The difference between GSK-3β and GSK-3β2 reside in their affinity for certain targets (Saeki et al., 2011). Subtle differences in substrate preference between isoforms and slice variants has been reported in brain (Soutar et al., 2010). GSK-3β is highly expressed in the brain and by neurons (Woodgett, 1990), making it easily accessible to tau. In post-mortem AD brain tissue, GSK-3β levels are increased by approximately 50% compared to non-diseased brains (Pei et al., 1997). In mice overexpressing GSK-3β, tau was hyperphosphorylated in the hippocampus with the appearance of pretangle-like structures and neuronal cell death and this was accompanied with cognitive deficits (Lucas et al., 2001; Spittaels et al., 2000). *In vitro*, tau phosphorylation by GSK-3 was shown to greatly reduce the ability of tau to associate with microtubules (Mandelkow et al., 1992) and the treatment of cells with a selective GSK-3 inhibitor, lithium, significantly reduced tau phosphorylation (Hong et al., 1997; Lovestone et al., 1999). Furthermore, lithium treatment in transgenic mice overexpression GSK-3β or mutant tau, reduced tau phosphorylation, tau aggregation and axonal degeneration (Engel et al., 2006; Leroy et al., 2010; Noble et al., 2005). It has been established that GSK-3β can phosphorylate tau at primed (e.g., Thr231) as well as unprimed (e.g., Ser202, Thr205, Ser396 and Ser404) epitopes. Priming occurs 4-6 residues C-terminal to the GSK-3β target site (Cole et al., 2006; Li et al., 2006) and can be performed by PKA, CK1 or Cdk5 (Li et al., 2006; Wang et al., 1998).

Cdk5 is regulated by a neuron-specific activator, p35, which is cleaved under neurotoxic conditions by calpain to form p25. It is the association of p25 with Cdk5 that causes the hyperphosphorylation of tau (Lee et al., 2000). In rodent models, overexpression of p25 led to tau hyperphosphorylation and neurodegeneration (Cruz et al., 2003; Noble et al., 2003), which was ameliorated by silencing of Cdk5 (Piedrahita

et al., 2010). Furthermore, phosphorylation of tau by Cdk5 has also been shown to induce neurotoxicity in Drosophila (Steinhilb et al., 2007).

Dephosphorylation of tau is equally as important, as the lack of phosphatase activity may lead to the hyperphosphorylated forms of tau found in disease. The five major protein phosphatases (PP), PP1, PP2A, PP2B, PP2C and PP5 are highly expressed in the brain. *In vitro*, all these protein phosphatases, with the exception of PP2C, can dephosphorylate tau (Buee et al., 2000) (for review). In addition, all of these have been shown to dephosphorylate tau in the brain to some varying degrees. However, PP2A has been shown to be the major tau phosphatase (Goedert et al., 1995; Liu et al., 2005). *In vitro* incubation of PP2A with tau aggregates was shown to rescue microtubule binding (Wang et al., 2007). Furthermore, the activities and expression of the two phosphatases PP1 and PP2A are reduced in selective areas of the AD brain (Gong et al., 1993). The observation that endogenous PP2A inhibitors are increased, colocalising with PP2A and hyperphosphorylated tau in neurons of AD brain tissue suggested that a reduction in dephosphorylation of tau may be of considerable importance for the aberrant hyperphosphorylation of tau (Tanimukai et al., 2005).

The overall level of tau phosphorylation is determined by the action of both protein kinases and phosphatases. The imbalance of these activities may thus contribute to the abnormal phosphorylation of tau observed in AD, and therefore be pathogenic.

1.1.2.3 Pathological functions of tau

NTFs are not only observed in AD but also in a family of neurodegenerative diseases called tauopathies such as frontotemporal dementia with parkinsonism linked to chromosome 17 (FTDP-17), Pick's disease, corticobasal degeneration, dementia pugilistica, and progressive supranuclear palsy. Although to date no mutations have been found in tau that lead to AD, there are tau mutations that do lead to other

neurodegenerative disorders such as FTDP-17 (Hutton et al., 1998). This adds to the idea that dysregulation of tau and/or its normal physiology contributes to neurotoxicity both in AD and other tauopathies. Indeed, it has been demonstrated, initially by Terry *et al*, that tau pathology correlates better with cognitive decline than amyloid pathology. Although, in fact, the best correlate with cognitive decline is neither tau nor amyloid pathology but loss of synapses (Terry et al., 1991). How tau exerts its neurotoxic properties has still not been fully established. Some tau becomes hyperphosphorylated and aggregates but tau aggregates are now not thought to be the toxic species as demonstrated by *in vivo* and *in vitro* experiments.

The isolation of abnormally hyperphosphorylated tau from cytosolic fractions of the AD brain and hyperphosphorylated recombinant tau, both self aggregate into PHFs *in vitro* and this process was reversed upon dephosphorylation (Alonso et al., 2001a). Other *in vitro* models that used pseudophosphorylated tau, induced a cytotoxic effect in PC12 cells compared to wild type cells, thereby mimicking the functional and structural aspects of AD (Fath et al., 2002). Additionally, the Drosophila GSK-3β homologue shaggy, requires the overexpression of human tau for its ability to exacerbate neurodegeneration due to neurofibrillary pathology (Jackson et al., 2002). This is further supported by the use of phosphatase inhibitors which induce tau to hyperphosphorylate and consequently induced tau fibrillisation (Perez et al., 2002). It has also been postulated that tau phosphorylation may inhibit its turnover rate, giving rise to intracellular levels of tau (Litersky and Johnson, 1992). Furthermore, hyperphosphorylated tau is also known to sequester normal tau and other MAPs, which can deplete microtubules from functional tau and cause the instability of microtubules (Alonso et al., 1996; Alonso et al., 1997). Leading on from this, an *in vivo* model of mice expressing human tau treated with the microtubule stabilising drug, (Paxceed), stabilised microtubules which consequently restored axonal transport defects and improved motor impairments (Zhang et al., 2005).

Taken together these *in vivo* studies along with the *in vitro* data demonstrate a causal relationship between hyperphosphorylation of tau and the formation of NFTs and that hyperphosphorylation of tau can cause its loss of biological function and a gain of toxicity. This is thought to influence the aggregation of tau into NFT.

As a matter of fact, tau phosphorylation occurs before the formation of NTFs (Braak and Braak, 1995; Iqbal and Grundke-Iqbal, 1991) and the survival of neurons bearing NTFs many years after tangle formation is thought to be a self-defense mechanism. In mouse and Drosophila models, soluble, non-aggregated, hyperphosphorylated tau induces a toxic effect. Furthermore, in a transgenic mouse model with the P301L human tau mutation, suppression of tau expression caused cognitive improvements and stabilised the neuron number, whilst NFTs continued to accumulate (Santacruz et al., 2005). This study demonstrates an association between the levels of soluble hyperphosphorylated tau and cognitive impairments. Interestingly, a Drosophila model demonstrated phosphorylation of Ser262 and Ser356 was a prerequisite for subsequent activation of tau kinases GSK-3 and Cdk5 (Nishimura et al., 2004). Likewise, staining of AD brains, revealed phosphorylation of Thr231, Ser262 and Thr153 sites associated with the neuronal pretangle state (Augustinack et al., 2002). Conversely, other groups found phosphorylation at the Ser262 and Ser214 epitopes protected against tau assembly into filaments (Schneider et al., 1999) and was shown to be anti-apoptotic (Kyoung Pyo et al., 2004). Together, these findings indicate that certain tau phosphorylation sites may be associated with the toxic or protective functions of soluble forms of tau.

Despite all the above the precise role of phosphorylated and aggregated tau remains unclear. A better understanding of the functional effect of tau phosphorylation at specific epitopes will greatly further our understanding of tau biology and how it then becomes dysregulated in disease.

1.1.3 Calcium and AD

Alterations in calcium (Ca^{2+}) homeostasis as the common cause for neurodegenerative diseases was first described by Khachaturian in 1989 (Khachaturian, 1989). Experimental studies supporting this theory in AD soon followed as fibroblasts from asymptomatic AD patients (Etcheberrigaray et al., 1998; Ito et al., 1994) and gene expression analysis of post-mortem AD brain tissue (Emilsson et al., 2006) indicated enhanced inositol-1,4,5-triphosphate (IP_3) receptor-mediated Ca^{2+} signalling. Recently, the drug, memantine, was approved as treatment for moderate to severe AD. Memantine targets the NMDA receptors of the glutamatergic system and blocks the permeability of NMDA receptors to Ca^{2+} thereby further confirming a role for Ca^{2+} signalling in AD.

Ca^{2+} signalling is central to a variety of neuronal functions, such as neurotransmitter release, signal transduction, gene expression, formation of radical species and cell death (Berridge, 1998). It is therefore important that Ca^{2+} signals are regulated. The Ca^{2+} concentration within the cytosol of a cell is low under minimal activity (50-300 nM). This is achieved by Ca^{2+} influx from the extracellular environment and Ca^{2+} release from intracellular stores; the endoplasmic reticulum (ER) (LaFerla, 2002). In contrast, the Ca^{2+} concentration is 1000 times higher within the ER. This concentration gradient within the cell is maintained by the presence of plasma membrane Ca^{2+}-ATPases and sodium/Ca^{2+} exchangers that pumps Ca^{2+} into the extracellular space whilst the sarco/endoplasmic reticulum Ca^{2+} ATPase (SERCA) on the ER membrane actively transports Ca^{2+} from the cytosol into the intracellular stores. Upon cellular activation, extracellular Ca^{2+} is influxed into the cytosol either via voltage-gated and/or ligand-gated channels (e.g. NMDA receptors), store-operated channels (eg. Transient receptor potential channels TRPC) or G-protein coupled receptors (GPCRs, e.g. metabotrophic glutamate receptors, mGluR). ER stores of Ca^{2+} are released via channels localised on the ER membrane; the IP_3 receptors (IP_3R) and ryanodine receptors (RyR). The activation of IP_3R requires IP_3 which is generated by

inositol-4, 5-biphosphate via GPCR-activated phospholipase C at the plasma membrane. The RyR are activated by small increases in cytosolic Ca^{2+} levels, a process known as Ca^{2+} induced Ca^{2+} release (Berridge, 1998).

There is evidence showing Ca^{2+} modulates the processing of APP. Treatment of human embryonic kidney 293 cells (HEK-293 cells) expressing APP with a Ca^{2+} ionophore (A23187) consistently increased the production of Aβ by approximately 3-fold (Querfurth and Selkoe, 1994). The same group also treated HEK-293 cells with caffeine, a RyR stimulator, that also increased the production of Aβ (Querfurth et al., 1997). Interestingly, another group reported that high levels of Ca^{2+} in the cytosol, generated from extracellular Ca^{2+} influx, impairs the non-amyloidogenic pathway and increases the production of intraneuronal $A\beta_{42}$ (Pierrot et al., 2004). Additionally it was shown that Ca^{2+} release from the ER alone is insufficient to induce the production of intracellular Aβ; Aβ production is only observed on sustaining a high cytosolic Ca^{2+} concentration by extracellular influx (Pierrot et al., 2004). Recently, a polymorphism in the CALHM1 gene was identified and proposed as a risk factor for LOAD (Dreses-Werringloer et al., 2008). CALHM1 encodes transmembrane glycoprotein that controls cytosolic Ca^{2+} and Aβ levels. In contrast to the study by Pierrot *et al*, the mutation in CALHM1 impairs plasma membrane Ca^{2+} permeability and reduces the cytosolic Ca^{2+} levels thereby increasing $A\beta_{42}$ production and $A\beta_{42}/A\beta_{40}$ ratio (Dreses-Werringloer et al., 2008). Conversely, other studies have, in turn, demonstrated the effects of APP and its metabolites on Ca^{2+} signalling. *In vitro*, the addition of Aβ to the media of hippocampal neurons increases Ca^{2+} concentration in the cytosol (Goodman and Mattson, 1994; Mattson et al., 1993). This may be mediated by the insertion of $A\beta_{42}$ and $A\beta_{40}$ oligomers into the plasma membrane via an interaction with phosphatidylserine, to form Ca^{2+} permeable pores (Arispe et al., 1993). Aβ oligomers can also modulate the activation of Ca^{2+} channels at the plasma membrane (De Felice et al., 2007; Nimmrich et al., 2008; Shankar et al., 2007) or ER-specific IP_3Rs and RyRs and initiate a rise in cytosolic Ca^{2+} concentration (Ferreiro et al., 2004). Disturbances in cytosolic Ca^{2+}

levels can trigger neurotoxic mechanisms such as free radical formation (Brustovetsky et al., 2003), lipid peroxidation (Lovell et al., 2001) and apoptosis (Bernardi et al., 2006). Interestingly, secreted APP may therefore have neuroprotective properties since they attenuate the elevation of intracellular Ca^{2+} caused by Aβ (Goodman and Mattson, 1994).

Ca^{2+} dysregulation can also affect the tight regulation of tau phosphorylation, leading to abnormally hyperphosphorylated tau and NFT formation. Transient increases in intracellular Ca^{2+} levels in the SHSY5Y neuronal cell line has been shown to activate the tau kinase, GSK-3β (Hartigan and Johnson, 1999). The activation of another tau kinase, Cdk5, is induced by the Ca^{2+}-dependent protease, calpain. Calpain generates p25 from the p35 precursor; p25 is a strong activator of Cdk5 (Maccioni et al., 2001). In cultured neurons, membrane depolarisation induced a transient Ca^{2+}-mediated tau phosphorylation by both of these tau kinases GSK-3 and Cdk5. Tau phosphorylation was followed by Ca^{2+}-dependent dephosphorylation (Pierrot et al., 2006). These studies demonstrate the effect of increases in cytosolic Ca^{2+} concentrations on the modification of tau phosphorylation. Many other Ca^{2+}-dependent proteins have been indicated to have an influence on tau pathology such as CaMK (Yoshimura et al., 2003) and the phosphatase calcineurin (Fleming and Johnson, 1995). CaMK can phosphorylate purified tau in solution (Baudier and Cole, 1987). Specifically, CaMKII immunoreactivity is enhanced in the hippocampal neurons of the CA1 and subiculum regions of post-mortem AD brain tissue, these regions are predisposed to NFT formation (McKee et al., 1990). CaMKII is thought to phosphorylate tau (Ser262 and Ser356 epitopes) at the site of its interaction with microtubules (Litersky et al., 1996). Calcineurin can also act directly to dephosphorylate recombinant tau or brain extracts (Drewes et al., 1993) and was found to dephosphorylate GSK-3β and Cdk5 in neuronal cells, demonstrating a role in the regulation of tau phosphorylation (Kim et al., 2009c; Pierrot et al., 2006).

Ca^{2+} plays a key role in cell signalling processes crucial to the normal functioning of neuronal cells. Although research is much more focused on the mechanism of Aβ and tau neurotoxicity in AD, accumulating evidence highlights the importance of disturbances in Ca^{2+} homeostasis and its contribution to AD pathogenesis.

1.2 Apolipoprotein E (ApoE) and AD

A genetic contribution to the development of AD is not limited to FAD but also to LOAD. In 1993 Allen Rose's group identified that the ε4 allele of the gene encoding apolipoprotein E (APOE) was strongly linked with AD (Saunders et al., 1993). Since then many susceptibility genes have been identified, although replications have been inconsistent and most were likely to be false positives (see Alzgene website for candidate gene study details www.alzgene.org) (Bertram et al., 2007). Recently, the completion of several very large scale genome-wide association studies has finally identified new susceptibility genes, including CLU, PICALM and CR1, ABCA7, MS4A, EPHA1, CD33 and CD2AP (Harold et al., 2009; Hollingworth et al., 2011; Lambert et al., 2009).

In humans, the APOE gene is polymorphic, being represented by three major alleles: ε2, ε3 and ε4. This gives rise to three homozygous (APOEε2/2, ε3/3 and ε4/4) and three heterozygous (APOEε3/2, ε4/3 and ε4/2) genotypes. Within Caucasian populations, the ε3 allele is the most common representing 77% of the population, followed by the ε4 allele accounting for 15% and the ε2 allele accounting for 2% (Farrer et al., 1997). Genetic studies have provided evidence that the ε4 allele confers the greatest risk of developing AD, whilst the ε3 allele confers intermediate risk and the ε2 allele may be a protective factor for AD (Corder et al., 1994). Relative to ε3, the risk of AD is increase by ~3 fold with one copy of the ε4 allele and by ~12 fold with two copies (www.alzgene.org), relative to ε2, ε4 increases the risk by over 500 fold. The

importance of APOEε4 in AD pathogenesis is highlighted by representing for 65-80% of all AD cases. Furthermore, the APOEε4 allele is present in ~50% of LOAD patients, compared to ~16% of age- and sex-matched controls (Saunders et al., 1993). In contrast to the autosomal inheritance of FAD genes, the APOEε4 allele itself does not cause disease but rather, evidence suggests it alters the risk of AD in a dose-dependent manner by lowering the mean age of onset from 85 to 68 years (Corder et al., 1993). Carriers of the APOEε4 gene do not necessary develop AD and therefore diagnosis of AD cannot rely on the presence of ε4, although the presence of ε2 is a likely exclusion criteria (Corder et al., 1995; Tiraboschi et al., 2004).

The mechanism by which APOEε4 confers greater susceptibility for AD remains unclear. There are conflicting reports about whether APOEε4 influences a rapid rate of cognitive and functional decline after the onset of AD. MRI studies have shown greater decreases in entorhinal cortex and hippocampus volume in APOEε4 positive AD patients (Bookheimer and Burggren, 2009). Similarly, cognitively normal children and adults carrying the APOEε4 allele also have a decrease in entorhinal cortex volume (Shaw et al., 2007). Additionally, cognitively normal APOEε4 carriers also have greater cognitive decline (Blair et al., 2005), and positron emission tomography studies have found that these individuals show cerebral glucose hypometabolism (Reiman et al., 2001) suggesting this may be an advance measure, predictive of dementia in their later lives. Neuropathologically, apoE has been immunohistochemically identified in Aβ plaques and NFTs of AD post-mortem brain tissue (Namba et al., 1991) which raises the idea that apoE may be directly involved in the pathological mechanisms leading to neurodegeneration. This is supported by the observation that mice expressing FAD forms of APP but which are apoE-null do not develop Aβ plaques.

1.2.1 ApoE structure, isoforms and function

Apolipoprotein E (apoE) is a key component of lipid transport and cholesterol metabolism not only within the periphery but also within the brain. The differences between the three isoforms of human APOE (ε2, ε3 and ε4) reside in single base differences giving rise to amino acid substitutions at residues 112 and 158 (Figure 1.4). APOEε2 has two cysteines (Cys) at these positions, APOEε3 has a Cys at 112 and an arginine (Arg) at 158 whilst APOEε4 has Arg residues at both positions (Weisgraber et al., 1981). ApoE is synthesised as a 34 kDa protein containing 299 amino acids and consists of two domains connected by a flexible hinge region; the N-terminal domain and C-terminal domain containing the receptor binding site and lipoprotein binding site, respectively (Weisgraber, 1994). An interaction between these two domains is stronger in the apoE4 isoform than the apoE2 or apoE3 isoforms. This domain interaction occurs when the Arg112 residue displaces the side chain of Arg61 in the amino-terminal that allows it to form a salt bridge with glutamic acid at position 255 at the C-terminal (Figure 1.5) (Dong and Weisgraber, 1996; Dong et al., 1994). Interestingly, Arg61 is unique to humans as all other 17 species in which the apoE gene has been sequenced have a threonine at the same position (Weisgraber, 1994). The differences in amino acids that alter the charge and structural properties of apoE, ultimately influences the functional properties of each apoE isoform.

Figure 1.4 Schematic representation of the APOE isoforms in human and mouse

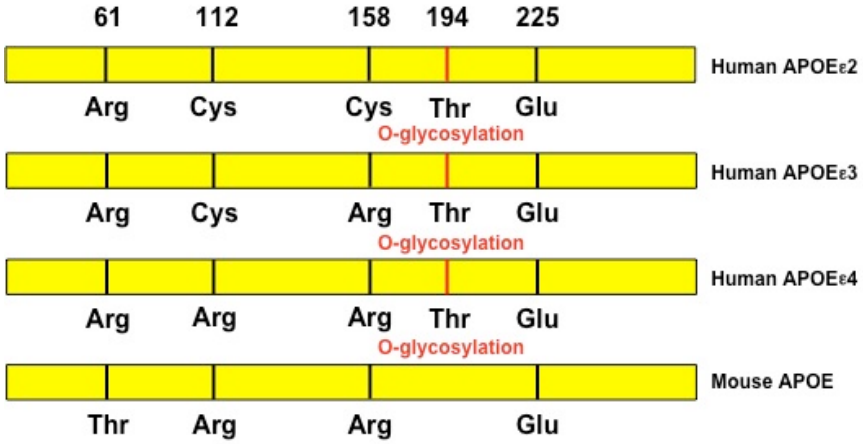

Human APOE is expressed as three isoforms; ε2, ε3 and ε4. These are distinguished by single amino substitutions at residues 112 and 158; APOEε2 has two cysteines (Cys), APOEε3 has a Cys at 112 and an arginine (Arg) at 158 whilst APOEε4 has two Arg. Domain interaction is a unique property of the APOEε4 isoform which occurs between Arg61 and Glu225 and is influenced by Arg112. Mouse APOE is similar to APOEε4 in that it contains an Arg112 however lacks domain interaction due to a threonine (Thr) at position 61. Human apoE is O-glycosylated at residue Thr194 (red), which is not conserved in mouse. This figure is adapted from (Vance and Hayashi, 2010).

Figure 1.5 Structure of lipid-free apoE

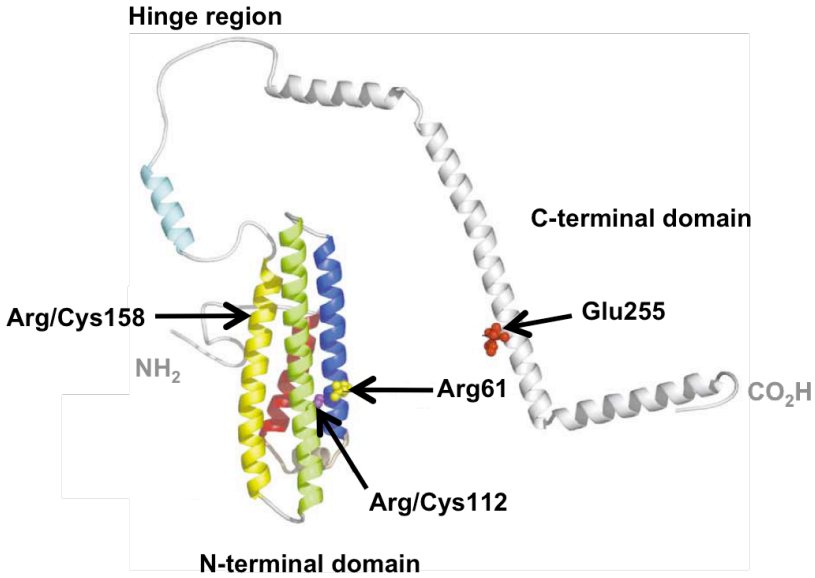

A ribbon diagram of lipid-free apoE. The C- and N-terminal domains are connected by a hinge region. The N-terminal domain consists of a four-helix bundle (helix 1-4 in red, blue, green and yellow, respectively). The receptor binding site is situated in helix 4 of the N-terminal, whilst the C-terminal domain (grey) contains the lipoprotein binding site. Highlighted are positions 112 and 158 that contain either arginine (Arg) or cysteine (Cys) residues in apoE2, apoE3 and apoE4 isoforms. Also highlighted is glutamic acid (Glu) 225 and Arg61 that forms a salt bridge in the apoE4 isoform, allowing domain interaction to occur. This figure is adapted from (Hatters et al., 2006).

In the periphery, most apoE originates from the liver as constituents of lipoprotein complexes, though it is also produced by several other cell types including macrophages, adrenal gland cells, and others. Lipoproteins consist of esterified and unesterified cholesterol, triglycerides and phospholipids which are delivered to cells for use as a source of energy, as building blocks for membrane synthesis and modulation of membrane fluidity. In addition, cholesterol is used as a substrate for the synthesis of a variety of sterols including vitamins, bile acids and steroid hormones. The continuous supply of cholesterol required by the body is acquired by *in vivo* cholesterol biosynthesis via the HMG-CoA pathway, which involves a series of 20 sequential

reactions regulated by the rate limiting enzyme, 3-hydroxy-3-methylglutaryl coenzyme A reductase (HMGCR), and also through diet. ApoE is found to be associated with four main classes of lipoproteins; chylomicrons, very low-density lipoprotein (VLDL), low-density lipoprotein (LDL) and high-density lipoprotein (HDL). The preferences for these lipoproteins lies in the structural difference of the APOE isoforms; apoE2 and apoE3 have preferential binding to small cholesterol-rich high-density lipoproteins such as HDLs whilst apoE4 preferably binds to lower-density lipoproteins such as VLDLs and LDLs (Weisgraber, 1990). ApoE serves as a ligand to the LDL receptor family on cell membranes, for the receptor mediated endocytosis of lipoprotein complexes. The apoE2 isoform has the lowest receptor binding affinity and has important implications in disease, such that elevated circulating levels of apoE2 protein is responsible for type III hyperlipoproteinemia (Weisgraber et al., 1982).

The brain has the second highest concentration of apoE after the liver (Elshourbagy et al., 1985), produced locally by astrocytes (Boyles et al., 1985), although microglia and neurons also synthesise apoE under certain normal physiological and pathological conditions (Bao et al., 1996; Han et al., 1994; Xu et al., 1999; Xu et al., 1996). Newly synthesised apoE assembles with phospholipids and cholesterol to form HDL-like particles. Unlike in plasma, cerebrospinal fluid (CSF) does not contain LDL or VLDL complexes and the assembly of apoE into HDL-like particles occurs without any known apoE isoform specificity (Bandaru et al., 2009; Pitas et al., 1987). Apart from apoE, the predominant lipoprotein within the CNS, other lipoproteins are also present including; apoAI, apoJ (also known as clusterin and also associated with AD) and apoD (Fagan et al., 1999; Pitas et al., 1987). Cholesterol in the brain is acquired by *de novo* synthesis as dietary cholesterol, carried on apoB-containing lipoproteins, is separated from CNS cholesterol by the blood brain barrier (BBB). *De novo* cholesterol synthesis mainly occurs in astrocytes and oligodendrocytes through the HMG-CoA pathway. In neurons, cholesterol synthesis is high in the developing CNS but rapidly declines to low levels in the mature brain (Bjorkhem and Meaney,

2004). Therefore, neurons depend on a supply of cholesterol secreted from astrocytes and glia in the form of HDL-like particles (Funfschilling et al., 2007). Lipidation of the HDL-like particle is assisted by the cholesterol transporter, ATP-binding cassette A1 (ABCA1) which transports cellular cholesterol and phospholipids to lipid-poor apolipoproteins. ApoE on HDL-like particles serves as a ligand for LRP1 and the LDLR, both present on neurons (Narita et al., 1997). Upon binding, the lipoprotein/receptor complex is internalised into endosomes and fuses with lysosomes containing hydrolytic enzymes which release lipids and cholesterol for use in axonal growth, neuronal repair and synapse formation and remodeling (Mauch et al., 2001). The resulting increase in intracellular cholesterol also provides a negative feedback mechanism to HMGCR, reducing endogenous cholesterol synthesis. Cholesterol homeostasis is maintained by converting excess cholesterol into a more hydrophilic oxysterol metabolite, 24S-hydroxycholesterol (24S-OHC) by the neuron specific enzyme 24S-hydroxylase (CYP27A1). 24S-OHC can pass the BBB and directly enters the blood stream for elimination by the liver (Lutjohann et al., 1996). *In vitro*, 24S-OHC released by neurons was shown to upregulate the transcription of APOE, ABCA1 and ABCG1 via a liver X-receptor mechanism to induce apoE-mediated cholesterol efflux (Abildayeva et al., 2006). This reduces cholesterol synthesis, increases cholesterol transport and storage thereby regulating cholesterol homeostasis.

In response to neuronal cell damage or traumatic brain injury, large amounts of apoE are synthesised presumably to clear and redistribute lipid and cholesterol debris to cells requiring membrane repair (Boyles et al., 1989; Ignatius et al., 1987). *In vitro* studies investigating the interaction between lipid and apoE isoforms have shown that apoE3 containing lipoproteins are more efficient at supplying cholesterol to neurons and enhances neurite outgrowth compared to apoE4 containing lipoproteins (Michikawa et al., 2000; Minagawa et al., 2009; Nathan et al., 2002). Furthermore, mice expressing human APOEε3, but not APOEε4, under the neuron-specific enolase (NSE) promoter are protected against excitotoxin-induced neuronal damage and age-

dependent neurodegeneration observed in the APOE knockout mice (Buttini et al., 1999). A number of other studies have focused on apoE isoforms and synaptic plasticity and synaptogenesis. Infusion of recombinant apoE3 and apoE4 into the brain were equally able to rescue presynaptic deficits and cognitive impairment in APOE knockout mice (Masliah et al., 1997). However, other studies found that the apoE4 isoform is less efficient at maintaining normal brain function and as such, APOEε4 mice display synaptic deficits and reduced excitatory synaptic transmission in the absence of Aβ deposition, NFTs or gliosis (Wang et al., 2005). These mice furthermore have impaired LTP and reduced dendritic spine formation (Ji et al., 2003). In support of this, examination of APOEε4 AD post-mortem brain tissue revealed significantly less plastic dendritic changes compared to AD post-mortem brain tissue without an APOEε4 allele (Arendt et al., 1997) thus suggesting poor synaptic remodeling capacity of the apoE4 isoform may contribute to the development of AD.

Attempts to understand the association of apoE isoforms with AD risk have thus focused on the role of lipid metabolism in AD. Disturbances in cholesterol homeostasis can alter the production of Aβ although reports have been controversial. One of the first reports showing a connection cholesterol and amyloid was by Sparks *et al*; rabbits fed a high cholesterol diet increased the accumulation of intracellular Aβ (Sparks et al., 1994). This finding was later replicated in an APPSwe transgenic mouse model (Levin-Allerhand et al., 2002). In cultured cells, proteolysis of APP occurs in cholesterol rich membrane microdomains and *in vitro* studies demonstrated that increasing the cholesterol content in lipid rafts induces β- and γ-secretase activities which led to the elevation of $A\beta_{40}$ and $A\beta_{42}$ species (Frears et al., 1999; Wahrle et al., 2002). Thus apoE might affect AD through a lipid-dependent effect on Aβ production. AD is also characterised by accumulation of tau-containing NFTs, however, a role for cholesterol in tau pathology is not clearly defined. Nevertheless, a recent study reported that increasing cholesterol levels in hippocampal neurons induces Aβ-dependent calpain

activation which generates the neurotoxic 17 kDa tau fragment that becomes hyperphosphorylated, aggregates and forms NFTs (Nicholson and Ferreira, 2009).

Taken together, apoE isoforms seem to have differential effects on the delivery of lipid and cholesterol to neurons and disturbances in this can lead to the formation of plaques and tangles.

1.2.2 ApoE and Aβ pathology

The overproduction of Aβ, leading to excesses of insoluble Aβ peptides, is considered to be one of the primary events leading to disease. Under normal conditions, Aβ is produced at the synapse and intracellularly, and can be found at high levels in CSF or plasma, therefore the balance between Aβ production and clearance may be a possible cause of AD pathology (Hardy and Selkoe, 2002). The discovery that apoE and Aβ form a complex in CSF prompted investigations into the direct involvement of apoE in disease mechanisms (Namba et al., 1991; Wisniewski and Frangione, 1992; Wisniewski et al., 1993). Although the role of apoE remains unclear, there is some evidence suggesting apoE isoform specific effects on Aβ is associated with disease progression.

The interaction between apoE and Aβ may play an important role in AD pathogenesis; it was initially demonstrated *in vitro* that delipidated apoE and lipidated apoE have different binding affinities for Aβ (LaDu et al., 1995). The incubation of delipidated apoE4 with Aβ allowed the rapid formation of Aβ fibrils and Aβ aggregation relative to the other apoE isoforms, in the order of ε4>ε3>ε2 (Sanan et al., 1994; Strittmatter et al., 1993; Wisniewski et al., 1993). In contrast, for lipidated apoE and Aβ fibril formation, the reverse is true, with apoE2 and apoE3 forming complexes with Aβ more rapidly than does apoE4 isoform (in the order of ε2>ε3>ε4) (LaDu et al., 1994; Tokuda et al., 2000). Since the order of binding between apoE and Aβ is inverse to the

risk of developing AD, it has been hypothesised the rate of Aβ clearance is enhanced by apoE2 and apoE3 compared to apoE4 (further discussed below). Neuropathological examination of AD post-mortem brain tissue revealed increased plaque load was associated with APOEε4 (Bales et al., 2009; Fagan et al., 2002; Fryer et al., 2005; Manelli et al., 2007; Manelli et al., 2004). This correlates with both pathological and neuroimaging studies showing APOEε4 carriers have earlier Aβ deposition and greater neuritic plaques (Tiraboschi et al., 2004). Moreover, identification of fibrillar Aβ aggregates using positron emission tomography radioligands (i.e. C11-labelled Pittsburgh compound C) found the highest amounts in cognitively normal APOEε4 carriers in a gene dose dependent manner (Reiman et al., 2009). This occurs with the simultaneous reduction in CSF $A\beta_{42}$ levels, which correlates with the observations from *in vitro* studies and indicates that APOEε4 promotes Aβ deposition in the brain (Fagan et al., 2006; Prince et al., 2004). Due to the rarity of APOEε2 carriers, the effect of APOEε2 isoform on Aβ pathology remains unclear (Berlau et al., 2009). However, in accordance with the above experiments, increased plaque deposition has been observed in APOEε4 transgenic mice expressing APP (Holtzman et al., 2000a). Indeed it has been shown that apoE is required for the formation and deposition of Aβ plaques (Bales et al., 1999; Bales et al., 1997; Holtzman et al., 2000b) and these can occur in an apoE isoform-dependent manner; in the order ε4>ε3>ε2 (Bales et al., 2009; Fagan et al., 2002; Fryer et al., 2005; Manelli et al., 2007; Manelli et al., 2004).

Studies investigating apoE isoforms on Aβ aggregation *in vitro* demonstrated that all three isoforms induced $A\beta_{42}$ fibrillisation or $A\beta_{40}$ aggregation which was enhanced in apoE4 relative to apoE3 or apoE2 (Castano et al., 1995; Ma et al., 1994; Wisniewski et al., 1994). These findings recapitulate those reporting increased amyloid load in APOEε4 subjects. On the other hand, some *in vitro* studies have reported opposite effects, with human isoforms decreasing Aβ fibrillisation (Beffert and Poirier, 1998; Evans et al., 1995; Webster and Rogers, 1996; Wood et al., 1996). These

conflicting findings are most likely due to differences in the apoE and Aβ preparations used.

In addition to their role in fibril formation, accumulating evidence also proposes apoE as an Aβ binding protein that facilitates it's clearance and degradation. Two pathways important for Aβ clearance are receptor mediated uptake by microglia and astrocytes, and receptor mediated transport across the BBB.

In vitro, several studies using various neuronal cell types demonstrated human apoE bind and facilitate the internalisation of soluble Aβ (Beffert et al., 1998, 1999; Cole and Ard, 2000; Yamauchi et al., 2002a; Yamauchi et al., 2000; Yang et al., 1999) and that apoE can faciliate cellular Aβ degradation (Jiang et al., 2008; Koistinaho et al., 2004). However, it is unclear whether these observations are apoE isoform dependent. Consistent with this, APP(V717F) mice lacking apoE have increased soluble Aβ levels prior to Aβ deposition (Dodart et al., 2002; Fagan et al., 2002). These findings apparently contradict *in vivo* studies showing that apoE deficiency reduces Aβ deposition. Nevertheless, Aβ can also be cleared from the brain to the periphery, mediated by the transport of apoE-Aβ complexes across the BBB, involving LRP1 (Deane et al., 2004; Shibata et al., 2000). This occurs in an apoE isoform-dependent manner (Castellano et al., 2011; Deane et al., 2008). Further experiments by Bell *et al* using real-time *in situ* microdialysis demonstrated that $A\beta_{40}$ is cleared more rapidly across the BBB via LRP1 than is $A\beta_{42}$ (Bell et al., 2007). In a similar experiment, Deane *et al* demonstrated that the binding of Aβ to apoE4 reduced the rate of clearance compared to apoE2 and apoE3 through a redirection of clearance from LRP1 to the VLDL receptor (Deane et al., 2008). These authors suggested the reduction in Aβ deposition observed in the apoE null APP mice is likely due to loss of apoE-mediated Aβ retention.

Finally, in other studies, apoE4 can enhance lysosomal leakage and ultimately apoptotic cell death. Treatment of apoE3 or apoE4 Neuro-2a cells treated with $A\beta_{42}$

demonstrate greater lysosomal leakage in apoE4 compared to apoE3 or control. It is hypothesised that the low pH of the lysosome work in concert with the structural interaction between the N- and C-terminal domains of apoE (see above) and $A\beta_{42}$ to cause membrane instability and lysosomal leakage (Ji et al., 2002).

Thus, it is clear that apoE isoforms can have differential effects on Aβ production, aggregation and clearance, which may account for the role of APOE in AD. However, apoE isoforms also play a role in tau pathology.

1.2.3 ApoE and tau pathology

The association between apoE and tau is much less clear. Studies in humans have produced inconsistent findings, whilst some reported a positive relationship between the APOEε4 genotype and NFTs (Ghebremedhin et al., 1998; Nagy et al., 1995; Ohm et al., 1995; Polvikoski et al., 1995), others found no clear association (Itoh et al., 1996; Landen et al., 1996; Morris et al., 1995; Olichney et al., 1996; Oyama et al., 1995). However, evidence from *in vitro* and *in vivo* experiments suggests binding differences between apoE isoforms and tau, independent of Aβ. *In vitro* experiments showed that recombinant tau bound to apoE3 more avidly than to apoE4 isoform (Strittmatter et al., 1994). Furthermore, the interaction between tau and apoE3 was prevented in a crude brain extract of phospho-tau, suggesting apoE3 binds to non-phosphorylated tau. This binding was mediated by interaction between the LDL receptor binding domain on apoE3 and MTB domain of tau and was thought to prevent self-aggregation of tau and therefore the formation of NFTs (Strittmatter et al., 1994).

There is evidence showing apoE is subjected to proteolysis in neurons and the apoE4 isoform appears to be more susceptible to proteolysis than the apoE3 isoform. The cleavage of apoE4 at residues methionine (Met) 272 by a neuron-specific chymotrysin-like serine protease and/or at leucine (Leu) 268 by thrombin cleavage generates neurotoxic C-terminal truncated fragments of 29 kDa and 10-20 kDa,

respectively (Harris et al., 2003). These fragments are toxic both *in vivo* and *in vitro* and weaken the neuronal response to injury (Harris et al., 2003; Huang et al., 2001; Ljungberg et al., 2002). Of the two truncated fragments, the 29 kDa fragment has been the most intensively studied. It can translocate into the cytosol and cause cytoskeletal changes such as formation of NFTs and disruption of mitochondrial processes (Chang et al., 2005). Examination of AD post-mortem brain tissue and the brains of mice expressing apoE in CNS neurons, revealed similar staining of C-terminal truncated fragments, which were furthermore associated with NFTs (Brecht et al., 2004; Harris et al., 2003; Huang et al., 2001). The accumulation of fragments from apoE4 is greater than from apoE3. Interestingly, accumulation of fragments coincides with the appearance of behavioural deficits and neurodegenerative changes in the APOEε4 transgenic mice (Brecht et al., 2004). It is believed that the lipid binding region within the 29 kDa fragment causes neurodegeneration, as neurodegeneration is absent in mice expressing apoE without this region (Harris et al., 2003). These fragments are increased in the post-mortem brain tissue of AD relative to control individuals, however, there are currently no reports showing an increase of these fragments in APOEε4 positive AD patients.

In transgenic mice specifically expressing APOEε3 or APOEε4 in neurons using the NSE promotor, age-dependent impairment in hippocampal dependent learning and memory was found in NSE-APOEε4 mice, but not NSE-APOEε3 mice (Raber et al., 1998). Similarly, APOEε4 knock in (KI) mice developed learning and memory deficits not observed in the APOEε3 KI mice (Bour et al., 2008), whilst APOEε3 mice were protected against excitotoxin-induced neurodegeneration compared to the APOEε4 mice (Buttini et al., 2000). Recently, the cellular origin of apoE in the brain of mice has been shown to effect its action-no effect of genotype on apoE excitoprotection was observed when expressed in astrocytes, whereas apoE4 but not apoE3 was excitotoxic when expressed in neurons (Buttini et al., 2010). Additionally, *in vivo*, mice expression of human APOEε4 in astrocytes did not increase tau phosphorylation whereas

expression of apoE in neurons did, showing a neuron-specific effect (Brecht et al., 2004). Other studies have shown higher levels of tau phosphorylation in APOEε4 KI mice compared to APOEε3 KI mice (Inbar et al., 2010; Kobayashi et al., 2003). Taken together, these studies show apoE isoform specific effects on AD pathology and experimentally confirm epidemiological studies that show that APOEε4 is detrimental in LOAD.

1.3 The metabolic syndrome, type 2 diabetes and AD

As well as the genetic influence on disease risk, such as APOE isoform, environmental factors also alter risk. A growing body of data indicates that the metabolic syndrome, a cluster of risk factors, characterised by impaired glucose tolerance, visceral obesity, hypertension, dyslipidemia, elevated triglycerides, elevated LDL cholesterol and low HDL cholesterol, contributes to the development of AD. The metabolic syndrome not only increases the risk for AD but also the risk of developing diabetes and cardiovascular disease.

Diabetes mellitus (DM) is a chronic metabolic disorder associated with cognitive impairments and damage to the CNS. The two major types of DM are defined as type 1 DM (T1DM) and type 2 DM (T2DM). T1DM (previously known as insulin-dependent diabetes), common in children and young adults, is due to an autoimmune destruction of pancreatic beta cells (β-cells), leading to a deficiency in insulin production. On the other hand, type 2 diabetes Mellitus (T2DM) (previously known as non-insulin-dependent diabetes), which is more prevalent in the elderly, is characterised by hyperinsulinemia and insulin resistance during the early stages of the disorder whilst in the later stages insulin resistance is maintained, glucose intolerance also develops (Gispen and Biessels, 2000; Ramlo-Halsted and Edelman, 1999). Insulin resistance is caused by a reduced response of insulin-responsive tissues to insulin. As a result the reduced glucose lowering effects of insulin lead to an elevation of blood glucose.

Diabetes is a multisystemic disorder associated with pathogenic changes in both large and small vessels, peripheral nerves, skin and eyes. These lead to renal failure, visual loss, autonomic and peripheral neuropathy, peripheral vascular disease, myocardial infarction, as well as cerebrovascular disease (Zhao et al., 2010). Thus, it is not surprising that T2DM also causes vascular dementia. However the connection between diabetes and AD is still not clear.

1.3.1 Type 2 diabetes and AD

The association between T2DM and AD is supported by several epidemiological studies (Biessels et al., 2006) (for systematic review). In 1997, Leibson *et al* reported the risk of AD in type 2 diabetics was elevated (Leibson et al., 1997). Later findings from other longitudinal studies have also confirmed this association of T2DM and AD (Arvanitakis et al., 2004; Cheng et al., 2011; Irie et al., 2008; Leibson et al., 1997; Luchsinger et al., 2004; Ott et al., 1999). On the other hand, there are some large population studies indicating no association between T2DM and AD (Akomolafe et al., 2006; Luchsinger et al., 2001; MacKnight et al., 2002; Xu et al., 2004). Additionally, in an early report of the Honolulu-Asia study, no association of mid-life diabetes and AD were found (Curb et al., 1999). However a follow up study with the same samples showed a high risk of AD in patients diagnosed with T2DM (Peila et al., 2002). This underlines the importance of examining the lifespan of T2DM as this disorder is more prevalent in the elderly and may not be diagnosed in the same patient at a young age. In some of these studies T2DM was associated with an increased risk of vascular dementia (Xu et al., 2004) as well as of AD (Ott et al., 1999; Peila et al., 2002), suggesting these are independent events. In addition, the co-occurrence of T2DM and APOEε4 was found to synergistically increase the risk of AD (Irie et al., 2008; Peila et al., 2002). Neuropathological studies within the same study reported the highest number of neuritic plaques and NFTs in the cortex and hippocampus of APOEε4 type 2 diabetic post-mortem brain tissue (Peila et al., 2002). Another group

also reported greater density of diffuse and neuritic plaques in T2DM post-mortem brain tissue (Janson et al., 2004). However other studies have produced conflicting findings and did not show an increase in AD-related pathology in post-mortem brain tissue of diabetics (Alafuzoff et al., 2009; Arvanitakis et al., 2006a; Heitner and Dickson, 1997).

In T2DM, an elevation in the levels of fasting plasma insulin precede many years before the development of hyperglycaemia. The underlying factor seems to be due to peripheral insulin resistance, which is associated with an increased risk of dementia. Studies have reported that insulin resistance alone, independent of diabetes, increases disease risk as fasting plasma insulin levels were shown to be increased in people with and without diabetes (Kuusisto et al., 1997). Similar results were found in a larger study (Luchsinger et al., 2004). Clinical studies further support these findings in that AD patients have elevations in fasting plasma insulin and reduced CSF insulin levels (Craft et al., 1998) and lower insulin-mediated glucose disposal rates (Craft et al., 1999b) compared to age-matched controls. Furthermore, the aforementioned studies suggest that the risk of insulin resistance in LOAD is independent of APOEε4 genotype.

The reduced levels of CSF insulin may be due to a reduced transport of peripheral insulin into the brain due to chronic hyperinsulinemia (Wallum et al., 1987), which strongly suggests defects of insulin action in the brain. At autopsy, post-mortem brain tissue from AD patients have reduced expression of insulin and insulin receptors (Steen et al., 2005). Additionally, downstream insulin signalling is reduced in AD brains. The ineffective insulin signalling within the brain might therefore initiate neurodegenerative processes leading to cognition dysfunction. The realisation that low insulin, insulin receptor levels and reduced glucose homeostasis confined to the AD brain has led this insulin resistant brain state to be classified as ‘Type 3 diabetes’.

1.3.2 Insulin and memory

It was once thought that the brain was insulin insensitive. However this theory was challenged by the identification of insulin and insulin receptors in the brain. Insulin mRNA has been detected in neurons (Devaskar et al., 1994; Schechter et al., 1988) and also in the rat hippocampus (Singh et al., 1997). In addition, insulin receptors are widely distributed in the CNS with the highest concentrations in olfactory bulb, hippocampus, amygdala, hypothalamus, cortex and cerebellum (Havrankova et al., 1978; Marks et al., 1990; Werther et al., 1987). At the cellular level, insulin receptors are enriched in neurons compared to glia and are concentrated at synapses (Abbott et al., 1999). This indicates that insulin plays a important role in enhancement of memory functions (for review see) (Park, 2001). However, it has now been shown that little or no insulin synthesis occurs in the brain (Woods et al., 2003) and the major source of brain insulin is believed to originate from the pancreas. Insulin from the periphery enters the brain via a receptor-mediated saturable transport mechanism across the BBB (Banks et al., 1997) to increase CSF insulin levels (Baura et al., 1993). The binding of insulin to insulin receptors mediates diverse functions such as energy and glucose homeostasis (Air et al., 2002; Pocai et al., 2005), growth (Rulifson et al., 2002) and neuronal plasticity (Chiu and Cline, 2010). The role of insulin in memory has been highlighted by the following studies.

Peripheral administration of insulin in patients with AD in euglycaemic conditions increased CNS insulin levels and led to the improvement in memory and performance (Craft et al., 1996; Kern et al., 2001). Moreover, intranasal administration of insulin, which results in the direct transport of insulin from the nasal cavity to the CNS, induces facilitation of working memory in humans (Benedict et al., 2004). Similarly, intranasal insulin treatment improved cognitive performance in rodents (Francis et al., 2008). Additionally, intracerebroventricular insulin administration in rodents raises CNS insulin levels (Bernstein et al., 1986), upregulates insulin receptors

on hippocampal neurons (Zhao et al., 1999) and acutely improves memory performance on a passive avoidance task (Park et al., 2000).

Insulin may affect memory through several mechanisms. Although insulin does not seem to play a role in the transport of glucose into the brain or participate in basal cerebral glucose metabolism, evidence indicates insulin may mediate glucose uptake in selective regions of the brain such as the hippocampus and hypothalamus. This may be due to the overlapping distributions of insulin, insulin receptors with insulin sensitive glucose transporters; GLUT4 (cerebellum, hippocampus, pituitary and hypothalamus) and GLUT8 (hippocampus and hypothalamus). By contrast, glucose independent mechanisms also exist, for example, Craft *et a*l demonstrated that memory in AD patients did not improve when plasma glucose levels were increased whilst insulin secretion was suppressed using somatostatin (Craft et al., 1999a). Furthermore, intravenous insulin infusion in patients with AD under euglycaemic conditions led to improvement in memory and performance (Craft et al., 1996).

Insulin also modulates the release and re-uptake of presynaptic neurotransmitters such as acetylcholine and norepinephrine, which influence cognitive function (Figlewicz et al., 1993; Kopf and Baratti, 1999). Insulin can also modulate synaptic plasticity, the formation of synaptic connections underlying learning and memory. Insulin has been shown to increase the expression of GABA (gamma aminobutyric acid) receptors on postsynaptic membranes and dendrites to modulate synaptic plasticity (Wan et al., 1997). Similarly, insulin promotes the internalisation of AMPA (alpha-amino-3-hydroxy-5-methyl-4-isoxazole-propionate) receptors from the postsynaptic membrane to cause depression of excitatory synaptic transmission in the hippocampus (Man et al., 2000) and cerebellum (Huang et al., 2003). Additionally, insulin can enhance NMDA (N-Methyl-D-aspartate) receptor mediated synaptic transmission in hippocampal slices (Liu et al., 1995) by transiently modulating the phosphorylation of NR2A and NR2B subunits (Christie et al., 1999). Activation of the NMDA receptor increases Ca^{2+} influx, which is presumed to activate CAMKII and other

Ca^{2+}-dependent enzymes leading to greater synaptic strength between neurons. These alterations in the expression and function of NMDA receptors has been implicated in the behavioural and electrophysiological abnormalities observed in insulin-deficient rats (Di Luca et al., 1999). Whilst in rat hippocampal slices insulin signalling was shown to mediate the induction of long-term depression (LTD) at the CA1 synapses in an activity, frequency, PI3K/Akt and NMDA receptor-dependent manner (van der Heide et al., 2005). Insulin appears to shift the NMDA receptor-dependent frequency response curve of activity-dependent synaptic plasticity, enabling the induction of both LTD and LTP at lower frequencies. Van der Heide *et al* suggested insulin may function as a neuromodulator of activity-dependent synaptic plasticity, setting the threshold for NMDA receptor-dependent LTD and LTP induction.

1.3.3 Insulin signalling and AD pathology

1.3.3.1 The insulin signalling pathway

The insulin receptor is a homodimer, composed of four subunits, two extracellular α subunits and two transmembrane β subunits held together by disulphide bonds. Each insulin receptor monomer originates from a single precursor protein which is cleaved to generate an extracellular α subunit and an intracellular β subunit linked together by intrinsic disulphide bonds. A insulin receptor monomer dimerises with another monomer to generate a functional receptor. The insulin signalling pathway is shown in Figure 1.6. Upon binding of insulin to the α subunits, the β subunits undergo conformational change resulting in autophosphorylation on a number of tyrosine residues (Van Obberghen et al., 2001). Insulin receptors then phosphorylate adaptor proteins containing phosphotyrosine-binding domains such as the insulin receptor substrate (IRS) family members, IRS1 and IRS2. Following this, the p85 regulatory subunit of phosphoinositide 3-kinase (PI3K) containing the Src homology 2 domain binds to tyrosine residues on IRS1 and leads to activation of the p110 catalytic subunit

of PI3K. Subsequently, p110 converts membrane lipids phosphatidylinositol 4,5-bisphosphate (PIP_2) to phosphatidylinositol 3,4,5-triphosphate (PIP_3). PIP_3 in turn activates phosphate dependent kinase-1 (PDK-1), which in combination with an as yet unidentified kinase, upregulates Akt (also known as PKB). Akt then phosphorylates Ser9 and Ser21 on the GSK-3α and β isoforms respectively, leading to their inactivation (Lizcano and Alessi, 2002; Saltiel and Kahn, 2001) (for review). Since GSK-3 is implicated in APP metabolism and tau phosphorylation, defects within the insulin signalling pathway are widely thought to impact upon AD pathology. GSK-3 also regulates the activity of glycogen synthase, an enzyme that catalyses the conversion of glucose into glycogen. The activity of glycogen synthase is inhibited when phosphorylated therefore activation of the PI3K pathway leading to the inactivation of GSK-3 promotes the storage of glucose as glycogen. In addition, insulin has a key role stimulating glucose uptake into cells to maintain peripheral blood glucose levels. On binding to insulin receptors, vesicles containing glucose transporters, GLUT4, translocate from the cytosol and fuses with the plasma membrane. GLUT4 are subsequently inserted into the membrane which permits the diffusion of glucose into the cell for glycolytic processes or stored as glycogen (Figure 1.6).

Figure 1.6 The insulin signalling pathway

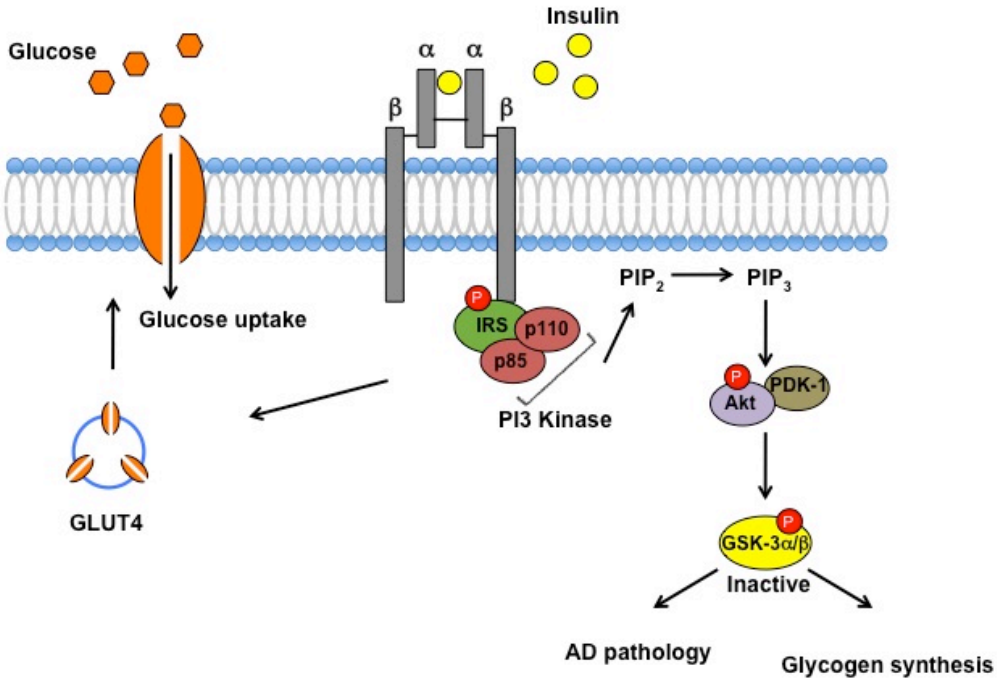

The insulin receptor is composed of two α and two β subunits tethered together by disulphide bonds. Binding of insulin induces autophosphorylation of the insulin receptor at a number of tyrosine residues which are recognised by the insulin receptor substrate (IRS) adaptor proteins. Phosphorylation of IRS leads to the binding of the p85 subunit of phosphoinositide 3-kinase (PI3K) which activates the p110 catalytic subunit of PI3K. p110 then converts membrane lipids phosphatidylinositol 4,5-bisphosphate (PIP_2) to phosphatidylinositol 3,4,5-triphosphate (PIP_3). The subsequent activation of phosphate dependent kinase-1 (PDK-1) and Akt leads to the phosphorylation of GSK-3 which becomes inactive. GSK-3 is involved in glycogen synthesis and can influence pathological processes related to AD. Activation of the insulin signalling pathway also stimulates glucose uptake in the cell by promoting GLUT4 translocation. This figure is adapted from (Saltiel and Kahn, 2001).

1.3.3.2 Insulin and Aβ pathology

APP metabolism is regulated by a variety of mechanisms, one of these is by insulin. Insulin has been shown to accelerate the trafficking of $A\beta_{40}$ and $A\beta_{42}$ peptides from the trans golgi network to the plasma membrane in neuronal cultures thereby increasing its secretion (Gasparini et al., 2001). This process was mediated by the Erk1/2 signalling pathway, suggesting reduced insulin levels can interfere with the trafficking of Aβ peptides and possibly leading to Aβ accumulation. In the SHSY-5Y cell line, insulin enhanced and shifted APP metabolism towards the non-amyloidogenic pathway, promoting α-secretase cleavage of APP (Solano et al., 2000). Conversely, GSK-3α has been shown to influence the production of Aβ peptides by regulating γ-secretase activity, with the inhibition of GSK-3α by lithium blocking the generation of $A\beta_{40}$ and $A\beta_{42}$ peptides (Phiel et al., 2003). Aβ has also been shown to act as a competitive inhibitor of insulin, competing with insulin for binding to the insulin receptor. This can reduce insulin receptor phosphorylation and thereby antagonise the downstream insulin signalling effects (Xie et al., 2002). Furthermore, Aβ can be degraded by two major proteases, neprilysin (NEP) and insulin degrading enzyme (IDE) (Ling et al., 2003). Both are metalloproteases involved in the degradation of proteins that form β-pleated sheet-rich amyloid fibrils. In APP transgenic mice, the overexpression of NEP or IDE reduced Aβ levels and prevented the formation of Aβ plaques (Iwata et al., 2000; Leissring et al., 2003; Poirier et al., 2006). It was also demonstrated that gene transfer of NEP by viral vector delivery could lower Aβ levels in the brain of NEP deficient and APP transgenic mice (Iwata et al., 2004). Similarly, this was shown to reduce Aβ deposition in APP transgenic mice (Marr et al., 2003). Conversely, the disruption or knockout of NEP (Farris et al., 2007; Huang et al., 2006; Iwata et al., 2001) or IDE (Farris et al., 2003; Miller et al., 2003) genes induces the accumulation of Aβ in the brain. The distinct subcellular distribution of NEP and IDE allows the degradation of Aβ at different subcellular compartments. NEP is a plasma membrane bound enzyme that is able to degrade monomeric and oligomeric forms of

$A\beta_{40}$ and $A\beta_{42}$ (Kanemitsu et al., 2003), both intracellullarly and extracellularly (Hama et al., 2004). In contrast, IDE is a cytosolic enzyme, exists as a mixture of dimers and tetramers (Authier et al., 1996; Duckworth et al., 1998) and degrades intracellular as well as extracellular Aβ (Sudoh et al., 2002). IDE is found in endosomes, at the cell surface and in the extracellular milieu (Qiu et al., 1998; Seta and Roth, 1997; Vekrellis et al., 2000). The secreted or cell surface associated form of CNS IDE is the dependent on cell type. In primary mouse microglia and the BV2 cell line, IDE was found to be secreted whilst in primary hippocampal neurons and differentiated PC12 cells, IDE was found to be membrane associated only (Mentlein et al., 1998; Qiu et al., 1998; Vekrellis et al., 2000). Insulin and Aβ are amongst the main substrates of IDE that compete for degradation (Qiu et al., 1998). *In vitro*, IDE degrades and clears soluble monomeric Aβ secreted by microglial and neurons (Qiu et al., 1998; Sudoh et al., 2002; Vekrellis et al., 2000). IDE also degrades intracellular Aβ and facilitates the degradation of AICD (Edbauer et al., 2002). In mice, insulin resistance induced by diet (Ho et al., 2004) or sweetened water (Luo et al., 2011) reduced the levels of IDE, and promoted the generation of Aβ, consistent with an increase in γ-secretase activity.

In AD, the activity of IDE is reduced and histopathological examination of the hippocampus in post-mortem AD brains revealed reduction in IDE expression compared to age-matched controls. Interestingly, this observation was detected in APOEε4 carriers only and patients homozygous for APOEε4 allele had the highest IDE reductions (Cook et al., 2003). Consistent with this, the apoE4 isoform reduced expression of IDE by activating NMDR receptors in hippocampal neurons (Du et al., 2009). At present the cause of this is unknown. However, studies using IDE knockout mice found increased accumulation of cerebral Aβ levels and a decrease in clearance of Aβ was observed in primary cortical neuronal cultures from the same mice (Farris et al., 2003). Taken together, these findings suggest IDE has a critical *in vivo* role in determining the amount of Aβ in the brain. Genetic studies support this association

between IDE and AD, as IDE is located on chromosome 10, close to the AD locus (Bertram et al., 2000).

1.3.3.3 Insulin and tau pathology

The insulin signalling pathway regulates the downstream activity of GSK-3, a major tau kinase, important in the formation of NFTs. A limited number of studies have shown direct effects of insulin on specific epitopes of tau phosphorylation. *In vitro*, insulin and insulin-like growth factor 1 (IGF1) treatment can downregulate GSK-3β activity, thereby reducing tau phosphorylation (Ser202/Thr205) and promoting the binding of tau to microtubules in human neuroblastoma cells (Hong and Lee, 1997). Following this, another study by Lesort *et al* demonstrated that insulin can transiently increase, then decrease tau phosphorylation at a range of epitopes including Ser202, Thr205, Ser396 and Ser404 in a neuronal cell line. This also corresponded to the sequential activation and deactivation of GSK-3β which was itself associated with the activity of Fyn kinase (Lesort et al., 1999), that was able to regulate GSK-3 activity by targeting the Tyr216 and Tyr279 site in GSK-3β and GSK-3α, respectively. A subsequent study confirmed these observations by showing the inhibition of GSK-3 activity by lithium treatment in primary cortical neurons prevented changes in tau phosphorylation (Ser202/Thr205) (Lesort and Johnson, 2000). It was also shown that transient changes in tau phosphorylation correlated with the transient interaction of tau with microtubules in these neuronal cultures (Lesort and Johnson, 2000). *In vivo*, peripheral injection of insulin induced hyperphosphorylation of various tau epitopes including Ser199, Ser202, Thr205, Thr212, Thr214, Thr231, Ser262, Ser396, Ser404 and Ser422 (Planel et al., 2004). The activity of GSK-3β was inhibited in this study however, JNK activity was increased whilst the activity of PP2A decreased (Planel et al., 2004). Similarly, another *in vivo* study demonstrated that peripheral insulin injection led to an increase in tau phosphorylation at the Ser202 epitope with inhibition of GSK-

3β activity however, the activity of Erk1/2 was increased (Freude et al., 2005). Collectively, these studies suggest insulin can promote changes in the phosphorylation of specific tau epitopes. However, it remains unclear exactly which kinases or phosphatases are specifically linked to the regulation of each phospho-epitope in tau.

In vivo studies have also demonstrated disruption in the insulin signalling pathway contributes to the hyperphosphorylation of tau. Thus, IGF1 knockout (Cheng et al., 2005), neuronal insulin receptor knockout (NIRKO) (Schubert et al., 2004) and IRS2 knockout (Killick et al., 2009; Schubert et al., 2003) mice all promote hyperphosphorylation of tau. Further studies using streptozotocin, a chemical toxic to pancreatic β-cells, to deplete peripheral circulating insulin levels in mice also caused increased tau phosphorylation in the brain (Clodfelder-Miller et al., 2006; Grunblatt et al., 2007; Planel et al., 2007; Qu et al., 2011). Interestingly, insulin (Jolivalt et al., 2008) or lithium (Qu et al., 2011) treatment in insulin deficient mouse models reversed tau pathology.

1.3.3.4 Regulation of tau kinases

GSK-3

As GSK-3 is central to numerous cell signalling processes and cellular functions, it is important that its activity is tightly regulated. One mechanism of regulation is by phospho-modifications at specific residues, which act to either inhibit or activate GSK-3. The effect of the insulin signalling pathway (described above) upon GSK-3 has been one of the most extensively studied. Within this pathway the phosphorylation of Ser21 and Ser9 for GSK-3α and GSK-3β respectively by Akt inhibits GSK-3 activity (Cross et al., 1995). This induces the formation of pseudo-substrate-like structures within the GSK-3 proteins which occupy its kinase domain and block their activities towards true substrates (Doble and Woodgett, 2003; Frame and Cohen, 2001). On the other hand, GSK-3 is a constitutively active kinase which is dependent

upon the phosphorylation of Tyr279 and Try216 in GSK-3α and GSK-3β respectively (Hughes et al., 1993). The basal activity has been shown to increase following nerve growth factor withdrawal (Bhat et al., 2000), whilst insulin treatment led to a transient increase in Tyr216 phosphorylation by the Src tyrosine kinase, Fyn (Lesort et al., 1999). Phosphorylation of Tyr279 and Try216 residues has also been proposed as an autophosphorylation event (Cole et al., 2004).

GSK-3 is also regulated by the wnt signalling pathway, in this instance by altering its cellular localisation. In the absence of a wnt signal, GSK-3 exists in a multiprotein complex consisting of β-catenin, axin, adenomatous polyposis coli (APC) and casein kinase 1 (CK1). In this complex, GSK-3 constitutively phosphorylates β-catenin, promoting its ubiquitination and proteosomal degradation. On binding of wnt to the frizzled (FZD) receptors, LRP5/6 is phosphorylated and activates dishevelled (Dvl). Dvl separates GSK-3 and β-catenin, thereby inhibits the proteolytic degradation of β-catenin and allows the entry of β-catenin into the nucleus to interact with members of the Tcf/Lef family of transcription factors (Chien et al., 2009). The mechanism by which wnt inhibits GSK-3 has not yet been fully resolved, two models have been proposed; a) axin may associate with GSK-3 and are then recruited together to the plasma membrane by the interaction between FZD, Dvl and axin. The phosphorylation motif on the cytoplasmic tail of LRP6, which binds to FZD, then acts as a pseudo-substrate for GSK-3, thus preventing GSK-3 targeting β-catenin (Cselenyi et al., 2008; Mi et al., 2006; Piao et al., 2008; Wu et al., 2009; Zeng et al., 2008), b) a more recent view is that wnt proteins induce compartmentalisation of GSK-3 into multivesicular bodies, further increasing the separation of GSK-3 from β-catenin (Taelman et al., 2010).

In addition to physical separation, negative regulation by phosphorylation also plays a role in wnt signalling. PKC directly inhibits GSK-3 activity and activates wnt signalling (Chen et al., 2000; Cook et al., 1996). P38 MAPK also participates in wnt signalling (Bikkavilli and Malbon, 2009). The PI3K/Akt pathway has been implicated in wnt signalling or stabilisation of β-catenin (Ponce et al., 2011; Voskas et al., 2010)

however, whether crosstalk exist between the two pathways again has not been fully resolved (Ng et al., 2009).

Cdk5

The activity of Cdk5 is regulated by p25, a truncated form of the neuron-specific activator, p35. The association of p25 with Cdk5 induces the hyperphosphorylation of tau (Lee et al., 2000). In rodent models, the overexpression of p25 leads to tau hyperphosphorylation and neurodegeneration (Cruz et al., 2003; Noble et al., 2003), which was also observed in Drosophila (Steinhilb et al., 2007). *In vitro*, the overexpression of p25/Cdk5 complex causes tau phosphorylation and impaired axonal transport of neurofilaments as shown by time-lapse imaging technology. The treatment of Neuro-2a cells with a Cdk5 inhibitor, roscovitine, reversed this defect in axonal transport (Zhou et al., 2010). In cells expressing p35, treatment with (Town et al., 2002) or without (Hashiguchi et al., 2002) $A\beta_{42}$ also increased phosphorylation of tau. Specifically, $A\beta_{25-35}$ treatment of SHSY-5Y cells caused tau phosphorylation at lipid rafts (Hernandez et al., 2009). Recently, Zheng *et al* identified a 24 residue peptide, p5, derived from p35 (Zheng et al., 2010). P5 inhibited p25/Cdk5 activity and reduced $A\beta_{42}$-induced tau phosphorylation and apoptosis in cortical neuronal cultures, therefore suggesting a possible therapeutic for AD. In HFD-induced obese mice, Cdk5 activation in adipose tissues induced the phosphorylation of PPARγ, a nuclear receptor involved in the regulation of adipogenesis fat cell gene expression. Phosphorylation of PPARγ led to the dysregulation of obesity-related genes which was reversed by the action of anti-diabetic ligands (rosiglitazone and MRL24). This evidence suggests that post-translational modification of PPARγ by Cdk5 may contribute to insulin resistance (Choi et al., 2010; Choi et al., 2011).

PP2A

PP2A is a major tau phosphatase (Goedert et al., 1995). It is a holoenzyme composed of a structural A subunit, catalytic C subunit, forming the core enzyme, and a regulatory B subunit that determines substrate specificity (Janssens and Goris, 2001; Lechward et al., 2001). The association of A and C subunits with one of a series of B subunits produces several species of holoenzymes with distinct functions. The activity of PP2A is regulated by post-translational modifications of the C subunit. The C-terminal sequence of the C subunit is highly conserved between species, containing two phosphorylation sites at Thr304 and Tyr307 and a methylation site at Leu309. Thr304 is subjected to phosphorylation by an autophosphorylation-activated protein kinase (Guo and Damuni, 1993), whilst Tyr307 is phosphorylated by $p60^{v\text{-}src}$, $p56^{lck}$, epidermal growth factor receptors, and insulin receptors (Chen et al., 1992). Phosphorylation at both sites consequently results in the inhibition of PP2A. Leu309 can be reversibly methylated by the PP2A methyltransferase and PP2A methlyesterase (Lee and Stock, 1993). Methylation promotes the assembly of the PP2A holoenzyme and facilitates the association of B subunits (Tolstykh et al., 2000; Wu et al., 2000). The C subunit of PP2A also interacts with endogenous inhibitor proteins, I_1^{PP2A} and I_2^{PP2A}, both of which have been found in human post-mortem brain tissue and were shown to specifically block phosphatase activity of PP2A towards tau phosphorylation (Tanimukai et al., 2005; Tsujio et al., 2005). In rat brain slices, inhibition of PP2A activity by okadaic acid increased phosphorylation and the accumulation of neurofilaments, as shown by western blotting and immunohistochemistry techniques (Gong et al., 2003). Additionally, inhibition of PP2A activity *in vivo* by the injection of calyculin A into the rat hippocampus also increased tau phosphorylation and caused spatial memory retention in the Morris water maze test (Sun et al., 2003). More recently, in an AD mouse model (Tg2576) crossed with IRS2 knockout mice, an increase in tau phosphorylation was shown to correlate with reduced PP2A activity (Killick et al., 2009).

1.4 The peroxisome proliferator-activated receptors (PPARs)

The peroxisome proliferator-activated receptors (PPARs) belong to the NR1C class of the nuclear hormone receptor superfamily of ligand-activated transcription factors and are expressed in a wide variety of cell types. The three PPAR isoforms; PPARα, PPARβ/δ and PPARγ participate in the regulation of metabolism, proliferation, differentiation, apoptosis and the immune response specific to the tissues in which they are expressed. The PPARs are organised into four functional domains (Figure 1.7); the N-terminal A/B domain has a ligand-independent transcriptional activating function; the DNA binding domain is responsible for attaching specific peroxisome proliferator response elements (PPREs) on the promoter of PPAR target genes; the hinge region interacts with co-repressors and co-activators; the C-terminal ligand binding region is involved in the dimerisation of PPARγ and retinoid X receptors (RXR) or other ligands and provides ligand-dependent transactivation function (AF-2) to the receptor (Luconi et al., 2010). PPARγ was originally identified in Xenopus by homology cloning (Dreyer et al., 1992) and then subsequently in mice (Zhu et al., 1993). The PPARγ gene produces two splice variants that generates two proteins, PPARγ1, and PPARγ2 which has an additional 28 amino acids within the A/B domain at the N-terminus. PPARγ1 is ubiquitously expressed, whilst PPARγ2 is adipose-specific (Berger and Moller, 2002). The post-translational modification of PPARγ can modulate its transcriptional activity, for example the phosphorylation site Ser82 in PPARγ1 or Ser112 in PPARγ2 (in mouse) have been described as targets of members of the MAPK family (Erk1/2, JNK, p38 MAPK). In mice, phosphorylation of Ser112 by Erk1/2 decreases the biological actions of the receptor and inhibits fat cell differentiation (Hu et al., 1996a).

Figure 1.7 Schematic representation of the domain structures in human PPAR isoforms

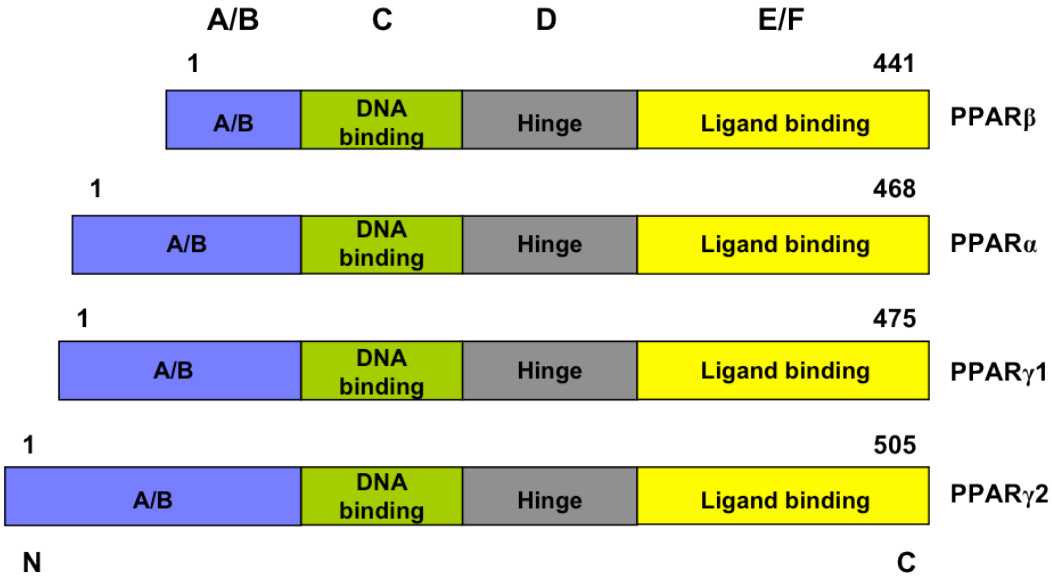

The PPARs are formed of four functional domains; A/B, C, D and E/F. The N-terminal A/B domain contains a ligand-independent transactivation function known as AF-1 and also contains a site for mitogen-activated protein kinase phosphorylation (Adams et al., 1997). The central region consists of a highly conserved DNA binding domain (C) that contains two zinc fingers responsible for binding of PPREs within the promoter region of specific target genes and a hinge region (D) that interacts with co-repressors and co-activators to modulate DNA binding affinity. The C-terminal ligand binding domain (E/F) dimerises with ligands such as the retinoid X receptors (RXR) and provides ligand-dependent transactivation function (AF-2) to the receptor. This figure is adapted from (Rosen and Spiegelman, 2001).

To date, a specific natural ligand for PPARγ has not been reported. Some of their endogenous ligands include various unsaturated fatty acids, prostaglandins (15ΔPGJ2), eicosanoids and oxidized low-density lipoprotein species, (Straus and Glass, 2007) (for review).

The action of PPARγ effects adipose differentiation, lipid storage and inflammation. Their mechanism of action can be divided into two parts; genomic effects and non-genomic effects. The genomic effects involve lipid regulation, glucose homeostasis, anti-inflammation and anti-cancer actions whilst non-genomic effects modulate intracellular second messengers. In the genomic effects, ligand bound PPARγ forms heterodimers with RXR, allowing high affinity binding to DNA (Kliewer et al., 1992). This displaces co-repressors and recruits transcriptional co-activators which together bind to sequence-specific PPRE present in the promoter region of target genes to initiate transcription (Tugwood et al., 1992). Non-genomic effects involve the extranuclear interaction of PPARγ with second messengers leading to rapid changes in signalling, such as Erk1/2 (Hu et al., 1996a) and MEK-1 (Burgermeister et al., 2007). This mechanism excludes the PPARγ interaction with DNA and offers a regulatory role for PPARγ activity. However, since PPARγ has no nuclear export signal sequence, trafficking from the nucleus to the cytosol must involve shuttle proteins, MEK-1 has been demonstrated to be one of these (Burgermeister et al., 2007).

The thiazolidinediones (TZDs), PPARγ agonists were initially discovered because of their insulin sensitising action in rodents which was consequently confirmed in humans and were identified as potential treatments for T2DM patients (Nolan et al., 1994). An interaction between TZD and PPARγ was first discovered by Harris and Kletzien reporting that pioglitazone increased transcriptional activation of ARF6DNA-binding complex on the fat selective adipocyte P2 (aP2) promoter (Harris and Kletzien, 1994). ARF6 was subsequently identified as the PPARγ/RXR heterdimer (Tontonoz et al., 1994) and it was later shown that TZDs are direct agonists for PPARγ (Lehmann et al., 1995). In humans, mutations in PPARγ are associated with insulin resistance (Agostini et al., 2006; Barroso et al., 1999), further supporting the evidence that TZDs act through binding to PPARγ to improve insulin sensitivity.

1.4.1 PPARγ and insulin resistance

PPARγ agonists such as the TZDs, are insulin sensitisers that improve the action of insulin and reduce blood glucose levels. Their site of therapeutic action was proven to be adipose tissue as mice with the deletion of adipose tissue specific PPARγ are deficient in their response to TZD treatment (He et al., 2003). The action of PPARγ agonists was shown to cause *de novo* differentiation of large adipocytes into smaller insulin-sensitive adipocytes (Okuno et al., 1998) and it is thought that PPAR activation in adipose tissue alters the secretion of adipokines, bioactive molecules that enters the circulation and affects whole-body insulin sensitivity. Adiponectin is a adipokine present in plasma which is inversely correlated to adipose tissue mass and directly correlated to insulin sensitivity (Hu et al., 1996b). In support of this, the administration of TZDs in rodents and humans was found to increase adiponectin expression and consequently plasma adiponectin levels were increased (Pajvani et al., 2004; Yu et al., 2002). Furthermore, mice lacking adiponectin have impaired response to TZDs (Nawrocki et al., 2006). PPARγ activation of adipocytes also decreases the production of tumor necrosis factor (TNF)α and resistin. Both TNFα and resistin are postulated to cause insulin resistance (Hotamisligil et al., 1993; Steppan et al., 2001), as knockout mouse models of TNFα or resistin improves insulin sensitivity (Banerjee et al., 2004; Uysal et al., 1997).

The insulin sensitising actions of TZDs, discussed above, was the basis that led to investigating their potential use as treatments for AD.

1.4.2 PPARγ agonists and AD

The TZD rosiglitazone was the first PPARγ agonist to be used in clinical trials with AD patients. Watson and colleagues performed a 6 month preliminary clinical trial using rosiglitazone in a subset of patients suffering from early stage AD which demonstrated to improve cognitive function (Watson et al., 2005). Following this,

Risner and colleagues conducted a larger rosiglitazone trial showing improvements in response to drug treatment in APOEε2/ε3 carriers whilst no improvement was found in APOEε4 carriers (Risner et al., 2006). *In vivo*, the administration of rosiglitazone in animal models of AD also attenuated learning and memory deficits (Pedersen et al., 2006). The APOE genotype specific effect may be due to the fact that APOEε4 negative patients are more likely to be insulin resistant (Craft et al., 1999b) and improving insulin sensitivity may result in an increased insulin uptake into the brain (Craft et al., 2003). However, it is also thought that rosiglitazone may have direct effects in the CNS by stimulating neuronal mitochondrial biogenesis thus enhancing glucose utilisation (Strum et al., 2007). Furthermore, as greater mitochondrial dysfunction has been detected in AD APOEε4 carriers (Gibson et al., 2000), it has been proposed that excessive mitochondrial damage may mean that APOEε4 AD patients could not obtain maximum benefit from the rosiglitazone drug treatment. Despite the above, a recent phase III clinical trial of rosiglitazone treatment in patients with early stage AD, did not support these findings and reported no beneficial effect of rosiglitazone treatment on cognitive function (Gold et al., 2010).

A potential explanation for the limited efficiency of rosiglitazone is the poor permeability through the BBB. It was initially thought that rosiglitazone was BBB impermeable (Pedersen et al., 2006; Watson et al., 2005), but a recent study by Strum *et al* has shown its presence in the brain after oral administration (Strum et al., 2007). An alternative TZD, pioglitazone, is thought to have higher permeability through the BBB compared to rosiglitazone. Although rosiglitazone is more potent in activity compared to pioglitazone; rosiglitazone has EC_{50} values of 0.043 μM and 0.076 μM, for the human and murine PPARγ receptors respectively, whilst pioglitazone has EC_{50} values of 0.58 μM and 0.55 μM, for the human and murine PPARγ receptors respectively (Willson et al., 2000). Recently, Geldmacher *et al* performed a pilot study on the safety of pioglitazone treatment in patients with mild to moderate AD and reported the drug was well tolerated and awaiting future clinical trials (Geldmacher et

al., 2011). Additionally, a 6 month clinical trial was conducted in a group of mild AD patients accompanied by T2DM. Pioglitazone treatment demonstrated improved cognitive function and enhanced insulin sensitivity in the diabetic AD patients, suggesting pioglitazone may offer a novel strategy for the treatment of AD (Sato et al., 2011). *In vivo*, the use of pioglitazone by two independent studies produced conflicting results; Yan *et al* found treatment in Tg2576 mice reduced soluble Aβ levels but had no effects on the accumulation of Aβ or inflammatory markers (Yan et al., 2003). A following study by Heneka *et al* using a larger dose of the drug in APP(V717I) mice found a reduction in accumulation of Aβ, reduction in $A\beta_{42}$ levels and reduced levels of inflammatory markers (Heneka et al., 2005). The authors of the first study claim their results were due to poor penetration of pioglitazone through the BBB. PPARγ activation has also been shown to reduce the phosphorylation of tau in neurons *in vitro* (d'Abramo et al., 2006).

All of the above suggests PPARγ agonists may offer therapeutic benefit for the treatment of AD. However, the mechanism(s) by which thiazolidinediones act upon PPARγ still remains unclear. A better understanding of their action upon pathways and proteins implicated in AD pathology would help determine how they affect AD-like pathological symptoms and help vindicate their use for the amelioration of AD.

1.5 Animal models of AD and impaired insulin signalling

That there may be a relationship between insulin resistance, as a consequence of T2DM, and AD is further supported by evidence from animal models. Insulin resistance occurs by a reduced reponse of insulin-responsive tissues to circulating insulin. Diabetes-like symptoms can be induced experimentally by a range of techniques and provide insights to the underlying mechanisms which may contribute to pathology. This approach may help identify targets for the development of future therapeutic intervention.

1.5.1 Streptozotocin models

The streptozotocin (STZ) approach is the most commonly used technique to model insulin deficiency in AD. STZ is a nitrosurea derivative isolated from *Streptomyces achromogenes*, an alkaylating substance, which is toxic to pancreatic β-cells; STZ enters β-cells via GLUT2 and alkaylates DNA, inducing DNA damage (Szkudelski, 2001). Systemic STZ injection therefore results in the development of insulin deficiency and glucose intolerance by the destruction of β-cells as the production of insulin is halted. The reduced levels of circulating insulin have an impact on brain insulin signalling since the major source of brain insulin is from the periphery. STZ administration has been shown to cause an increase in tau phosphorylation at a number of epitopes in the cortex and hippocampus of C57BL/6 mice (Clodfelder-Miller et al., 2006; Kim et al., 2009a; Planel et al., 2007). Whilst tau phosphorylation changes did not correlate with change in kinase activities such as GSK-3β, Cdk5, Erk1/2, JNK and CAMKII, a decrease in PP2A levels has been reported (Clodfelder-Miller et al., 2006; Planel et al., 2007), suggesting the hyperphosphorylation of tau was due to a decrease in phosphatase activity. STZ has also been administered in Swiss Webster mice which reduced expression of IDE, reduced activation of the insulin receptor and Akt thereby increased GSK-3 activity leading to increased tau phosphorylation at the Thr231 epitope, elevated Aβ levels and induced learning deficits (Jolivalt et al., 2008). Interestingly, in the studies by Coldfelder-Miller *et al* and Jolivalt *et al*, 15 minutes insulin treatment in animals reversed tau phosphorylation at some epitopes (Thr231, Ser396/404) but did not restore PP2A activity (Clodfelder-Miller et al., 2006), whilst 8 weeks of insulin treatment partially reversed phosphorylation of the insulin receptor, GSK-3β activity and tau phosphorylation in addition to improving the learning performance in animals (Jolivalt et al., 2008). The difference between these two studies may be attributed to the length of STZ treatment (3 days in Coldfelder-Miller *et al* and 9 weeks in Jolivalt *et al*), demonstrating the reversibility of tau phosphorylation at selective sites after short term insulin deficiency. In rats administered with STZ,

increased tau phosphorylation also correlated with the reduction in phosphorylation of Akt, GSK-3 and PP2A. However, insulin treatment did not change tau phosphorylation but lithium treatment reversed all tau phosphorylation sites by 30 days (Qu et al., 2011). Additionally, STZ treatment in the pR5 tau mouse model with the P301L human tau mutation, the deposition of hyperphosphorylated insoluble tau was evident along with the formation of NFTs (Ke et al., 2009).

In two APP transgenic models; APP double transgenic (London V717I and Swedish K670M/N671L) mice and the APP/PS1 double transgenic line, STZ treatment increased GSK-3 activity leading to an increase in Aβ production and a concomitant increase in Aβ plaques (Jolivalt et al., 2010), which associated with impaired memory performance (Wang et al., 2010). Additionally, tau phosphorylation was increased in the APP double transgenic mice (Jolivalt et al., 2010). Furthermore, direct intracerebroventricular (ICV) injection of STZ target GLUT2 in the brain and mimics the insulin resistant brain state. This approach selectively decreases brain insulin without disturbing systemic insulin and glucose levels. STZ was found to impair glucose and energy metabolism and also impaired learning and memory in rats (Lannert and Hoyer, 1998). ICV STZ injected brains also exhibit neurodegenerative features in that they appear reduced in size, likely due to cell loss and gliosis as evidenced by increased p53 immunoreactivity (Lester-Coll et al., 2006). The activation of GSK-3β increased phosphorylation of tau and elevated Aβ levels (Lester-Coll et al., 2006). In the APP transgenic model Tg2576 (overexpressing the APPswe mutation), ICV STZ treatment increased GSK-3 activity leading to an increase in Aβ production and a concomitant increase in Aβ plaques, which coincided with impaired memory performance (Plaschke et al., 2010). Interestingly, a recent study demonstrated ICV STZ injection resulted in deficits in hippocampal LTP and indicated synaptic dysfunction was due to reduced expression of NMDA receptor subunits, NR2A and NR2B (Shonesy et al., 2011).

1.5.2 Spontaneous diabetes models

Spontaneous diabetes models are genetically predisposed to developing T1DM or T2DM. In rats, both Bio-Breeding/Worcester (BB/Wor) (T1DM) and Bio-Breeding Zucker diabetic rat (BBZDR)/Wor (T2DM) models develop diabetes around 2 months of age and by 10.5 months of age neuronal loss in the frontal cortex was visible, noticably higher in the BBZDR/Wor rats which was accompanied by a nine-fold increase in dystrophic neurites. In both models, the expression of the IGF1-receptor was reduced and phosphorylation of Akt and GSK-3β were reduced. In the type 2 diabetic BBZDR/Wor rats, this led to more than two-fold increase in the levels of APP, BACE and Aβ as well as a significant increase in tau phosphorylation (Ser396) (Li et al., 2007). These findings indicate T2DM more likely influences the development of AD pathology. In another study using db/db (homozygous for diabetic gene (db) that encodes a point mutation for the leptin receptor) mice, which develop T2DM by 5 weeks of age, tau phosphorylation and tau cleavage was increased in the cortex and hippocampus by 8 weeks of age (Kim et al., 2009a). In contrast, another study found no change in tau phosphorylation at 8 weeks of age in the same mice (Jolivalt et al., 2008). Recently, Takeda *et al* generated mouse models that genetically develop T2DM and AD by crossing APP23 mice with ob/ob (leptin deficient) or Nagoya-Shibata-Yasuda (NSY) type 2 diabetic mice (Takeda et al., 2010). Both APP^+-ob/ob and APP^+-NSY mice showed features of diabetic phenotype but exhibit different pathogenic mechanisms. APP^+-ob/ob mice exhibited early onset of diabetes and early onset of learning deficit in the Morris water maze test. Aβ deposition was not detected but cerebrovascular Aβ deposition was prominent and associated with increased RAGE immunoreactivity, increase reactive astrogliosis and reduced cholinergic fibres in the hippocampus. Insulin signalling was disturbed as levels of insulin, PIP_3 and Akt phosphorylation were suppressed. Similar observations were observed in APP^+-NSY mice when fed a high fat diet (HFD) for 5 months. The authors suggested that

cerebrovascular dysfunction and altered brain insulin signalling may play a mechanistic role between T2DM and AD.

1.5.3 Diet-induced models of insulin resistance and diabetes

Diet-induced insulin resistance is more reflective of modern lifestyles in man and the development of T2DM. In Tg2576 mice, feeding HFD for 5 months induced obesity, impaired glucose tolerance and resulted in high fasting plasma insulin levels. Impairments in the insulin signalling pathway were shown in reduce insulin receptor activation, phosphorylation of Akt and phosphorylation of GSK-3. $A\beta_{40}$ and $A\beta_{42}$ levels were elevated accompanied by the generation of $A\beta$ plaques which corresponded to an increase γ-secretase and a reduction in IDE activities (Ho et al., 2004). Furthermore, impairment in performance of the Morris water maze task was observed (Ho et al., 2004). Feeding HFD to the same mice for 3 months by another group also induced insulin resistance and $A\beta_{40}$ and $A\beta_{42}$ levels increased however, authors did not examine components of the insulin signalling pathway (Kohjima et al., 2010). These observations were strengthened by a group using the triple transgenic AD mouse (APP[APPswe], PS1 [PS1M146V], and tau [P301L]), which after being fed a HFD showed increased levels of $A\beta_{40}$ and $A\beta_{42}$, as well as soluble tau. Instead of memory tests, decreased levels of the synaptic marker, drebrin, were found (Julien et al., 2010). On the contrary, Moroz *et al* found no AD pathology in C57BL/6 mice fed HFD for 16 weeks, despite developing glucose intolerance and hyperinsulinemia (Moroz et al., 2008). Although changes in brain expression levels of tau, insulin, IGF1 receptor, IRS1, IRS4, ubiquitin, GFAP and β-actin were detected and insulin receptor binding was reduced. The authors concluded that T2DM contributes to the development of AD but is not sufficient to cause AD. Two other papers have reported the intake of 10% sweetened sucrose water for 25 or 16 weeks in APP/PS1 double transgenic mice (Cao

et al., 2007) or rats (Luo et al., 2011) respectively, exacerbates memory impairment and Aβ deposition.

1.5.4 Models with genetic manipulations

Studies have targeted components of the insulin signalling pathway in an attempt to identify the level of signalling which would have the greatest impact on AD pathology. In NIRKO mice, the PI3K signalling pathway is reduced and thus Akt activity was reduced. This led to an increase of GSK-3β activity that corresponded to the hyperphosphorylation of tau. However, the absence of neuronal damage, impaired cognition or basal brain glucose metabolism suggests other factors must interact for the development of AD (Schubert et al., 2004). Similarly, IRS2 knockout mice displayed hippocampal NFTs containing hyperphosphorylated tau, corresponding to a reduction of the PP2A catalytic subunit (Schubert et al., 2003). A further study queried the effect of IRS2 knockout on amyloid pathology by crossing the IRS2 knockout mice with Tg2576 mice. As previous studies, tau phosphorylation was increased due to a reduction in the tau phosphatase PP2A, however the Aβ burden was significantly reduced, accompanied by an improvement in cognitive function of mice (Killick et al., 2009). The reduction in Aβ plaques correlated with an increase in the Aβ binding protein, transthyretin, indicating increased Aβ clearance in the brain. Interestingly, another study using the same mice, Tg2576 crossed with IRS2 knockout mice, reported a delay in Aβ accumulation which rescued the premature mortality of Tg2576 mice (Freude et al., 2009). Furthermore, the IDE knockout mice displayed increased cerebral Aβ accumulation, elevation of AICD and peripheral hyperinsulinemia and glucose intolerance, features of both AD and T2DM respectively (Farris et al., 2003). These results show IDE hypofunction might be related to the connection between AD and T2DM.

Taken together, although the mechanisms underlying the increased risk of AD in diabetics are not yet clear, evidence from animal models has provided some clues towards the underlying cause. However, as in man, these *in vivo* models are complex with some apparently contradictory evidence coming from type 1 versus type 2 and from genetic versus dietary models. Future studies are essential to confirm these complex interactions, which trigger disease progression and to identify targets for therapeutic intervention.

1.6 Aims and objectives of the current study

The overall aim of this thesis was to investigate the effects of PPARγ agonism on insulin signalling processes relevant to AD pathogenesis and to determine if any such effects are APOE genotype dependent. This could give insight with regard to the possible use of TZDs as treatments for AD.

The principle objectives were:

1. To determine the effect of APOE genotype in modulating the influence of insulin signalling on APP metabolism and tau phosphorylation *in vivo*.

2. To determine whether PPARγ agonists modulate the influence of insulin signalling on APP metabolism and tau phosphorylation *in vivo* and if they do, whether this is in an APOE-dependent manner.

3. To determine the mechanism of effect of PPARγ agonists in this context - specifically, whether it is mediated through a direct action on neurons, via cholesterol related mechanisms.

4. To investigate the effects of diet-induced insulin resistance on the brain transcriptome of APOE mice.

CHAPTER 2

Materials and Methods

2.1 Materials

All reagents were obtained from Sigma Aldrich (UK) or Roche (UK) unless stated otherwise. Solutions were prepared using ultra-pure water from an Elga Maxima water purification system.

2.1.1 Commonly used reagents

Sigma

Ammonium persulphate (APS)

Beta-Mercaptoethanol (β-mercaptoethanol)

Boric acid

Ethylenediaminetetraacetic acid (EDTA)

Ethylene glycol tetraacetic acid (EGTA)

Glycine for electrophoresis

Glycerol 2-phosphate disodium salt hydrate

Phenylmethanesulphonyl fluoride (PMSF)

Phosphate buffered saline (PBS) tablets

Ponceau S

Sodium azide

Sodium fluoride

Sucrose

TEMED (N,N,N',N'- Tetramethylethylenediamine)

Trichloroacetic acid

Tris-HCl (pH 7.4)

Triton X-100

Tween 20

Ultrapure agarose

Roche

Mini complete protease inhibitor tablets

Mini complete phosphatase inhibitor tablets

Tris

2.1.2 General solutions

Ammonium persulphate

10% APS

Azide

1% Sodium azide

Ponceau S

0.2% Ponceau S

5% Trichloroacetic acid

2.1.3 Solutions for electrophoresis

Tris-Borate-EDTA (TBE) buffer for agarose electrophoresis:

89 mM Tris

89 mM Boric acid

2 mM EDTA

Running buffers for western blotting:

8% Sodium dodecyl sulphate-polyacrylamide gel electrophoresis (SDS-PAGE)

SDS PAGE Tank Buffer (10x) Tris-Glycine SDS (Geneflow)

10x buffer was diluted to 1x in ddH_2O before use

16% Tricine gels

Novex Tricine SDS Running Buffer (10x) (Invitrogen)

10x buffer was diluted to 1x in ddH_2O before use

Transfer buffer:

1.88 M Glycine

20% Methanol (VWR)

5 M Tris

Wash buffer:

PBS-tween (PBST);

PBS 1x

0.1% Tween

Blocking buffer:

5% Dried skimmed milk (Marvel) in PBST

2.1.4 Transgenic mice

All transgenic mice; APOE KO, APOEε3 and APOEε4, were purchased from Taconic and together with the same background strain C57BL/6 mice (Charles River) were bred in-house at The Frythe, GlaxoSmithKline. Judy Latcham, Michael Fulleylove, Jason Smith and Sylvia Fung from GlaxoSmithKline were involved with the animal husbandry.

Mice with human APOE genes replacing murine APOE genes (henceforth described as 'APOE mice') were generated as published (Knouff et al., 1999; Piedrahita et al., 1992; Sullivan et al., 1997). In brief, the mice were created by gene targeting of the endogenous murine APOE gene locus with the human APOE alleles; APOEε3 or APOEε4. Consequently, mice expressed human apoE isoforms under the control of murine APOE regulatory sequences and have similar apoE expression levels to the non-transgenic apoE expressing mice. Further details are described in chapter 3.

2.1.4.1 Assessment of metabolic changes

Oral glucose tolerance test

+D-Glucose (Sigma)

Plasma insulin levels

Mouse insulin ultrasensitive enzyme-linked immunosorbent assay (ELISA) (DRG, Germany. EIA 3440)

Plasma adiponectin levels

Mouse adiponectin immunoassay (R&D Systems, Minneapolis USA. MRP300)

2.1.5 Protein extraction and sample preparation

2.1.5.1 Sucrose homogenisation buffer

250 mM sucrose

20 mM Tris-HCl (pH 7.4)

1 mM EDTA

1 mM EGTA

100 mM PMSF

1 mini complete phosphatase inhibitor cocktail tablet

1 mini complete protease inhibitor cocktail tablet

1% Triton X-100

2.1.5.2 Protein sample buffer

8% SDS-PAGE

2x Laemmli Sample Buffer (BioRad)

β-mercaptoethanol

16% Tricine gels

2x Tris-glycine SDS sample buffer containing NuPage sample reducing agent (Invitrogen)

2.1.6 Western blotting

2.1.6.1 Protein molecular weight markers

8% SDS-PAGE gels

Precision Plus Protein Kaleidoscope Standards (Bio Rad)

16% Tricine gels

Novex Sharp Prestained Protein Standard (Invitrogen)

2.1.6.2 SDS-PAGE

Resolving gel

4x ProtoGel Resolving Buffer (1.5 M Tris-HCl, 0.4% SDS, PH 8.8) (Geneflow)

Ultra Pure ProtoGel- 30% (w/v) Acrylamide: 0.8% (w/v) Bis-Acrylamide stock solution (37.5:1) (Geneflow)

APS

99% TEMED (N,N,N',N'- Tetramethylethylenediamine)

Stacking gel

ProtoGel Stacking Buffer (0.5 M Tris-HCl, 0.4% SDS, PH 6.8) (Geneflow)

Ultra Pure ProtoGel- 30% (w/v) Acrylamide: 0.8% (w/v) Bis-Acrylamide stock solution (37.5:1)

APS

99% TEMED (N,N,N',N'- Tetramethylethylenediamine)

Pre-cast gels

16% Novex Tricine Gel (Invitrogen)

2.1.7 Antibodies

Primary antibodies

All antibody sources, specificity and dilutions used are summarised in table 2.1. These were diluted in blocking solution PBST containing 5% milk and used for western blotting. Protein bands were normalised to β-actin or α-tubulin III antibodies.

Secondary antibodies

Goat anti-rabbit, goat anti-mouse or donkey anti-goat secondary antibodies conjugated to fluorophors (Molecular Probes, Invitrogen) emitting at wavelengths of either 700 or 800 nm were used. Donkey anti-rabbit and donkey anti-mouse HRP-conjugated secondary antibodies (GE Healthcare, UK) were used for the detection of APP processing and β-actin.

Table 2.1 List of antibodies used for western blotting

Antibody	Type	Source	Dilution		
			Plasma	Brain lysates	Cell lysates
Primary antibodies					
Apolipoprotein E	Goat polyclonal	Millipore	1:5000	-	-
AT8 (Ser202/Thr205)	Mouse monoclonal	Pierce	-	1:1000	-
AT180 (Thr231)	Mouse monoclonal	Pierce	-	1:1000	-
Phospho-tau (Ser396)	Mouse monoclonal	Cell signalling Technology	-	1:1000	-
PHF1	Mouse monoclonal	Peter Davies	-	-	1:2000
Total Tau	Rabbit polyclonal	Dakocytomation	-	1:50,000	1:50,000
Phospho-GSK-3 (Ser21/9)	Rabbit polyclonal	Cell signalling Technology	-	1:1000	1:2000
Total GSK-3	Mouse monoclonal	Stressgen	-	1:1000	1:2000
Phospho-Akt (Ser473)	Rabbit polyclonal	Cell signalling Technology	-	1:1000	1:2000
Total Akt	Rabbit polyclonal	Cell signalling Technology	-	1:1000	1:2000
Phospho-PP2A (Tyr307)	Rabbit polyclonal	Cell signalling Technology	-	1:1000	-
Total PP2A	Goat polyclonal	Santa Cruz	-	1:1000	-
p35/25	Rabbit polyclonal	Cell signalling Technology	-	1:1000	-
Anti-APP 369	Rabbit polyclonal	(Buxbaum et al., 1990)	-	1:1000	-
β-Actin	Mouse monoclonal	Abcam	-	1:5000	1:5000
β-Tubulin III	Rabbit polyclonal	Sigma	-	1:5000	1:5000
Secondary antibodies					
Goat anti-rabbit 800 (flurophore)	Rabbit polyclonal	Molecular Probes, Invitrogen	-	1:6000	1:6000
Goat anti-mouse 680 (flurophore)	Mouse polyclonal	Molecular Probes, Invitrogen	-	1:6000	1:6000
Donkey anti-goat 680 (flurophore)	Donkey polyclonal	Molecular Probes, Invitrogen	1:6000	1:6000	-
Donkey anti-rabbit (HRP)	Rabbit polyclonal	GE Healthcare	-	1:5000	-
Donkey anti-mouse (HRP)	Mouse polyclonal	GE Healthcare	-	1:5000	-

2.1.8 Abeta (Aβ) enzyme-linked immunosorbent assays (ELISAs)

Mouse soluble Aβ 1-40 and Aβ 1-42 were measured using the BetaMark Beta Amyloid x-40 (SIG-38950) and x-42 (SIG-38952) chemiluminescent ELISA kits (Covance). Both ELISA kits detect human and rodent Aβ 1-40 and Aβ 1-42.

2.1.9 Cell culture reagents

Poly-D-Lysine Hydrobromide (Sigma), 1 mg/ml

Insulin (Sigma)

Trypsin (PAA Laboratories)

PBS tablets (Sigma)

Pioglitazone (ChemPacific)

2.1.9.1 Culture Media

CHO cell culture media

F12/DMEM (PAA Laboratories) supplemented with:

10% Fetal bovine serum (Sera Labs International)

Penicillin/Streptomycin (PAA Laboratories)

Neuronal cell culture media

Neuralbasal media (Gibco, Invitrogen) supplemented with:

B27 supplement with insulin (Invitrogen) or B27 supplement without insulin (Invitrogen)

200 mM L-Glutamine (PAA Laboratories)

Penicillin/Streptomycin

G418 disulfate salt solution (Sigma)

2.1.10 Affymetrix microarray

All Affymetrix GeneChip Mouse Genome 430 v2.0 arrays, GeneChip Hybridisation Wash and Stain kits and GeneChip IVT Express kits were purchased from Affymetrix, UK. Agilent RNA 6000 Pico chips to assess the quality of RNA, were purchased from Agilent Technologies, UK. Tissues were lysed in Matrix lysing D tubes from Qbiogene and RNA extracted using the RNase-Free DNase Set from Qiagen, UK, which incorporates a DNase step to remove any genomic DNA contamination.

2.2 Methods

2.2.1 Transgenic mice

2.2.1.1 Dietary conditions

APOE KO, APOEε3 and APOEε4-transgenic mice together with background strain C57BL/6 mice, at 3 months of age, were kept on a low fat diet (LFD) (10% fat, Research Diets, D12450B) (n = 12 per genotype) or a high fat diet (HFD) (60% fat, Research Diets, D12492) (n = 12 per genotype) for 32 weeks. Details of diets are shown in Table 2.2 and 2.3, respectively. Mice were housed individually under controlled conditions of temperature and lighting and given free access to food and water. Metabolic changes were assessed until mice fed on a HFD developed insulin resistance.

Table 2.2 Formula of low fat diet with 10% kcal fat

Table is adapted from the Research Diets, D12450B datasheet.

Product	**D12450B (LFD)**	
	gm %	**kcal %**
Protein	19.2	20
Carbohydrate	67.3	70
Fat	4.3	10
Total		100
kcal/gm	3.85	
Ingredient	**gm**	**kcal**
Casein, 80 Mesh	200	800
L-Cystine	3	12
Corn Starch	315	1260
Maltodextrin 10	35	140
Sucrose	350	1400
Cellulose, BW200	50	0
Soybean Oil	25	225
Lard*	20	180
Mineral Mix S10026	10	0
DiCalcium Phosphate	13	0
Calcium Carbonate	5.5	0
Potassium Citrate, 1 H_2O	16.5	0
Vitamin Mix V10001	10	40
Choline Bitartrate	2	0
FD&C Yellow Dye #5	0.05	0
Total	**1055.05**	**4057**

*Typical analysis of cholesterol in lard = 0.95 mg/gram

Cholesterol (mg)/4057 kcal = 19

Cholesterol (mg)/kg = 18

Table 2.3 Formula of high fat diet with 60% kcal fat

Table is adapted from the Research Diets, D12492 datasheet.

Product	**D12492 (HFD)**	
	gm %	**kcal %**
Protein	26.2	20
Carbohydrate	26.3	20
Fat	34.9	60
Total		100
kcal/gm	5.24	
Ingredient	**gm**	**kcal**
Casein, 80 Mesh	200	800
L-Cystine	3	12
Corn Starch	0	0
Maltodextrin 10	125	500
Sucrose	68.8	275.2
Cellulose, BW200	50	0
Soybean Oil	25	225
Lard*	245	2205
Mineral Mix, S10026	10	0
DiCalcium Phosphate	13	0
Calcium Carbonate	5.5	0
Potassium Citrate, 1 H_2O	16.5	0
Vitamin Mix, V10001	10	40
Choline Bitartrate	2	0
FD&C Blue Dye #1	0.05	0
Total	**773.85**	**4057**

*Typical analysis of cholesterol in lard = 0.95 mg/gram

Cholesterol (mg)/4057 kcal = 232.8

Cholesterol (mg)/kg = 300.8

2.2.1.2 Drug treatment

APOE KO, APOEε3 and APOEε4-transgenic mice together with background strain C57BL/6 mice, at 3 months of age, were kept on a 60% HFD for 30 weeks. During the last 3 weeks of diet, mice were divided into vehicle and pioglitazone treatment groups. The pioglitazone treatment group (n = 12 per genotype) were orally dosed with pioglitazone (20 mg/kg) (ChemPacific) whilst the vehicle group (n = 12 per genotype) received 1% methylcellulose. Mice were dosed twice daily (8am and 8pm).

Mice were housed individually at 3 months of age under controlled conditions of temperature and lighting and given free access to food and water.

2.2.1.3 Oral glucose tolerance test

Glucose tolerance tests were conducted to assess the level of circulating glucose prior to commencing each study and then at 6 or 12 weekly intervals following the initiation of study. Mice were fasted overnight. The next morning, mice were placed in a warming chamber prior to blood sampling and blood was taken by direct venopuncture. Mice were then given a single oral dose of glucose (3 g/kg dose volume 10 ml/kg) and serial blood samples collected from the tail tip post-dose at 30, 60, 90, 120 and 180 min. Glucose levels were accessed using the Ascensia blood glucose meter (Bayer Diabetes Care, UK).

2.2.1.4 Collection of plasma

Blood samples collected from the tail vein at baseline into anti-coagulation tubes were centrifuged at 3000 x g for 5 min. Plasma was aliquoted into separate tubes and then stored at -80°C until analysis.

2.2.1.5 Measurement of plasma insulin levels and homeostatic model assessment of insulin resistance (HOMA-IR)

ELISAs used to measure insulin were ran according to the manufacturer's instructions.

All reagents and samples were brought to room temperature before use. The ELISA is based on the direct sandwich ELISA technique (Figure 2.1) in which 5 μl plasma sample plus 50 μl secondary peroxidase conjugate were loaded into a insulin

antibody coated 96-well plate. During the 2 h incubation, shaking at room temperature, insulin within the sample binds with the secondary and anti-insulin antibodies in the microtitration well. The unbound enzyme labelled antibodies were removed by washing the plate six times with 350 μl of wash buffer. Peroxidase substrate (200 μl of 3,3',5,5'-tetramethylbenzidine (TMB)) was then added and incubated for a further 30 min before the addition of stop solution (1 M sulphuric acid, H_2SO_4). The plate was placed onto a shaker for 5 sec to ensure mixing of the substrate and stop solution before measuring on the SpectraMax M2 microplate reader (Molecular Devices, UK) at 450 nm absorbance. The SoftMax Pro v5 software to was used to analyse the data. Animals with a lack of effect of high fat feeding on insulin sensitivity were removed from the corresponding data analyses.

The HOMA-IR (Matthews et al., 1985) was calculated using the following formula: (fasting blood glucose (mg/dL) * fasting insulin (μU/ml))/405.

Figure 2.1 Diagram of the direct sandwich ELISA technique

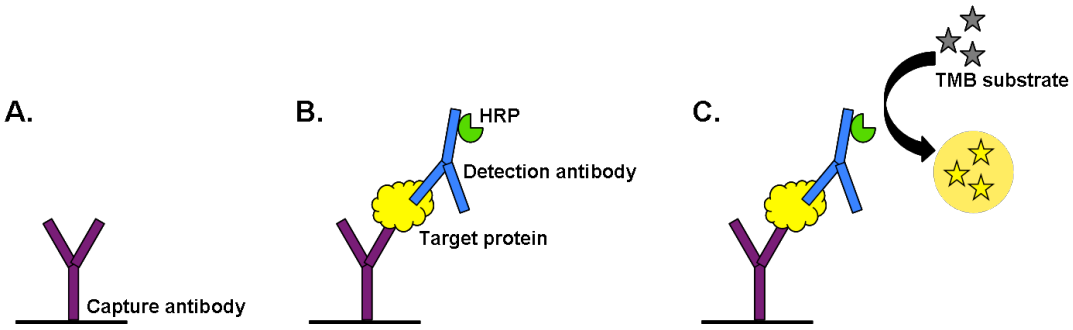

Each well of a 96-well plate is coated with capture antibodies for the protein of interest (A). During the assay, the sample is loaded into the well. The target proteins are recognised by the capture antibodies and are immobilised onto the plate surface (B). Following incubation, the well is subjected to washes that remove unbound samples. The addition of an enzyme conjugated secondary antibody allows the detection of the target protein when a substrate is added (C).

2.2.1.6 Measurement of plasma adiponectin levels

Adiponectin levels were measured using a commercial ELISA kit according to the manufacturer's instructions.

All reagents and plasma samples were brought to room temperature before use. The ELISA is based on a direct sandwich technique. Samples were diluted 2000-fold with the calibrator diluent provided in the kit. Diluted samples (50 μl) along with 50 μl assay diluent were loaded into an anti-adiponectin monoclonal antibody coated 96-well plate and allowed to bind during incubation for 3 h at room temperature. Unbound substances were removed by washing the plate with 400 μl of wash buffer five times. An HRP enzyme-linked polyclonal antibody specific for mouse adiponectin (100 μl) was then added into the well for 1 h at room temperature. Following five 400 μl plate washes to remove any unbound enzyme, 200 μl of substrate solution containing hydrogen peroxide and TMB was added to each well and incubated for 30 min, protected from light. The reaction was ended by the addition of stop solution (100 μl of hydrochloric acid, (HCl)) and mixed gently before reading the absorbance at 450 nm on the SpectraMax M2 microplate reader (Molecular Devices, UK). The SoftMax Pro v5 software to was used to analyse the data.

2.2.1.7 Tissue preparation

At termination of each study, mice were sacrificed by a lethal overdose of anesthetic, pentobarbitone sodium. Brains were removed, and each hemisphere was subdissected into the following regions: cortex, hippocampus, cerebellum and rest of brain. One hemisphere was fresh frozen in liquid nitrogen and subsequently stored at -80˚C until use. The other hemisphere was preserved immediately in 10 volumes (~10μl per mg tissue) of RNA*later* (Qiagen, UK) per 1g of tissue for 2 days at 4°C before removing the reagent and storing at -80°C until use. RNA*later* is a tissue permeant

stabiliser and protectant of RNA. Samples of the liver were also collected, fresh frozen in liquid nitrogen and subsequently stored at -80˚C.

2.2.2 Genotyping of transgenic mice

2.2.2.1 Extraction of DNA

The DNeasy Blood and Tissue kit (Qiagen) was used to extract DNA from livers of transgenic mice according to the manufacturer's instructions.

Livers from transgenic mice were weighed and placed in microcentrifuge tubes with Buffer ATL (180 μl). Proteinase K was added to each tube, mixed thoroughly by vortex and allowed to incubate at 56°C in a thermomixer to lyse the tissue. Following lysis, tubes were vortexed for 15 sec before the addition of Buffer AL (200 μl) and mixed thoroughly. Ethanol (200 μl, 100%) was added to each sample and mixed thoroughly. The mixture from each tube was transferred into a DNeasy Mini spin column and centrifuged at 8000 rpm for 1 min. The flow-through was discarded. Buffer AW1 (500 μl) was added to each DNeasy spin column and centrifuged at 8000 rpm for 1 min before discarding the flow-through. Buffer AW2 (500 μl) was added to each DNeasy spin column and centrifuged at 14,000 rpm for 3 min. Finally to elute the DNA, DNeasy spin columns were placed into a fresh microcentrifuge tube and the Buffer AE (100 μl) was added directly onto the DNeasy membrane, incubated at room temperature for 1 min and centrifuged at 8000 rpm for 1 min. In order to obtain maximum yield, the elution step was repeated once more. Eluted DNA samples were stored at -20°C until use.

2.2.2.2 Polymerase chain reaction (PCR)

PCR amplification was carried out in a master mix shown in table 2.4 containing AmpliTaq Gold DNA Polymerase (Applied Biosystems), Gold buffer (Applied

Biosystems), $MgCl_2$ (Applied Biosystems), dNTPs (Roche), forward and reverse primers (Eurofins MWG, table 2.5) and 10 ng of genomic DNA as a template. DNA (2 μl) was added into a PCR Thermal-Fast 96-well microplate (ThermalScientific) before the addition of the master mix (18 μl per reaction). The plate was subjected to a brief spin to collect the mixture at the bottom of the plate before placing in the BioRad DyadDisciple thermal cycler controlled by the Opticon Monitor 3 software. The following thermal cycling conditions were used:

1. $T_{melting}$ 95°C 1 min
2. 95°C 10 sec
3. $T_{annealing}$ 63°C 10 sec
4. $T_{extension}$ 72°C 30 sec
5. Repeat steps 2-4, 30 times
6. End, hold at 4°C

Table 2.4 Reagents within the master mix prepared for one PCR reaction

Reagent	**Volume (μl)**
10 x buffer	2
Primer 1 (10μM)	2
Primer 2 (10μM)	2
dNTP (2 mM)	2
Taq polymerase	0.1
DNA (5 ng/μl)	2
$MgCl_2$ (25 mM)	1.6
DNase-free H_2O	8.3

Table 2.5 Primers for PCR APOE genotyping

Gene		Primer sequence
Neomycin	Forward	cgttggctacccgtgatatt
	Reverse	gcctgcttttccaattcttg

2.2.2.3 Agarose gel electrophoresis of PCR products

PCR products were analysed on 1.5% agarose gels. Ultrapure agarose was dissolved in boiling 1x TBE buffer, cooled and ethidium bromide was added into the mixture before cast onto a tray with a suitable comb. Gels were placed in the electrophoresis tank containing 1x TBE buffer to cover the surface of the gel. PCR products were diluted in gel loading buffer prior to loading into the gel with a 100 bp DNA ladder (TrackIt, Invitrogen) and run at 115 V for 50 min. Gels were visualised using the AlphaImager Mini (Alpha Innotech) emitting ultraviolet light.

2.2.2.4 TaqMan genotyping

TaqMan small nucleotide polymorphism (SNP) Genotyping Assays are performed using a 5' nuclease chemistry for the amplification and detection of specific polymorphisms in genomic DNA samples. The assay used was pre-designed and validated by Applied Biosystems. The assay was performed together with Dr. Michelle Lupton, King's College London.

DNA was extracted from the livers of mice by using the Qiagen DNeasy blood and tissue kit as described in section 2.2.2.1. The concentration of each sample was measured using the NanoDrop 1000 (ThermoScientific) and prepared to a concentration of 5 ng/μl in working plates. DNA from each sample (1 μl) was transferred to an optically clear 384 well plate (Thermo-fast diamond, ABgene) and left

to dry by evaporation. A reaction mixture containing 1x ABsolute QPCR ROX Mix (ABgene) and 1x genotyping assay (Applied biosystems) was then added to each well, to disperse the DNA before sealed with an optically clear “absolute QPCR” adhesive cover (ABgene). The PCR reaction was carried out using the following parameters:

1. 95°C for 15 min
2. 92°C for 15 sec
3. 60°C for 1min 30 sec
4. Repeat steps 2-3, 49 times
5. End, hold at 4°C

On completion of the PCR amplification, an endpoint plate read was performed using the Applied Biosystems 7900HT Fast Real-Time PCR System according to manufacturer’s instructions. Fluorescent measurements (FAM and VIC) obtained from each well were plotted by the Sequence Detection System (SDS) software. The plotted fluorescence signals indicate which alleles are in each sample by use of a clustering algorithm. The plate was analysed with a quality value of 95% and an automatic allele call. The allele calls were converted to genotype as the two different report dyes FAM and VIC show the presence of each allele (APOEε3 or APOEε4). The calls are positioned on the plot due to the level of fluorescence for each allele (Figure 3.4).

APOE genotypes

The APOE gene consists of three main alleles; ε2, ε3 and ε4. The difference between these alleles are due to 2 residues therefore the APOE allele is a haplotype consisting of two SNPs. Between the ε3 and ε4 alleles there is one differing SNP, ε3 was detected as rs429348T and ε4 detected as rs429348C.

2.2.3 Analysis of brain samples

2.2.3.1 Protein extraction

Individual regions of interest were weighed whilst frozen and then homogenised rapidly in 10-fold volume of a detergent free tissue homogenisation buffer on ice. A sample of total brain homogenate was collected and stored at -80°C until use for the Aβ ELISAs. Homogenates were then centrifuged at 47,000 rpm for 20 min at 4°C in a Beckman TLA 55 rotor (Beckman, Palo Alto, CA, USA). The soluble supernatant (S1 fraction) was collected and the pellet resuspended in a same volume of the above buffer with the addition of 1% Triton X-100, then subjected to centrifugation again. The resultant supernatant (S2 fraction) was collected and stored at -80°C with the S1 fraction and the pellet, P2, until use.

2.2.3.2 Bradford assay

The concentration of protein in brain lysates were determined by using the Bradford Protein assay from BioRad, according to the manufacturer's instructions. The assay is based on the dye-binding method described by Bradford (Bradford, 1976). It utilises an acidic solution of Coomassie Brilliant Blue G-250 which shifts from 465 nm to 595 nm on binding of a protein. Samples were diluted 1:10 dilution with ddH_2O and then 10 μl diluted sample was incubated with 190 μl Bradford reagent for 30 min in the dark, at room temperature. Absorbance was recorded at 595 nm using the Wallac spectrophotometer (Perkin Elmer) and measurements were compared to a standard curve prepared from a set of bovine serum albumin standards (0-2 mg/ml).

2.2.3.3 Western blotting

2.2.3.3.1 8% and 12% SDS-PAGE

S1 and S2 samples were diluted in an equal volume of 2x reducing laemmli sample buffer and boiled at 100°C for 5 min. Denatured samples were separated on 8% and 12% SDS-PAGE gels at 150 V for 1 h at room temperature. Proteins were then transferred onto nitrocellulose membranes (Whatman, UK) at 80 V for 1 h. Membranes were incubated in a blocking solution PBST for 1 h and then probed with primary antibody overnight at 4°C. The membranes were washed three times with PBST then incubated with either goat anti-rabbit, goat anti-mouse or donkey anti-goat secondary antibodies conjugated to fluorophors emitting at wavelengths of either 700 or 800 nm for 1 h at room temperature. Membranes were washed three times again with PBST. Proteins were detected using an Odyssey infrared imager (Licor, UK) and densitometry performed using ImageJ.

2.2.3.3.2 16% Tricine gels

S2 samples were diluted in an equal volume of 2x Tris-glycine SDS sample buffer containing NuPage sample reducing agent and heated for 3 min at 85°C. Samples were spun briefly then separated on 16% Tricine gels at 130 V for 2 h. Proteins were then transferred onto 0.2 μm pore size nitrocellulose membranes (Invitrogen, UK) at 200 mA for 2 h at room temperature. Membranes were boiled by microwave for 5 min in 1x PBS then incubated in a blocking solution for 1 h then probed with primary antibody overnight at 4°C. The membranes were washed three times with PBST incubated with either goat anti-rabbit or goat anti-mouse HRP-conjugated secondary antibodies for 1 h at room temperature. Membranes were washed three times with PBST. Immunoreactivity was visualised using enhanced chemiluminescence reagents (GE Healthcare, UK), x-ray film (Fuji, UK) and developer. ImageJ was used for quantification.

2.2.3.4 Aβ ELISAs

The levels of mouse soluble $A\beta_{40}$ and $A\beta_{42}$ were measured according to the manufacturer's instructions. The ELISAs are based on a sandwich ELISA technique and 50 μl total brain homogenates from the cortex were diluted with 50 μl working incubation buffer containing the HRP detection antibody before adding in duplicate (2x 100 μl) into the antibody coated plate. The ELISA plate was incubated overnight at 4°C to allow binding of sample and antibody. Subsequently, the plate was washed with 300 μl of wash buffer 5 times before the addition of chemiluminescent substrate and measured using a Wallac luminometer (Perkin Elmer). The resultant Aβ ELISA data was normalised to the total protein levels within each brain sample, as determined by the Bradford assay.

2.2.4 Cell Culture

2.2.4.1 Chinese hamster ovary (CHO) cells

ApoE3 and apoE4 stable CHO cells were generated in house (unpublished studies). In brief, cDNAs encoding the human ε3 and ε4 alleles of APOE were cloned into pEGFP-C1 to add C-terminal tags. These constructs were transfected into CHO cells and stable clones established using G418 selection.

2.2.4.2 Rat cortical neuronal cultures

Sprague-dawley rats (Charles River Laboratories) at gestational day 18 were culled by cervical dislocation in accordance with Schedule 1 of the Animals (Scientific Procedures) Act 1986. Embryos were decapitated and whole brains removed into ice-cold Hanks buffered saline solution (HBSS). Cortices were dissected, meninges removed and the whole cortex was incubated in papain solution at 37°C for 30 min and then triturated using a sterile Pasteur pipette to dissociate the tissue. The mixture was

filtered through a 70 μm nylon strainer (BD Biosciences) then centrifuged at 1200 rpm for 5 min at room temperature. The supernatant was discarded and cell pellet resuspended in HBSS containing albumin-ovomucoid inhibitor and DNase. The cell suspension was carefully overlayed on top of 5 ml ovomucoid solution, then centrifuged at 600 rpm for 5 min at room temperature. The supernatant containing membrane fragments was discarded whilst the pellet containing the dissociated cells was resuspended in neural basal media supplemented with B27 containing insulin. Viable cell numbers were estimated using trypan blue (Sigma) and a haemocytometer. Cells were plated on poly-D-Lysine coated 6-well or 12-well plates at a density of 750,000 and 500,000 per well respectively. Cells were maintained in a humidified incubator (5% CO_2 atmosphere at 37°C).

2.2.4.3 Treatment of cortical neurons with CHO-apoE conditioned media

Media was removed from the cortical neuronal cultures 24 h post seeding and replaced with neurobasal media supplemented with B27 without insulin. Neurons were maintained in culture for a further 6 days. On day 6, 600 μl of the media from these cultures were transferred into confluent 6-well plates containing wild type (WT) CHO, CHO-apoE3 and CHO-apoE4 cells for 24 h to make "conditioned" media (CM). On day 7, neurobasal media was removed from the neurons and replaced with CM from WT CHO, CHO-apoE3 and CHO-apoE4 cells. Neurons were incubated in CM for 24 h with or without 10 μM pioglitazone.

Neurons were lysed in 150 μl of 2x reducing Laemmli sample buffer containing 0.5 M β-glycerolphosphate and heated to 100°C for 5 min. Samples were immunoblotted using 8% SDS-PAGE gels as described in section 2.2.3.3.1. For qRT-PCR, neurons were collected in 500 ml Trizol/well (of a 12-well plate) and stored at -80°C for subsequent total RNA extraction.

2.2.4.4 Non-radiolabelled "pulse-chase like" experiment

WT CHO and CHO-apoE CM was applied onto 6-well plates of 1 week old cortical neurons as described above and incubated for 24 h at 4°C or 37°C. At the end of the experiments, neurons were washed twice with cold 1x PBS. Lysates were collected in 150 μl 2x reducing Laemmli sample buffer for immunoblotting on 12% SDS-PAGE gels. Blots were probed for apoE using an apoE antibody (Calbiochem) as described in section 2.2.3.3.1.

2.2.4.5 Insulin time-response experiment

Neurons (12-well plates) treated with WT CHO or CHO-apoE CM were also treated with 50 nM insulin for 15 min, 30 min, 1 h, 3 h and 24 h at 37°C. Lysates were collected in 150 μl of 2x reducing Laemmli sample buffer for immunoblotting on 8% SDS-PAGE gels as described in section 2.2.3.3.1. Blots were probed with PHF1, total tau, phospho-GSK-3 and total GSK-3 antibodies.

2.2.4.6 Insulin dose-response experiment

Neurons treated with WT CHO and CHO-apoE CM were treated with 10, 50, 100, 500 or 1000 nM for 15 min at 37°C. Lysates were collected in 150 μl 2x reducing Laemmli buffer for western blotting on 8% SDS-PAGE gels as described in section 2.2.3.3.1. Blots were probed with PHF1, total tau, phospho-GSK-3 and total GSK-3 antibodies.

2.2.4.7 Live dead assay

Neurons were assessed for cytotoxicity using a dual staining kit from Promokine, UK. This assay is based on the differential uptake of 2 compounds which

stain healthy cells (green) and dead cells (red) using calcein AM and ethidium homodimer III (EthD-III) respectively. Calcein AM penetrates through the plasma membrane of living cells and is hydrolysed by intracellular esterases, enabling calcein to release green fluorescence at 515 nm whilst ethidium homodimer III can only intercalate with DNA through damaged membranes of dying cells, and emits in the spectrum of red at 635 nm. Neurons on coverslips were treated with WT CHO, CHO-apoE3 or CHO-apoE4 CM with or without pioglitazone for 24 h. Cells were labeled according to manufacturer's instructions as follows: to remove serum esterase activity neurons grown on coverslips were washed gently three times with 1x PBS. Neurons were then fixed with 4% paraformaldehyde for 10 min, washed and stained with a solution consisting of 2 μM calcein AM and 4 μM EthD-III at 37°C. After 45 min, the Calcein AM/EthD-III solution was aspirated and coverslips were mounted onto slides then sealed with nail polish to prevent evaporation. Labeled cells were visualised using a fluorescence microscope (Zeiss Axiovert).

2.2.4.8 RNA extraction

Lysates were collected in 500 μl Trizol, in RNase-free Eppendorf tubes. Chloroform (100 μl) was then added, vortexed and subjected to centrifugation at 13,000 rpm for 5 min. The supernatant was transferred into fresh RNase-free Eppendorf tubes and 200 μl isopropanol was added to precipitate the RNA. The tubes were vortexed briefly before centrifuged again at 13,000 rpm for 5 min. The supernatant was removed without disturbing the pellet and washed with 200 μl 70% ethanol to clean the pellet. Tubes were centrifuged at 13,000 rpm for 5 min. The supernatant was discarded and the pellet was resuspended in 15 μl of RNase-free H_2O, concentrations and quality measured using a NanoDrop 1000 (ThermoScientific) and stored at -20°C until use.

2.2.4.9 Reverse transcription of RNA into cDNA

The extracted total RNA was reversed transcribed using a TaqMan reverse transcription kit (Promega). The content of the kit was prepared as a master mix (MM) shown in Table 2.6. The MM (6.15 μl) was added to 1 μg total RNA in a final volume of 3.85 μl per reaction, in 0.2 ml PCR tubes and kept on ice. The reaction was performed on a G-Storm thermal cycler using the following parameters: 25°C for 10 min, 48°C for 30 min and 95°C for 5 min. The cDNA was diluted at 1:10 ready for use.

Table 2.6 Reagents within the master mix prepared for the reverse transcription of RNA to cDNA for one reaction

Reagent	**Volume (μl)**
10x buffer	1
$MgCl_2$	2.2
dNTP	2
Hexamers	0.5
RNase inhibitor	0.2
Reverse transcriptase enzyme	0.25

2.2.4.10 Quantitative real time polymerase chain reaction (qRT-PCR)

Primer sets were designed using the Universal Probe Library package (Roche, UK) as shown in Table 2.7, which were diluted at 1:10 in RNase-free H_2O prior to use. A master mix (MM) shown in table 2.8 was prepared and targets were amplified using 8 μl MM with 2 μl of 1:10 diluted cDNA on 96-well plates on ice. The 96-well plates were subjected to a brief spin to collect mixtures at the bottom of the plate and cycling was performed using the BioRad DyadDisciple thermal cycler controlled by the Opticon

Monitor 3 software under the following thermal cycling conditions: 3 min at 95°C followed by 40 cycles of 95°C for 20 sec and 60°C for 30 sec. Mean values for the genes of interest were normalised to the mean value obtained for β-actin. The absolute threshold cycle values (Ct values) for each gene was then converted to relative quantities using the comparative Ct method.

Table 2.7 Primers used for qRT-PCR

Gene		**Primer sequence**
HMGCR	Forward	GACCTTTCTAGAGCGAGTGCAT
	Reverse	GCTATATTCTCCCTTACTTCATCCTG
MVD	Forward	TGGCGTCAGTGAACAACTTC
	Reverse	ACCCGGGCCAAGGTATAG
LSS	Forward	GAACAGACGGGGCTAGAGG
	Reverse	TGTTTGAGCTTTAGGTAAGTTCTTGA
DHCR7	Forward	CACCGCCTGTGACAGCTA
	Reverse	AGCCAGGAGTAAAGCAGCAC
ABCA1	Forward	CAGACGATATCTCGATTCATGG
	Reverse	GAGCGTGACTTCGGTTGG
ABCG1	Forward	GGACCTTTCTTACTCCGTACCC
	Reverse	CCTTTCAAAAGGGTCTTGTATCC

Table 2.8 Reagents within the master mix prepared for one qRT-PCR reaction

Reagent	**Volume (μl)**
SYBR green polymerase	5
Primer 1	0.5
Primer 2	0.5
RNase-free H_2O	2

2.2.5 Affymetrix microarray

Gene expression was performed on the cortical region using 3-4 microarray chips for each condition as follows: WT LFD (n = 4), APOEε3 LFD (n = 4), APOEε4 LFD (n = 4), APOE KO LFD (n = 3), WT HFD (n = 3), APOEε3 HFD (n = 4), APOEε4 HFD (n = 4) and APOE KO HFD (n = 4).

2.2.5.1 RNA extraction

The Qiagen RNeasy Lipid Tissue Mini Kit was used according to manufacturer's instructions as follows.

RNA*later* stabilised brain tissue from 30 samples in the LFD vs HFD study were homogenised in matrix lysing D tubes, in QIAzol (1 ml) in a FastPrep Automated Homogeniser (MP, UK). The lysates were left at room temperature for 5 min before being transferred into RNase-free tubes. Chloroform (200 μl) was added to each tube, vortexed, and left at room temperature for 3 min and then centrifuged at 13,000 rpm for 15 min at 4°C. The upper aqueous phase of the supernatant, which contains the RNA, was transferred into a new RNase-free tube, and an equal volume of 70% ethanol was added and then mixed thoroughly by vortexing. Samples were transferred into RNeasy mini spin columns placed in collection tubes and centrifuged at 10,000 rpm for 15 sec at room temperature, with the flow-through discarded. The spin column membranes were washed by the addition of 700 μl Buffer RW1 and then centrifuged at 10,000 rpm for 15 sec before discarding the flow-through. Columns were then washed two more times with 500 μl Buffer RPE and centrifuged at 10,000 rpm for 15 sec and 2 min respectively, with the flow-through was discarded. The RNeasy spin columns were then placed in new collection tubes before being centrifuged at maximum speed spin for 1 min to eliminate possible RPE buffer carry over. To elute the RNA, RNeasy columns were placed into Eppendorf tubes and 60 μl RNase-free water was added

directly onto the membranes. The column was spun at 10,000 rpm for 1 min and eluents stored at -80°C until use.

2.2.5.1.1 RNA quantification

RNA yields were determined using the NanoDrop 1000 (Thermal Scientific). Protein and solvent contamination were determined by the optical density readings OD_{260}/OD_{280} and OD_{260}/OD_{230} respectively. OD_{260}/OD_{280} should fall between 1.7-2.1 as a measure of RNA purity.

2.2.5.1.2 RNA integrity

High quality RNA is required for microarray analysis, and thus the quality was assessed using the Agilent RNA 6000 Pico kit (Agilent Technologies), which provides a RNA integrity number (RIN). This is a measure of RNA quality on a scale of 0-10, with 10 being maximal. In this study samples had RIN ≥7.30.

2.2.5.2 Affymetrix Genechip process

The process involved seven stages as illustrated in Figure 2.2. Each of these stages was carried out according to the manufacturer's instructions and is described below.

Figure 2.2 An illustrative overview of the microarray process

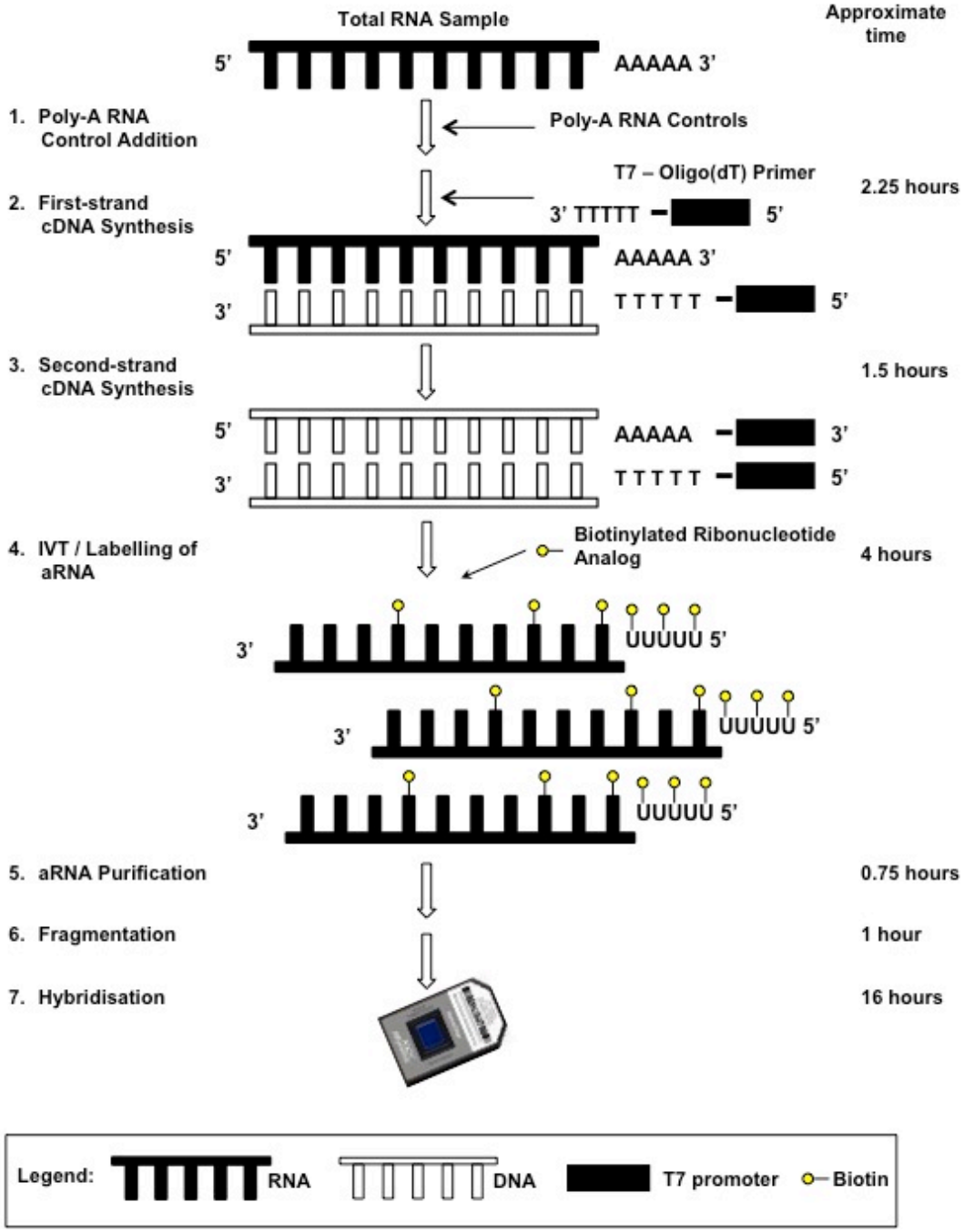

[1] Poly-A is added to RNA for [2] reverse transcription to synthesise the first strand of cDNA using the T7 oligo (dT) primer. [3] Second strand cDNA synthesis converts the single stranded cDNA into double stranded cDNA and is ready for *in vitro* transcription. [4] *In vitro* transcription generates biotin-modified amplified RNA (aRNA) and is [5] purified to remove unincorporated NTPs, salts, enzymes and inorganic phosphate. [6] Labelled aRNA is fragmented for [7] hybridisation onto GeneChip 3' expression arrays. This figure is adapted from the Affymetrix GeneChip 3' IVT Express Kit manual.

2.2.5.2.1 Poly-A RNA control addition

Poly-A RNA controls (*lys*, *phe*, *thr* and *dap*) are exogenous positive controls that monitor the whole RNA labelling process. The set of poly-A RNA controls provided in the GeneChip 3' IVT Express Kit are obtained from several *B.subtilis* genes, absent in eukaryotic samples. The Poly-A Control Stock was diluted in RNase-free centrifuge tubes with Poly-A Dil Buffer to achieve the final concentrations required when spiked into the RNA samples. The control was diluted by serial dilutions based on the guideline of 250 ng of total RNA as starting material.

2.2.5.2.2 Reverse transcription to synthesise first-strand cDNA

The first strand synthesis reagents (First-strand buffer mix and First-strand enzyme mix (5x first strand reaction mix, 0.1 M DTT and 10 mM dNTP)) were assembled into a master mix on ice before being vortexed and then centrifuged briefly. The first strand master mix (5 μl) was transferred to individual tubes for each of the 30 samples and 5 μl of the total RNA/poly-A control Mixture was aliquoted into the corresponding tubes. Tubes were mixed thoroughly by gently vortexing and subjected to a brief spin before incubated for 2 h at 42°C in a thermal cycler. After the incubation, tubes were centrifuged briefly and placed on ice ready for the next step.

2.2.5.2.3 Second-strand cDNA synthesis

The second-strand master mix (Nuclease-free water, second-strand buffer mix, second-strand enzyme mix (5x second strand reaction mix, 10 mM dNTP, E.coli DNA ligase, E,coli DNA polymerase I and RNase H)) was assembled on ice and mixed gently by vortexing before being centrifuged briefly. The master mix (20 μl) was transferred to each of the cDNA samples. Tubes were vortexed before being subjected to a brief spin and incubated for 1 h at 16°C followed by 10 min at 65°C in a thermal

cycler. Tubes were centrifuged briefly to collect mixtures at the bottom of the tube and then place on ice immediately before proceeding to the *in vitro* transcription step.

2.2.5.2.4 *In vitro* transcription (IVT) to synthesise labeled amplified RNA (aRNA)

The IVT master mix (reaction buffer, ATP solution, CTP solution, UTP solution, GTP solution, enzyme mix) was prepared at room temperature in a nuclease-free tube and centrifuged briefly to collect the master mix at the bottom of the tube. The IVT master mix (30 μl) was transferred to each double-stranded cDNA sample, mixed thoroughly by gently vortexing and centrifuged briefly before placing in a thermal cycler block and incubated for 4 h (250 ng) at 40°C. The aRNA was frozen immediately at -20°C overnight.

2.2.5.2.5 aRNA purification

The purification of aRNA is required to remove enzymes, salts and unincorporated nucleotides. The aRNA binding mix was prepared at room temperature, consisting of RNA binding beads and aRNA binding buffer concentrate. The binding mix (60 μl) was added to each sample and transferred into a 96-well plate and then mixed by pipetting. To bind the sample to the RNA binding beads, 100% ethanol (120 μl) was added to each sample and mixed thoroughly by pipetting and shaking gently for 2 min on a plate shaker. RNA binding beads were captured by placing the plate onto a 96-well magnetic-ring stand (Ambion) for 5 min. Once the capture was complete, the mixture became transparent and the RNA binding beads formed pellets against the magnets in the magnetic field. The supernatant was removed and discarded. Beads were washed by the addition of 100 μl aRNA washing solution to each sample, shaken at moderate speed for 1 min and then placed on the magnetic stand again to capture the RNA binding beads. The washing step was repeated a second time. The plate was

moved to a plate shaker and shaken vigorously for 1 min to evaporate the residual ethanol from the beads. Purified aRNA from the RNA binding beads were eluted by the addition of 50 μl preheated (50-60°C) aRNA elution solution to each sample. The plate was shaken vigorously for 3 min to disperse the beads. The plate was moved onto the magnetic stand to capture the RNA binding beads once again. The supernatant containing the eluted aRNA was transferred to a nuclease-free tube and placed on ice for the next step.

2.2.5.2.6 Fragmentation

The concentration of the aRNA was quantified using the NanoDrop 1000 spectrophotometer (Thermo Scientific). All samples were diluted to 15 μg with nuclease-free water and the aRNA fragmentation mixture was added before incubation at 94°C for 35 min. The reaction was then immediately placed on ice.

2.2.5.2.7 Target hybridisation

The hybridisation cocktail was mixed for a 49 standard format array consisting of fragmented and labelled aRNA (15 μg), control oligonucleotide B2 (50 pM), hybridisation controls (*bioB* (1.5 pM), *bioC* (5 pM), *bioD* (25 pM), *cre* (100 pM)) (heated at 65°C for 5 min), 1x hybridisation mix, 10% DMSO, nuclease-free water. The hybridisation cocktail was then preheated to 99°C for 5 min and then immediately transferred to a 45°C heat block for 3 min. Meanwhile, a volume of the pre-hybridisation mix was pipetted through the septa of each probe arrays equilibrated to room temperature and incubated at 45°C for 10 min rotating. The pre-hybridisation mix was then removed and replaced with an appropriate volume of hybridisation cocktail. The arrays were incubated in the hybridisation oven at 45°C for 16 h rotating at 60 rpm.

2.2.5.2.8 Array washing and staining

The hybridisation cocktail was removed from the array and was filled with a volume of non-stringent wash buffer A (6x SSPE (0.9 M NaCl, 0.06 M NaH_2PO_4, 0.006 M EDTA), 0.01% Tween-20). The arrays were then immediately washed and stained using the Affymetrix GeneChip Fluidics Station 450/250, which was prepared with the appropriate buffers. The arrays were stained with streptavidin-phycoerythrin (2x stain buffer (100 nM MES, 1 M Na^+, 0.05% Tween-20), 50 mg/ml BSA, 1 mg/ml streptavidin phycoerythrin) and the fluorescent signal was amplified with biotinylated anti-streptavidin antibody (2x stain buffer, 50 mg/ml BSA, 10 mg/ml goat IgG, 0.5 mg/ml biotinylated anti-streptavidin). An automated protocol (Fluidic Script FS450-0001) was used on the fluidics station.

2.2.5.2.9 Array scan

Once the arrays were stained, they were scanned using an Affymetrix GeneChip Scanner 3000. The image from each array were saved as .DAT files.

2.2.5.3 Analysis of microarray data

Affymetrix GeneChip analysis was performed together with Dr. Caroline Johnston, King's College London. All analyses were carried out in Bioconductor. The simpleaffy package was used to assess array quality. The arrays were then normalised using Robust Multichip Average (RMA), consisting of three stages; 1) background correction, 2) quartile normalisation and 3) summarisation. The expression data was then log transformed before using LIMMA, a bioconductor package for MA analysis and moderated t-tests. P-values were corrected for multiple testing according to the false discovery rate (FDR) procedure of Benjamini and Hochberg (Benjamini and Hochberg, 1995).

2.2.5.4 Bioinformatics-Functional categorisation and pathway analysis

Genes were categorised into Gene Ontology (GO) biological processes according to the GO Consortium (http://www.geneontology.org/). This was performed using NetAffx and searches on GeneCards or NCBI Gene databases. Biological pathway analysis was performed using Ingenuity Pathway Analysis (IPA) software (http://www.ingenuity.com).

2.2.5.5 WebQTL

WebQTL is a internet based resource containing, amongst other data sets, biological traits and microarray-based gene expression data from more than 30 BXD recombinant inbred (RI) strain lines. RI lines were derived from a cross between the two common progenitor strains C57BL/6 (B) and DBA/2 (D) (BXD), followed by repeated sibling intercross of the F2 progenies. The recombination events are fixed in each RI line and therefore provides recombinant animals of the same genotype that are unlimited in number. By combining web-based analysis software with the database, webQTL can be used for searching for associations between a trait and genotypes at known marker loci for mapping quantitative trait loci (QTL) or for searching for correlations among traits. This web-based tool was used to identify the correlation of genes found in the current study with the expression of other genes across the BXD strains in hippocampal brain tissue.

2.2.6 Statistics

Statistical analysis was performed using either a one-way analysis of variance (ANOVA), two-way ANOVA, both followed by a Tukey *post hoc* test. The Students t-test was used where two groups were compared. These analyses were used when appropriate, as indicated in the text. All analysis was performed in SPSS version 15.0

or in Microsoft Excel. Data are presented as mean±SEM. In all analyses, significance was set at $p \leq 0.05$.

CHAPTER 3

Characterisation of the Humanised APOEε3 and APOEε4 Mouse Model

3.1. Introduction

Apolipoprotein E (apoE) is a key component of lipid transport and cholesterol metabolism not only within the periphery but also within the brain. The brain has the second highest concentration of apoE (Elshourbagy et al., 1985), produced locally by astrocytes (Boyles et al., 1985), although microglia and neurons also synthesise apoE under certain physiological and pathological conditions (Bao et al., 1996; Han et al., 1994; Xu et al., 1999; Xu et al., 1996). In human and mouse, the APOE gene consists of four exons and three introns. Human APOE is located at q13.31 on chromosome 19 (Olaisen et al., 1982; Paik et al., 1985), whilst the mouse APOE gene is located on band A2 of chromosome 7. In both human and mouse genes, exon 1 is non-coding (Horiuchi et al., 1989; Paik et al., 1985). ApoE is synthesised with a N-terminal signal peptide (Zannis et al., 1984) which undergoes intracellular processing before being secreted as a 34,200 Da (Mahley, 1988) mature glycoprotein consisting of 299 amino acids (Rall et al., 1982). The three isoforms of human apoE are distinguished by single amino acid differences that alter each isoform's structure and consequently their function (Figure 1.4).

Since the discovery of an association with the APOEε4 gene and Alzheimer's disease (AD) by Strittmatter and colleagues in 1993 (Strittmatter et al., 1993), the need to understand the role of apoE in the central nervous system (CNS) has grown enormously. As such, APOE mouse models have been increasingly used to understand the pathogenesis of AD.

The APOE models used in this project were originally generated by Dr Nobuyo Maeda and colleagues to study atherogenesis using gene targeting replacement technology. These mice were generated to overcome problems with earlier work where the creation of transgenic mice by pronuclear injection of human DNA resulted in expression of varying levels of the transgene, which was on a background of endogenous mouse apoE expression.

Gene targeting by homologous recombination in embryonic stem cells provides a means to generate animals with changes in specific genes and to more specifically study the effects of the transgene. In target replacement, mice retain the murine apoE regulatory sequences and thus produce solely human apoE proteins within the normal physiological range. The tissue distribution and levels are also identical to that of the endogenous gene.

The APOE KO model was generated using a plasmid containing a modification of the murine apoE locus where a portion of the WT mouse APOE gene that had been replaced by the marker genes, neomycin resistance and thymidine kinase, was electroporated into E14TG2a cells (Figure 3.1). Sucessfully electroporated cells were identified by positive neomycin resistance and were injected into blastocytes of C57BL/6J mice to produce chimeric mice (Piedrahita et al., 1992). Similarly, APOEε3 (Sullivan et al., 1997) and APOEε4 (Knouff et al., 1999) transgenic mice were achieved by electroporation of embryonic stem cells with a target construct containing the human coding sequence (exons 2-4) in combination with flanking sequences from mouse as shown in Figure 3.2. The resultant transgenic mice were homozygous for human APOEε3 or APOEε4.

Here I describe the genotyping of all mice used in the main studies of this project; chapters 4, 5 and 7 of this thesis.

Figure 3.1 Homologous integration of the APOE KO replacement gene

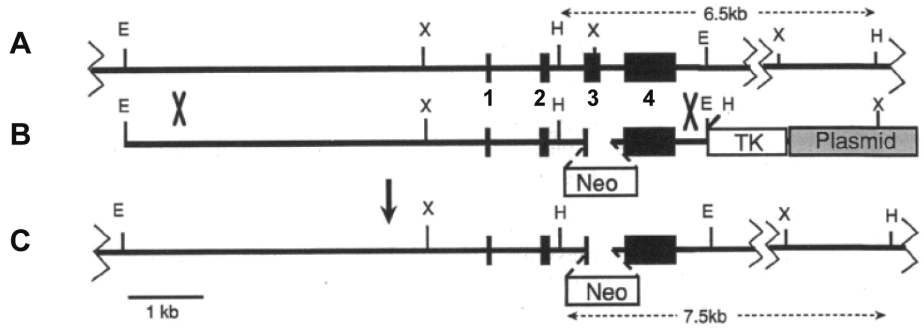

The structure of the WT mouse APOE locus shown in A), was targeted with the plasmid construct B) containing the neomycin resistance (Neo) and thymidine kinase (TK) genes for the selection of targeted embryonic stem cells. C) Shows the APOE locus after homologous recombination. Mouse exons 1-4 are indicated by solid boxes. Mouse regulatory and flanking sequences are indicated by solid lines. E, *Eco*RI; X, *Xmn*I; H, *Hin*dIII. This figure was taken from the original paper (Piedrahita et al., 1992).

Figure 3.2 Homologous integration of the human APOEε3 and APOEε4 transgenes

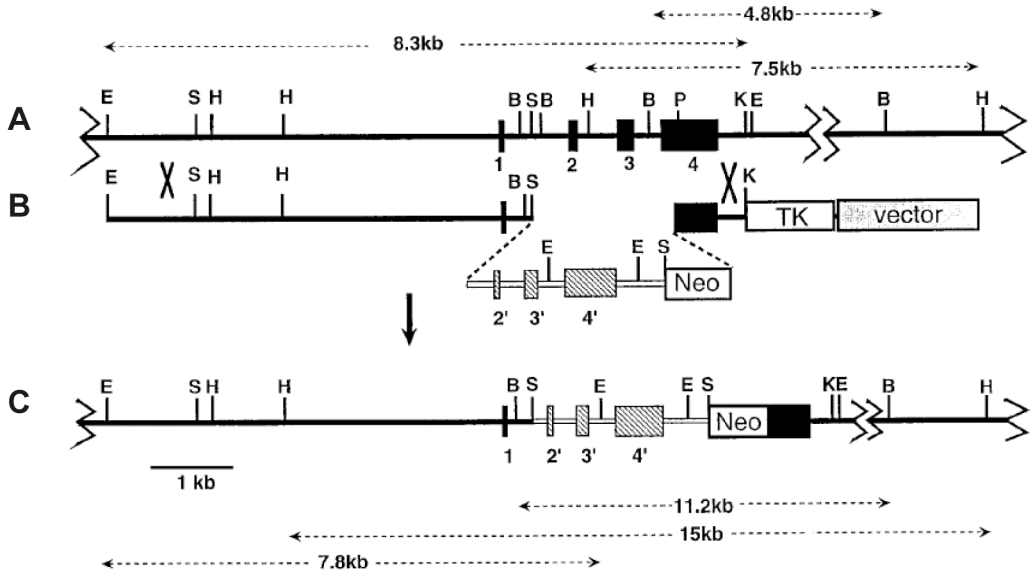

A) The structure of the WT mouse endogenous APOE locus was targeted with a construct containing the human APOEε3 or APOEε4 exons indicated by striped boxes and clear lines, and neomycin resistance (Neo) and thymidine kinase (TK) genes for the selection of targeted embryonic stem cells B). The structure of the genes after homologous recombination is shown in C). E, *Eco*RI; S, *Sac*I; H, *Hin*dIII; P, *Pv*uI; K, *Kpn*I; X, *Xba*I; B, *Bam*HI. Figure was taken from the original paper (Sullivan et al., 1997).

3.2 Results

All transgenic mice; APOEε3, APOEε4, together with APOE knockout (KO) and background strain C57BL/6 (WT) were genotyped by GlaxoSmithKline at the beginning of each *in vivo* study, discussed in the following chapters. However, once these studies were completed we ensured the APOE genotypes of all mice were correctly labeled. The APOE genotypes of transgenic mice were determined using a range of techniques in order to distinguish human APOE from mouse APOE, as described below.

3.2.1 Identification of APOE mice by western blotting

Terminal bleeds from all mice were processed and the plasma was taken for the detection of apoE by western blotting. Protein bands were detected as a doublet around 34 kDa in all mice transgenic for the human APOEε3 or APOEε4 genes. In WT mice, a lower band at 32 kDa was observed for mouse apoE. Protein bands were absent for apoE in APOE KO mice (Figure 3.3).

Figure 3.3 Western blot of apoE in mouse plasma

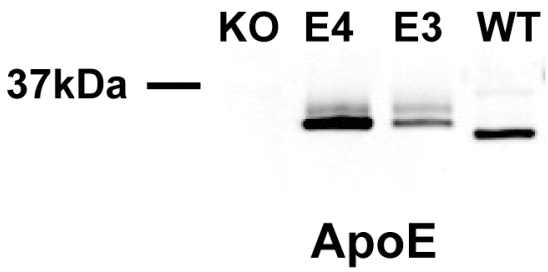

APOEε3 and APOEε4 transgenic mice show a protein band as a doublet around 34 kDa, WT mice show a band at 32 kDa, whilst in APOE KO mice no protein bands were detected. Samples were collected by colleagues at GlaxoSmithKline.

3.2.2 Genotyping of mice by the TaqMan and the polymerase chain reaction

As the western blotting method was unable to distinguish between the human isoforms of APOE, the TaqMan SNP assay was used to identify mice carrying the APOEε3 or APOEε4 alleles. In these experiments we used liver tissue as an alternative source to plasma and because a greater quantity of DNA can be extracted from liver. Fluorescent signals from the TaqMan assay were plotted as shown in Figure 3.4; two different reporter dyes (FAM and VIC) at the endpoint plate read indicate the presence of either a APOEε3 (blue dots) or APOEε4 (red dots) allele within a sample. Samples in which the reaction failed during the assay are represented by the black crosses on the graph. Within the APOE transgenic mice, a total of 53 out of the 82 expected samples were called positive for either the APOEε3 or APOEε4 allele. The assay was repeated with the samples expected to have an APOEε3 or APOEε4 allele however, the assay failed repeatedly. Consequently, we had to rely on the combination of genotyping data provided by GlaxoSmithKline and data from western blotting.

The remaining samples which were uncalled (black crosses) from the TaqMan assay consisting of APOE KO and WT mice were distinguished from each other by PCR. Primers were designed specifically to recognise a region of the neomycin gene. This gene is one of the selectable markers that replaced part of the murine APOE gene during the generation of APOE KO mice and were also included in the transgenic APOEε3 and APOEε4 plasmid constructs. Thus, when the PCR products were ran on an agarose gel, only APOE KO, APOEε3 and APOEε4 mice would show the presence of a band at 170 bp (Figure 3.5).

Figure 3.4 TaqMan allelic discrimination plot

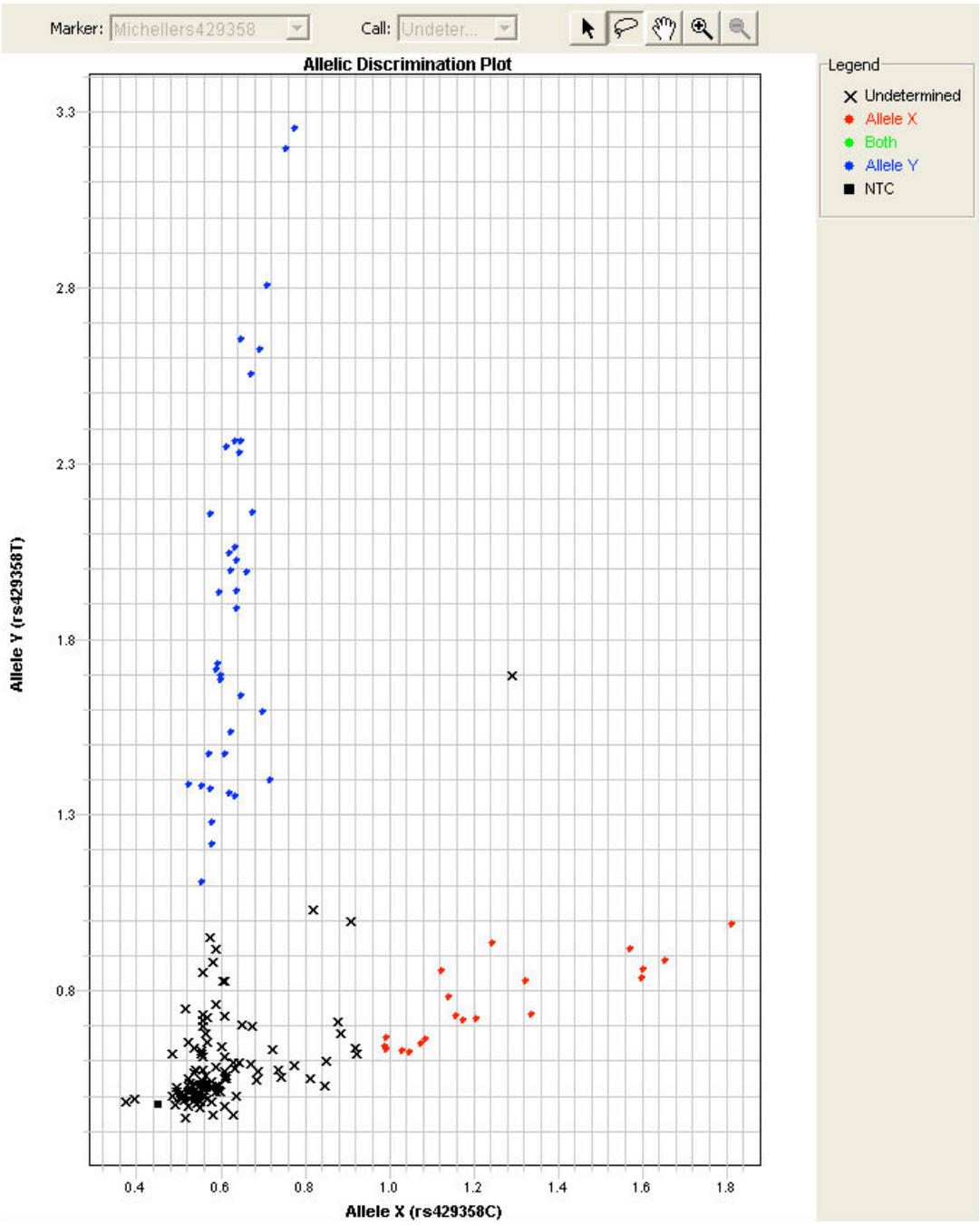

There is one differing amino acid between the ε3 and ε4 alleles, ε3 was detected as rs429348T (Allele Y) and ε4 detected as rs429348C (Allele X). The blues dots represent transgenic mice with the APOEε3 allele, the red dots represent transgenic mice with the APOEε4 allele. The wells where the reaction failed are uncalled and are indicated by black crosses.

Figure 3.5 Electrophoresis of PCR products from using primers for the neomycin gene

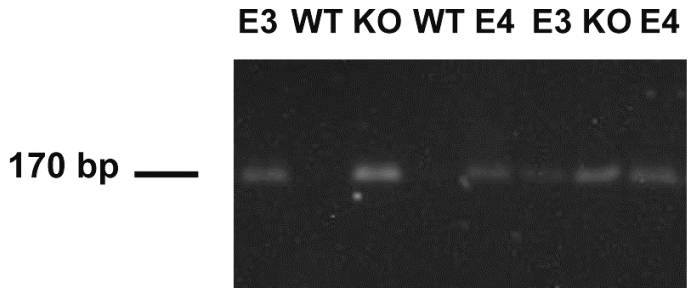

Bands visualised at 170 bp represents the neomycin gene present in the APOE KO, APOEε3 and APOEε4 target constructs. The normal WT mouse APOE gene does not contain the neomycin resistance gene.

3.3 Discussion

In this chapter, genotyping experiments were set up to determine the APOE genotype of mice used in the studies described in the following chapters. A range of techniques was used to distinguish human APOE from mouse APOE and both of these from APOE KO mice.

The three APOE mouse models (APOE KO, APOEε3 and APOEε4) were generated by the Maeda group using the concept of gene targeting in embryonic stem cells (Knouff et al., 1999; Piedrahita et al., 1992; Sullivan et al., 1997). By replacing the coding sequence for mouse apoE with human apoE allows the expression of human apoE with identical tissue distribution and levels to that of WT mouse apoE.

In the TaqMan assay 29 samples which we expected to be APOEε3 or APOEε4 failed to be identified, despite repeated runs of the assay. This is likely due to poor DNA quality or a high level of impurities in the DNA samples. However, western blotting data showed these samples contain human apoE and with the information given by GlaxoSmithKline we were confident these samples were correctly identified. We also successfully identified all APOE KO from WT mice that failed to give a fluorescent signal in the TaqMan assay by PCR. All APOE KO samples showed a band at 170 bp as a product of the PCR reaction with the neomycin primer. Both of these techniques (TaqMan and PCR) confirm results observed in western blotting.

Human apoE is posttranslationally modified and was detected as two bands by western blotting. The lower band represents the mature apoE protein whilst the upper band represents the sialylated form of apoE. Contrastingly, mouse apoE is detected as one band only. In humans, the apoE protein is subject to O-linked glycosylation by the addition of sialic acid (Jain and Quarfordt, 1979; Zannis and Breslow, 1981) to the threonine (Thr) 194 residue (Wernette-Hammond et al., 1989). The lack of sialylation in WT mouse apoE is because the Thr194 residue is not conserved (Weisgraber, 1994). Interestingly apoE in the brain is more sialylated (Pitas et al., 1987) and is detected as

multiple bands which can be removed upon neuraminidase treatment (Zannis and Breslow, 1981). The role of sialylation is unclear but as the addition of carbohydrate groups renders proteins biologically active, and in brain there is increased sialylation of apoE, it may be indicative of an important CNS function. It has been speculated that apoE sialylation is involved in neuronal growth, regeneration of the peripheral and central nervous systems and recently in formation of lipid particles and the deposition of Aβ in the brain (Kawasaki et al., 2009; Sugano et al., 2008).

The function of mouse and human apoE are similar however human apoE exists as three isoforms, differing by arginine (Arg) or cysteine (Cys) residues at positions 112 and 158, whilst mice have one form only. An interaction between the N- and C-terminal domains is a unique property of the apoE4 isoform, mediated by a salt bridge between glutamine (Glu) 225 and Arg61, promoted by Arg112. Regarding structure, mouse apoE is similar to human apoE4 containing the equivalent Arg112 and Glu225 but lacks Arg61, instead mouse has a threonine residue at this position (Figure 1.4). Thus, domain interaction by formation of a salt bridge between Arg61 and Glu225 is prevented making mouse apoE functionally more similar to human apoE3, including its preferential binding to high density lipoproteins (Weisgraber, 1994). Furthermore, introducing the Thr61Arg mutation in mice creates a human apoE4-like molecule (Raffai et al., 2001).

Mouse models of APOE have long been used for the studies of atherosclerosis and cholesterol metabolism (Breslow, 1996; Meir and Leitersdorf, 2004) because there were no adequate *in vitro* systems were available. After the discovery of an association between apoE and AD, the APOE mouse models were made use for investigating AD pathogenesis. Mouse models used for research in the AD field not only include gene target replacement mice which replaces murine apoE with human apoE but also mice that express human apoE in astrocytes and neurons under the GFAP (glial fibrillary acidic protein) or for example the NSE (neuron-specific enolase) promoters, respectively (Huber et al., 2000; Lesuisse et al., 2001; Raber et al., 1998; Sun et al.,

1998; Tesseur et al., 2000). These have proven to be particularly useful in the analysis of cell specific effects of apoE isoforms on Aβ and tau pathology.

In summary, all transgenic mice were characterised with regard to APOE genotype. Tissues from these mice were then subsequently analysed as described in the following chapters.

CHAPTER 4

The Effects of Diet-Induced Insulin Resistance on Tau Phosphorylation and Aβ Metabolism in Humanised APOEε3 and APOEε4 Mice

4.1 Introduction

Type 2 diabetes mellitus (T2DM) is a risk factor of Alzheimer's disease (AD). T2DM is characterised by a gradual decline in insulin action due to insulin-responsive tissues developing a reduced response to insulin, and is described as insulin resistance (Gispen and Biessels, 2000). As a consequence, the β-cells of the pancreas compensate by increasing the secretion of insulin to maintain the normal glucose levels in the blood. Of the 2.6 million individuals currently diagnosed with diabetes in the UK, T2DM accounts for 90% of the cases (Diabetes UK). This figure is still set to rise because the population is aging and obesity is increasing.

Insulin resistance is regarded as the underlying cause of the metabolic syndrome (Gallagher et al., 2010). Interestingly, there is evidence of a synergistic interaction between T2DM and APOE, in particular, the APOEε4 isoform of APOE. T2DM patients carrying the APOEε4 allele have an increased risk for AD, and neuropathological studies have reported the highest number of AD lesions in brain tissue of ε4 diabetic patients compared to age-matched controls (Peila et al., 2002). However, other studies have produced conflicting findings and have failed to show an increase in AD-related pathology in diabetic brain (Alafuzoff et al., 2009; Arvanitakis et al., 2006b; Heitner and Dickson, 1997).

Further evidence for a link between insulin signalling and AD comes from rodent models. The use of rodent models has greatly increased our knowledge of neuropathological disease mechanisms. However, these *in vivo* models are complex with some apparently contradictory evidence coming from genetic versus dietary, and from type 1 versus type 2 diabetes models. For example, diet-induced insulin resistance accelerates Aβ pathology (Ho et al., 2004), whilst peripheral insulin injection induces tau phosphorylation in brain (Freude et al., 2005). Gene deletion experiments of the neuronal insulin receptor (NIRKO) and insulin receptor substrate 2 (IRS2) in mice, which induces insulin resistance, reduces Aβ deposition (Killick et al., 2009) and

yet, counter-intuitively, increase tau phosphorylation (Killick et al., 2009; Schubert et al., 2003; Schubert et al., 2004).

Since it is unclear what role apoE may play in APP metabolism and tau phosphorylation when insulin signalling is impaired, we explored this by utilising an APOE humanised mouse model. Mice lacking the mouse APOE gene and is replaced with the human APOEε3 or APOEε4 gene (Knouff et al., 1999; Piedrahita et al., 1992; Sullivan et al., 1997). In order to model diet-induced insulin resistance, these mice were fed on a high fat diet.

4.2 Results

4.2.1 Mice fed HFD develop diet-induced insulin resistance

APOE KO, APOEε3, APOEε4 and WT mice were fed either a high fat diet (HFD, 60% fat) or low fat diet (LFD, 10% fat) for 32 weeks to induce insulin resistance. Throughout the 32 weeks, food consumption and body weights were monitored weekly. Metabolic tests were carried out at 6 week intervals to monitor diet-induced insulin resistance in mice.

4.2.1.1 High fat feeding promotes weight gain

Throughout the 32 weeks, HFD fed mice gained significantly more weight than LFD fed mice. All mice displayed a similar weight prior to initiation of the study. It is apparent in both dietary conditions that WT mice gained the least weight; WT mice weighed less than the other HFD fed mice from the beginning of the study but all mice fed on a HFD followed a similar pattern of weight gain (Figure 4.1). Mice fed with HFD gained weight as early as 6 weeks: APOE KO gained 13.9±0.8 g higher than baseline weight, APOEε3 gained 13.2±1.2 g, APOEε4 gained 14.0±1.2 g and WT gained 8.7±1.0 g (Figure 4.1B). On the other hand, LFD fed mice showed a slight increase in body weight compared to their starting weight: APOE KO 4.4±0.4 g, APOEε3 4.6±0.5 g, APOEε4 4.4±0.6 g and WT 1.7±0.3 g (Figure 4.1A). As the weeks progressed, the body weights of mice fed on a HFD increased dramatically. At the end of the study (week 32), HFD mice gained an average weight of APOE KO 31.5±0.8 g, APOEε3 25.2±0.6 g, APOEε4 26.9±1.4 g and WT 25.6±1.0 g (Figure 4.1B). In contrast LFD fed mice showed a modest increase body weight gain: APOE KO 11.4±0.8 g, APOEε3 12.5±1.7 g, APOEε4 11.7±1.3 g and WT 8.0±0.9 g (Figure 4.1A). APOE KO, APOEε3 and APOEε4 mice weighed significantly more than the WT mice throughout the study as indicated in Figure 4.1A and B.

Figure 4.1 Body weight increases in HFD fed mice

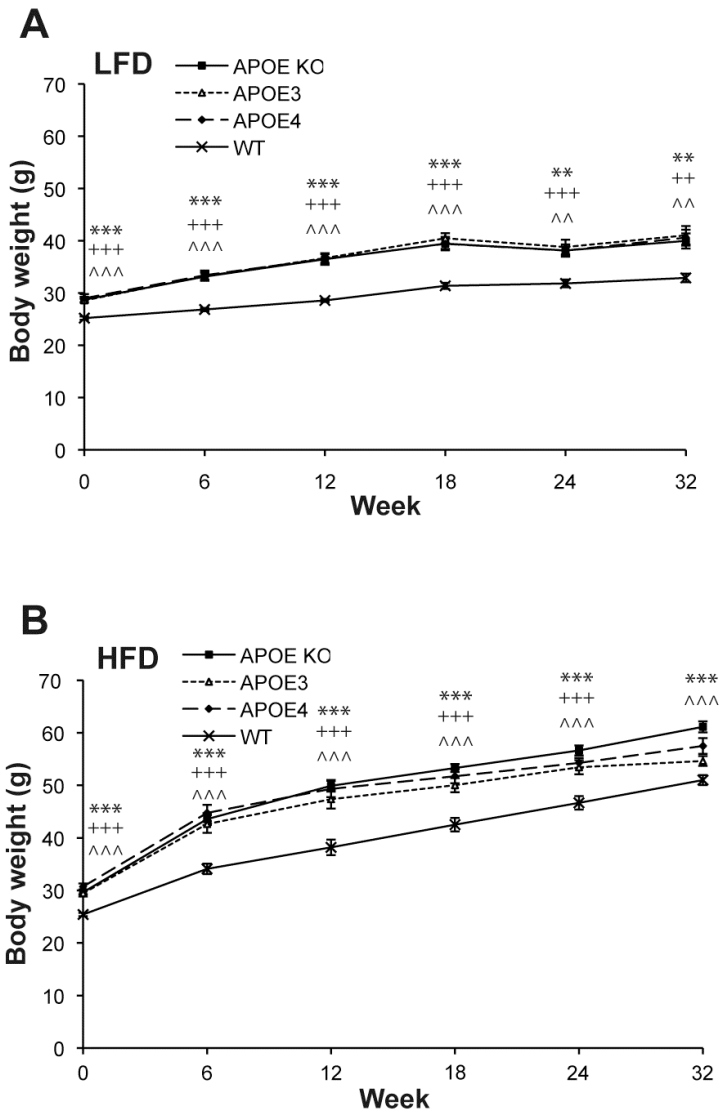

Body weight of APOE KO, APOEε3, APOEε4 and WT mice over 32 weeks of A) low fat diet (LFD) and B) high fat diet (HFD), starting from 3 months of age. Data were generated by colleagues at GlaxoSmithKine. Data are represented as mean±SEM, n = 10-12. Body weights in A) and B) reached **p<0.01, ***p<0.001 by one-way ANOVA with Tukey *post hoc* test at all weeks indicated compared to WT mice. Significance is indicated by * APOE KO, + APOEε3, ^ APOEε4.

4.2.1.2 Mice fed HFD develop impaired glucose metabolism

The oral glucose tolerance test (OGTT) was taken at baseline and at 6 weekly intervals following the initiation of study. This test was used to assess for impaired glucose metabolism in mice throughout the study. OGTT measures the ability of the body to metabolise glucose and to clear it from the blood stream; glucose is given orally after an overnight fast and blood samples are taken for glucose measurement over a time course of 180 minutes. In a normal OGTT curve, blood glucose at baseline fasting state rises steeply after the administration of a bolus of glucose, which reaches a peak around 30 minutes. At this time, insulin production increases within the pancreas and blood glucose levels begin to fall. Insulin causes the liver and muscles to remove glucose from the blood and to convert it into glycogen stores, thus the OGTT curve falls. The OGTT curve gradually tails off as blood glucose levels are bought to the normal fasting levels towards the end of 180 minutes. The key findings of the OGTT between LFD and HFD mice are as follows.

- All mice have normal OGTT curves at week 0 baseline (before commencement of study) (Figure 4.2A and B).

LFD fed mice:

- In all LFD mice, throughout weeks 6, 12, 18, 24 and 32, the OGTT curve appears to be normal and similar shape to week 0 baseline; blood glucose peaks at 30 minutes, falls by 60 minutes and gradually tails off over time towards 180 minutes when blood glucose returns to fasting levels (Figures 4.2C, E, G, I and K).

HFD fed mice:

- At week 6, all HFD mice begin to show signs of impaired glucose metabolism as glucose elimination occurred at a slower rate (Figure 4.2D).

- At weeks 6 and 12, APOEε3 and APOEε4 mice glucose metabolism seem to be more impaired compared to WT and APOE KO mice (Figures 4.2D and F). Glucose levels in APOEε3 and APOEε4 mice peaked at 60 minutes and elimination occurred at a much slower rate.

- Throughout weeks 18, 24 and 32 glucose metabolism in all HFD mice became increasingly impaired (Figure 4.2H, J and L). Blood glucose was increasingly removed at a much slower rate compared to week 6. The peak and the tail of the OGTT curve are less well defined in all mice.

Figure 4.2 Mice develop impaired glucose metabolism over 32 weeks of high fat feeding

Oral glucose tolerance tests (OGTT) were conducted at baseline and then at 6 weekly intervals. Mice were fasted overnight. The following morning, mice were placed in a warming chamber prior to blood sampling and blood was taken by direct venopuncture. Mice were then given a single dose of glucose by oral gavage (3 g/kg, dose volume 10 ml/kg) and serial blood samples collected from the tail tip post-dose at 30, 60, 90, 120 and 180 min. Glucose levels were accessed using a blood glucose meter by colleagues at GlaxoSmithKline. Graphs show plasma glucose concentrations at weeks 0, 6, 12, 18, 24 and 32 of APOE KO, APOEε3, APOEε4 and WT mice fed A, C, E, G, I, K) LFD and B, D, F, H, J, L) HFD. Data were generated by colleagues at GlaxoSmithKine. Data are represented as mean±SEM, n = 10-12. *p<0.05, **p<0.01, ***p<0.001 versus WT mice by one-way ANOVA with Tukey *post hoc* test. Significance is indicated by * APOE KO, + APOEε3, ^ APOEε4.

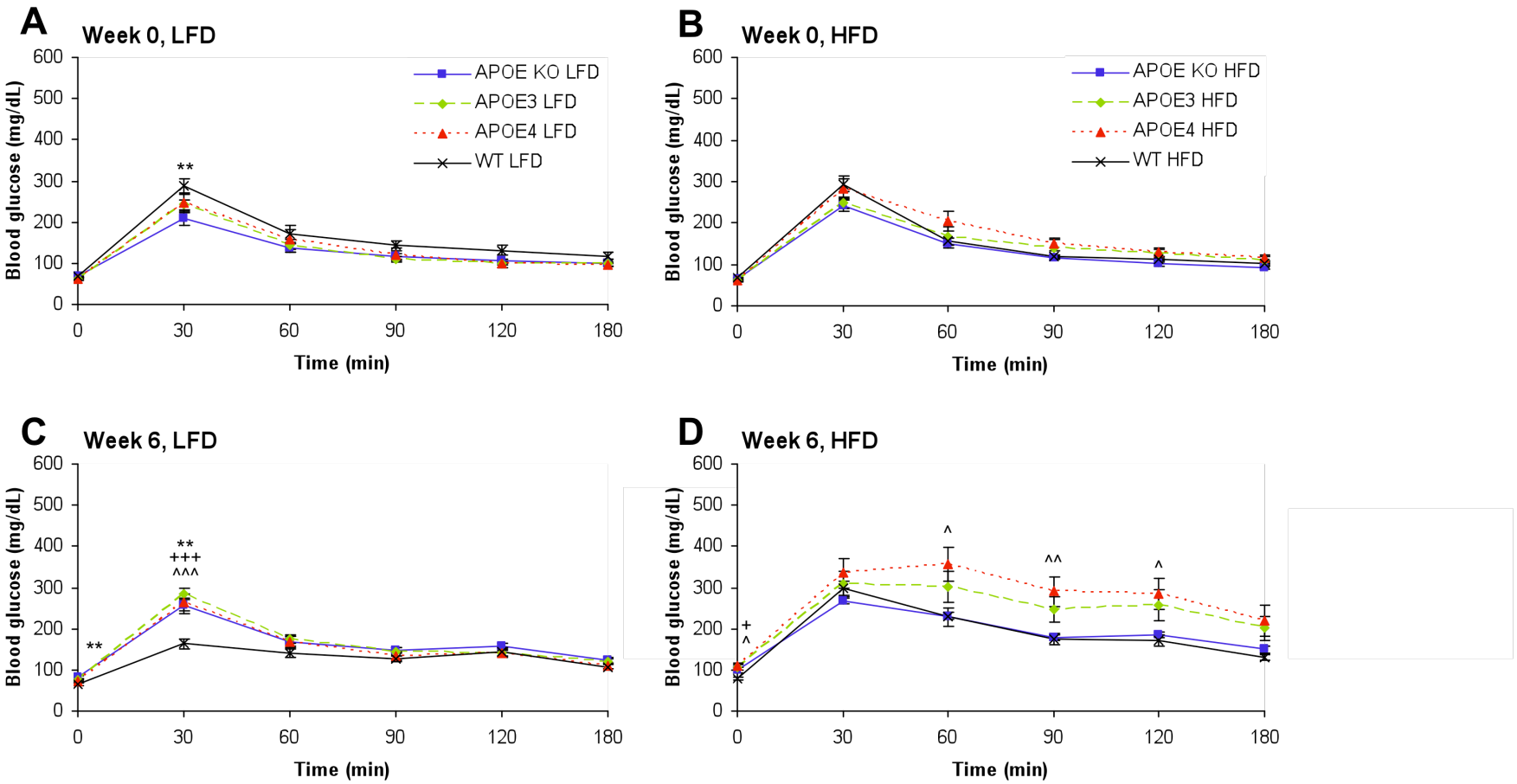
A
Week 0, LFD
APOE KO LFD
APOE3 LFD
APOE4 LFD
WT LFD
Blood glucose (mg/dL)
Time (min)
B
Week 0, HFD
APOE KO HFD
APOE3 HFD
APOE4 HFD
WT HFD
Blood glucose (mg/dL)
Time (min)
C
Week 6, LFD
Blood glucose (mg/dL)
Time (min)
D
Week 6, HFD
Blood glucose (mg/dL)
Time (min)

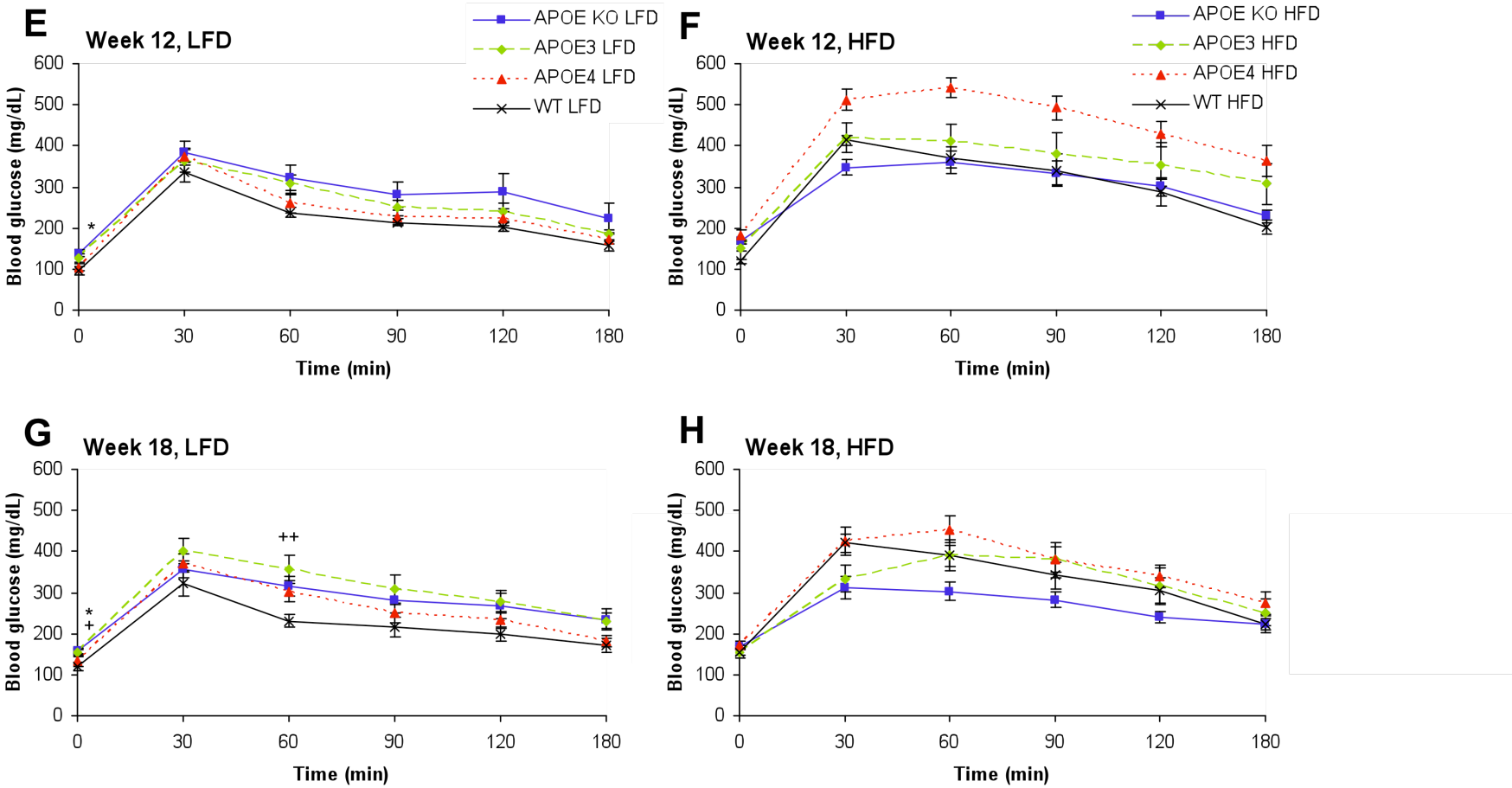
E
Week 12, LFD
APOE KO LFD
APOE3 LFD
APOE4 LFD
WT LFD
Blood glucose (mg/dL)
Time (min)
F
Week 12, HFD
APOE KO HFD
APOE3 HFD
APOE4 HFD
WT HFD
Blood glucose (mg/dL)
Time (min)
G
Week 18, LFD
Blood glucose (mg/dL)
Time (min)
H
Week 18, HFD
Blood glucose (mg/dL)
Time (min)

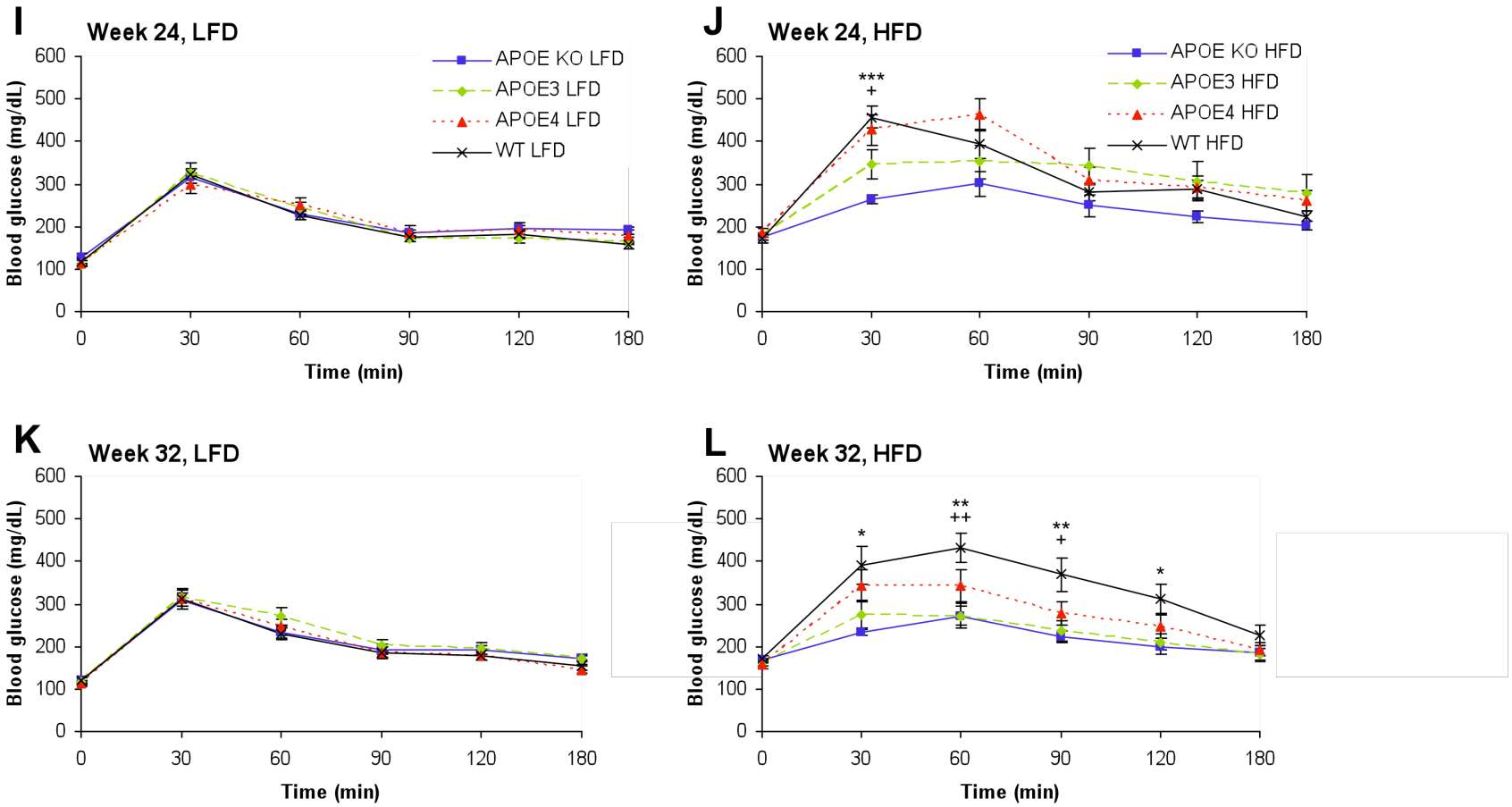
I
Week 24, LFD
APOE KO LFD
APOE3 LFD
APOE4 LFD
WT LFD
Blood glucose (mg/dL)
Time (min)
J
Week 24, HFD
APOE KO HFD
APOE3 HFD
APOE4 HFD
WT HFD
***
+
K
Week 32, LFD
L
Week 32, HFD
**
++
*

4.2.1.3 Fasting plasma insulin levels increase in HFD fed mice

Blood samples from fasted mice were taken at 6 weekly intervals, before the OGTT was carried out. Blood was processed and plasma was measured for insulin levels by ELISA.

At baseline, all mice had similar levels of plasma insulin. Beginning from week 6 and as the weeks progressed plasma insulin levels elevated which accompanied hyperglycaemia in all groups of HFD fed mice. At the end of the 32 weeks study, all the HFD group of mice had statistically significantly elevated levels of plasma insulin in comparison to the LFD group, with the highest in APOEε4 (5.9±0.5 μg/l) followed by APOEε3 (5.2±0.6 μg/l), APOE KO (4.8±0.5 μg/l) and then WT (3.5±0.6 μg/l) (Figure 4.3B). In contrast, mice fed with LFD had similar levels of insulin at the end of the 32 weeks study compared to baseline: APOE KO 0.8±0.1 μg/l, APOEε3 0.8±0.1 μg/l, APOEε4 0.8±0.2 μg/l and WT 0.4±0.1 μg/l (figure 4.3A).

The homeostatic model assessment of insulin resistance (HOMA-IR) was calculated as a measure of insulin sensitivity. HOMA-IR did not differ between diet groups prior to the initiation of study however, HOMA-IR was significantly increase ($p<0.001$) in all HFD fed mice compared to LFD fed mice within each genotype after 32 weeks of feeding (Figure 4.3C).

Figure 4.3 HFD fed mice develop diet-induced insulin resistance

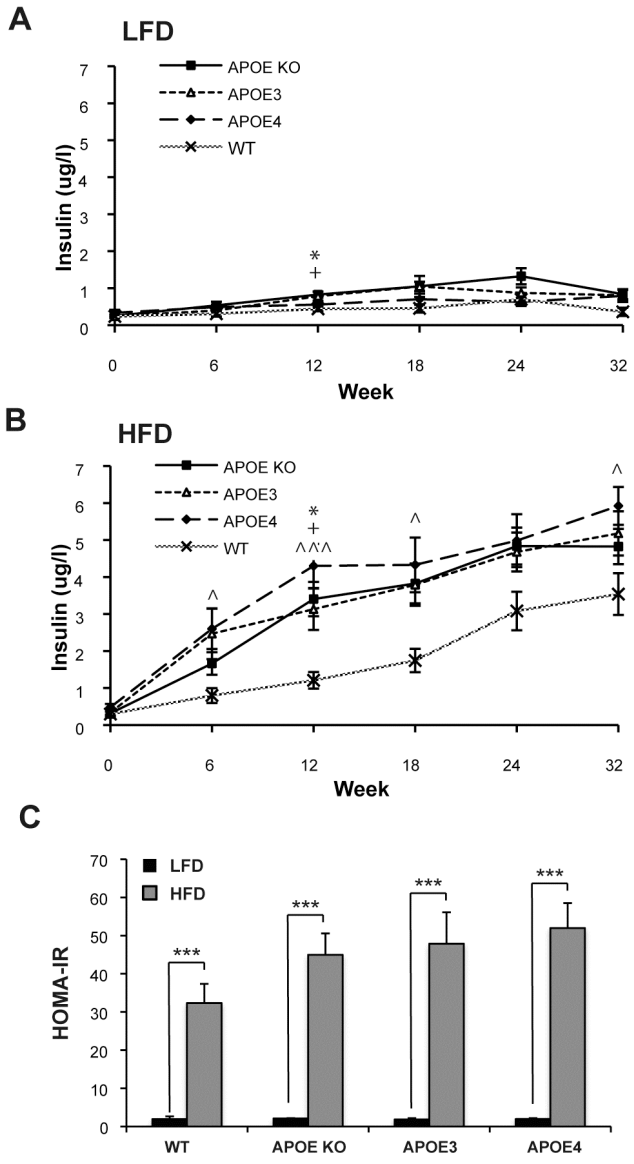

Plasma insulin levels were measured in APOE KO, APOEε3, APOEε4 and WT mice over 32 weeks of feeding with A) LFD and B) HFD. Blood samples from the tail vein at each OGTT were collected and plasma was analysed for ifasting nsulin levels by ELISA. C) Homeostatic model assessment of insulin resistance (HOMA-IR) after 32 weeks of HFD, HOMA-IR was calculated using the formula (fasting blood glucose*fasting insulin)/405. In A) plasma insulin levels in all LFD fed mice reached *p<0.05 by one-way ANOVA with Tukey *post hoc* test compared to WT mice. In B) plasma insulin levels in HFD fed mice reached *p<0.05, **p<0.01 or ***p<0.001 by one-way ANOVA with Tukey *post hoc* test compared to WT mice as indicated. Significance is indicated by * APOE KO, + APOEε3, ^ APOEε4. In C) ***p<0.001 by Student's t-test.

Samples were provided by colleagues at GlaxoSmithKline. Data are represented as mean±SEM, n = 10-12.

4.2.2 Tau phosphorylation is reduced in HFD fed mice

Three phospho-tau epitopes (Ser396, Ser202/Thr205 and Thr231) were examined on western blots; immunoreactivity for tau was observed around the 50 kDa size marker with each of these phospho-epitope specific sera and with a non-phospho dependent antibody, Dako A0024, raised against human tau. Phospho and non-phospho tau immunoreactivity was detected using an near infrared scanner and quantitated using IMAGEJ software. Phospho-immunoreactivity was determined from the ratio of phospho-specific to total tau immunoreactivity on the same blots. In the comparison between HFD and LFD fed mice, a decrease in tau phosphorylation was detected in the insulin resistant mice at all three tau epitopes. This decrease was preserved across all genotypes with a significant decrease in tau phosphorylation in HFD fed WT and APOEε4 mice at the Ser202/Thr205 ($p=0.01$ and $p=0.03$, respectively) and Thr231 ($p=0.04$ and $p=0.04$, respectively) epitopes, and a trend towards reduction at Ser396 (Figure 4.4B). Analysis of all genotypes and all phospho-tau epitopes by two-way ANOVA shows a significant interaction between diet and tau phosphorylation ($p<0.05$) but no effect of genotype. Combining all genotypes and comparing LFD and HFD groups shows a highly significant effect of tau phosphorylation at all three epitopes examined (Ser396 $p=0.03$, Ser202/Thr205 (AT8) $p<0.001$ and Thr231 (AT180) $p=0.008$) (Figure 4.4C, F and I).

Figure 4.4 Tau phosphorylation is reduced in HFD fed mice, independent of APOE genotype

The cortical brain region from mice were homogenised in sucrose homogenisation buffer, lysates were then immunoblotted with the indicated antibodies. A, D, G) Western blot of tau antibodies in the frontal cortex of APOE KO, APOEε3, APOEε4 and WT mice fed LFD or HFD. B, E, H) Density of phosphorylated tau normalised against total tau. C, F, I) Tau phosphorylation is dependent on diet. Phosphorylated tau is normalised to total tau, data is grouped by diet. Analysis of all genotypes and all phospho-tau epitopes by ANOVA shows a significant interaction between diet and tau phosphorylation ($p<0.05$). Samples were provided by colleagues at GlaxoSmithKline. Data are represented as mean±SEM, n = 8-12, *$p<0.05$; **$p<0.01$; ***$p<0.001$ by Student's t-test.

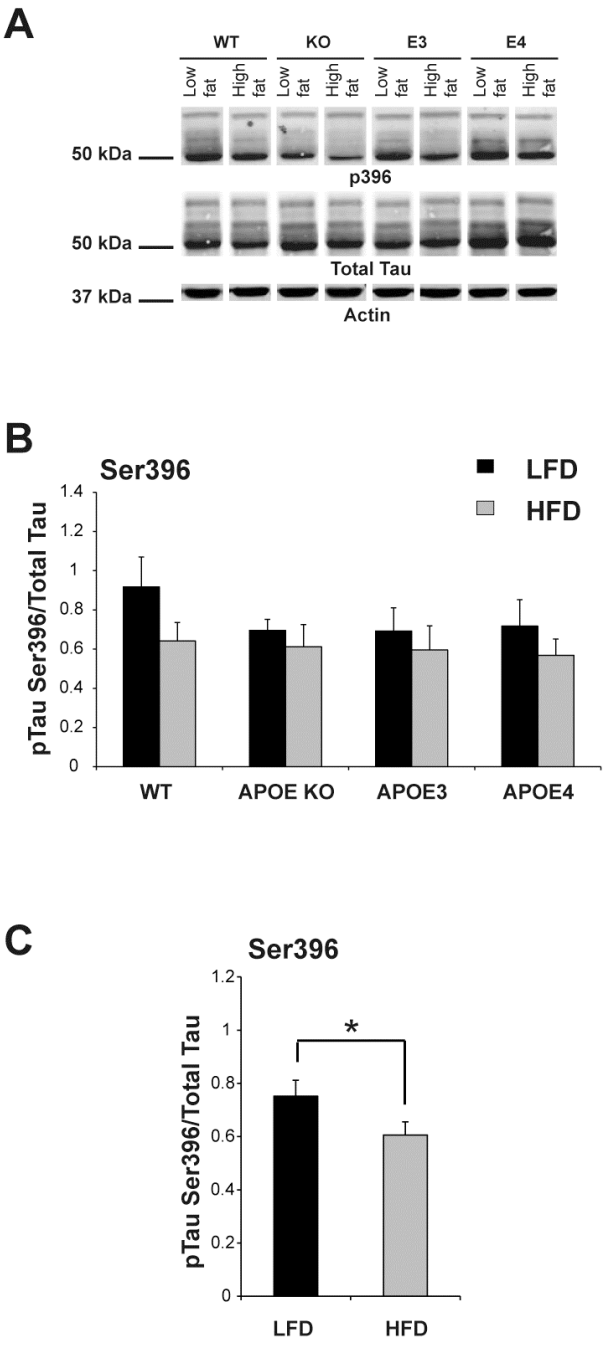
A
WT
KO
E3
E4
Low fat
High fat
50 kDa
p396
Total Tau
37 kDa
Actin
B
Ser396
LFD
HFD
pTau Ser396/Total Tau
WT
APOE KO
APOE3
APOE4
C
Ser396
pTau Ser396/Total Tau
*
LFD
HFD

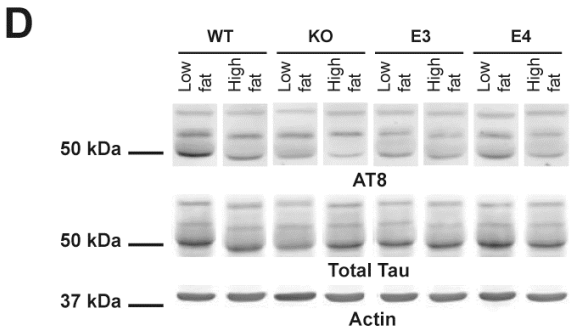
D
WT
KO
E3
E4
Low fat
High fat
50 kDa
AT8
50 kDa
Total Tau
37 kDa
Actin

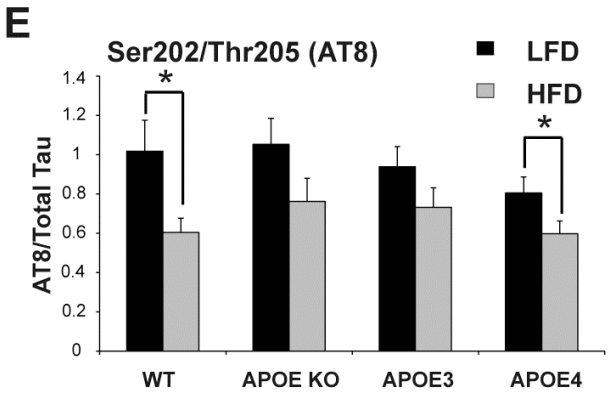
E
Ser202/Thr205 (AT8)
LFD
HFD
AT8/Total Tau
1.4
1.2
1
0.8
0.6
0.4
0.2
0
*
*
WT
APOE KO
APOE3
APOE4

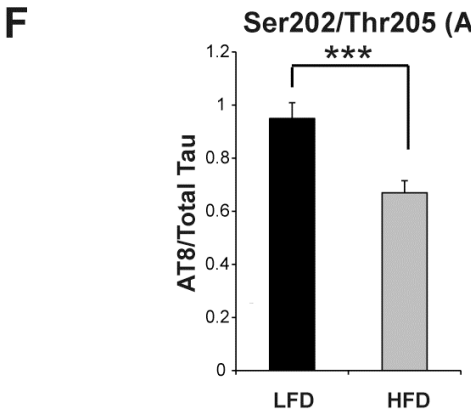
F
Ser202/Thr205 (AT8)
***
AT8/Total Tau
1.2
1
0.8
0.6
0.4
0.2
0
LFD
HFD

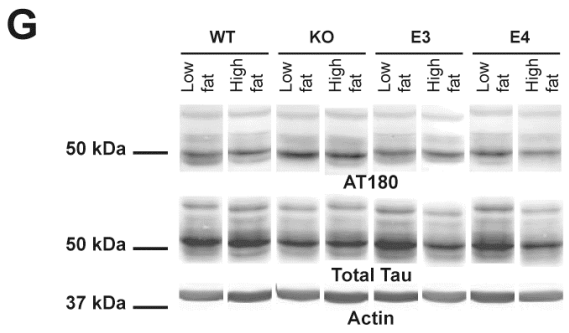
G
WT
KO
E3
E4
Low fat
High fat
50 kDa
AT180
50 kDa
Total Tau
37 kDa
Actin

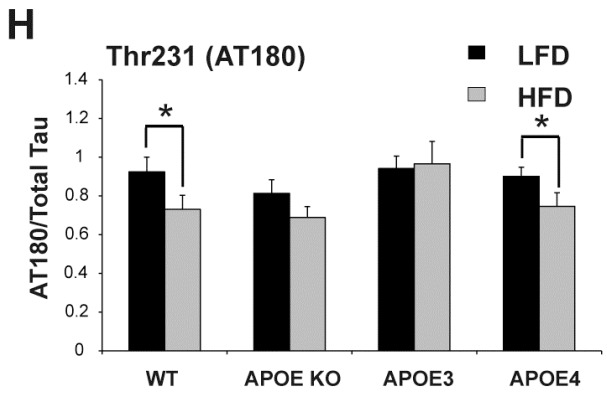
H
Thr231 (AT180)
LFD
HFD
AT180/Total Tau
1.4
1.2
1
0.8
0.6
0.4
0.2
0
*
*
WT
APOE KO
APOE3
APOE4

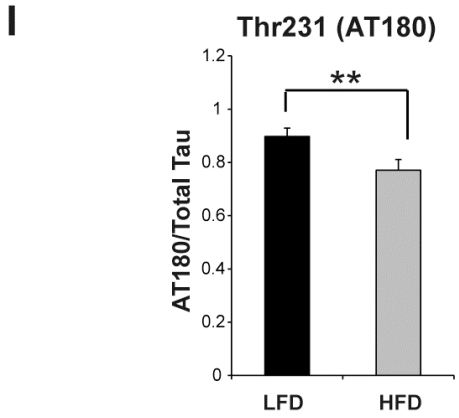
I
Thr231 (AT180)
AT180/Total Tau
1.2
1
0.8
0.6
0.4
0.2
0
**
LFD
HFD

4.2.3 APP metabolism is unchanged in HFD fed mice

The levels of soluble $A\beta_{40}$ and $A\beta_{42}$ were measured by ELISA. A trend was detected whereby HFD fed WT, APOEε3 and APOEε4 mice had higher levels of $A\beta_{40}$ whereas in APOE KO mice fed HFD, a reduced level was observed (Figure 4.5A). Similarly, $A\beta_{42}$ levels appeared higher in WT, APOE KO and APOEε4 mice fed HFD whereas in APOEε3 mice lower levels of $A\beta_{40}$ were detected (Figure 4.5B). These alterations in both Aβ species did not reach statistical significance.

For APP processing, the Triton-soluble fraction from brain samples were measured by western blotting (section 2.2.3.3). Figure 4.6A shows three bands around 110 kDa representing full length APP, whilst five bands were resolved for the phosphorylated forms of APP C-terminal fragments (APP-CTFs); C83, C89 and C99, between 10 kDa-15 kDa. The non-amyloidogenic and amyloidogenic processing (α- and β-processing respectively) of APP was assessed by measuring the levels of APP-CTFs C83 & C89 (non-amyloidogenic) and C99 (amyloidogenic). The levels of full length APP were not significantly altered when mice were grouped by genotype or diet (Figure 4.6B and C). No significant changes were observed in the APP-CTFs C83 & C89 and C99 when mice were grouped by genotype or diet (Figure 4.6D-G).

Figure 4.5 Levels of soluble $A\beta_{40}$ and $A\beta_{42}$ in mice fed LFD or HFD for 32 weeks

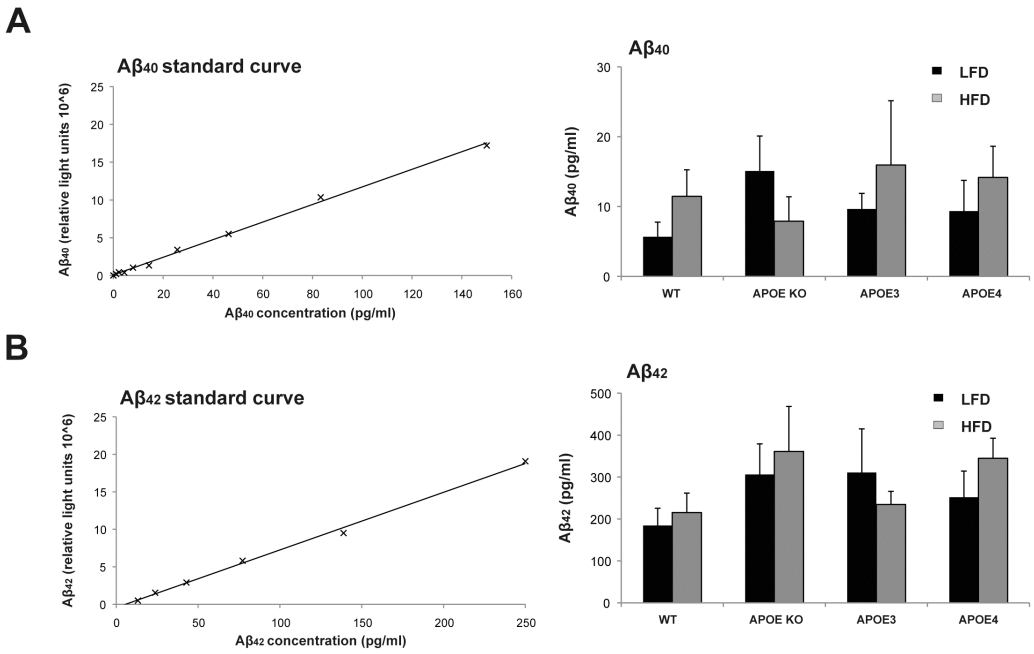

Soluble levels of Aβ were analysed by ELISA. A) Standard curve and $A\beta_{40}$ levels, and B) standard curve and $A\beta_{42}$ levels, in the brain of mice fed LFD or HFD. Samples were provided by colleagues at GlaxoSmithKline. Data are represented as mean±SEM, n = 5-9.

Figure 4.6 APP processing is not altered in mice fed HFD

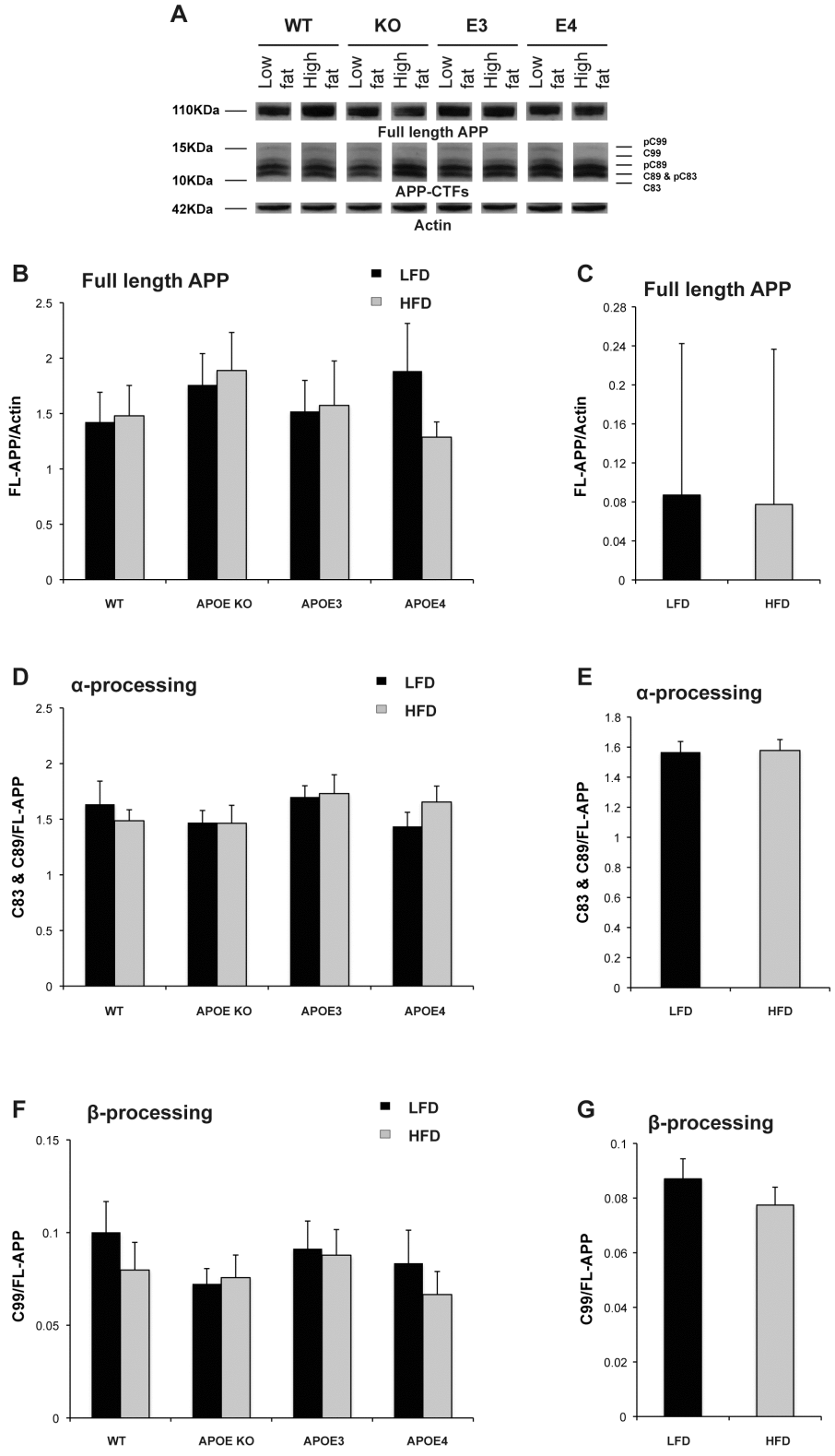

A) Immunoblot of APP processing in the cortical brain region of mice fed LFD and HFD. Triton-soluble lysates from the cortical brain region were run on 16% Tricine gels

and immunoblotted with the 369 antibody for full length (FL)-APP and APP-CTFs. Three bands around 110 kDa were observed for FL- APP whilst five bands were resolved for the phosphorylated forms of APP-CTFs between 10 kDa and 15 kDa. No differences in the levels of B), C) FL-APP or D), E) C83 & C89 or F), G) C99 between APOE KO, APOEε3, APOEε4 or WT mice were observed. FL-APP was normalised to β-actin and APP-CTFs were normalised to FL-APP for quantification. Samples were provided by colleagues at GlaxoSmithKline. Data are represented as mean±SEM, n = 8-12.

4.2.4 Regulators of tau phosphorylation are not altered

Given the changes in tau phosphorylation due to the dietary conditions, the insulin signalling pathway and level of active tau kinases and tau phosphatases were measured; Akt and GSK-3 by using antibodies to phospho-epitopes at sites reflective of activation state of the kinases, Cdk5 by using the p35/25 specific antibody and the tau phosphatase, PP2A. Surprisingly, no significant changes in the brain were found in Akt, GSK-3, Cdk5 or PP2A by APOE genotype or diet (Figure 4.7).

Figure 4.7 Proteins of the insulin signalling pathway, tau kinases and tau phosphatases were not altered in HFD fed mice

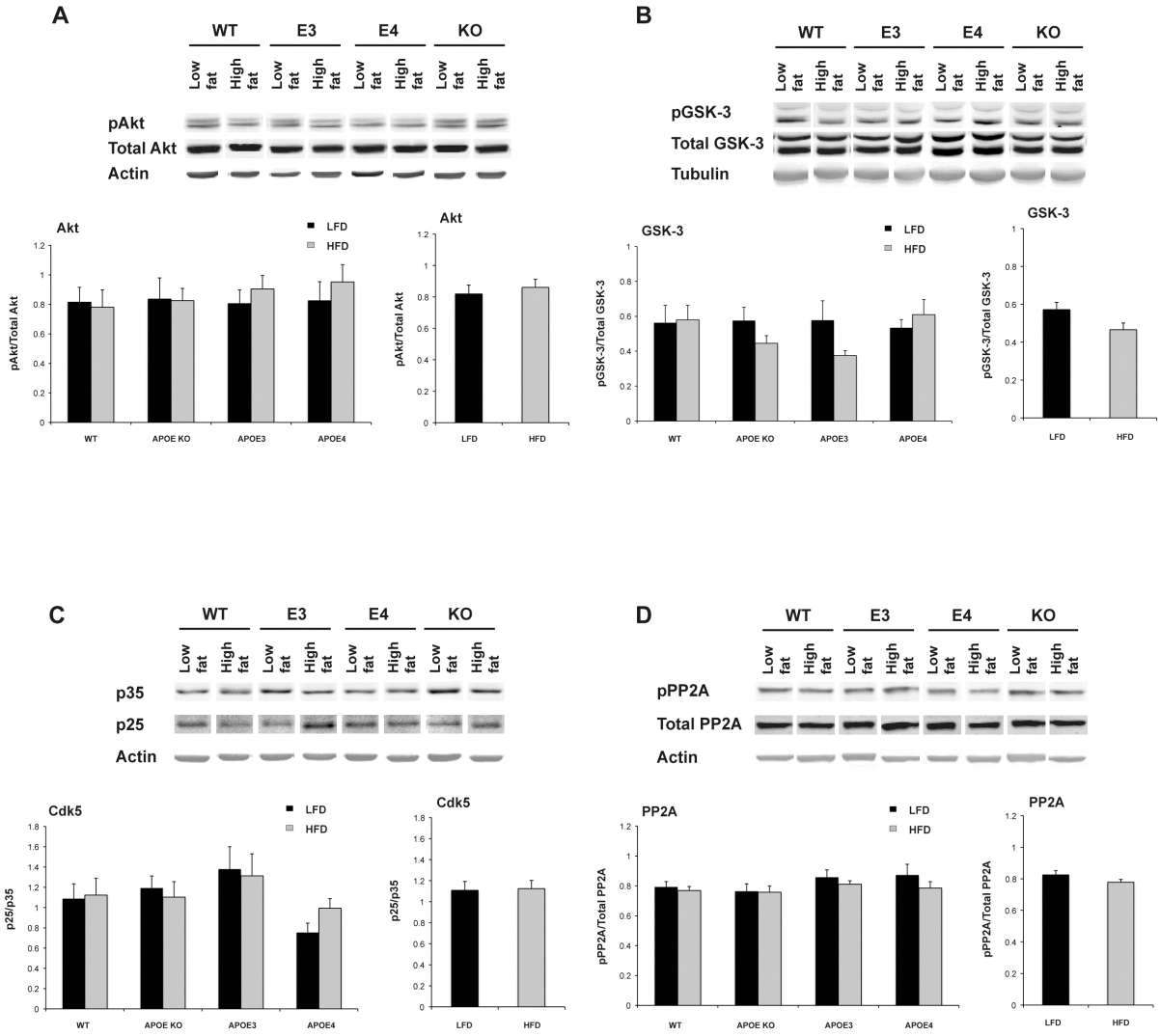

The activity of A) Akt, B) GSK-3, C) Cdk5 and D) PP2A did not change in mice fed a HFD. Samples were provided by colleagues at GlaxoSmithKline. Data are represented as mean±SEM, n = 8-12.

4.3 Discussion

The aim of this set of experiments was to determine whether AD-like pathology in diet-induced insulin resistant mice might be modulated in an APOE-dependent manner.

Diabetes can be induced experimentally by a range of techniques. The model used here manifests most of the features of patients with a predisposition to T2DM; obesity, weight gain, hyperinsulinemia, insulin resistance and glucose intolerance (Srinivasan and Ramarao, 2007). These are the exact features we observed in our HFD fed APOE transgenic mice with a C57BL/6 background, consistent with those initially reported in HFD fed C57BL/6 mice by Surwit *et al* (Surwit et al., 1988). Reassuringly, the metabolic tests used in our study such as the oral glucose tolerance test (OGTT), show similar curves to published studies using the same APOE transgenic mice (Arbones-Mainar et al., 2010; Karagiannides et al., 2008) as early as 6 months of age. There is also a similar OGTT trend to that reported by Arbones-Mainer and colleagues where APOEε4 animals show greater glucose intolerance compared to APOEε3 animals (Arbones-Mainar et al., 2010). Additionally, it has been suggested that the APOEε4 genotype can elevate fasting plasma insulin and glucose levels in obese men (Elosua et al., 2003). Fasting insulin levels are expected to rise in HFD fed mice over time due to the gradual decline in pancreatic β-cell function, this is also very similar to our observations.

The results from this set of data show an effect of diet upon tau phosphorylation; HFD reduces tau phosphorylation compared to LFD fed mice, independent of APOE genotype. These observations are contrary to our predictions, as well as other published findings that have shown insulin resistance or the disruption of insulin signalling causes AD pathology and this may be due to the differences in animal models used. In particular, our results are contrary to a recent finding by Moroz *et al* where HFD had no effect on tau phosphorylation despite an increase in tau gene

expression (Moroz et al., 2008). Although their study uses the same strain of mice and the same 60% HFD as our study, it is possible that our results are different because their mice were examined at a considerably younger age; mice were sacrificed and examined at 4 months by Moroz *et al*., and at 11 months in this study. In addition, in the former study the duration of feeding was shorter, 16 weeks compared to 32 weeks used in this study. Therefore, our observations on tau phosphorylation are likely due to long-term high fat feeding. Our observation is also counter to that of Freude and colleagues (Freude et al., 2005), where peripheral hyperinsulinemia promoted tau pathology in mouse brain. In this study, peripheral hyperinsulinemia was initiated with an acute insulin challenge; 20 minutes after peripheral injection, tau phosphorylation was increased in the brain. This study by Freude and colleagues is not comparable to the data reported in this section where tau phosphorylation was reduced in the context of long-term HFD induced hyperinsulinemia; arguably a model more representative of diet-induced hyperinsulinemia in man. The presence of insulin and insulin receptors in the brain is well established. In post-mortem brain tissue of AD patients, reduced expression of both insulin and insulin receptors has been found (Steen et al., 2005). Since insulin signalling inhibits the activity of the tau kinase, GSK-3, a reduction in insulin signalling might be expected to reduce inhibition of GSK-3, leading to an increase in tau phosphorylation. This is evidenced from gene deletion models such as the NIRKO, IRS1 and IRS2 knockout mice, all of which exhibit increased brain tau phosphorylation (Killick et al., 2009; Schubert et al., 2003; Schubert et al., 2004). Interestingly, intravenous infusion of insulin whilst maintaining euglycaemic conditions in AD patients resulted in an improvement in memory and performance (Craft et al., 1996). This indicates peripheral insulin may have a role in rescuing the impairment of insulin metabolism within the brain. Consequently, a further clinical study by Reger and colleagues found daily intranasal insulin raised the level of brain insulin and improved memory in AD patients (Reger et al., 2008). It is thought that by means of intranasal administration, insulin bypasses the blood brain barrier and reaches the CNS via the olfactory and trigeminal neural pathways (Hanson and Frey, 2008). Thus, any defect in

brain insulin signalling is corrected. Improved cognitive performance has also been demonstrated in animals administered with intracerebroventricular insulin (Park et al., 2000) or intranasal insulin (Francis et al., 2008), which also improved diabetic brain neuropathy (Francis et al., 2009). Putting this into context with our study, it is possible that the peripheral hyperinsulinemia in the HFD mice may induce increased entry of insulin into the brain, which, *in the absence of brain insulin resistance,* results in a reduction in the levels of phosphorylated tau.

Furthermore, in contrast to previous studies we found tau phosphorylation was independent of APOE genotype (Genis et al., 1995; Harris et al., 2004; Hoe et al., 2006; Kobayashi et al., 2003; Tesseur et al., 2000). Whilst we are unable to provide a full explanation for this, one possible source of discrepancy is the difference between our study and in both papers by Tesseur (Tesseur et al., 2000) and Harris (Harris et al., 2004) is the use of transgenic mice expressing neuronal apoE3 and apoE4. Previously, the cellular origin of apoE in the brain has been shown to affect its actions-astrocytic expression of apoE3 or apoE4 had no effect on excitoprotection whereas neuronal expression of apoE4 but not apoE3 was excitotoxic (Buttini et al., 2010). It is possible that such differences in the models used in the experiments underlie our conflicting observations.

Insulin resistance has also been shown to cause Aβ pathology in rodents (Bales et al., 2009; Cao et al., 2007; Ho et al., 2004; Kohjima et al., 2010; Luo et al., 2011). In the current study, LFD versus HFD, trends in increased levels of soluble $A\beta_{40}$ and $A\beta_{42}$ was observed in HFD fed WT and APOEε4 mice. In APOE KO mice, HFD caused a reduction in levels of $A\beta_{40}$ whilst the more toxic form, $A\beta_{42}$, was increased. In HFD APOEε3 mice, the reverse was observed; levels of $A\beta_{40}$ increased whilst the more toxic form, $A\beta_{42}$, reduced. However, this data, in addition to the data from APP processing, did not reach statistical significance when pooled regardless of APOE genotype or diet. This is surprising since it has been reported (Bales et al., 2009; Cao et al., 2007; Ho et al., 2004; Kohjima et al., 2010; Luo et al., 2011) that diet-induced insulin resistance

promotes the generation of $A\beta_{40}$ and $A\beta_{42}$. However, since these published studies used transgenic mice overexpressing mutant human APP (Tg2576 mice carry the Swedish mutations K670N/M671L, and the double transgenic APP/PS1 mice carry the Swedish mutations K670N/M671L with PS1 deleted in exon 9), animals are predisposed to the formation of toxic Aβ oligomers that are detected with human APP only, as APP in non-transgenic mice do not generate oligomeric species. Toxic Aβ oligomers are thought to induce Aβ aggregation leading to the formation of Aβ plaques that has the potential to cause tau phosphorylation. This may allow the detection of a significant effect with diet or APOE genotype, which we failed to find. In agreement with many studies, our data suggests the APOEε3 genotype is protective for amyloid pathology in HFD mice. According to the amyloid cascade hypothesis of AD, it is the formation or deposition of Aβ that initiates the formation of neurofibrillary tangles (Hardy and Allsop, 1991). In our mice, human Aβ is not expressed therefore Aβ oligomers cannot be formed and cause downstream pathological effects. Our data therefore suggest that in our APOE model of diet-induced T2DM, tau phosphorylation arises due to a process independent of Aβ.

Several of the published studies previously mentioned have identified upstream candidates responsible for tau phosphorylation and increased Aβ levels. In our study; LFD versus HFD, we did not detect any changes in activation of members of the insulin signalling pathway (Akt, GSK-3), tau kinases (GSK-3, Cdk5) or the tau phosphatase, PP2A. The lack of differences in Akt, GSK-3 or Cdk5 phosphorylation indicates the possibility of other proteins affecting the reduction in tau phosphorylation. However, this was not due to PP2A, as we detected no changes in this tau phosphatase. Moreover, in addition to serine phosphorylation, GSK-3 activity is regulated by tyrosine (Tyr) phosphorylation at residues Tyr279 and Tyr216 in GSK-3α and GSK-3β respectively (Hughes et al., 1993). Under physiological conditions, GSK-3 is constitutively active and phosphorylation at these sites is thought to augment its activity, thus for future experiments, these phosphorylation sites should be

investigated. Despite our findings, many tau phosphatases and kinases have been identified to date (Chung, 2009) and further examination of these may help us identify the possible candidates responsible for dephosphorylation of HFD-induced tau phosphorylation, such as PKA, JNK, MAP Kinases and PTEN. Furthermore, it is probable that the period required to increase sufficient levels of insulin in the brains of these mice by HFD feeding led to a failure in detecting changes in the insulin signalling cascade. This may have occurred transiently at an earlier time point.

In summary, this chapter has found an effect of diet on tau phosphorylation, independent of APOE genotype. That is, a reduction of tau phosphorylation in HFD fed mice with no changes in amyloid pathology or activity of components of the insulin signalling pathway.

CHAPTER 5

The Effect of Pioglitazone on Tau Phosphorylation and Aβ Metabolism in High Fat Fed Humanised APOEε3 and APOEε4 Mice

5.1 Introduction

New therapeutics are urgently needed to prevent or slow down the progression of cognitive decline seen in Alzheimer's disease (AD). Current evidence points towards the role of a dysregulation of the insulin signalling pathway as a possible cause of amyloid beta (Aβ) and tau pathology in the AD brain and in memory loss. This is supported by the observations that the expression of both insulin and insulin receptors are reduced in post-mortem AD brain tissue (Frolich et al., 1998; Steen et al., 2005). Based on this concept, treatments aimed at restoring the adequate levels of brain insulin have been proposed as a therapeutic approach for AD. As such, the administration of insulin via peripheral (Craft et al., 2003; Craft et al., 2000) or intranasal (Reger et al., 2006; Reger et al., 2008) routes has been found to facilitate memory in AD patients. Some of these effects were shown to be more prominent in non-APOEε4 carriers (Craft et al., 2000; Reger et al., 2006). Intranasal insulin treatment in animal models has also demonstrated to improve cognitive performance (Francis et al., 2008). These results have provided a strong rationale for use of the thiazolidinediones (TZDs) as therapeutic agents for AD. TZDs are a class of insulin sensitising drugs that reduce peripheral insulin resistance and blood glucose levels, by targeting peroxisome proliferator-activated receptor gamma (PPARγ). Since these drugs are prescribed to type 2 diabetes (T2DM) patients and T2DM is a risk factor for AD, TZDs would provide additional therapeutic benefits to these patients. In two early clinical trials, rosiglitazone (Avandia) improved memory and cognition in patients with mild to moderate AD (Watson et al., 2005) in an APOE-dependent manner (Risner et al., 2006). More recently, pioglitazone (Actos) also slowed cognitive decline in AD (Sato et al., 2011). Consistent with these observations, treatment with the same insulin sensitising agents in experimental models attenuated learning and memory deficits (Pedersen et al., 2006), reduced the accumulation of Aβ, reduced $A\beta_{42}$ levels and reduced levels of inflammatory markers (Heneka et al., 2005). PPARγ activation has also been shown to reduce the phosphorylation of tau *in vitro* (d'Abramo et al., 2006),

whilst the overexpression of PPARγ reduces the accumulation of Aβ (Camacho et al., 2004; d'Abramo et al., 2005).

The observations in man that increased risk of AD with T2DM is APOE dependent, that insulin affects Aβ pathology in an APOE-dependent manner and that in the early clinical trials with TZDs there was a stratification of effect by APOE led to the hypothesis that diet-induced insulin resistance and subsequent treatment with TZDs in animal models would have APOE-dependent effects on 'downstream' AD pathology. In order to explore this, the experiments in this chapter sought to determine the effects of the PPARγ agonist, pioglitazone, on tau phosphorylation and Aβ metabolism in diet-induced insulin resistant APOE mice.

5.2 Results

5.2.1 Body weights of mice increase during high fat feeding and pioglitazone treatment does not alter body weight

Feeding mice on a high fat diet (HFD) is known to be sufficient for the development of diet-induced insulin resistance and was observed previously in chapter 4. Here, mice also gained weight throughout 27 weeks of high fat feeding; APOE KO mice gained the most weight followed by APOEε3, APOEε4 and WT mice (Figure 5.1A and B). Although WT mice weighed less compared to the other HFD mice at the beginning of the study, a similar pattern in weight gain was observed. APOE KO, APOEε3 and APOEε4 mice weighed significantly more than the WT mice throughout the study. At week 27, mice were divided into vehicle and pioglitazone treatment groups for the final 3 weeks of the study whilst continuing to receive HFD. In the HFD mice given vehicle treatment, there was no significant change in body weight in APOEε3 and APOEε4 mice but body weight was significantly reduced in the APOE KO ($p=0.02$) and WT ($p<0.001$) mice (Figure 5.1A). In all HFD mice given pioglitazone treatment, no significant change in body weight was observed (Figure 5.1B).

Figure 5.1 Body weights of mice fed HFD for 30 weeks and treated with pioglitazone in the final 3 weeks

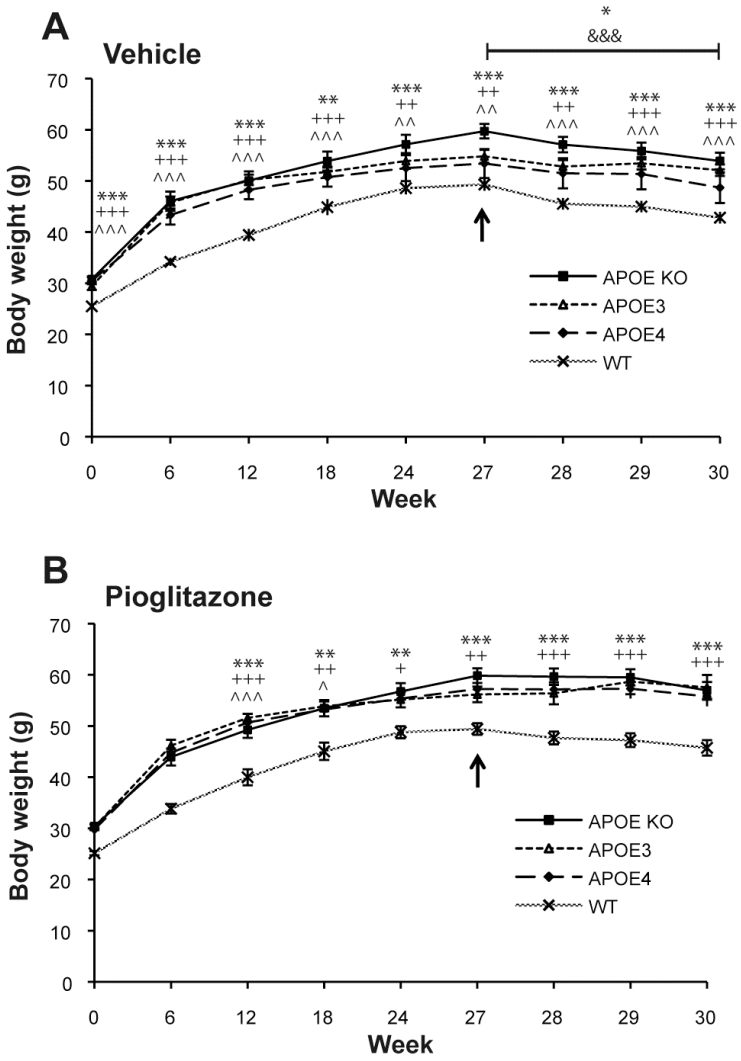

Body weights of APOE KO, APOEε3, APOEε4 and WT mice over 30 weeks of HFD, where in the final 3 weeks mice were given A) vehicle or B) pioglitazone treatment (indicated by the arrow). Data were generated by colleagues at GlaxoSmithKine. Data are represented as mean±SEM, n = 9-12. *p<0.05, **p<0.01; ***p<0.001 versus WT mice by one-way ANOVA with Tukey *post hoc* test. Significance is indicated by * APOE KO, + APOEε3, ^ APOEε4, & WT.

5.2.2 Glucose metabolism is impaired in mice fed HFD before treatment with pioglitazone

All mice had normal glucose tolerance profiles at week 0, before being given a HFD. The oral glucose tolerance test (OGTT) curve shows plasma glucose levels rising rapidly and reaches a peak at 30 minutes after being given a single oral dose of glucose. Thereafter, glucose levels falls sharply at 60 minutes as insulin production by the pancreas increases and glucose is eliminated from the bloodstream. The curve falls gradually and forms a tail as blood glucose returns to normal levels at 180 minutes (Figure 5.2A and B). The key findings of the OGTT are as follows.

- At week 12 of HFD, all mice show signs of impaired glucose metabolism (Figure 5.2C and D). Glucose took longer to reach peak levels in APOEε3 and APOEε4 mice and in all mice glucose elimination occurred at a much slower rate compared to week 0 baseline.

- At week 24, glucose metabolism continued to be increasingly impaired in all mice; the peak and the tail of the OGTT curve is less well defined compared to the start of the study (Figure 5.2E and F). WT mice appeared to have an increased impairment in glucose metabolism at all time points compared to all other mice.

- Mice were divided into two groups 3 weeks before the termination of the study. One group was given the vehicle 1% methylcellulose whilst the other group was given 20 mg/kg pioglitazone by oral gavage. After 3 weeks treatment of vehicle or pioglitazone at week 30, blood glucose levels were reduced in all animals of both treatment groups. The glucose peak was less pronounced and blood glucose remained steady during the OGTT (Figure 5.2G and H).

Figure 5.2 Oral glucose tolerance tests in mice fed a HFD for 30 weeks and treated with pioglitazone in the final 3 weeks

Oral glucose tolerance tests (OGTT) were conducted at baseline and then at 12 weekly intervals thereafter. Mice were fasted overnight. The next morning, mice were placed in a warming chamber prior to blood sampling and blood was taken by direct venopuncture. Mice were then given a single oral dose of glucose (3 g/kg, dose volume 10 ml/kg) and serial blood samples were collected from the tail tip post-dose at 30, 60, 90, 120 and 180 minutes. Glucose levels were accessed using a blood glucose meter. Graphs show glucose concentrations before vehicle and pioglitazone treatment at week; A,B) 0, C,D) 12 and E,F) 24 of HFD. At week 30, mice fed HFD were given 3 weeks of G) vehicle or H) pioglitazone treatment. Data were generated by colleagues at GlaxoSmithKine. Data are represented as mean±SEM, n = 9-12. *p<0.05, **p<0.01; ***p<0.001 versus WT mice by one-way ANOVA with Tukey *post hoc* test. Significance is indicated by * APOE KO, + APOEε3, ^ APOEε4.

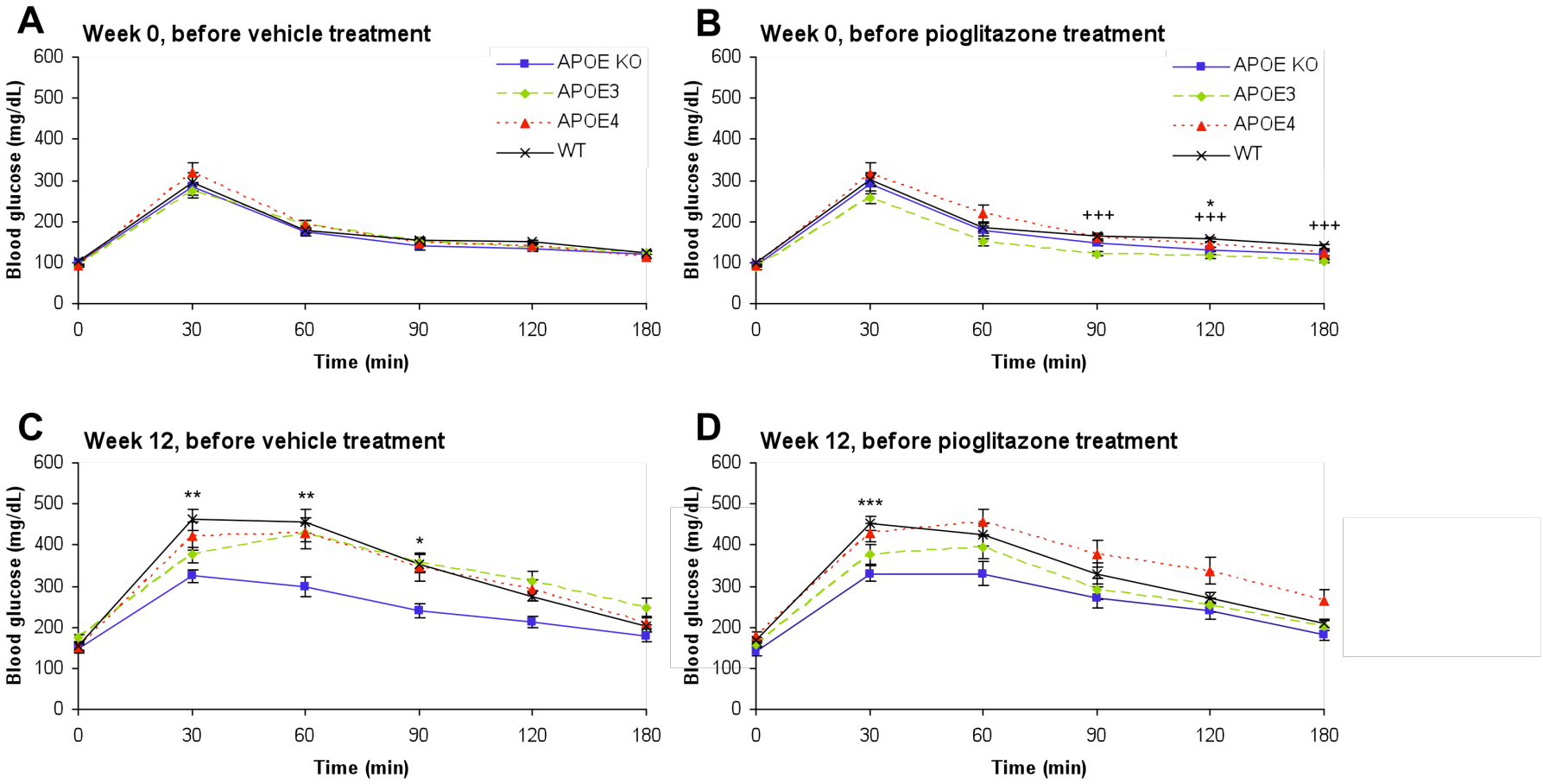
A
Week 0, before vehicle treatment
B
Week 0, before pioglitazone treatment
C
Week 12, before vehicle treatment
D
Week 12, before pioglitazone treatment
APOE KO
APOE3
APOE4
WT
Blood glucose (mg/dL)
Time (min)
0
30
60
90
120
180
100
200
300
400
500
600
+++
*
**
***

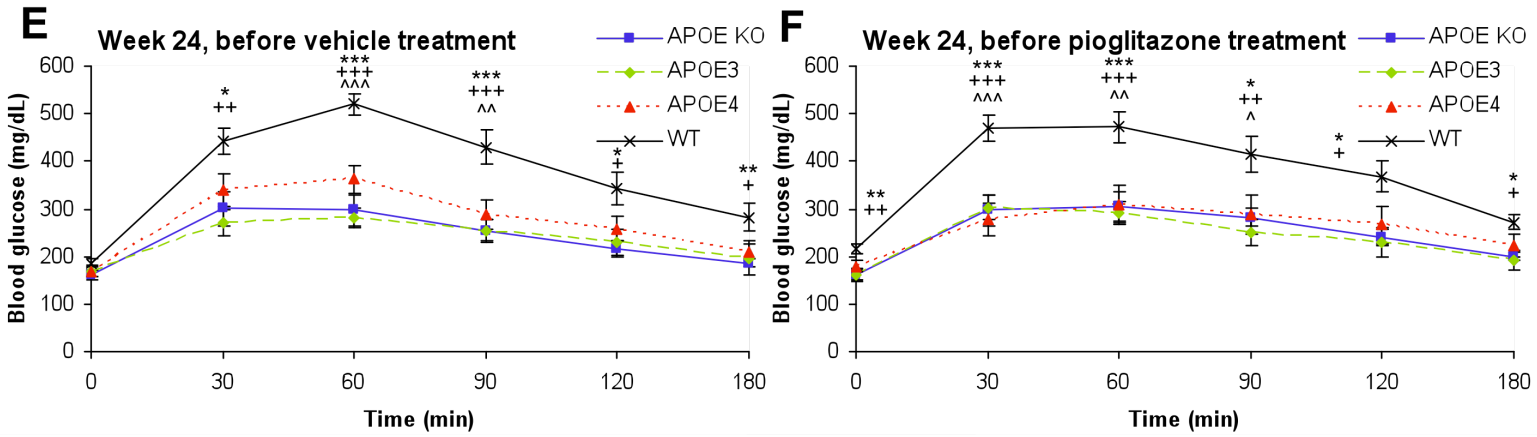
E
Week 24, before vehicle treatment
APOE KO
APOE3
APOE4
WT
Blood glucose (mg/dL)
Time (min)
F
Week 24, before pioglitazone treatment
APOE KO
APOE3
APOE4
WT
Blood glucose (mg/dL)
Time (min)

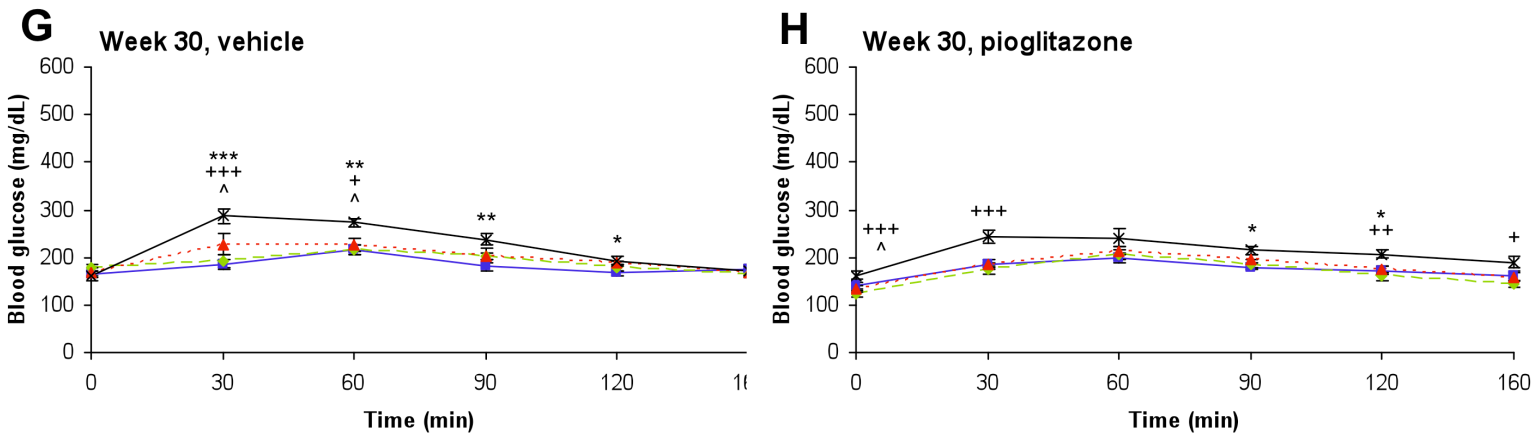
G
Week 30, vehicle
Blood glucose (mg/dL)
Time (min)
H
Week 30, pioglitazone
Blood glucose (mg/dL)
Time (min)

5.2.3 Levels of fasting plasma insulin reduce in insulin resistant mice after 3 weeks of pioglitazone treatment

Fasting levels of plasma insulin increased in all mice given a HFD from week 0 to week 24 (Figure 5.3A and B). Mice were divided into vehicle or pioglitazone treatment groups at week 27, the drug was administered for 3 weeks. At the end of the treatment period no significant changes in plasma insulin levels was observed in mice given vehicle treatment (Figure 5.3A). In mice given pioglitazone treatment, plasma insulin levels tended towards a decrease and reached significance in the APOEε4 and WT mice, $p=0.02$ and $p=0.03$ respectively (Figure 5.3B).

The homeostatic model assessment of insulin resistance (HOMA-IR) was calculated as a measure of insulin sensitivity. HOMA-IR levels were statistically significantly increased ($p<0.001$) after 24 weeks of HF feeding in all mice, indicating all mice were increasingly insulin resistant (Figure 5.3.C and D). After three weeks of pioglitazone treatment, HOMA-IR levels decreased within each genotype in comparison to the HOMA-IR levels before treatment (Figure 5.3D). In contrast, in all mice given vehicle treatment, HOMA-IR levels were similar to before treatment (Figure 5.3C). By comparing HOMA-IR levels at week 30, after vehicle and pioglitazone treatment within mice of the same genotype (Figure 5.3E), reduced levels of HOMA-IR in all mice given pioglitazone was detected, however this difference did not reach statistical significance. Significant differences were recorded for WT ($p=0.004$) and APOEε3 mice ($p=0.018$).

Figure 5.3 Levels of fasting plasma insulin is reduced in insulin resistant mice after 3 weeks of pioglitazone treatment

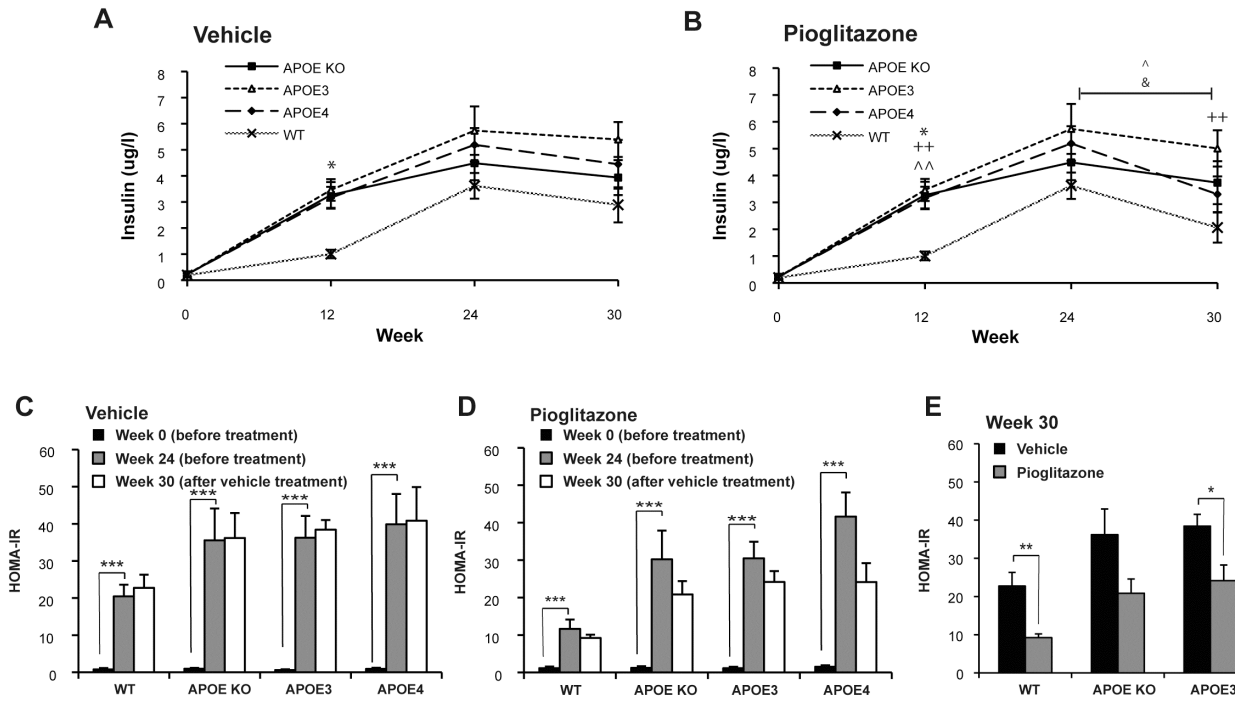

Levels of fasting plasma insulin were measured by ELISA in APOE KO, APOEε3, APOEε4 and WT mice over 24 weeks of HFD and a further 3 weeks of HFD with A) vehicle or B) pioglitazone treatment. The homeostatic model assessment of insulin resistance (HOMA-IR) was calculated at baseline (week 0), before (week 24) and after (week 30) treatment with either C) vehicle or D) pioglitazone. E) Comparison of HOMA-IR in mice treated with 3 weeks of vehicle or pioglitazone. In A) and B) plasma levels reached *p<0.05, **p<0.01 versus WT mice by one-way ANOVA with Tukey *post hoc* test. Significance is indicated by * APOE KO, + APOEε3, ^ APOEε4, & WT. in C), D) and E) **p<0.01, ***p<0.001 by Student's t-test. Samples were provided by colleagues at GlaxoSmithKine. Data are represented as mean±SEM, n = 9-12.

5.2.4 Levels of plasma adiponectin increase on the administration of pioglitazone in HFD fed mice

Adiponectin is an insulin sensitising hormone and plasma levels of adiponectin were measured as an indication of the effectiveness of pioglitazone treatment. In all HFD fed mice given vehicle treatment, there was no significant change in fasting plasma adiponectin levels between week 24 and week 30 (Figure 5.4A). However, in HFD fed pioglitazone treated mice, as expected, there was a highly significant increase ($p<0.001$ for all mice) in plasma adiponectin levels between week 24 and week 30 in the order of; 1.9±0.1 to 8.7±1.2 ng/ml in APOEε3, 2.1±0.1 to 8.1±0.5 ng/ml in APOE KO, 2.8±0.2 to 7.4±0.4 ng/ml in WT mice and 1.1±0.1 to 6.9±0.3 ng/ml in APOEε4 (Figure 5.4B).

Figure 5.4 Levels of plasma adiponectin increase on the administration of pioglitazone in HFD fed mice

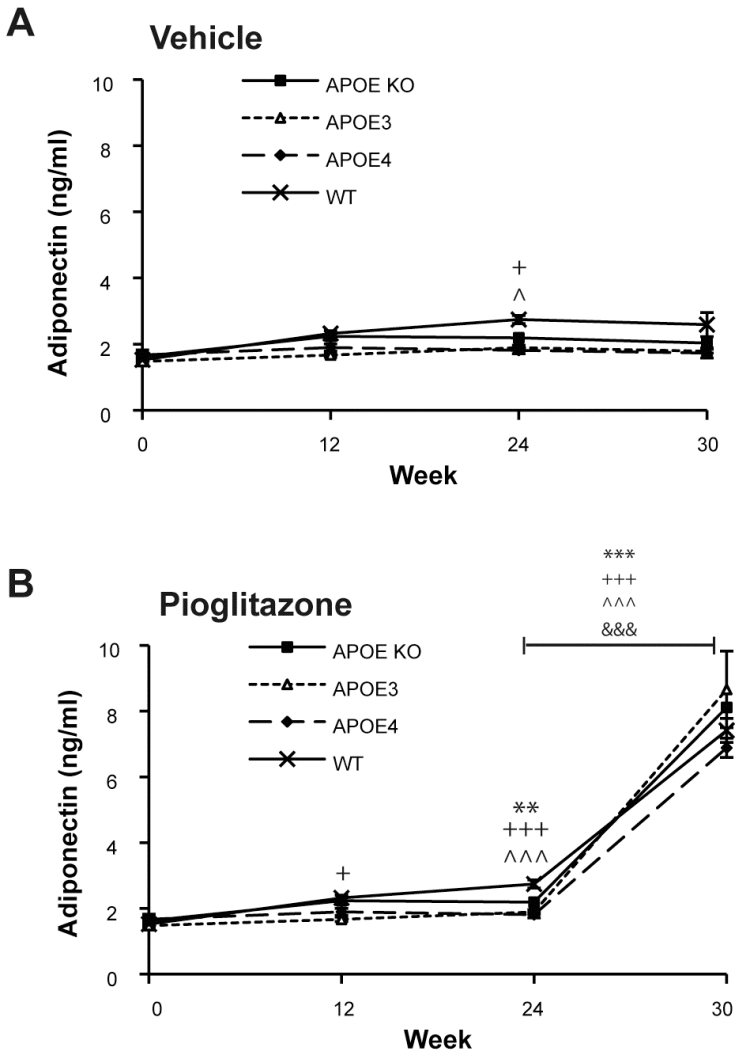

Levels of fasting plasma adiponectin was measured by ELISA in APOE KO, APOEε3, APOEε4 and WT mice over 24 weeks of HFD and a further three weeks of HFD with A) vehicle or B) pioglitazone treatment. Samples were provided by colleagues at GlaxoSmithKine. Data are represented as mean±SEM, n = 9-12. *p<0.05, **p<0.01; ***p<0.001 versus WT mice by one-way ANOVA with Tukey *post hoc* test. Significance is indicated by * APOE KO, + APOEε3, ^ APOEε4, & WT.

5.2.5 Pioglitazone treatment selectively lowers the phosphorylation of tau at the Ser202/Thr205 epitope in APOEε3 mice

Tau phosphorylation was not significantly altered after vehicle or pioglitazone treatment at any of the three tau epitopes (Ser396, Ser202/Thr205 or Thr231) (Figure 5.5B,E and H). However, there was a genotypic effect with APOEε3 mice showing a decrease in tau phosphorylation at the Ser202/Thr205 epitope ($p=0.01$) and the reverse, a significant increase in tau phosphorylation in APOEε4 mice ($p=0.03$) with pioglitazone treatment (Figure 5E). This trend was also detected with the AT180 antibody which recognises the Thr231 phospho-tau epitope (Figure 5.5H).

Figure 5.5 Pioglitazone treatment selectively lowers tau phosphorylation at the Ser202/Thr205 epitope in APOEε3 mice

Mice fed HFD for 30 weeks were treated with vehicle or pioglitazone for the final 3 weeks. The cortical brain region from mice were homogenised in sucrose homogenisation buffer, lysates were then immunoblotted with the indicated antibodies as shown in A, D and G). The density of phosphorylated tau was normalised against total tau. B, C) ptau Ser396, E, F) Ser202/Thr205 (AT8), H, I) Thr231 (AT180). Samples were provided by colleagues at GlaxoSmithKine. Data are represented as mean±SEM, n = 9-12. *$p<0.05$ by Student's t-test.

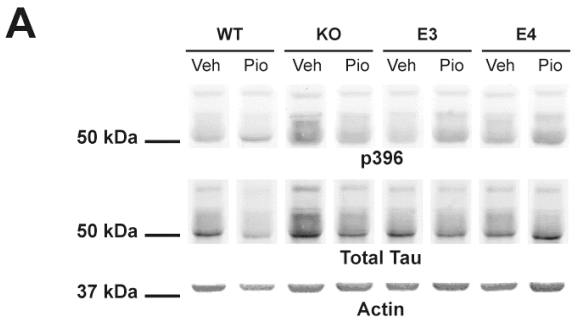
A
WT
KO
E3
E4
Veh
Pio
Veh
Pio
Veh
Pio
Veh
Pio
50 kDa
p396
50 kDa
Total Tau
37 kDa
Actin

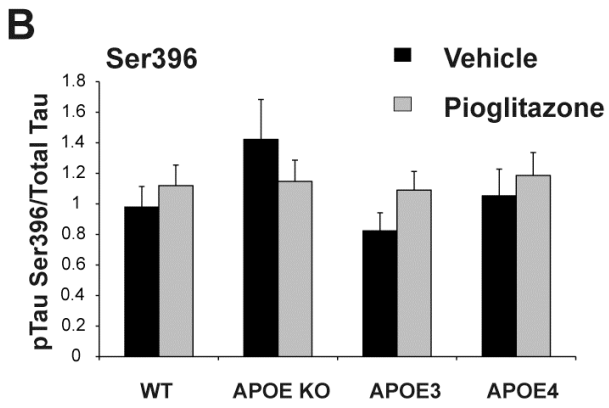
B
Ser396
Vehicle
Pioglitazone
pTau Ser396/Total Tau
1.8
1.6
1.4
1.2
1
0.8
0.6
0.4
0.2
0
WT
APOE KO
APOE3
APOE4

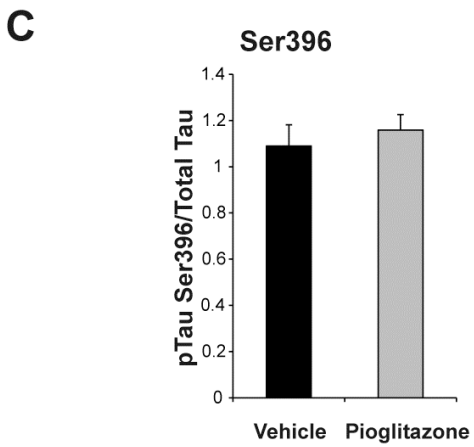
C
Ser396
pTau Ser396/Total Tau
1.4
1.2
1
0.8
0.6
0.4
0.2
0
Vehicle
Pioglitazone

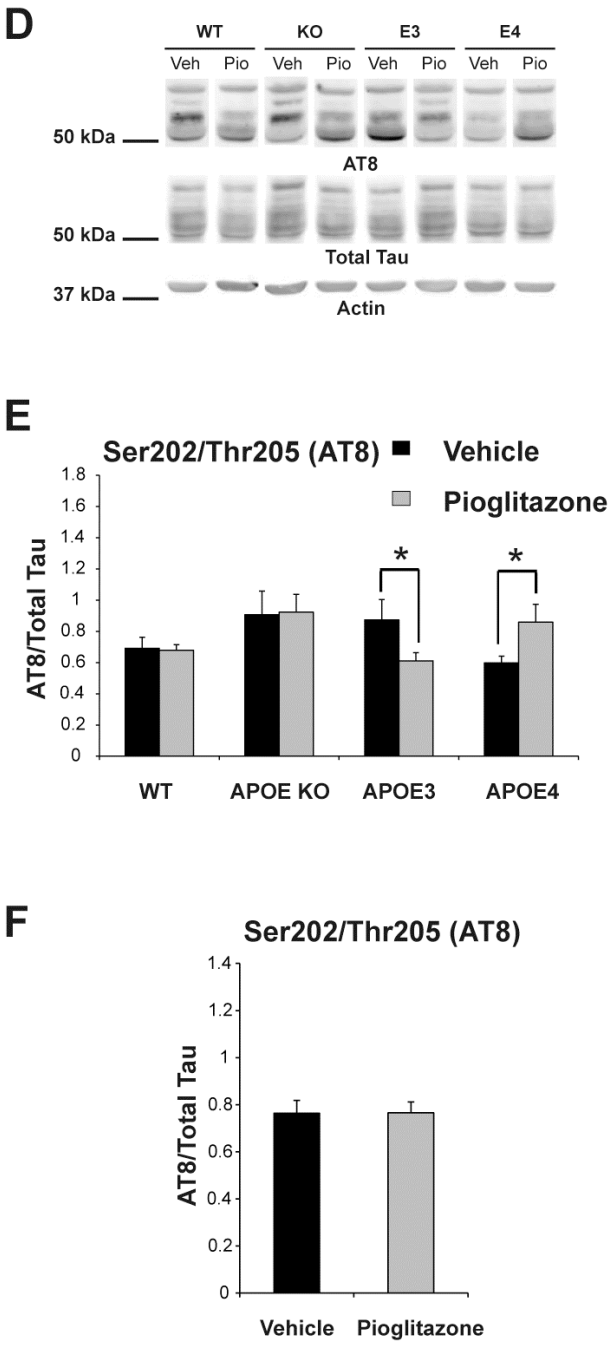
D
WT
KO
E3
E4
Veh
Pio
Veh
Pio
Veh
Pio
Veh
Pio
50 kDa
AT8
50 kDa
Total Tau
37 kDa
Actin
E
Ser202/Thr205 (AT8)
Vehicle
Pioglitazone
AT8/Total Tau
1.8
1.6
1.4
1.2
1
0.8
0.6
0.4
0.2
0
*
*
WT
APOE KO
APOE3
APOE4
F
Ser202/Thr205 (AT8)
AT8/Total Tau
1.4
1.2
1
0.8
0.6
0.4
0.2
0
Vehicle
Pioglitazone

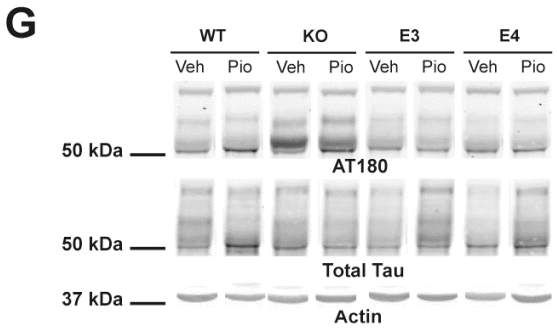
G
WT
KO
E3
E4
Veh
Pio
Veh
Pio
Veh
Pio
Veh
Pio
50 kDa
AT180
50 kDa
Total Tau
37 kDa
Actin

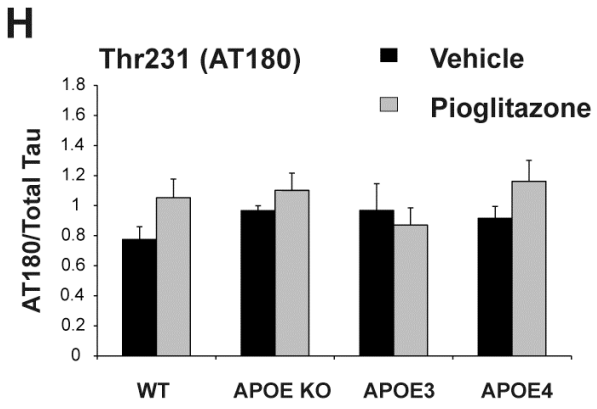
H
Thr231 (AT180)
Vehicle
Pioglitazone
AT180/Total Tau
1.8
1.6
1.4
1.2
1
0.8
0.6
0.4
0.2
0
WT
APOE KO
APOE3
APOE4

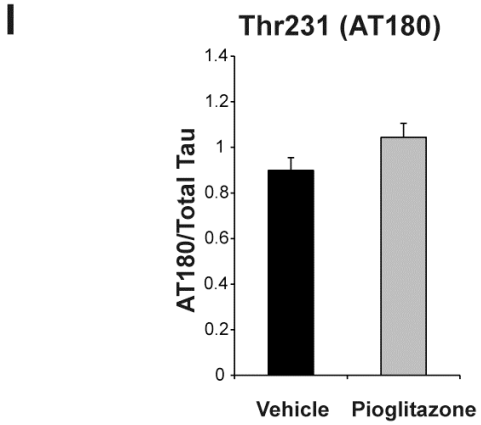
I
Thr231 (AT180)
AT180/Total Tau
1.4
1.2
1
0.8
0.6
0.4
0.2
0
Vehicle
Pioglitazone

5.2.6 Pioglitazone treatment on APP processing and soluble Aβ levels

Pioglitazone treatment has been shown to lower amyloid load in animal models (Heneka et al., 2005; Yan et al., 2003). In our study, we measured the levels of soluble $A\beta_{40}$ and $A\beta_{42}$. On comparison of $A\beta_{40}$ levels within each genotype, $A\beta_{40}$ tended towards a decrease although these did not reached statistical significance (Figure 5.6A). Similarly, alterations in the levels of $A\beta_{42}$ were statistically insignificant; in WT, APOE KO, APOEε3 and APOEε4 mice fed HFD and treated with pioglitazone, $A\beta_{42}$ was reduced, albeit this change was very small in APOEε3 mice (Figure 5.6B).

The non-amyloidogenic and amyloidogenic processing (α- and β-processing respectively) of the amyloid precursor protein (APP) was assessed by measuring the levels of C-terminal fragments C83 & C89 (non-amyloidogenic) and C99 (amyloidogenic). The levels of full length APP were not significantly altered when mice were grouped by genotype or treatment groups (Figure 5.7B and C). In pioglitazone treated APOEε3 mice, the levels of C83 & C89 were significantly reduced compared to vehicle treated APOEε3 mice ($p=0.001$) whilst no significant changes were detected in the levels of C99 (Figure 5.7D and F). In the pioglitazone treated APOE KO, APOEε4 and WT mice the levels of C83 & C89 and C99 were not significantly altered (Figure 5.7D and F). There was no significant change in APP processing when mice were combined into vehicle or pioglitazone groups (Figure 5.7E and G).

Figure 5.6 Levels of soluble Aβ_{40} and Aβ_{42} in HFD fed mice treated with or without pioglitazone

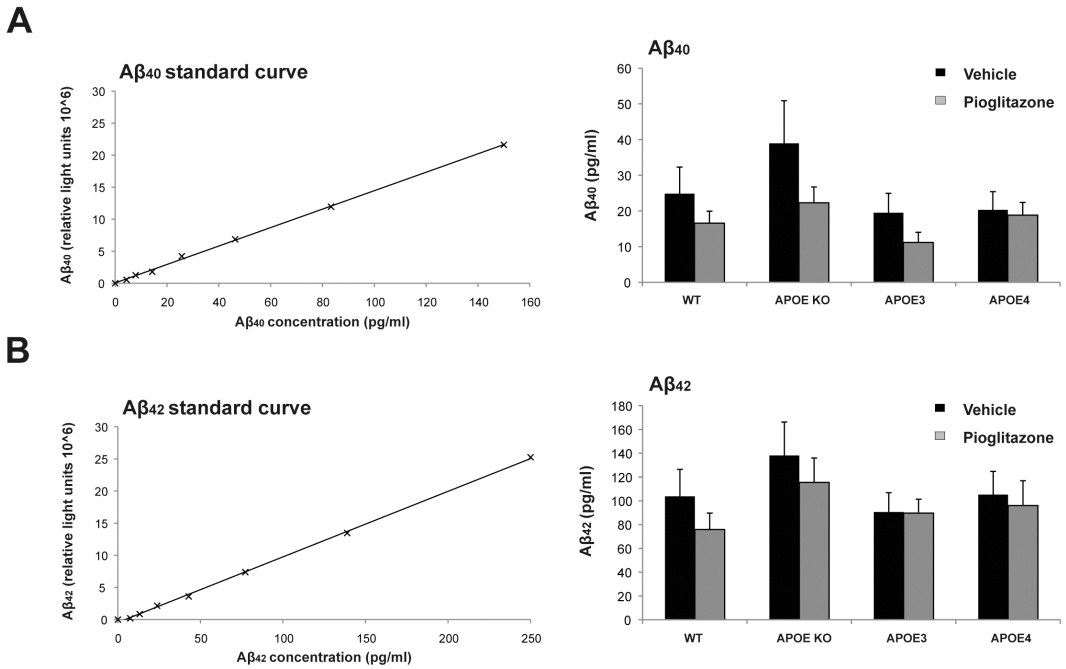

Soluble levels of Aβ were analysed in the cortical brain region of mice by using chemiluminescent ELISA kits. A) Standard curve and Aβ_{40} levels, and B) standard curve and Aβ_{42} levels, in the brain of mice fed HFD and treated with vehicle or pioglitazone. Samples were provided by colleagues at GlaxoSmithKine. Data are represented as mean±SEM, n = 7-11. *$p<0.05$ by Student's t-test.

Figure 5.7 APP processing in mice fed HFD with or without pioglitazone treatment

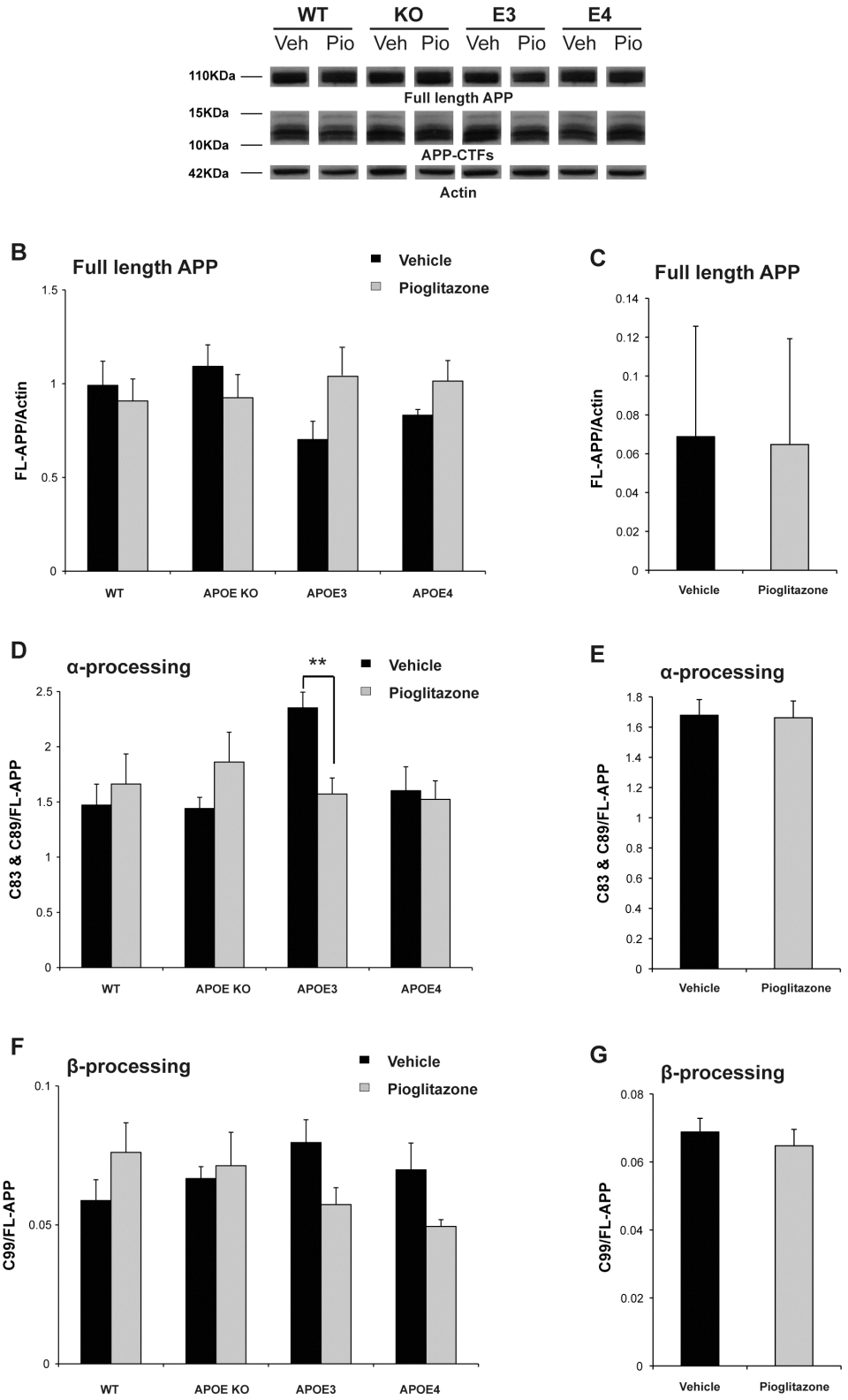

The dissected cortical regions from mice were homogenised in brain homogenisation buffer containing 1% Triton. A) Lysates were immunoblotted on 16% Tricine gels and probed with a C-terminal specific APP antibody for full-length (FL)-APP and C-terminal fragments (CTFs). CTFs were normalised against FL-APP. B) and C) FL-APP, D) and E) α- (non-amyloidogenic) processing and F) and G) β- (amyloidogenic) processing. Samples were provided by colleagues at GlaxoSmithKine. Data are represented as mean±SEM, n = 9-12. **p<0.01 by Student's t-test.

5.2.7 Regulators of tau phosphorylation are not altered

Given the APOE isoform specific change in tau phosphorylation at the Ser202/Thr205 epitope, the level of active tau kinases GSK-3 and Cdk5, the tau-phosphatase PP2A and changes in Akt, a component of the insulin signalling pathway were measured. However, we found no significant changes correlating to the APOE isoform specific effect in tau phosphorylation (Figure 5.8).

Figure 5.8 Regulators of tau phosphorylation are not altered

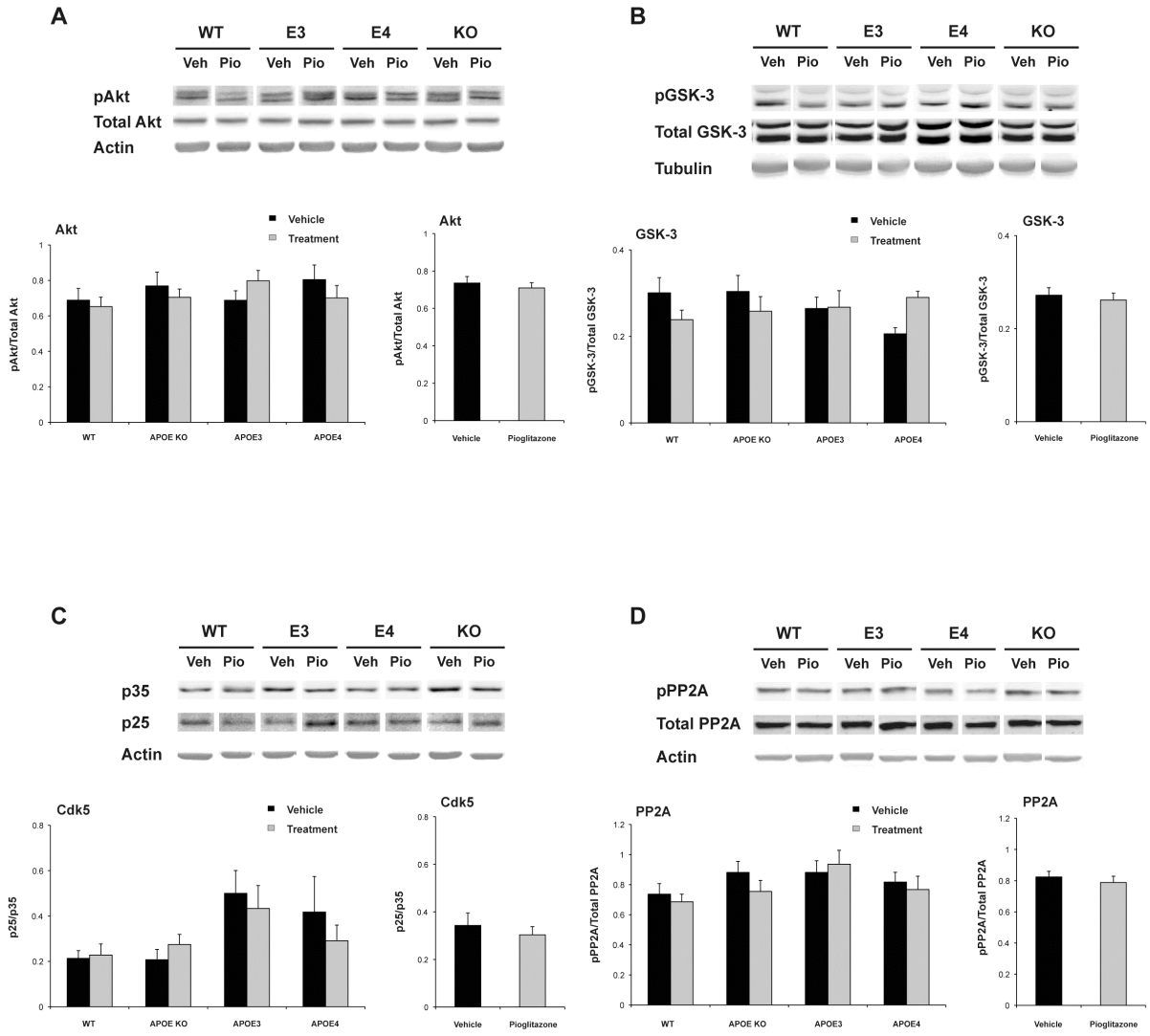

Lysates from the cortical brain region of mice were subjected to SDS-PAGE and were immunoblotted for some of the regulators of tau phosphorylation A) Akt, B) GSK-3, C) Cdk5 and D) PP2A. The density of phosphorylated forms of the proteins were normalised against the total form of the same protein. Samples were provided by colleagues at GlaxoSmithKine. Data are represented as mean±SEM, n = 9-12.

5.3 Discussion

This set of experiments was designed to examine the effect of the PPARγ agonist, pioglitazone, on tau phosphorylation and APP metabolism in diet-induced insulin resistant APOE mice.

The HFD fed C57BL/6 mouse has been shown to be a good model for studying the mechanisms and treatment of T2DM (Winzell and Ahren, 2004). As such, we used APOE mice on a background strain of C57BL/6 for this study. In the previous chapter (chapter 4), we developed a diet-induced insulin resistance mouse model. In this section, we used these same conditions and went on to investigate the effects of the PPARγ agonist, pioglitazone.

The PPARs are members of the NR1C class of the nuclear hormone receptor superfamily of ligand-activated transcription factors that are expressed in a variety of cell types. The three PPAR isoforms; PPARα, PPARβ/δ and PPARγ are involved in adipocyte differentiation, lipid storage and glucose metabolism. PPARs are activated upon binding of a natural or synthetic ligand which causes conformational changes in PPAR (Berger et al., 1996). This change in conformation promotes the recruitment of transactivator complexes and the subsequent transcription of target genes. The TZDs; rosiglitazone, pioglitazone and troglitazone are all pharmacological ligands of the PPARγ isoform (Lehmann et al., 1995). They control blood glucose concentration by binding PPARγ with various affinities and are therefore able to exert their insulin-sensitising and hypoglycaemic effects. PPARγ is predominately expressed in adipose tissue (Chawla et al., 1994), allowing the direct actions of TZDs on adipose cells. For example, mice with the deletion of adipose tissue specific PPARγ are deficient in their response to TZD treatment (He et al., 2003). PPAR agonists also promote the differentiation of preadipocytes into adipocytes (Chawla et al., 1994; Lehmann et al., 1995; Sandouk et al., 1993; Tontonoz et al., 1994). Additionally, two recent papers reported that neuronal PPARγ signalling is also required for the hepatic insulin

sensitising effects of TZDs. By using various techniques to inactivate PPARγ in the brain, authors demonstrated rosiglitazone-induced hyperphagia and weight gain were abolished (Lu et al., 2011; Ryan et al., 2011). Currently, rosiglitazone and pioglitazone are the only Food and Drug Administration-approved TZDs clinically prescribed to T2DM patients.

In this study, we chose to use pioglitazone as it has a higher permeability through the blood brain barrier (BBB) compared to rosiglitazone. Although it was initially thought that rosiglitazone was BBB impermeable (Pedersen et al., 2006; Watson et al., 2005), a recent study by Strum and colleagues has shown its presence in the brain after oral administration (Strum et al., 2007). The effectiveness of pioglitazone treatment in mice was assessed by measuring plasma adiponectin levels. Adiponectin is an insulin sensitising hormone secreted by adipocytes in adipose tissue and enhances insulin sensitivity in the body by carrying out three key roles: 1) increased uptake of glucose on tissues and accelerating fatty acid clearance (Yamauchi et al., 2001); 2) reduction in hepatic glucose production (Berg et al., 2001); and 3) reduced levels of circulating insulin (Winzell et al., 2004). As PPARγ acts directly on adipocytes, circulating adiponectin levels increase upon the administration of these TZDs (Miyazaki et al., 2004), acting as a biomarker for the restoration of insulin sensitivity. As we observed an increase in plasma adiponectin levels, this demonstrates the effectiveness on the target of the drug used in this study, at both the dose and length of treatment specified. All mice given 20 mg/kg pioglitazone treatment for 3 weeks by oral gavage showed a concomitant increase ($p<0.001$) in plasma adiponectin. Accompanying the striking increase in levels of plasma adiponectin, was a decrease in fasting plasma insulin levels in mice receiving pioglitazone treatment. In contrast, fasting levels of plasma insulin in vehicle treated mice reached a plateau and remained at the same level from week 24 to week 30. This observation was expected because TZDs increase the levels of circulating adiponectin and the action of adiponectin reduces the level of plasma insulin. In the final measurement of the OGTT

at week 30, the expected improvement of glucose metabolism in HFD fed and pioglitazone treated mice was not observed. Both the vehicle and pioglitazone treatment groups, after 3 weeks of treatment, had a reduction in glucose levels, despite the fact that vehicle treated mice were expected to have a continuation in the impairment of glucose metabolism. It is obvious that this observation was not due to inadequate drug treatment as our adiponectin and insulin data indicates pioglitazone treatment was effective and it is highly likely that something went wrong during the OGTT process, for example mice were not given the correct dose of glucose.

Despite that TZDs improve glycaemic control and insulin sensitivity in T2DM patients, one of the negative side-effects is the potential to cause weight gain (Mori et al., 1999; Patel et al., 1999). Similarly, TZD treatment in rodents has also been shown to cause weight gain (Eldershaw et al., 1995; Fujiwara et al., 1991; Hallakou et al., 1997; Kaufman et al., 1995), although in one study they failed to do so (Fujiwara et al., 1988). Several studies have attempted to elucidate the mechanisms behind improved tissue insulin sensitivity and simultaneous weight gain; these include adipocyte proliferation (Chawla et al., 1994; Kletzien et al., 1992) and reduced leptin production (Kallen and Lazar, 1996; Shimizu et al., 1998). In this study, pioglitazone treatment in HFD fed mice did not cause weight gain and it is possible that increases in body weight may have appeared if mice were given pioglitazone for a longer period.

Our data from biochemical analysis of the cortical region of the brain shows that pioglitazone has an APOE genotype specific effect at the Ser202/Thr205 phosphoepitope of tau; in pioglitazone treated HFD APOEε3 mice, a reduction of tau phosphorylation was observed in comparison to APOEε3 mice treated with vehicle. The reverse, an increase in tau phosphorylation was observed in pioglitazone treated HFD APOEε4 mice. Whilst in the APOE KO or WT mice, no significant change in tau phosphorylation by pioglitazone treatment was detected. This trend, although not reaching statistical significance, was also observed at the Thr231 phosphoepitope of tau. These results are consistent with the results from an early rosiglitazone clinical trial

in which drug treatment improved cognition in APOEε4 negative patients with mild to moderate AD (Risner et al., 2006), However, rosiglitazone was not shown to be effective in a recent phase III clinical trial (Gold et al., 2010). A recently published paper also observed APOE isoform dependent effects of rosiglitazone in adipose tissue (Arbones-Mainar et al., 2010). As mentioned earlier, there is some evidence of a synergistic interaction between the APOEε4 allele and T2DM and the risk of AD is higher amongst APOEε4 carriers with T2DM (Irie et al., 2008; Peila et al., 2002). Evidence on mitochondrial dysfunction as part of the pathophysiology of both AD (Bubber et al., 2005) and T2DM (Lowell and Shulman, 2005) is also emerging. Greater mitochondrial dysfunction has been detected in AD APOEε4 carriers (Gibson et al., 2000) and significant evidence shows that this is the cause of apoE4 protein fragments (Nakamura et al., 2009), as apoE4 is more susceptible to degradation compared to the apoE2 and apoE3 isoforms (Huang et al., 2001). One hypothesis is that the formation of C-terminal truncated fragments by neuron-specific cleavage of the apoE4 protein escapes through the secretory pathway, enters the cytosol and interacts with mitochondria via its hydrophobic lipid-binding region (Chang et al., 2005). This leads to perturbation of mitochondrial function and therefore diminishes the participation of mitochondria in the glycolytic processes. Via the same route, apoE4 truncated fragments can also induce tau phosphorylation, as shown *in vivo* and *in vitro* (Brecht et al., 2004; Harris et al., 2003; Huang et al., 2001; Ljungberg et al., 2002; Zhou et al., 2006). Since a direct role of PPARγ agonism is to stimulate mitochondrial biogenesis (Bolten et al., 2007; Miglio et al., 2009; Wang et al., 2002; Wilson-Fritch et al., 2004), this suggests that perhaps neurotoxic C-terminal fragments in our APOEε4 mice caused excessive damage to the mitochondria in neurons. Accordingly, APOEε4 mice did not respond to pioglitazone treatment, like that of APOEε3 mice. A higher dose of pioglitazone may possibly overcome the detrimental effects of the APOEε4 isoform by upregulating mitochondrial biosynthesis.

In relation to amyloid, we analysed the processing of full-length APP and soluble levels of $A\beta_{40}$ and $A\beta_{42}$ in the same brain samples from the mice. Full-length APP is metabolised by two competing pathways; the non-amyloidogenic pathway (α-processing) gives rise to soluble APPα and C83 & C89 whereas the amyloidogenic pathway (β-processing) yields soluble APPβ and C99. C99 is further cleaved by γ-secretase to produce the $A\beta_{40}$ and $A\beta_{42}$ species. Biochemical analyses revealed a significant decrease in α-processing of APP in the pioglitazone treated APOEε3 mice. This finding is intriguing because we also observed changes in tau phosphorylation with the same mice, however because there are no reported mechanisms between apoE isoforms, TZDs and APP, further work is required to investigate this interaction. In other studies, a recent *in vivo* study using PDAPP transgenic mice expressing human APOE isoforms (Castellano et al., 2011) and in an *in vitro* study using cell lines expressing human APOE (Biere et al., 1995), both studies demonstrate no significant alterations in APP processing. Furthermore, soluble levels of $A\beta_{40}$ and $A\beta_{42}$ were not significantly altered in this study when HFD fed mice were administered with pioglitazone. However, a trend was observed in all mice showing pioglitazone treatment reduced both Aβ species. In addition, higher levels of both soluble $A\beta_{40}$ and $A\beta_{42}$ were detected in APOE KO mice in comparison to mice with the APOE gene, which has also been demonstrated in another study (Dodart et al., 2000). The idea that APOE KO animals cannot clear Aβ from brain has been suggested (Shibata et al., 2000), it being proposed that the clearance of Aβ from the brain to the periphery is mediated by the transport of apoE-Aβ complexes across the BBB via LRP1 (Deane et al., 2004; Shibata et al., 2000). An alternative explanation is that APOE KO mice have an altered plasma lipid profile due to apoE protein deficiency, which is essential for the transport and metabolism of lipids. APOE KO mice begin to develop atherosclerotic lesions rapidly at 3 months of age (Zhang et al., 1992) and the progression of atherosclerosis can be accelerated by HFD feeding (Plump et al., 1992). In APOE KO mice fed HFD, the integrity of the BBB is altered (Mulder et al., 2001), this can lead to

increased lipid peroxidation and subsequently an increase in the generation of Aβ (Chen et al., 2008; Pratico et al., 2001). In the current study, to test for the evidence of leakage at the BBB, the levels of BBB integrity markers such as the S100β protein (Kapural et al., 2002) could be examined in a tail tip bleed from the APOE KO mice. This could contribute to further work for this study. S100β is a marker of astrocytic damage (Griffin et al., 1989) and has been implicated as a possible mechanism underlying the progression of neuropathological changes in AD (Hu et al., 1997; Mrak et al., 1996; Sheng et al., 1997). Furthermore, our results did not replicate the finding of a reduction in Aβ levels following pioglitazone treatment, as reported in two earlier *in vivo* studies using Tg2576 mice (Yan et al., 2003) and APPV717I mice (Heneka et al., 2005). This is most likely due to the use of different mouse models and both groups may have seen a more pronounced effect with Aβ, as their models are engineered to develop amyloid pathology.

In this study of HFD together with pioglitazone treatment, we did not detect any changes in any of the regulators of tau phosphorylation examined; components of the insulin signalling pathway (Akt, GSK-3), tau kinases (GSK-3, Cdk5) or the tau phosphatase PP2A. Further investigation using other tau kinases and phosphatases or a whole brain transcriptomic study (chapter 7) may help to identify possible pathways relating to our genotypic effect in tau phosphorylation.

To summarise, this set of experiments found an APOE-dependent effect of pioglitazone on tau phosphorylation. The APOEε3 genotype responded to pioglitazone treatment, which is in line with an early clinical trial using rosiglitazone in AD patients. We found that pioglitazone treatment was effective at reducing tau phosphorylation at the Ser202/Thr205 epitope, with a trend also observed at the Thr231 phospho-tau site. Pioglitazone treatment also reduced α-processing of APP in the APOEε3 pioglitazone treated mice, this observation requires further investigation. Further work will also be required to identify possible pathways correlating to the change in tau phosphorylation observed.

CHAPTER 6

The Effects of ApoE3 and ApoE4 Isoforms and Pioglitazone on Tau Phosphorylation and Cholesterol Biosynthesis *In Vitro*

6.1 Introduction

Apoliproteins are proteins that bind lipids such as cholesterol to form lipoprotein particles. In the periphery, lipoproteins are delivered in the plasma to cells in the body requiring cholesterol for the production of cell membranes, to maintain membrane fluidity or for the synthesis of vitamin D and hormones. ApoE is the most studied member of this protein family and in the brain, apoE is thought to serve similar functions. It is clear that the brain has its own system of cholesterol supply to meet its need for cholesterol in processes such as membrane remodeling during synapse formation and increases in dendritic arbourisation. This is acquired through *de novo* cholesterol synthesis which involves a series of sequential modifications in a 20 step reaction, the 5 key steps are as follows: Acetyl Co A is firstly converted to 3-hydroxy-methylglutaryl-CoA (HMG-CoA) and then to mevalonate; mevalonate is phosphorylated to isopentenyl pyrophosphate (IPP) and other isoprenoid units which form squalene; squalene is finally converted to lanosterol which, subsequently, will finally form cholesterol (Leduc et al., 2010). Cholesterol synthesis is thought to mainly occur in astrocytes and oligodendrocytes and delivers cholesterol to neurons via high density lipoprotein (HDL)-like particles. The formation of HDL-like particles containing apoE is assisted by the cholesterol transporters, ATP-binding cassette, subfamily A, member 1 (ABCA1), which transports cellular cholesterol and phospholipids to lipid-poor apolipoproteins and also ATP-binding cassette, subfamily G, member 1 (ABCG1). Newly synthesised HDL-like particles migrate in a gradient dependent manner towards the apoE receptors on the plasma membranes of neurons for uptake and subsequent release of cholesterol.

Cholesterol homeostasis is maintained by synthesis, degradation and transport processes, and disturbances in brain cholesterol homeostasis can alter brain function. Rabbits fed a high cholesterol diet were found to have increased amyloid beta (Aβ) accumulation in hippocampal neurons (Sparks et al., 1994). The APP processing enzymes, β- and γ-secretase, are found in cholesterol rich membrane microdomains

and increasing the cholesterol content in these lipid rafts induces amyloidogenic processing, leading to the increased generation of $A\beta_{40}$ and $A\beta_{42}$ species (Frears et al., 1999; Wahrle et al., 2002). Accordingly, the use of cholesterol lowering drugs such as the statins (HMG-CoA inhibitors), reduced Aβ production in mice (Fassbender et al., 2001). Excess cholesterol has also been identified in tau bearing neurons from AD and Niemann-Pick C (NPC) post-mortem brain tissue (Distl et al., 2001). NPC is a hereditary cholesterol storage disorder with Alzheimer-like tau pathology appearing in youth or adolescence, without amyloid plaque deposition. Statins have also been shown to reduce tau phosphorylation in NPC mice (Ohm et al., 2003). In addition, some epidemiological studies suggests that statins may reduce the incidence of AD (Haag et al., 2009; Li et al., 2004; Simons et al., 2002; Sparks et al., 2005).

In respect to apoE, isoform-specific effects have been observed on cholesterol delivery. For example, *in vitro*, apoE3 was shown to deliver cholesterol more efficiently to neurons than apoE4 (Michikawa and Yanagisawa, 1998). Since the apoE4 isoform is a major risk factor for AD (Strittmatter et al., 1993), this implies that altered cholesterol metabolism may have an impact on Aβ and tau pathologies. In fact, the interaction between Aβ and native apoE isoforms (associated with lipid particles) has different affinities, and as a consequence this may affect the trafficking and deposition of Aβ (LaDu et al., 1994). For tau, the inhibition of cholesterol biosynthesis *in vitro* increases tau hyperphosphorylation (Fan et al., 2001) and the apoE4 isoform has been reported to impair neurite outgrowth and be neurotoxic (Nathan et al., 1994; Nathan et al., 1995).

Interestingly, in a recent publication from our group, transcriptomic analysis of neurons treated with the thiazolidinedione (TZD), pioglitazone, showed an upregulation in cholesterol biosynthetic genes at the 6 hours time point and by 24 hours these genes were downregulated with the subsequent upregulation of the cholesterol transporters ABCA1 and ABCG1 (Cocks et al., 2010). However, these observations were via a PPARγ independent mechanism as co-treatment of neurons with the PPARγ

antagonist, GW9662, did not reduce the effects. Other studies have shown that another TZD, rosiglitazone, can upregulate the transcription of ABCA1 (Chawla et al., 2001; Chinetti et al., 2001), which can protect against diabetes as the absence of ABCA1 in β-cells of the pancreas was shown to increase cholesterol content and impair β-cell function (Brunham et al., 2007). Taken together, these findings indicate PPARγ agonists have a role on the influence of cholesterol biosynthesis.

Given there is evidence that cholesterol metabolism is differentially affected by the different apoE isoforms, and given the relationship with APOE genotype and both amyloid and tau pathologies discussed above, we hypothesised that the APOEε3 and ε4 isoforms may differentially modulate the effects of the pioglitazone, on tau phosphorylation and cholesterol biosynthesis. I established an *in vitro* model to determine if this is the case. Primary neuronal cultures were incubated with native apoE preparations, insulin and with or without pioglitazone. Insulin was used to mimic the HFD-induced hyperinsulinemia observed in mice. Measures of tau phosphorylation and cholesterol biosynthesis were subsequently performed, using western blotting and qRT-PCR, respectively.

6.2 Results

6.2.1 Neuronal uptake of human apoE from the conditioned media

To model neurons expressing human apoE *in vitro*, we applied conditioned media (CM) from Chinese hamster ovary (CHO) cells expressing EGFP-tagged human apoE3 or apoE4 to cortical neuronal cultures. As a control, we applied WT CHO CM onto the neuronal cultures. Figure 6.1 shows that lysates from untransfected, WT CHO cells barely express apoE, whilst very robust bands are detected in the CHO cells containing the human APOE constructs. This blot also shows that the expression levels of each APOE construct are comparable. It can also be observed that, as expected, apoE is secreted into the media and that there is no isoform specific effect on secretion. This sets the basal conditions for the subsequent experiments. Thus, a non-radiolabelled "pulse-chase like" experiment was carried out to investigate the neuronal uptake of apoE from WT CHO or CHO-apoE CM. Neurons were cultured in WT CHO or CHO-apoE CM for 24 h at 4°C or 37°C. Incubation at these two temperatures would allow us to track the uptake process because cellular processes are reduced within a cell at 4°C compared to 37°C. Lysates were collected after 24 h to assess neuronal uptake of apoE from the CM by western blotting. Figure 6.2 shows an immunoblot of the lysates from neurons incubated at 4°C or 37°C with WT CHO, CHO-apoE3 or CHO-apoE4 CM. A distinct band at 60 KDa can be observed corresponding to the apoE protein. ApoE is normally detected at 34 kDa, however due to it being tagged with EGFP (27 kDa), the band detected in the presented blots ran at ~60 kDa. In neurons incubated overnight at 4°C, a faint band was detected in those exposed to CHO-apoE3 or CHO-apoE4 CM, with neuronal uptake of apoE appearing to be similar. However, when neurons were incubated overnight at 37°C, a more intense band corresponding to apoE was detected exclusively in the neurons exposed to apoE3 and apoE4 CM, therefore showing a greater uptake of apoE.

Figure 6.1 CHO cells express the apoE protein

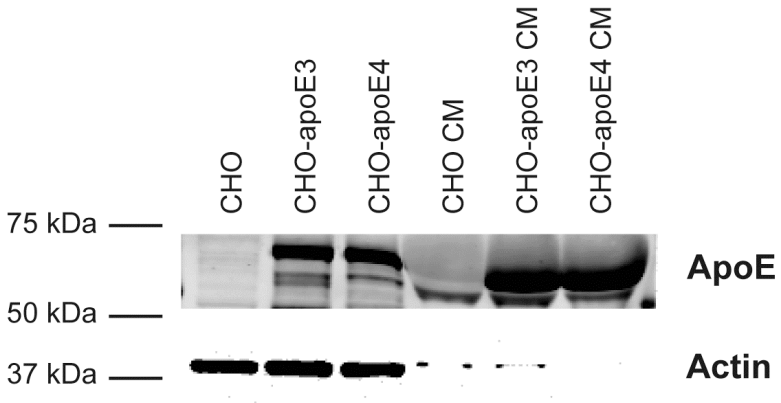

Western blot of apoE protein in lysates and conditioned media (CM) from WT CHO cells and CHO cells transfected with the human APOEε3 or APOEε4 EGFP-tagged constructs, indicated as CHO, CHO-apoE3 and CHO-apoE4, respectively.

Figure 6.2 Neuronal uptake of apoE from CHO-apoE conditioned media

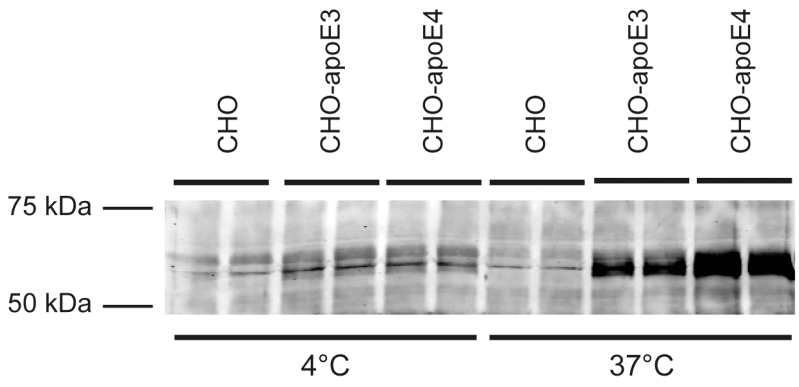

Pulse chase-like experiment to show the uptake of apoE in neurons incubated with CHO-apoE CM for 24 h at 37°C and the decrease rate of this process also for 24 h at 4ºC.

6.2.2 Treatment of neurons with CHO-apoE conditioned media improves cell viability

Neuronal cultures were treated with WT CHO, CHO-apoE3 or CHO-apoE4 CM with or without 10 μM pioglitazone for 24 h. A live dead staining assay was used as a measure of cell viability; calcein AM stains healthy cells green whilst ethidium homodimer III stains dead cells in red (Figure 6.3A-F). In neurons treated with WT CHO CM, approximately 34% of the neurons were dead after 24 h. Surprisingly, incubating neurons with CHO-apoE3 or CHO-apoE4 CM for the same period (24 h) appeared to reduce cell death compared to neurons incubated with WT CHO CM, by 8% and 6% respectively, although this reduction in cell death was non-significant. This pattern was also observed after 24 h pioglitazone treatment and there was a statistically significant reduction in cell death in neurons exposed to CHO-apoE3 CM compared to WT CHO CM ($p= 0.02$) (Figure 6.3G).

Figure 6.3 Calcein AM and ethidium homodimer III dual staining for cell viability

Immunofluorescence of healthy and dead neurons which were cultured in A) WT CHO CM, B) CHO-apoE3 CM, C) CHO-apoE4 CM, D) WT CHO CM with 10 μM pioglitazone, E) CHO-apoE3 CM with 10 μM pioglitazone and F) CHO-apoE4 CM with 10 μM pioglitazone. G) Bar chart showing the percentage of dead neurons with the corresponding treatments shown in A-F. Data shown is mean±SEM, *$p<0.05$ by Student's t-test. Scale bar: 100 μm, picture was taken at 20x magnification.

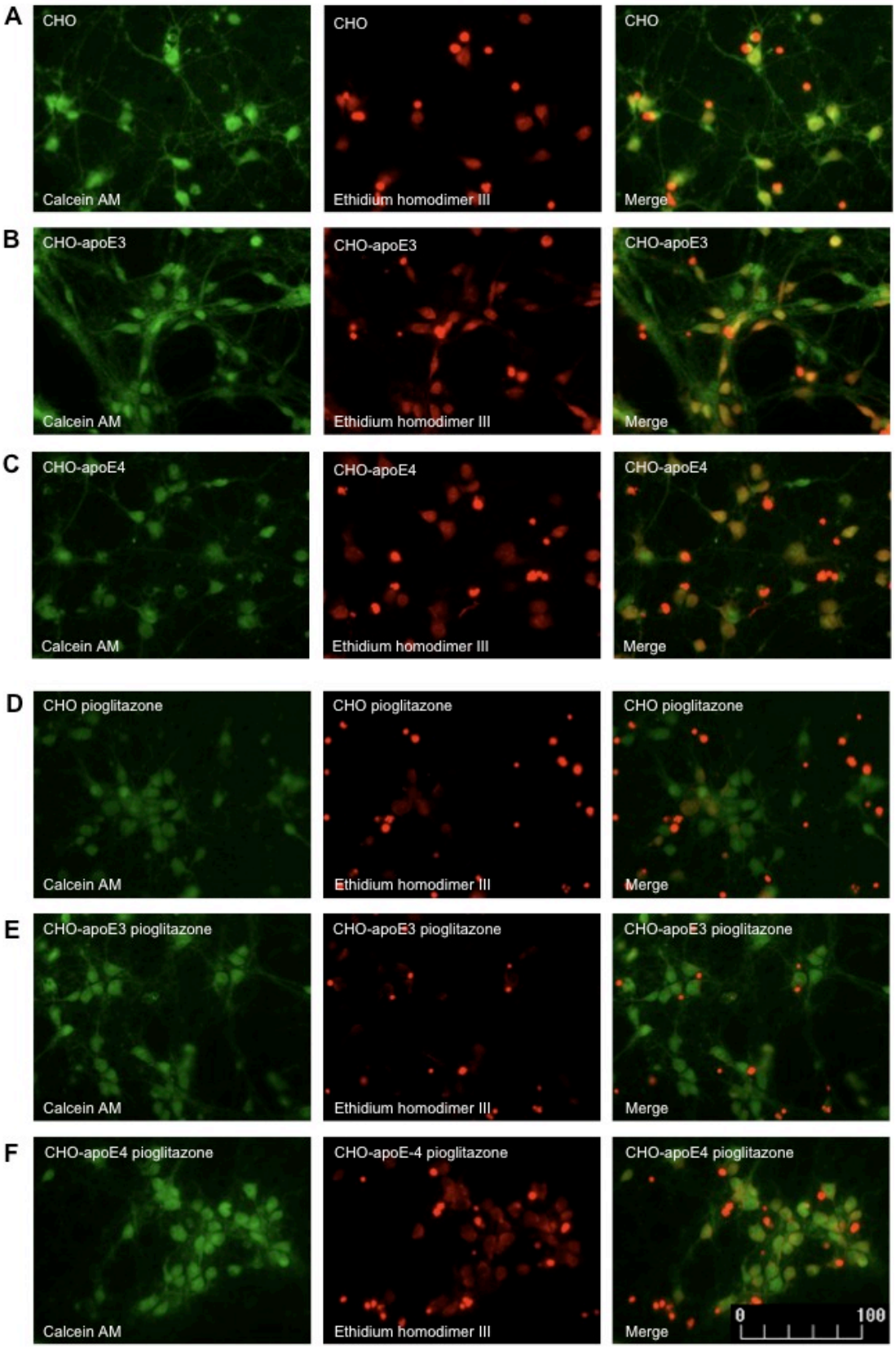
A
CHO
Calcein AM
CHO
Ethidium homodimer III
CHO
Merge
B
CHO-apoE3
Calcein AM
CHO-apoE3
Ethidium homodimer III
CHO-apoE3
Merge
C
CHO-apoE4
Calcein AM
CHO-apoE4
Ethidium homodimer III
CHO-apoE4
Merge
D
CHO pioglitazone
Calcein AM
CHO pioglitazone
Ethidium homodimer III
CHO pioglitazone
Merge
E
CHO-apoE3 pioglitazone
Calcein AM
CHO-apoE3 pioglitazone
Ethidium homodimer III
CHO-apoE3 pioglitazone
Merge
F
CHO-apoE4 pioglitazone
Calcein AM
CHO-apoE-4 pioglitazone
Ethidium homodimer III
CHO-apoE4 pioglitazone
Merge
0
100

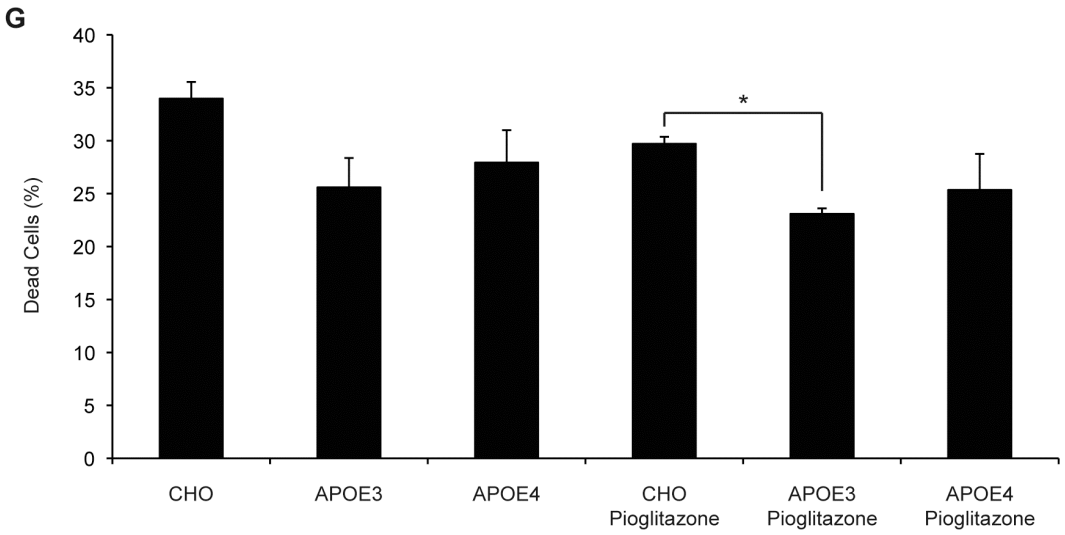

6.2.3 The effect of insulin treatment on neuronal cultures

Preliminary experiments were carried out in an attempt to determine the most effective dose and time course of insulin treatment. Neurons were treated with 50 nM insulin at 15 min, 30 min, 1 h, 3 h or 24 h. Neurons were also treated with 10, 50, 100, 500 or 1000 nM insulin for 15 min. However despite repeated experiments, results were inconclusive, which may in part be due to the reported biphasic temporal effect of insulin on GSK-3 activity. It was therefore decided to remove insulin treatment from these experiments.

6.2.4 Levels of tau and GSK-3 phosphorylation in neurons incubated with CHO-apoE conditioned media and pioglitazone treatment

Neurons treated with CHO-apoE conditioned media alone or with 10 μM pioglitazone for 24 h were immunoblotted for tau phosphorylation with the PHF1 antibody recognising the Ser396/404 epitope and for the phosphorylation of GSK-3 (Ser21/9). The dose of pioglitazone drug treatment used on neurons was determined

previously by this lab (Cocks et al., 2010). Although the levels of phosphorylated Akt were also measured, the signal was very weak, even with increased loading, and could not be measured reliably by densitometry. Comparison of the neurons cultured with WT CHO CM and CHO-apoE3 CM shows a significant reduction in tau phosphorylation ($p=0.01$) whilst no significant difference was detected between neurons treated with WT CHO CM and CHO-apoE4 CM (Figure 6.4A). Treatment of neurons cultured in WT CHO or CHO-apoE CM with 10 μM pioglitazone did not cause significant changes in tau phosphorylation (Figure 6.4B).

The same samples were immunoblotted for phospho-GSK-3. No significant differences were observed for neurons cultured in WT CHO CM and CHO-apoE CM (Figure 6.4C). We therefore tried treating neurons briefly with 500 nM insulin to test if GSK-3 was in an inactive state. Insulin treatment for 15 min significantly increased GSK-3 phosphorylation ($p<0.001$), hence showing GSK-3 was not in an inactive state. Treatment of neurons with 10 μM pioglitazone for 24 h in the various CHO CM did not alter the phosphorylation of GSK-3 (Figure 6.4D).

Figure 6.4 Levels of tau and GSK-3 phosphorylation in neurons cultured with CHO-apoE conditioned media and pioglitazone treatment

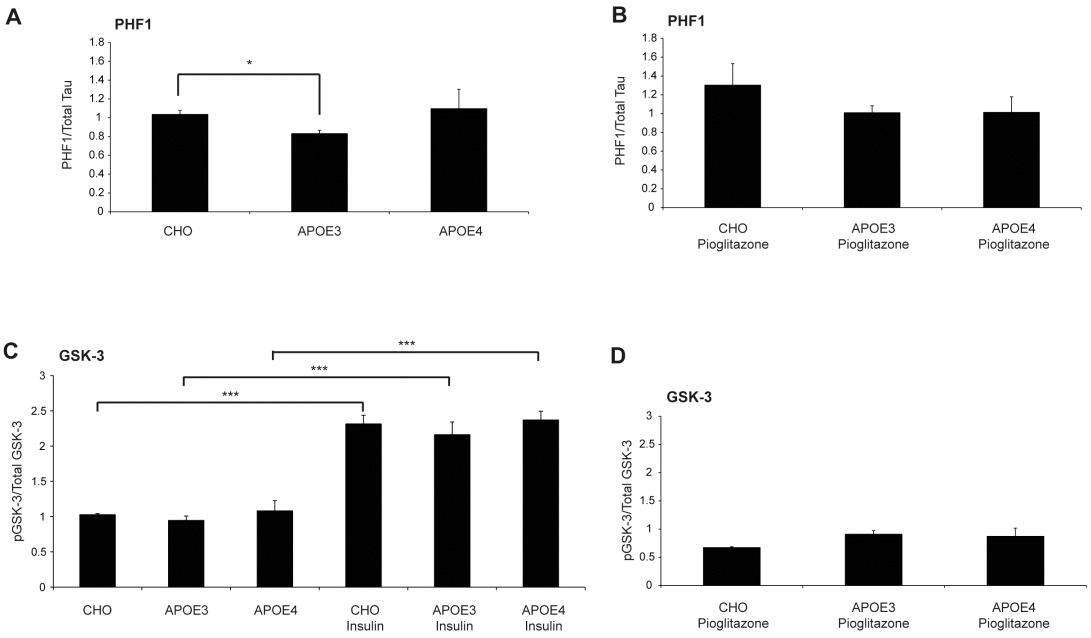

Lysates were immunoblotted for A, B) tau phosphorylation at the Ser396/404 epitope with the PHF1 antibody and C, D) phosphorylation of GSK-3 at Ser21/9 epitope. Data are represented as mean±SEM, n = 6, *p<0.05, ***p<0.001 by Student's t-test.

6.2.5 Effects of pioglitazone on the expression of cholesterol biosynthesis genes in neurons cultured with CHO-apoE conditioned media

To investigate whether apoE isoforms have differential effects on cholesterol biosynthesis we treated neurons as above with WT CHO, CHO-apoE3 or CHO-apoE4 CM with 10 μM pioglitazone for 6 h or 24 h. The following genes were investigated due to their critical involvement in cholesterol synthesis: HMG-CoA reductase (HMGCR), mevalonate decarboxylase (MVD), lanosterol synthase (LSS) and 7-dehydrocholesterol reductase (DHCR7). We also looked at cholesterol transporters; ATP-binding cassette, subfamily A, member1 (ABCA1) and ATP-binding cassette,

subfamily G, member1 (ABCG1). These particular genes and time points were chosen based on a previous study from our lab. Results showed a trend towards an increase in cholesterol biosynthetic genes at the 6 h time point in neurons cultured with WT CHO CM and pioglitazone treatment (Figure 6.5A). However, only LSS reached statistical significance ($p=0.04$). At the 24 h time point, there seem to be a trend towards a reduction in the expression of these genes except for DHCR7. Expression levels of DHCR7 remained similar to the 6 h time point (Figure 6.5A). In neurons cultured in CHO-apoE3 and CHO-apoE4 CM, genes involved in cholesterol biosynthesis were not significantly altered (Figure 6.5B and C). Additionally, the levels of ABCA1 and ABCG1 genes were not altered in neurons cultured with WT CHO or CHO-apoE3 CM (Figure 6.5A and B). However, in neurons cultured with CHO-apoE4 CM, ABCA1 expression increased significantly at the 24 h timepoint compared to 6 h ($p=0.02$), whilst no changes in the level of ABCG1 expression was observed (Figure 6.5C).

Figure 6.5 Expression of genes in the cholesterol biosynthesis pathway in neurons cultured with CHO-apoE conditioned media and treated with pioglitazone

Neuronal cultures were incubated in A) WT CHO CM, B) CHO-apoE3 CM and C) CHO-apoE4 CM. Following pioglitazone treatment for 6 h or 24 h, expression of the following genes were measured by qRT-PCR: HMG-CoA reductase (HMGCR), mevalonate decarboxylase (MVD), lanosterol synthase (LSS), 7-dehydrocholesterol reductase (DHCR7), ATP-binding cassette, subfamily A, member 1 (ABCA1) and ATP-binding cassette, subfamily G, member 1 (ABCG1). Data are represented as normalised against control, mean±SEM, n=6, *$p<0.05$ by Student's t-test.

A

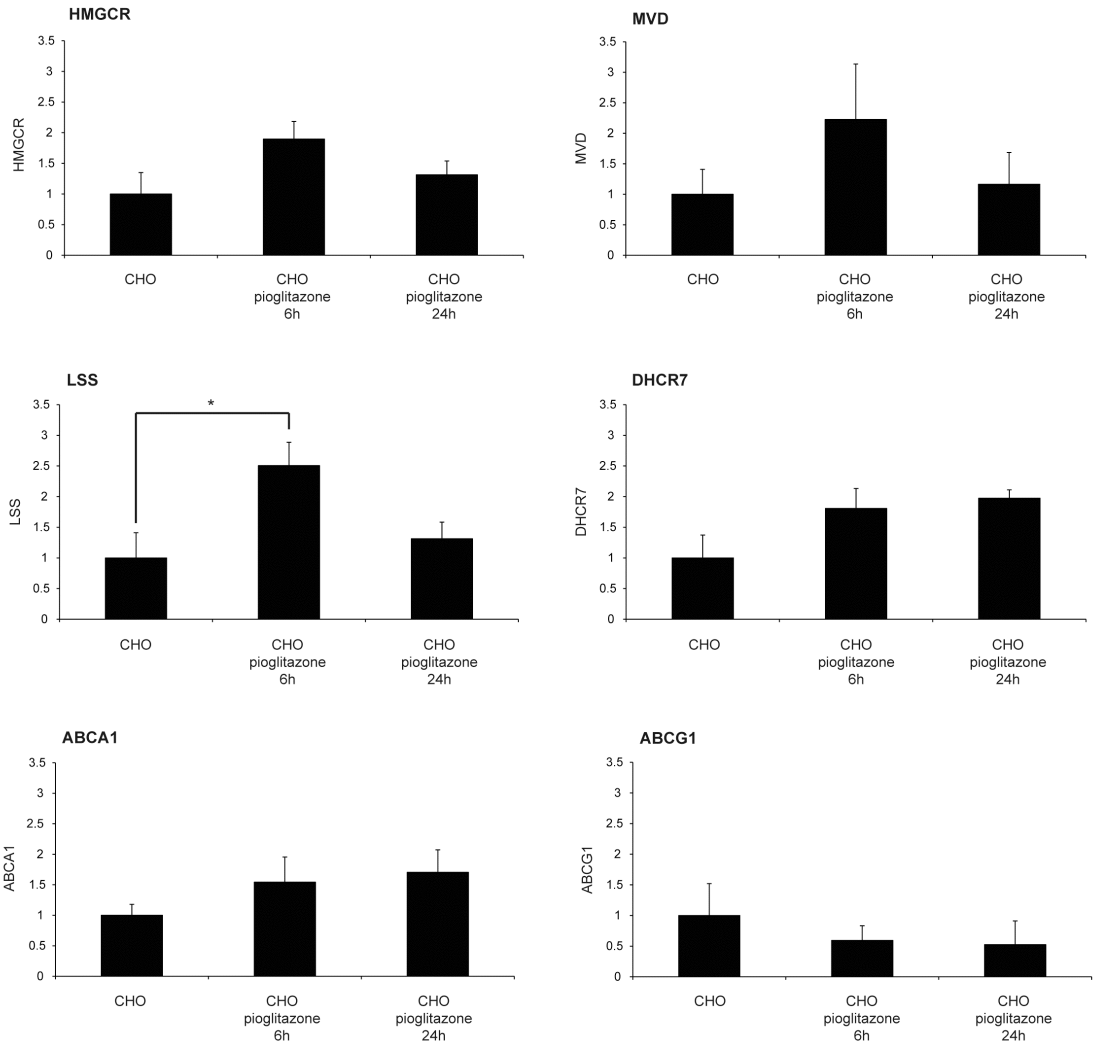
HMGCR
HMGCR
3.5
3
2.5
2
1.5
1
0.5
0
CHO
CHO pioglitazone 6h
CHO pioglitazone 24h
MVD
MVD
LSS
LSS
*
DHCR7
DHCR7
ABCA1
ABCA1
ABCG1
ABCG1

B

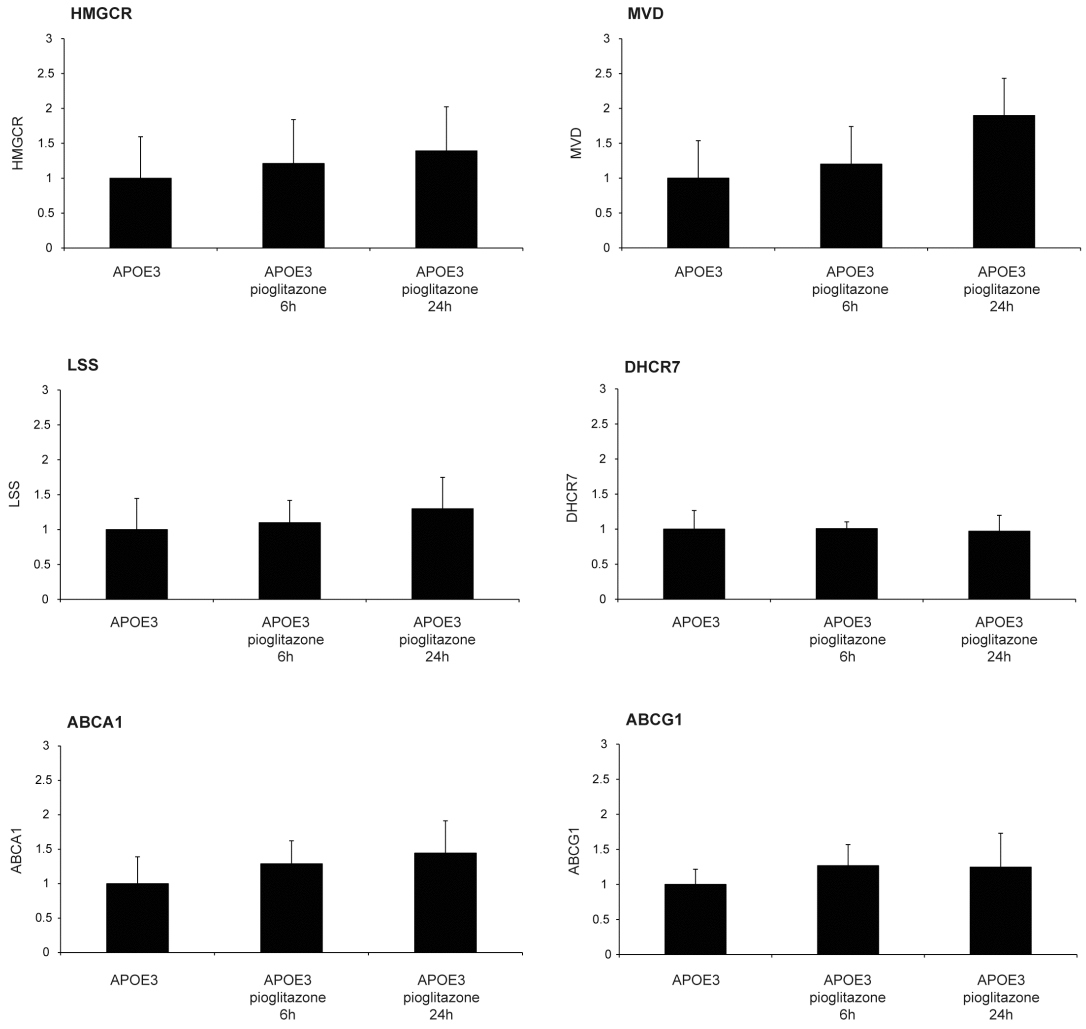
HMGCR
HMGCR
MVD
MVD
LSS
LSS
DHCR7
DHCR7
ABCA1
ABCA1
ABCG1
ABCG1
0
0.5
1
1.5
2
2.5
3
APOE3
APOE3 pioglitazone 6h
APOE3 pioglitazone 24h

C

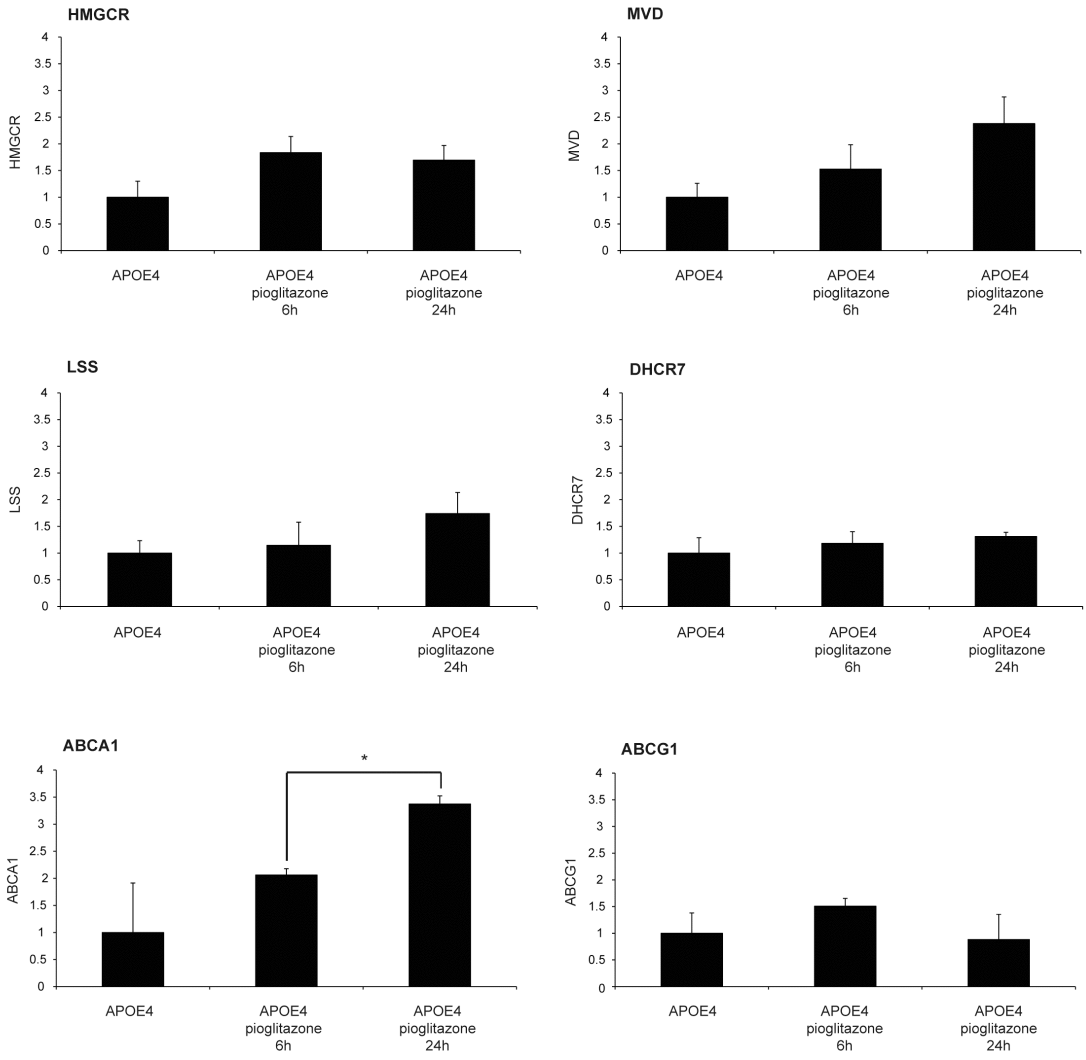
HMGCR
HMGCR
4
3.5
3
2.5
2
1.5
1
0.5
0
APOE4
APOE4 pioglitazone 6h
APOE4 pioglitazone 24h
MVD
MVD
LSS
LSS
DHCR7
DHCR7
ABCA1
ABCA1
*
ABCG1
ABCG1

6.3 Discussion

In this set of experiments, we sought to determine the effects of apoE isoforms and pioglitazone on tau phosphorylation and cholesterol biosynthesis *in vitro*.

In this *in vitro* model, we were able to show in neurons cultured in CHO-apoE CM, the movement of apoE from CM into neurons by a pulse chase-like experiment. We chose to use native preparations of apoE because the biologically active form of apoE requires lipid association (LaDu et al., 1995). By incubating neurons with CM at 37°C, apoE isoforms were transported into neurons and were visible in lysates after 24 h whereas the incubation of neurons at 4°C decreased the rate of this effect. The very small amounts of apoE protein visible on the immunoblot at 4°C most likely represents the presence of apoE bound to cell surface LRP receptors, the most preferentially expressed apoE receptor in neurons (Rebeck et al., 1993). A similar *in vitro* model has been used previously by LaDu and colleagues using CM from HEK-293 cells transfected with the human APOE3 or APOE4 constructs, to look at the interaction between apoE and Aβ (LaDu et al., 1994).

In our experiments, neurons cultured with CHO-apoE3 or CHO-apoE4 CM were equally protective and although insignificant, reduced the number of dead cells compared to neurons cultured in WT CHO CM. When neurons were treated with pioglitazone, cell death was again reduced in neurons cultured with CHO-apoE3 or CHO-apoE4 CM. ApoE isoform-specific effects on tau phosphorylation was observed in neurons cultured in CHO-apoE CM; apoE3 significantly reduced tau phosphorylation in neurons whilst apoE4 did not. This observation, that apoE3 seems to be protective is in agreement with other publications. Previously, *in vitro* experiments demonstrated that the apoE3 isoform has a greater avidity for tau thereby forms more stable complexes with tau compared to the apoE4 isoform (Strittmatter et al., 1994). It has been suggested that this might form the basis of the neuroprotective effects of apoE3 compared to the apoE4 isoform in AD. In these experiments, it was shown that apoE binds to the microtubule domains on tau and was proposed to protect tau from

abnormal phosphorylation thereby reducing its propensity to undergo self-assembly into paired helical filaments. Other studies further supports this hypothesis showing that the interaction between apoE3 and tau could be abolished by the phosphorylation of tau within the microtubule binding domain (Huang et al., 1995). Furthermore, *in vitro* studies have shown apoE isoforms have differential effects on neuronal protection. Thus, apoE2 and apoE3 isoforms promote neurite outgrowth, whilst apoE4 is associated with the depolymerisation of microtubules (Bellosta et al., 1995; Fagan et al., 1996; Holtzman et al., 1995; Nathan et al., 1994; Nathan et al., 1995).

Treatment of neurons cultured in the various CHO-apoE CM with pioglitazone for 24 h showed a trend towards a decreased in tau phosphorylation however, this did not reach statistical significance. This observation is in line with another study using a similar drug, rosiglitazone, which reduced tau phosphorylation in a human SHSY-5Y neuron-like cells transfected with tau (Yoon et al., 2010). Furthermore, this group reported that GSK-3 activity was not associated with tau phosphorylation, an observation we have also made.

A recently published microarray study from our lab shows cholesterol biosynthesis is upregulated with treatment of 10 μM pioglitazone at 6 h and downregulated at 24 h. At 24 h, the cholesterol efflux transporters ABCA1 and ABCG1 were upregulated (Cocks et al., 2010). In the experiments within this chapter, we looked at the effects of a range of the cholesterol biosynthesis genes identified by Cocks and colleagues by pioglitazone treatment at 6 h and 24 h in neurons cultured with different CHO-apoE CMs. In line with their study, we observed a trend of increased cholesterol gene expression (HMGCR, MVD and LSS) in neurons treated with WT CHO CM at 6 h, which were subsequently reduced at 24 h. In neurons cultured with the CHO-apoE3 or CHO-apoE4 CM and treated with pioglitazone, cholesterol gene expression was not significantly altered, although there were some indication of increased gene expression by 24 h, for example, MVD in CHO-apoE3 and CHO-apoE4 CM treated neurons. The gene expression of the cholesterol transporter,

ABCA1, was not altered in neurons incubated with WT CHO and CHO-apoE3 CM, however, in neurons cultured with CHO-apoE4 CM, ABCA1 expression increased at 24 h compared to 6 h. ABCG1 expression was not altered in neurons cultured with each of the three CMs. The different observations between these results and that of Cocks and colleagues may be because these experiments require further repeats, which may give more conclusive results. Our findings showing no significant apoE isoform-specific effects on cholesterol biosynthesis are different to those published by Michikawa and colleagues who have shown the neurotoxic effects of apoE4 are mediated by suppression of *de novo* cholesterol synthesis (Michikawa and Yanagisawa, 1998). However, they are in line with published data from Jansen and colleagues, showing that cholesterol biosynthesis is independent of apoE genotype (Jansen et al., 2009).

In summary, the experiments in this chapter show an *in vitro* model system whereby neurons gain the effects of human apoE by the uptake of apoE protein from CHO CM. The uptake of these apoE isoforms has pro-survival effects on cell viability. In these neurons, tau phosphorylation is reduced with uptake of the apoE3 isoform and this is not correlated with GSK-3 activity. Finally in this *in vitro* system no significant changes in cholesterol gene expression were observed.

CHAPTER 7

Analysis of the Cortical Transcriptome in Low Fat and High Fat Fed Humanised APOEε3 and APOEε4 Mice

7.1 Introduction

It is well documented that impairments in brain insulin signalling can influence Alzheimer's disease (AD) pathology. This may be associated with peripheral insulin resistance, a feature of type 2 diabetes mellitus (T2DM), which is a risk factor for AD (Watson and Craft, 2003). Circulating insulin is thought to enter the brain by a receptor mediated transport process (Banks et al., 1997) and binds to insulin receptors that are highly expressed in neurons. Insulin has many roles in the brain including maintaining synaptic plasticity, neuronal growth, phosphoinositide 3-kinase (PI3K) signalling, and regulating amyloid beta (Aβ) production and tau phosphorylation (de la Monte, 2009). Furthermore, Aβ itself can inhibit PI3K/Akt signalling (Lee et al., 2009). Disruption of insulin signalling can be detrimental, leading to neurotoxicity and synaptic defects. As the metabolic syndrome becomes more prevalent, combined with a greater incidence of AD, the need to develop effective treatments, which will slow down and possibly ameliorate pathology due to impaired insulin signalling in the brain, has never been more urgent. Rosiglitazone or pioglitazone, drugs currently used to treat diabetes, have been shown to improve cognition in AD patients, at least in early phase clinical studies (Risner et al., 2006; Sato et al., 2011; Watson et al., 2005). However, rosiglitazone was not shown to be effective in a phase III clinical trial (Gold et al., 2010). More recently, metformin, another anti-diabetic drug, has also been shown to ameliorate neuronal insulin resistance and AD-like changes in an *in vitro* model (Gupta et al., 2011). At present, it is unclear the extent to which peripheral insulin resistance accompanying T2DM may impact processes within the brain and exacerbate AD pathology. In addition, diabetics possessing the APOEε4 allele have an increased risk of developing AD (Irie et al., 2008; Peila et al., 2002). This suggests APOE may mediate specific pathological changes in the insulin resistant brain.

One approach to understanding the molecular link between insulin signalling and AD pathology is to explore signalling processes in relevant models using gene expression. Gene expression can be measured at a whole genome level by a

microarray based approach. Several such studies on post-mortem AD brain tissue have been reported (Courtney et al., 2010; Liang et al., 2008) (for review) as well as in a range of AD mouse models, such as Tau23 (Woo et al., 2010), Tg2576 (George et al., 2010) PDAPP (APPV717F) (Selwood et al., 2009) and AD11 mice (Arisi et al., 2011). Transcriptomics has also been used to study insulin resistance in a streptozotocin model (Grunblatt et al., 2004).

In chapter 4, we developed an *in vivo* model of diet-induced insulin resistance. These mice developed hyperinsulinemia, impaired glucose metabolism and tau pathology in the brain. The aim of this chapter is to elucidate the molecular mechanisms underlying diet-induced insulin resistance in the brain of mice by using microarray gene expression technology. The objectives were:

- To identify APOE genotypic changes in brain gene expression by comparing WT mice, APOE KO, APOEε3 and APOEε4 transgenic mice (fed a "normal" low fat diet-LFD)
- To identify diet-responsive changes by comparing the brain transcriptome of mice fed a LFD with that of mice fed a high fat diet (HFD) (within each genotype).
- To identify APOE genotypic changes that may interact with diet-responsive changes by comparing brain gene expression in WT mice, APOEε3 and APOEε4 transgenic mice fed HFD.

7.2 Results

In chapter 4, we showed that all mice used in this study develop insulin resistance when fed a HFD for 32 weeks. This hyperinsulinemia is accompanied by changes in tau phosphorylation. To gain insight into the mechanism(s) responsible for this and to identify key pathways, we performed microarray analyses on the contralateral brain region from the same mice used for protein analyses in chapter 4.

7.2.1 The effect of APOE genotype on the brain transcriptome

As we ultimately aimed to investigate the effect of HFD on brain gene expression, and how this may be affected by APOE genotype, we initially investigated the effect APOE genotype had on cortical gene expression in mice fed a LFD. There were 49 genes that were significantly differentially expressed in APOE knockout mice (KO) compared to normal wild-type (WT) mice at an FDR corrected q-value ≤0.05 (Table 7.1). Reassuringly, one of the most significant changes, with the greatest fold change in expression was the APOE gene (~52, log2fold). To elucidate the molecular mechanisms by which APOE may act centrally, functional categories were assigned to the transcripts using NetAffx, GeneCards or NCBI Gene searches. The remaining 48 genes that were altered encoded a diverse range of functions including apoptosis, metabolic processes, signal transduction, transcription and translation. We next compared gene expression between normal WT mice and those where murine APOE had been deleted, and replaced with human APOEε3 (E3) (Table 7.2) or APOEε4 (E4) (Table 7.3) We identified in these comparisons 51 genes and 47 genes respectively that reached an FDR corrected q-value ≤0.05. Genes that featured in all three tables (7.1 to 7.3) are likely to be genes affected by the deletion of murine APOE, whilst genes unique to table 7.2 or 7.3, are likely due to the effect of humanised APOEε3 or APOEε4 respectively on brain gene expression. To clarify, we built a Venn diagram

(Figure 7.1) to identify the number of genes, which were unique or common to the three comparisons.

Figure 7.1 Venn diagram showing the number of common genes differentially expressed between APOE KO, APOEε3 or APOEε4 and WT mice fed LFD

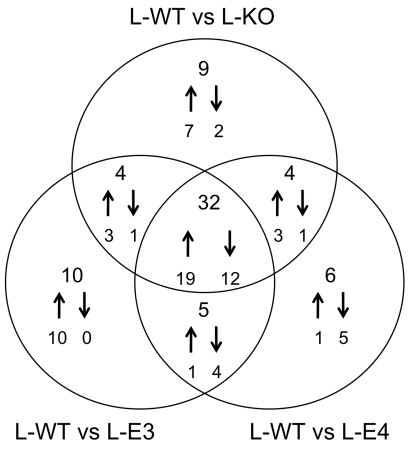

The up and down arrows indicate upregulation or downregulation of genes respectively. (L-WT = WT mice fed LFD; L-KO = APOE KO mice fed LFD; L-E3 = APOEε3 mice fed LFD; L-E4 = APOEε4 mice fed LFD).

We identified 32 genes altered in all three comparisons, which are presumably due to the deletion of murine APOE (Table 7.4a). Classification of the 19 upregulated transcripts revealed genes involved in apoptosis, cell differentiation, development, metabolic processes, proteolysis, signal transduction, transcription, translation and ubiquitination. On the other hand 12 genes were downregulated that are involved in cytoskeletal organisation, metabolic processes, protein modification, signal transduction, transcription and transport. We also identified five genes altered by introducing human APOE genes (Figure 7.1; Table 7.4b). The only upregulated gene,

ZFP772, currently has no identifiable biological function. There were four downregulated genes; BLVRB (biliverdin reductase B) that catalyses the final step of heme metabolism, PSG16 (pregnancy specific glycoprotein 16), DMPK (dystrophia myotonica-protein kinase) and EXOC3L2 (exocyst complex component 3-like 2).

There were 10 genes significantly altered uniquely in APOEε3 mice compared to WT mice (Figure 7.1; Table 7.4c). All 10 transcripts were upregulated with biological functions enriched in transcription, as well as sugar binding (LGALS4), transport (ARL5A) and a regulator of protein modification by phosphorylation (FAM129A).

In contrast, the presence of APOEε4 altered the transcripts of 6 different genes (Figure 7.1; Table 7.4d). The only upregulated gene, ZFP180, is involved in gene transcription, whilst biological processes of the other five genes included transport (NAPA), signal transduction (ICOSL), development (CLPTM1) and protein phosphorylation (PRKD2).

7.2.2 The effect of diet on the brain transcriptome

As brain insulin signalling can influence AD pathology as in T2DM, we were interested to investigate the effects of diet on brain transcription. As we had identified a number of gene expression differences between WT and transgenic mice in section 7.2.1, we felt it was important to compare LFD and HFD fed mice within each genotype. When we compared the brain transcriptomes of all mice fed LFD and HFD, we found no differentially expressed genes when using a FDR corrected q-value ≤0.05. Although this method was adequate for identifying differences between our WT and transgenic mice, we felt it may be too stringent to detect more subtle changes caused by dietary modifications. As such, we therefore decided to identify the top 50 genes when ranked by significance of change, using an uncorrected p-value, to identify central changes that may be associated with HFD feeding (Tables 7.5, 7.6, 7.7 and 7.8).

Genes differentially expressed in WT mice fed a LFD versus HFD, are presented in Table 7.5. To elucidate the mechanisms and pathways involved centrally in diet-induced insulin resistance, we again assigned functional categories to the transcripts using NetAffx, GeneCards or NCBI Gene searches.

Differentially expressed transcripts encoded proteins from many diverse functional categories. These included cytoskeletal organisation, development, phosphorylation, proteolysis, signal transduction and transport (Table 7.5).

7.2.3 The effect of diet on the brain transcriptome in APOE KO transgenic mice

As we identified both a number of genes that were altered in the brain due to deletion of the murine APOE gene (Table 7.1), and others altered in the brain as a consequence of diet in WT mice (Table 7.5), we therefore decided to investigate whether different genes are altered in APOE KO mice fed a HFD compared to those fed a LFD (Table 7.6). Differentially expressed transcripts encoded genes related to development, signal transduction, transcription, translation and transport. Of particular interest was the increased expression of the cholesterol transporter ABCA1 (ATP-binding cassette sub-family A member 1), as ABCA1 is associated with clearance of Aβ in the brain.

7.2.4 The effect of diet on the brain transcriptome in transgenic mice expressing human APOE transgenes.

As we had shown that diet has a small effect on brain gene expression in trangenic mice with the APOE gene deleted (Table 7.6), we thus decided to investigate whether the introduction of human APOEε3 and ε4 alleles, which increase the risk of developing AD in humans, could result in different genes being altered during dietary changes.

In APOEε3 transgenic mice, HFD feeding altered the expression of transcripts related to development, metabolic processes involving mitochondria and lipids, signal transduction, transcription, translation and transport (Table 7.7).

In APOEε4 transgenic mice, differentially expressed genes in HFD fed animals were involved in kinase and phosphatase activities, signal transduction, transcription, translation and transport (Table 7.8). Also noteworthy is the increased expression of ADRA2A, which encodes an adrenergic, G-protein coupled receptor that is associated with insulin secretion (Fagerholm et al., 2004). This gene did not feature in tables 7.5, 7.6 or 7.7, and is thus associated with the presence of the human APOEε4 transgene and HFD, and provides a possible interaction between diet and genotype in regulating insulin levels.

7.2.5 The interaction between diet and APOE genotype in regulating brain cortical gene expression.

Although we did not observe any APOE isoform-dependent effects on tau phosphorylation in these HFD fed mice, we went on to investigate the effects of APOE isoform on the cortical transcriptome in mice fed this HFD. It was hoped this may be informative as to the possible mechanisms underlying the APOE isoform-dependent effects on tau phosphorylation observed in pioglitazone treated HFD fed mice, as presented in chapter 5.

To establish the effect of loss of APOE in mice, we looked at the effect of HFD feeding in APOE KO mice compared to WT mice (Table 7.9). Using an FDR corrected q-value ≤0.05, we found 55 transcripts differentially expressed. We were interested to compare this list to the list of genes significantly different in APOE KO mice compared to WT mice fed LFD, and to the list of genes significantly different when comparing APOE KO mice fed LFD and HFD. As such, we produced a Venn diagram (Figure 7.2)

of these three comparisons to help us identify which genes may be important in mediating the effect of diet in the absence of the APOE gene.

Figure 7.2 Venn diagram showing the number of common genes differentially expressed between APOE KO mice fed LFD or HFD with WT mice fed LFD or HFD and APOE KO mice fed HFD compared to those fed LFD

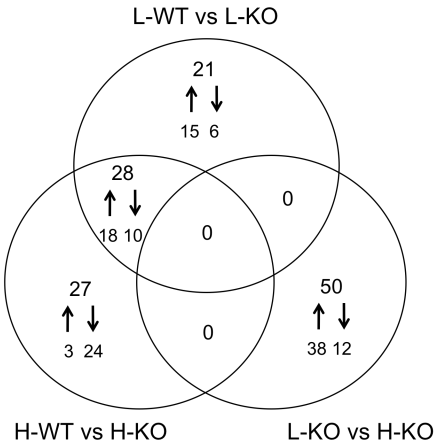

The up and down arrows indicate upregulation or downregulation of genes respectively. (L-WT = WT mice fed LFD; L-KO = APOE KO mice fed LFD; H-WT = WT mice fed HFD; H-KO = APOE KO mice fed HFD).

A total of 28 genes were altered in APOE KO mice, regardless of diet, of these genes 18 were upregulated whilst ten were downregulated (Table 7.10a). As expected, this list of genes was very similar to the list of genes in the centre of Venn diagram Figure 7.1, which were genes that are affected by deletion of murine APOE. Extra genes that are not common to those listed in the centre of Venn diagram in Figure 7.1 include CCDC123 (upregulated), the biological function of which is unknown, MTHFD2

(upregulated) that has a role in magnesium ion binding and KPTN (downregulated), which is involved in actin cytoskeleton organisation.

Unique to the loss of APOE and not related to dietary changes are 21 transcripts, of which 15 were upregulated and 6 were downregulated (Table 7.10b). In contrast, unique to the loss of APOE, combined with HFD feeding is 27 transcripts; 3 upregulated and 24 downregulated (Table 7.10c). Within this list (H-WT vs H-KO), upregulated include transcripts encoding a sugar binding protein, LGALS4 and CEACAM2, which has a role in signal transduction. The exact function of Ceacam2 is unclear however it has recently been reported that within the brain, Ceacam2 regulates feeding behaviour, energy balance and insulin sensitivity (Heinrich et al., 2010). Downregulated transcripts were enriched in kinases, metabolic processes, transcription and translation. Another interesting gene is NAPA, which is part of the SNARE complex that allows docking and fusing of vesicles to their target surface on the plasma membrane. Napa has been reported to be associated with GLUT4 vesicles that are insulin responsive and increases the absorption of glucose (Mastick and Falick, 1997). The downregulation of NAPA in our list may reduce association of GLUT4 vesicles with the plasma membrane and dysregulate storage of glucose in the brain of HFD fed APOE KO mice.

No overlapping genes were found between APOE KO mice fed LFD and HFD with APOE KO mice compared to WT mice fed LFD or HFD. The genes in the APOE KO mice fed LFD and HFD comparison were compiled by identifying the top 50 genes ranked by significance of change, using an uncorrected p-value (discussed in section 7.2.3). The fact that we have identified significant changes, which however do not pass FDR correction suggests HFD does cause gene expression changes in the brain, but we may have too few mice in our study to detect subtle changes in expression.

After identifying genes that may be altered as a consequence of dietary changes, in the absence of APOE, we then went on to investigate whether human APOE transgenes may impact on cortical gene expression in mice fed a HFD.

Genotypic comparisons between WT and either APOEε3 or APOEε4 mice fed HFD using a FDR-corrected q-value ≤0.05 revealed a total of 50 transcripts (Table 7.11) and 71 transcripts (Table 7.12) differentially expressed respectively. As we have identified a number of diet responsive genes, which are altered in transgenic mice expressing APOEε3 or APOEε4, we were interested to examine first whether the same genes or different genes were altered in transgenic mice expressing APOEε3 or APOEε4 fed HFD, as this would give us an insight into the molecular mechanisms that could be involved in the interaction between diet and APOE genotype in affecting brain gene expression. For ease of illustration this has been displayed as a Venn diagram (Figure 7.3). Of our 50 genes that were significantly altered in transgenic mice expressing APOEε3 fed HFD and 71 genes altered in transgenic mice expressing APOEε4 fed HFD, 38 featured in both lists (Table 7.13a). GO processes in this common gene list included enzymes involved with metabolic processes, kinase and phosphatase activities, transcription and translation. Reassuringly, all 38 genes showed the same direction of chance in both transgenic groups. These genes could be altered due to either the deletion of murine APOE, the insertion of human APOE (regardless of allele), or an interaction of genotype with diet. To investigate this further, we searched for these 38 genes in both table 7.1 (genes altered in KO mice compared to WT mice) and tables 7.2 and 7.3 (genes altered in APOEε3 fed LFD and genes altered in APOEε4 fed LFD, respectively). Altogether, 37 genes were also identified in tables 7.1, 7.2 and 7.3. The transcript for DEDD2 (death effector domain containing DNA binding protein 2) was the only gene not identified in these lists and therefore could be due to an interaction between genotype and diet (highlighted in Table 7.13a).

Genes unique to APOEε3 were also compared to tables 7.7 (genes altered in APOEε3 mice fed HFD compared to LFD) and 7.2 (genes altered in APOEε3 mice compared to WT mice fed LFD). A total of 8 genes were identified as not featuring in neither tables 7.7 or 7.2. These genes are likely due to an interaction between APOEε3 and diet (highlighted in Table 7.13b).

Finally, we compared genes unique to APOEε4 to tables 7.8 (genes altered in APOEε4 mice fed HFD compared to LFD) and 7.3 (genes altered in APOEε4 mice compared to WT mice fed LFD). In comparison to tables 7.8 and 7.3, 21 transcripts were different and could therefore be due to interaction between APOEε4 allele and diet (highlighted in Table 7.13c).

We found 12 genes (6 upregulated, 6 downregulated) that were uniquely differentially expressed in APOEε3 mice compared to WT mice fed HFD but not in APOEε4 mice. These genes encode proteins involved in processes such as development, phosphatase activity, signal transduction, synaptic vesicle recycling, transcription and translation (Table 7.13b). The genes unique to the HFD APOEε4 vs HFD WT comparison consisted of 9 upregulated genes, which were mostly involved in calcium or magnesium binding, development, signal transduction, transcription and translation, and 14 downregulated genes representing the following processes; iron homeostasis (TRFR2 (transferrin receptor 2)), proteolysis and vesicle transport (STX17 (syntaxin 17) and AP1G2 (adaptor-related protein complex 1, γ2 subunit)), signal transduction, transcription and translation (Table 7.13c).

Figure 7.3 Venn diagram showing the number of common genes differentially expressed between WT mice fed HFD and APOEε3 or APOEε4 mice fed HFD

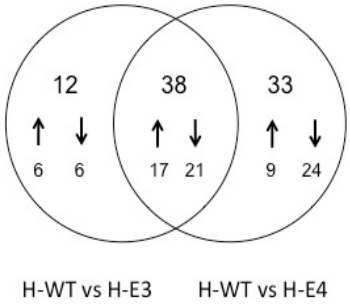

The corresponding gene lists are presented in tables 7.13a (overlapping genes), 7.13b (genes unique to WT vs APOEε3 comparison) and 7.13c (genes unique to WT vs APOEε4 comparison). The up and down arrows indicate upregulation or downregulation of genes respectively. (H-WT = WT mice fed HFD; H-E3 = APOEε3 mice fed HFD; H-E4 = APOEε4 mice fed HFD).

7.2.6 Pathway analysis and webQTL

In this chapter we have identified 71 genes that are significantly altered in the brains of transgenic mice expressing human APOEε4 when fed HFD. Of these, 21 were believed to be due to a combination of the presence of the ε4 allele and a HFD, as they were not observed in other comparisons. These genes are particularly interesting as they may be important molecular mechanisms by which diet-induced diabetes may increase the risk of AD in at risk individuals. In chapter 5, we demonstrated that pioglitazone reduced tau phosphorylation in APOEε3 mice fed HFD but not in APOEε4 mice fed HFD. As we did not find components of the insulin signalling pathway (Akt, GSK-3), tau kinases (GSK-3, Cdk5) or the tau phosphatase PP2A altered in our protein studies, network analysis using ingenuity pathway analysis (IPA) may indicate pathways associated with changes in tau phosphorylation at a transcriptional level. We therefore compared gene expression levels between APOEε3 mice fed HFD and APOEε4 mice fed HFD (Table 7.14), IPA revealed one of the top-scoring canonical pathways was axonal guidance signalling (Figure 7.4). In this network, tubulin is directly related to some of the genes from our list (TUBB4, CNP, MAG) and together suggests cytoskeletal changes related to the microtubular network is fundamental to the remodelling of dendrites and axons. Tubulin is also indirectly related to Erk1/2 and Igf1 signalling via Akt or Cnpase. Furthermore, Akt is associated with p38 MAPK, JNK and the calcineurin protein. This network suggests that the altered tau phosphorylation by APOE genotype observed in chapter 5 may be mediated by the above mentioned kinases and phosphatases.

Figure 7.4 Network for APOEε3 mice fed HFD vs APOEε4 mice fed HFD

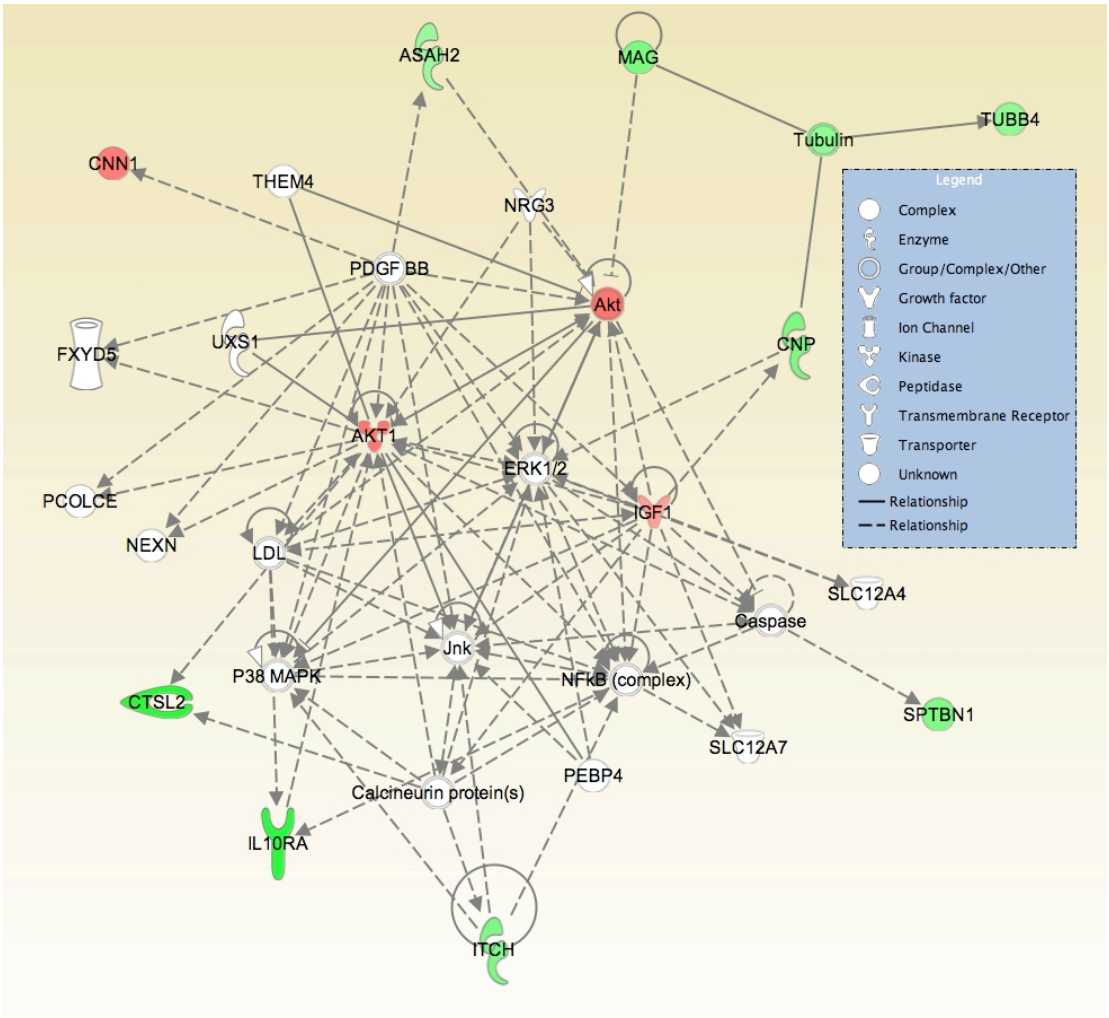

IPA revealed axonal guidance signalling as one of the top-scoring canonical pathways. The intensity of the node colour indicates upregulated (red) or downregulated (green) genes. Solid and dashed lines indicate direct or indirect relationship respectively.

Many transcripts were altered when murine APOE was absent or when human APOE was introduced, regardless of diet. Two genes of interest, WDFY1 and NUDT19, were differentially expressed in these lists. To identify genes that are co-ordinately expressed with WDFY1 and NUDT19, and thus could also be involved in susceptibility to tau phosphorylation, these genes were entered individually into the webQTL database. Searches were run on the BXD Hippocampal Consortium M430v2 database. Among the brain regions for which data is available, hippocampus was chosen because it is one of the most affected brain regions in AD. The top 15 Pearson correlations for WDFY1 and NUDT19 are shown in tables 7.15 and 7.16. Of particular interest for this study was the neuropeptide Y receptor Y2 (NPY2R) gene, which showed the 6th highest correlation with WDFY1 (Table 7.15). The neuropeptide Y receptor family has been shown to have a diverse range of biological roles, one of which is the regulation of body weight and control of food intake (Naveilhan et al., 1999). Also of interest, due to its link to AD, was the high correlation of presenilin enhancer 2 (PSENEN) with NUDT19 (Table 7.16). Psenen is the most recently identified component of the γ-secretase complex, which is an enzyme intimately involved in Aβ production and a key regulator of the relative abundance of the most amyloidogenic form, Aβ_{42}.

7.3 Discussion

To further our findings from chapters 4 and 5, we have used microarray analyses in this chapter to identify transcriptional changes occuring in the brains of HFD induced insulin resistance mice. We have also investigated the effect APOE genotype has on cortical gene expression alone, and in combination with HFD.

We identified firstly 32 genes, which we believed were altered as a response to the deletion of murine APOE, a further 5 genes that were altered as a response to the presence of human APOE transgenes, with a further 10 and 6 being altered by the presence of APOEε3 and APOEε4 respectively. Of the 32 genes altered in response to the absence of APOE, the most interesting finding was the downregulation of a number of genes involved in apoptosis, as this is a prominent feature of AD. VOPP1 (vesicular, overexpressed in cancer, prosurvival protein 1) is associated with apoptotic response and BOK induces apoptosis. ApoE plays an important role in lipid homeostasis within the CNS and is synthesised in large amounts in response to neuronal cell damage or traumatic brain injury (Boyles et al., 1989). Additionally, neurodegeneration is increased during aging by apoE deficiency (Masliah et al., 1995). Research by Hayashi *et al* have shown that apoE containing lipoproteins protects apoptosis in neurons via phospholipase Cγ1 activation (Hayashi et al., 2007, 2009) and thus may explain the upregulation of apoptosis associated genes when apoE expression is absent. Another interesting finding was the downregulation of the WDFY1 gene (WD repeat and FYVE domain containing 1), a protein localised on endosomes. Wdfy1 contains a FYVE domain that mediates the recruitment of proteins involved in cell signalling and also trafficking of proteins to phosphatidylinositol 3-phosphate containing membranes. APOE has been reported to activate Akt phosphorylation via the PI3K pathway in Neuro-2a cells (Laffont et al., 2002) and was suggested to affect neuronal cell metabolism. The downregulation of WDFY1 in the absence of APOE identified in our list suggests activation of the Akt pathway is reduced, which may interfere with cellular metabolism in neurons. Also noteworthy was the downregulation of PSG16 in mice

expressing either APOEε3 or APOEε4. PSG16 is a member of the carcinoembryonic antigen gene family, which is a member of the immunoglobulin gene superfamily. The function of this group of proteins is unclear, however evidence suggests they induce the secretion of some cytokines, including the interleukins IL-6, IL-10 and TGF-β. It is thus plausible that the introduction of human APOE transgenes may reduce inflammatory events in the brain.

Although we were able to identify highly significant changes in gene expression that occurred in response to changes in APOE genotype, we did not identify any genes that passed our stringent FDR correction when comparing the effect of diet on gene expression, within each genotype. This was likely due to a number of reasons, including the low power of the study, the brain region examined, and the likelihood that changes associated with diet would be more subtle. Despite this, we looked at the 50 most significant genes in the uncorrected data. Uncorrected p-values still highlight genes that are altered but must be analysed with caution, hence we limited the analysis to just the top 50 genes. Within each genotype, comparing LFD with HFD revealed transcripts with many diverse functions. Some of these genes are diet or feeding related, however they have not been shown to have direct effects on the brain. For example, in WT mice fed HFD compared to LFD, FURIN was downregulated, which is involved in the processing of progrehlin, the precursor for grehlin, a hormone that stimulates hunger (Takahashi et al., 2009); DIO1 (deiodinase, iodothyronine, type I), which is upregulated in the liver of an mouse model resistant to diet-induced obesity (Kalaany et al., 2005) and MT2 (metallothionein 2), which has been shown to prevent HFD induced cardiac contractile dysfunction (Dong et al., 2007). Additionally, in APOEε4 mice, genes associated with diet include Il-7R (interleukin 7 receptor) the expression of which was decreased in blood mononuclear cells of humans that consumed a mediterranean diet (Konstantinidou et al., 2010) and decreased expression of CLDN5 (claudin 5) which is related to impaired blood brain barrier (BBB) integrity in rats that are fed a high energy diet (Kanoski et al., 2010). This is particularly

interesting in the context of this study as BBB integrity is reduced in chronic neurodegenerative diseases, such as AD, for which T2DM is a risk factor. Another gene associated with feeding, which we expected to be altered in expression levels was neuropeptide Y (Beck et al., 1990). Although neuropeptide Y is widespread in the brain (Larhammar et al., 1987), it is plausible that this gene may be upregulated in other brain regions that are more susceptible to dietary changes, such as the hypothalamus.

It was interesting to see an upregulation of the cholesterol transporter ABCA1 in APOE KO animals which highlights the association between these two proteins. ABCA is a subfamily of the large superfamily of ABC transporters responsible for the translocation of various substrates across the plasma membrane by using energy from ATP hydrolysis (Luciani et al., 1994). The ABCA1 transporter mediates cholesterol and phospholipid efflux to lipid poor lipoprotein particles. ABCA1 is transcriptionally regulated by the Liver X Receptor and is required for the generation and lipidation of apoE (Koldamova et al., 2003). In the brain and cerebrospinal fluid (CSF) of ABCA1 knockout mice, levels of cholesterol and apoE are reduced (Kim et al., 2007; Wahrle et al., 2004) and the presence of small, poorly lipidated and unstable apoE containing lipoproteins in the CSF and that secreted from primary astrocytes indicated impaired cholesterol and phospholipid efflux to apoE. This role of ABCA1 in the lipidation of apoE and the formation of lipoprotein particles was also observed in human primary neurons (Kim et al., 2007). A series of reports have also revealed the role of ABCA1 in Aβ clearance and deposition. Deletion of ABCA1 in APP/PS1, APP23 or PDAPP mice, was shown to increase Aβ deposition and cerebral amyloid angiopathy with no change in APP processing or Aβ production therefore suggesting an impairment in Aβ clearance (Hirsch-Reinshagen et al., 2005; Koldamova et al., 2005; Wahrle et al., 2005). These observations were reversed in the PDAPP/ABCA1 double transgenic mouse model by Holtzman's group (Wahrle et al., 2008). The overexpression of ABCA1 in the brain driven by the mouse prion promoter resulted in almost complete

absence of Aβ plaques and less Aβ deposition in the hippocampal dentate gyrus, a phenotype resembling PDAPP/APOE-/- mice. In addition, CSF and conditioned media from the primary astrocytes of these mice increased lipidation of apoE-containing particles. Taken together, it was concluded that ABCA1 mediated lipidation of apoE can reduce Aβ burden in the brain and that increasing ABCA1 function may have a therapeutic effect in AD. In humans, genetic studies have reported the possibility for an association of some of the ABCA1 genetic variants with risk for AD (Koldamova et al., 2010) (for review). More recently, the ABCA7 member of the ABCA subfamily has been identified in a genome wide association study as a new susceptibility locus for AD (Hollingworth et al., 2011).

Intriguingly in APOEε4 mice, HFD upregulated ADRA2A encoding the α2A-adrenergic receptor. α2A-adrenergic receptors mediate adrenergic suppression of insulin secretion (Fagerholm et al., 2004), thus insulin secretion is enhanced in ADRA2A KO mice (Devedjian et al., 2000). Recently, Rosengren *et al* identified a genomic 1.4 Mb locus linking impaired insulin granule docking at the plasma membrane and reduce β-cell exocytosis in diabetic Goto-Kakizaki rats (Rosengren et al., 2010). In this locus ADRA2A, was significantly overexpressed. Antagonists to the receptor, silencing of the receptor expression or blockade of downstream effectors rescued insulin secretion in the β-cells. Rosengren and colleagues further identified a single-nucleotide polymorphism (SNP) in the human ADRA2A gene which causes its overexpression and increases the risk for T2DM (Rosengren et al., 2010). The upregulation of this gene in APOEε4 mice fed HFD, but not in any other genotypes may support findings that patients with the APOEε4 genotype have a high risk of developing T2DM (Irie et al., 2008; Peila et al., 2002). Linking to these findings, Ronnemaa and colleagues recently reported that impaired insulin secretion increase the risk of AD (Ronnemaa et al., 2008). Taken together, this could mean the reduction in insulin secretion or insulin deficiency, specifically in APOEε4 carriers with T2DM, can induce impairment of downstream insulin signalling effects including Aβ trafficking and

accumulation, tau hyperphosphorylation and cognition. For example, insulin stimulates the uptake of apoE-enriched lipoproteins via the LRP receptor (Descamps et al., 1993) and apoE binds and facilitates the cellular degradation of soluble Aβ peptides (Jiang et al., 2008; Koistinaho et al., 2004). A reduction in insulin could result in reduced degradation of Aβ peptides by microglia leading to Aβ accumulation and formation of Aβ plaques.

APOEε4 transgenic mice fed HFD had altered expression of many genes associated with cytoskeletal organisation compared to APOEε3 mice fed HFD. Although these genes did not meet the vigorous FDR correction, they still demonstrate important functional changes occurring in the cortex. Cytoskeletal changes are required for the formation of synapses during learning and memory. The downregulation of actin and microtubule related proteins in the brain, particularly within neurons, may be associated with the cognitive impairments observed in APOEε4 mice compared to APOEε3 mice (Grootendorst et al., 2005; Wang et al., 2005). *In vitro* studies have demonstrated APOE isoform specific effects on neurite outgrowth and microtubule depolymerisation; apoE4 depolymerises microtubules and inhibits neurite outgrowth (Nathan et al., 1995). Our network analysis by IPA revealed an indirect relationship between microtubule associated proteins with Erk1/2 and Igf1 signalling via Akt and Cnpase (2',3'-cyclic nucleotide 3' phosphodiesterase). Interestingly, the serine/threonine phosphatase calcineurin, and the kinases p38 MAPK and JNK, all of which are able to target tau (Goedert et al., 1997; Goto et al., 1985; Reynolds et al., 1997a; Reynolds et al., 1997b) are also present in the network. This analysis suggests that the Erk1/2, p38 MAPK, JNK and calcinerin may play a role in the tau phosphorylation changes we previously described in chapter 5. Further experiments are needed to determine whether there is a direct link between these pathways and tau phosphorylation.

Robust changes in gene expression were observed in both APOEε3 and APOEε4 mice fed HFD compared to WT fed HFD, even when data was corrected for

multiple testing. Many transcripts were altered similarly in both APOEε3 and APOEε4 mice, indicating these may not be allele-dependent.

Two of the most differentially expressed genes of interest, in the absence of murine APOE or introduction of human APOE, regardless of diet, were WDFY1 and NUDT19. Both genes have been previously identified in the AD11 mouse model as potential biomarkers for AD (Arisi et al., 2011). In this study, NUDT19 was downregulated and was identified as a brain marker of early (1-3 months) disease, whilst WDFY1 was upregulated in the brain in both early and late (6-15 months) stages, across multiple brain regions. Wdfy1 and Nudt19 are both associated with mitochondria. The FYVE domain of Wdfy1 recruits cell signalling proteins to phosphatidylinositol 3-phosphate containing membranes (He et al., 2009). Nudt19 is a coenzyme A diphosphatase that converts CoA esters into fatty-acyl-CoA esters for β-oxidation and has recently been identified in a kidney proteomic study of diabetic patients (Zhang et al., 2011a). Our study demonstrates that these two genes are differentially expressed in the opposite direction when mice are insulin resistant. More importantly, our study clearly demonstrates that expression of these candidate genes are not APOE genotype specific, which is important in the context of Arisi and colleagues *in vivo* AD biomarker work; as all APOE variants are relatively common, an allele specific effect on WDFY1 and NUDT19 would significantly diminish the translatability of their work to human studies. These two genes may also be relevant to the peripheral insulin resistance-induced processes within the brain. Our webQTL analysis associated WDFY1 with the NPY2R gene. Although neuropeptide Y receptors are associated with stimulation of food intake, recent research has suggested they may have a protective role in the CNS, inhibiting release of the neurotransmitter glutamate during excitotoxic insults (Silva et al., 2005). Additionally, Nudt19 was significantly correlated to Psenen, a component of the γ-secretase complex. This finding may support the idea that the impaired insulin signalling activates GSK-3, which subsequently dysregulates Aβ generation by γ-secretase activity (Phiel et al., 2003). Of

further interest, the promoter sequences of WDFY1 and NUDT19 were entered into the DNAstar software application, Genequest, and found that both genes contain PPARγ1 and PPARγ2 sites in their promoter regions, indicating that both genes may be possible targets of thiazolidinediones.

There were more genes uniquely dysregulated in APOEε4 mice fed HFD, than in APOEε3 mice fed HFD, compared to WT mice fed HFD. Particularly noteworthy was the downregulation of the transferrin receptor 2 (TRFR2) gene, which may result in the disruption of iron homeostasis in mitochondria (Horowitz and Greenamyre, 2010). Mitochondrial dysfunction is frequently described in AD brain (Eckert et al., 2011), and is believed to be caused by oxidative stress due to the release of reactive oxygen species (ROS), such as O_2^- and OH^-. Since neurons are highly sensitive to free radicals due to their post-mitotic nature, ROS is a major cause of neuronal cell death. Mitochondria dysfunction has been shown to cause tau phosphorylation and iron has been found to contribute to the development of Aβ plaques and has been detected in neurofibrillary tangles (Good et al., 1992; Mantyh et al., 1993). In addition, two vesicle transporters syntaxin 17 (STX17) and adaptor protein complex AP-1, γ2 subunit (AP1G2) were downregulated. Disruption of these may disrupt protein trafficking and could cause the build up of proteins leading to their aggregation, For example, syntaxin 5 has been shown to be involved in the secretion of Aβ peptides (Suga et al., 2005).

In summary, transcriptomic analysis suggests that the tau phosphorylation changes observed previously in chapter 5 might be associated with Erk1/2, p38 MAPK, JNK and calcineurin. It also highlights the association between APOE and ABCA1 and the role in lipidation of lipoproteins and Aβ clearance. Transcriptomic analysis also suggests the ADRA2A gene, which mediates insulin secretion, may provide an underlying link between the APOEε4 isoform and the risk of developing T2DM. Furthermore the observation that the two genes WDFY1 and NUDT19 both have PPAR binding sites in their regulatory elements suggest they may be targeted by PPARγ directed drugs such as the pioglitazones. Further work will be required to

validate some of these genes and the pathways, with relation to tau phosphorylation. The expression of individual genes is routinely assayed using real-time PCR (RT-PCR). It would be of particular interest to examine the expression of the two common genes WDFY1 and NUDT19 in the brains of mice treated with pioglitazone in chapter 5, across multiple brain regions, and particularly to look for correlations between expression and the degree of tau phosphorylation. We would also use RT-PCR to determine whether the feeding associated genes neuropeptide Y and leptin, which were not differentially expressed in the cortex of mice fed HFD compared to LFD, are in fact altered in other brain regions. Moreover, the expression of a gene does not always correlate with its protein expression and there are other approaches to transcript analysis including exon arrays which identifies splice variants (resulting from alternative splicing of mRNA), next generation sequencing-a high through-put DNA sequencing process and exome resequencing which selectively sequences the coding regions of the human genome and can potentially identify genes associated with common diseases such as AD.

CHAPTER 8

Discussion and Future Perspectives

The overall aim of this thesis was to investigate what effects activation of peroxisome proliferator-activated receptor-γ (PPARγ) signalling might have on Alzheimer's disease (AD)-like pathologies resulting from experimentally induced insulin resistance, in the hope of identifying the molecular mechanisms underlying the action of both insulin and PPARγ in this regard. Specifically, my working hypothesis was that diet-induced insulin resistance would cause APOE isoform-dependent effects on AD pathology and the subsequent treatment with the PPARγ agonist, pioglitazone, would reverse diet-induced insulin resistance as well as AD pathology, possibly in an APOE isoform-dependent manner.

The concept that the AD brain is in an insulin resistant state and that impaired insulin signalling contributes to pathology has generated a great deal of research effort. The evidence supporting an increased risk of AD in patients with type 2 diabetes mellitus (T2DM) has led the search to find therapeutics that restore brain insulin signalling. Recently, the thiazolidinediones (TZDs) rosiglitazone and pioglitazone have both been shown to improve cognitive function in patients with AD and in animal models. Since a definite diagnosis of AD can only be by the examination of the brain at autopsy, using animals has the advantage of gaining insight into the effects of drug action on brain pathology. However, it is unclear if APOE genotype, a well established risk factor of AD, has any effect on brain insulin resistance or how the APOE genotype affects the intervention of TZDs on the development of AD-like pathologies.

Firstly, in this study, insulin resistance was induced in WT, APOE KO, APOEε3 and APOEε4 mice by feeding a high fat diet (HFD). Mice manifested key features of T2DM; obesity, insulin resistance and impaired glucose metabolism. In the cortical region of the brain, tau phosphorylation was consistently reduced at three phospho-tau epitopes, in all insulin resistant mice, independent of APOE genotype. APP metabolism was not altered (as determined by Aβ ELISAs and measures of relative amounts of APP C-terminal fragments). Surprisingly, examination of some of the components of

the insulin signalling pathway, including the tau kinases GSK-3 and Cdk5 or the phosphatase PP2A were also not altered.

I went on to show that 3 weeks pioglitazone treatment, in insulin resistant mice significantly altered tau phosphorylation in an APOE-dependent manner at one of the phospho-tau epitopes (Ser202/Thr205) examined. A significant reduction in tau phosphorylation at this epitope was observed in APOEε3 mice whilst, the reverse, a significant increase in tau phosphorylation at the same epitope was seen in the APOEε4 mice. Although changes in tau phosphorylation were observed, components of the insulin signalling pathway, the tau kinases GSK-3 and Cdk5, and also the tau phosphatase PP2A were again unaltered. Further to this, pioglitazone treatment reduced α-processing (non-amyloidogenic) in APOEε3 mice. The soluble levels of $A\beta_{40}$ and $A\beta_{42}$ were not altered in pioglitazone treated compared to non-treated mice. However, in the APOE KO mice fed HFD and treated with or without pioglitazone, the soluble levels of $A\beta_{40}$ and $A\beta_{42}$ appeared to be higher compared to all other animals.

I then investigated the effects of the apoE isoforms and pioglitazone treatment on tau phosphorylation and cholesterol biosynthesis *in vitro.* I investigated this by treating primary cortical neurons with Chinese hamster ovary (CHO)-apoE3 or CHO-apoE4 conditioned media (CM). In both cases, improved cell viability relative to the neurons incubated with WT CHO CM was observed. In neurons incubated with CHO-apoE3 CM tau phosphorylation was significantly reduced however this did not correlate to a change in GSK-3 activity. In neurons incubated with CHO-apoE3 or CHO-apoE4 CM and treated with pioglitazone, no change in tau phosphorylation was observed. Furthermore, pioglitazone treatment in neurons incubated with CHO-apoE3 or CHO-apoE4 CM did not alter cholesterol biosynthesis when measured by qRT-PCR.

Finally, I examined the effects of diet and genotype on the cortical transcriptome of WT, APOE KO, APOEε3 and APOEε4 mice. A number of differences were observed. I found that feeding HFD in APOE KO mice increased the expression

of the cholesterol transporter ABCA1. In HFD fed APOEε4 mice, the expression of ADRA2A, a gene encoding the α2A-adrenergic receptor was increased which is known to be involved in T2DM. In the genotype comparisons, APOEε3 vs APOEε4 mice fed HFD revealed differentially expressed genes related to cytoskeletal organisation, post-investigation with the ingenuity pathway analysis (IPA) revealed that these were related to the axonal guidance signalling pathway. The IPA network showed microtubule changes relating to insulin growth factor 1 (Igf1), p38 MAPK, Erk1/2, Akt, JNK and calcineurin. The comparisons of WT vs APOEε3 and WT vs APOEε4 mice all fed HFD, revealed two interesting genes in common, WDFY1 and NUDT19, being decreased and increased in expression respectively in both APOEε3 and APOEε4 mice. Genes differentially expressed in the APOEε4 mice as compared to WT controls included; transferrin receptor 2 (TRFR2), syntaxin 17 (SYX17) and adaptor-related protein complex 1, γ2 (AP1G2), the expression of each being reduced in the APOEε4 mice.

Our observation that diet-induced insulin resistance reduces tau phosphorylation, in all mice, independent of APOE genotype is contrary to many other published findings. Diabetes-like symptoms can be induced experimentally by a range of techniques and the discrepancy between our findings and other published data may be due to differences in animal models used. For example the majority of published studies that mimic insulin resistance in AD use streptozotocin (STZ), a nitrosurea derivative isolated from *Streptomyces achromogenes*. STZ cannot permeate through the blood brain barrier (BBB) but is toxic to pancreatic β-cells; STZ enters cells via the glucose transporter, GLUT2, and alkaylates DNA, inducing DNA damage (Rees and Alcolado, 2005). As a result, insulin resistance and glucose intolerance develop because β-cells are destroyed and the production of insulin is halted. The systemic hypoinsulinemia effect on the brain in these animal models mimics type 1 diabetes mellitus (T1DM); a disorder due to primary failure of the insulin generating β-cells of the pancreas. As there is less evidence of a link between T1DM and AD compared to T2DM, STZ treated animals are therefore not a good model of insulin resistance in AD

and are not directly comparable to our study. These animals show Aβ pathology or tau phosphorylation as a consequence of the interruption of the insulin signalling pathway resulting in a loss of inhibitory control of GSK-3, the predominant tau kinase. Additionally, STZ can be intracerebroventricularly injected into the brain. In the brain, GLUT2 are widely expressed (Brant et al., 1993) and can be targeted by STZ which selectively reduces insulin production without disturbing systemic insulin and glucose levels. This has been shown to cause chronic reductions in glucose and glycogen metabolism in the cortex and hippocampus of rats (Plaschke and Hoyer, 1993) accompanied with the inhibition of insulin receptor function (Hoyer et al., 2000) and insulin signalling (Lester-Coll et al., 2006). This impairment in the insulin signalling pathway was shown to cause Aβ pathology (Plaschke et al., 2010; Salkovic-Petrisic et al., 2006), tau pathology (Deng et al., 2009) and learning and memory deficits in rodents (Lannert and Hoyer, 1998; Salkovic-Petrisic et al., 2006). Other studies use spontaneous diabetic models, which have a genetic deposition to T2DM, for example the BBZDR/Wor rats (Li et al., 2007) and db/db mice (Kim et al., 2009a), both of which have shown enhanced amyloidogenic APP metabolism, Aβ pathology, tau phosphorylation and tau cleavage. Gene deletion experiments can also induce insulin resistance by ablating some components of the insulin signalling pathway. Examples of these are the neuronal insulin receptor knockout (NIRKO) (Schubert et al., 2004) and insulin receptor substrate 2 (IRS2) knockout mice (Killick et al., 2009; Schubert et al., 2003). In NIRKO mice, the loss of insulin mediated activation of phosphoinositide 3-kinase (PI3K) resulted in a reduction of phosphorylated Akt and GSK-3β which led to an increase in tau phosphorylation. In the IRS2 knockout mouse, an increase in tau phosphorylation correlated to a reduction in PP2A activity but not GSK-3 activity. Likewise in the APP Tg2576 mice crossed with the IRS2 knockout mice (Killick et al., 2009), tau phosphorylation was increased due to reduced levels of PP2A. However, these mice also displayed a reduction in Aβ plaques, which correlated with an increase of the Aβ binding protein, transthyretin, which may have facilitated Aβ clearance from

the brain. This was also accompanied by improvement in cognitive function in the Tg2576/IRS2 knockout mice. Taken together, these findings show the deletion of specific steps of the insulin signalling pathway does not necessarily result in evident AD pathology and may act in a protective manner.

Diet-induced models of insulin resistance, which mimic the onset of T2DM, is more reflective of modern lifestyles in man. However, to date only a few studies have used diet-induced models of insulin resistance to investigate pathological processes related to AD. In chapter 4 (section 4.3), the discrepancies between these published reports and our own were discussed; feeding regimes, age of mice, different mouse models including transgenic mice predisposed to amyloid pathology. Moreover, APOE genotype dependent changes in AD pathology observed by other groups are likely to be caused by the constitutive expression of apoE under different promoters for example, neuron-specific enolase (NSE) and glial fibrillary acidic protein (GFAP) expressing apoE in neurons and astrocytes respectively, may drive the pathological features of AD, whereas in our study APOE was driven by the mouse APOE gene promoter leading to the expression of human apoE with identical tissue distribution and levels to that of the endogenous mouse gene. In the current study, diet-induced insulin resistance by HFD in mice demonstrated a reduction in tau phosphorylation. This is contrary to the hypothesis, that insulin resistance would cause impairments in downstream insulin signalling and therefore the resultant loss of inhibition in GSK-3 activity would increase tau phosphorylation and alter Aβ metabolism. In fact, it is possible that in our hyperinsulinemic mice, there was an increased entry of insulin from the periphery into the brain across the BBB. This increase in the levels of insulin binds to the insulin receptors and mediates PI3K signalling, leading to the activation of Akt and inhibition of GSK-3 activity. Subsequently, in the absence of insulin resistance, levels of phosphorylated tau are reduced as observed in the brains of HFD fed mice. In support of this idea, intravenous infusion of insulin was shown to increase the levels of cerebrospinal fluid (CSF) insulin (Wallum et al., 1987), which demonstrated that

peripheral insulin can be transported into the brain. Intravenous infusion of insulin under euglycaemic conditions in AD patients improves memory (Craft et al., 1996), and indicates that peripheral insulin may have a role in rescuing the impairment of insulin metabolism within the brain. Furthermore, clinical studies have shown that raising brain insulin levels by intranasal insulin is also beneficial and improves memory in AD patients (Reger et al., 2008). Similarly, intranasal insulin treatment in mice improved cognitive performance (Francis et al., 2008). Further supporting our observations, it was shown in mice that peripheral insulin treatment reverses tau phosphorylation in the brain (Jolivalt et al., 2008). Interestingly, a very recent study similar to our study was carried out in humans. Bayer-Carter and colleagues studied high-saturated/high glycemic index (HIGH) diet or a low-saturated/low glycemic index (LOW) diet in AD patients, amnestic mild cognitive impairments or healthy adults for 4 weeks (Bayer-Carter et al., 2011). The outcome measures included CSF $A\beta_{42}$ concentrations, which are normally reduced in AD patients due to the deposition of $A\beta_{42}$ peptides into plaques. Intriguingly, in healthy individuals LOW diet reduced CSF $A\beta_{42}$ whilst HIGH diet increased CSF $A\beta_{42}$. Although the authors proposed their observations might reflect the presymptomatic stage of AD in which a rise in $A\beta_{42}$ levels occurs before plaque deposition, nevertheless this study shows that a HFD could account for differences observed between ours and other studies.

The failure to identify changes in the components of the insulin signalling pathway suggests there may be other mechanisms related to the action of insulin in the brain. In addition to serine phosphorylation, the activity of constitutively active tau kinase, GSK-3, is augmented by tyrosine (Tyr) phosphorylation at residues Tyr279 (GSK-3α) and Tyr216 (GSK-3β). The phosphorylation state of both Tyr residues were not investigated in this study and should be considered in future experiments. It is also important to further examine possible alterations of these kinases and phosphatases in membrane fractions and compare these to cytosolic fractions. Furthermore, combining HFD with mouse models lacking these kinases and phosphatases for example, GSK-3

double knockout mice, p35 or Cdk5 knockout mice, may confirm our observations showing that HFD reduces tau phosphorylation. Alternatively, it is likely that the period of feeding required to increase levels of insulin sufficiently to affect the brain, may have led to a failure to detect changes in the insulin signalling components that could have occurred transiently at earlier time points. Feedback mechanisms may have led to the establishment of steady state levels similar to that of the time points we examined. Furthermore, it has been recently hypothesised that a decrease in brain glucose metabolism may contribute to neurodegenerative mechanisms (Gong et al., 2006). Tau can also be posttranslationally modified by O-glycosylation. Specifically, O-glycosylation by the attachments of the monosaccharide beta-N-acetylglucosamine (O-GlcNAcylation). O-GlcNAcylation and phosphorylation of tau are reciprocal to each other, in that they can compete for the same Ser/Thr residues (Liu et al., 2004). In support of this hypothesis, examination of AD post-mortem brain tissue found a correlation between reduced O-GlcNAcylated tau and hyperphosphorylated tau (Liu et al., 2009a; Liu et al., 2009b; Liu et al., 2008). This finding was also observed in T2DM post-mortem brain tissue (Liu et al., 2009b, 2011). These authors proposed that the observations are due to a reduction in glucose uptake via the neuronal glucose transporters GLUT1 and GLUT3 (Liu et al., 2009b; Liu et al., 2008) and/or reduced brain insulin signalling (Liu et al., 2011). Thus, for further work, it would be interesting to investigate whether the reduction in tau phosphorylation detected in HFD fed APOE mice was due to increases in O-GlcNAcylation.

Having shown that HFD feeding induces insulin resistance in mice and causes a reduction of tau phosphorylation independent of APOE genotype. We then explored the effects of PPARγ agonism on diet-induced insulin resistant mice. Pioglitazone treatment in diet-induced insulin resistant mice caused APOE allele-dependent changes in tau phosphorylation. The APOEε3 mice responded to treatment which reduced tau phosphorylation at the Ser202/Thr205 phospho-tau epitope in comparison to the vehicle treated APOEε3 mice, whilst the reverse, an increase in tau

phosphorylation was detected in the pioglitazone treated APOEε4 mice compared to vehicle treated APOEε4 mice. These observations are consistent with the findings from an early rosiglitazone clinical trial in which treatment stabilised cognition in mild to moderate APOEε4 negative AD patients (Risner et al., 2006). To date, there are only two publications that have examined TZD treatment on tau phosphorylation *in vivo*. Rosiglitazone reduced the number of tau aggregates containing Ser202/Thr205 phospho-tau epitope in the hippocampus of human APP (K670N/M671L and V717F) double transgenic mice (Escribano et al., 2010), whilst in OLETF rats, which develop spontaneous T2DM, rosiglitazone also reduced tau phosphorylation at Ser202/Thr205 epitope (Yoon et al., 2010). Both of these studies, along with our own, show that the Ser202/Thr205 phospho-tau epitope might be a common target of TZDs. Our observation correlating changes in tau phosphorylation with APOE genotype points towards the underlying cause as due to mitochondrial defects because the apoE protein is cleaved by a neuronal specific protease and the apoE4 isoform is the most susceptible to truncation. Histopathological staining of AD brains has shown the appearance of truncated fragments of apoE in NFT-like inclusions in neurons and mitochondrial damage in AD appears greater in APOEε4 carriers. It is thought that truncated C-terminal fragments of apoE escapes the secretory pathway and enters the cytosol and then impacts upon mitochondrial function. Since a possible role of PPARγ is to stimulate neuronal mitochondria biogenesis (Strum et al., 2007), the excessive damage inflicted on mitochondria in APOEε4 mice or APOEε4 patients therefore renders APOEε4 genotype less able to respond to TZD treatment. Furthermore, out of the apoE isoforms, apoE4 is the only one with an N- and C-terminal domain interaction, which is postulated to be responsible for it's pathogenic effects. A recent paper has provided evidence that neuronal cultures of NSE-apoE4, significantly reduced the levels of all subunits of mitochondrial respiratory complexes compared to NSE-apoE3 cultures. The fact that this observation was not found in primary cultures from transgenic mice expressing astrocytic apoE (GFAP-apoE3 and GFAP-apoE4)

demonstrates this is mitochondria damage is specific to neurons. Furthermore, apoE4 domain interaction can be abolished by the ArgThr61 mutation and this amended respiratory complex levels in Neuro-2a cells, indicating mitochondrial dysfunction is due to domain interaction, specific to the apoE4 isoform (Chen et al., 2011).

In response to pioglitazone treatments, the APOE-dependent changes in tau phosphorylation did not correlate to changes in the components of the insulin signalling pathway (Akt, GSK-3), the tau kinases (GSK-3, Cdk5) or the tau phosphatase PP2A. As we only examined phosphorylation of the serine residues (Ser21/9) in GSK-3, it is possible that tyrosine phosphorylation (Tyr279/216) may correlate to the APOE-dependent changes on tau phosphorylation and this would contribute to further experiments. Also, it cannot be ruled out that a shift of the kinases and phosphatase within subcellular compartments may have occurred, that would not have been detected in the total lysate preparations. Since we also have the membrane fractions for all mice, it would be interesting to compare the amount of active kinases and phosphatase between cytosolic and membrane fractions.

Interestingly, in a very recent study, Choi *et al* found that PPARγ can be phosphorylated at the Ser273 epitope via Cdk5 upon incubation of 3T3-L1 adipocytes with obesity related cytokines TNFα, IL-6 and fatty acids (Choi et al., 2010). The expression of cytokines that are increased during obesity, activates Cdk5 by causing the cleavage of p35 into the more stable p25 subunit (Dhavan and Tsai, 2001). The observation in 3T3-L1 adipocytes was replicated *in vivo*; HFD fed mice that became obese had increased PPARγ phosphorylation and Cdk5 activity in adipose tissue, as early as 7 weeks compared to mice fed the standard chow diet. Furthermore, Choi *et al* found that phosphorylation of PPARγ at Ser273 neither activated nor suppressed transcriptional activity of the receptor but dysregulated the expression of a subset of genes, including key metabolic regulators adipsin and adiponectin. On the application of the PPARγ ligands rosiglitazone (a full PPARγ agonist) and MRL24 (a partial PPARγ agonist) *in vivo*, phosphorylation of PPARγ in adipose tissue was reduced, alongside

improvement in glucose tolerance, reduction in fasting insulin levels, and most importantly, no alteration in body weight. Both rosiglitazone and MRL24 reversed the gene expression changes. By using hydrogen/deuterium exchange linked to mass spectrometry, the group found that binding of PPARγ ligands to the PPARγ ligand binding domain caused conformational changes which obstructed the access of Cdk5 to the Ser273 epitope.

In contrast to the study by Choi *et al* which was carried out in adipose tissue, in our study we have shown that p35 and p25 levels, and therefore Cdk5 activity was not altered in the cytosolic brain fractions of HFD fed mice treated with or without pioglitazone. If further work for our study shows no differences in Cdk5 activity between cytosolic and membrane fractions, it may suggest that a brain-specific mechanism exists for PPARγ and its ligands within the brain. Other further work would include examining the phosphorylation state of PPARγ at Ser273 in brain samples of our APOE mice treated with or without pioglitazone and also the phosphorylation state of PPARγ at Ser273 in the brain of Cdk5 knockout mice. These experiments would confirm whether Cdk5 has a role in PPARγ modification in the brain.

Following their work on showing PPARγ-based drugs are not only anti-diabetic as agonists for the nuclear receptor but also block obesity-linked phosphorylation of PPARγ by Cdk5, Choi *et al* developed synthetic compounds that blocked Cdk5-mediated phosphorylation albeit having high affinity for PPARγ and lacking classical agonism (Choi et al., 2011). One of these compounds, SR1664, demonstrated anti-diabetic activity; lowering of glucose levels, reduction of fasting insulin levels and no change in body weight in obese mice. SR1664 also did not cause the side effects of many PPARγ drugs such as fluid retention and weight gain. This paper by Choi and colleagues suggests the promising potential of a new class of anti-diabetic drugs over the current TZD agonists which causes side effects in patients. It would be interesting to see how this new class of anti-diabetic drugs affects Cdk5 activity in the brain, specifically on tau pathology in relation to AD.

Having shown *in vivo* that diet-induced insulin resistance can reduce tau phosphorylation and pioglitazone has APOE-dependent effects on tau phosphorylation, I went on to investigate, *in vitro,* whether these effects are mediated through direct action on neurons via cholesterol related mechanisms. This was because there is evidence showing cholesterol metabolism is differentially affected by the isoforms of apoE and that the TZDs can influence cholesterol biosynthesis (discussed in section 6.1). To investigate apoE isoform specific effects, primary neurons were incubated with native preparations of apoE from the CM of CHO cells stably expressing human APOEε3 (CHO-apoE3) or APOEε4 (CHO-apoE4). Native preparations of apoE were used because the biologically active form of apoE requires lipid association (LaDu et al., 1995). ApoE from the CHO-apoE3 or CHO-apoE4 CM were taken up by neurons, as demonstrated by the pulse chase-like experiment. This most likely occurred via the LRP receptor, the most preferentially expressed apoE receptor in neurons (Rebeck et al., 1993). ApoE isoform specific effects on tau phosphorylation were observed in neurons cultured in CHO-apoE CM; apoE3 significantly reduced tau phosphorylation in neurons whilst apoE4 did not. This suggests the apoE3 isoform is protective, an observation that has also been demonstrated by other groups. The basis for the neuroprotective effects of apoE3 in comparison to the apoE4 isoform was proposed to be due to the greater avidity of the apoE3 isoform for tau which thereby forms more stable complexes with tau compared to the apoE4 isoform (Strittmatter et al., 1994). In addition, it was shown that apoE3 binds to the microtubule domains on tau and was proposed to protect tau from abnormal phosphorylation, thereby reducing its propensity to undergo self assembly into paired helical filaments (Strittmatter et al., 1994). Treatment of neurons cultured in the various CHO-apoE CM plus pioglitazone for 24 h showed a trend towards a decreased in tau phosphorylation however this did not reach statistical significance. This could be due to the length of pioglitazone treatment and longer treatment may show more pronounced effects. Furthermore, the genes related to cholesterol biosynthesis were examined in neurons incubated with WT CHO, CHO-apoE3 or CHO-apoE4 CM and pioglitazone. Whilst neurons incubated with the WT

CHO CM and pioglitazone revealed some changes in cholesterol gene biosynthesis as reported by Cocks and colleagues; a trend in increased cholesterol gene expression (HMGCR, MVD and LSS) at 6 h, which were subsequently reduced at 24 h, neurons incubated with the CHO-apoE CM and pioglitazone did not revealed any significant changes in genes related to cholesterol biosynthesis or apoE isoform specific effects. Our findings are different to those published by Michikawa and colleagues who have shown that the neurotoxic effects of the apoE4 isoform are mediated by suppression of *de novo* cholesterol synthesis (Michikawa and Yanagisawa, 1998). However, further experiments are required to confirm our findings. Additionally, the discrepancy between our results and findings from other groups who have reported apoE isoform specific differences on neuronal cultures may be due to various factors. For example, the preparation of apoE (some groups have used recombinant apoE), the source of apoE, the type of cells or neuronal cultures and the precise culture conditions (addition of Aβ may allow apoE isoforms to show more prominent effects). For future experiments, an alternative *in vitro* model would be co-cultures of astrocytes and neurons from apoE transgenic mice. These cultures would give a more natural source of apoE thus eliminating variations noted above. This may give us a clearer indication of the role apoE isoforms plays in cholesterol biosynthesis, in the presence of a PPARγ agonist.

Given that we showed a decrease in tau phosphorylation in relation to diet-induced hyperinsulinemia and an APOE genotypic specific change in tau phosphorylation but did not observe changes in the known tau kinases, GSK-3, Cdk5 or phosphatase, PP2A, we then explored signalling by measuring genome-wide transcriptomic changes by microarray. I firstly identified APOE genotypic changes by comparing WT mice with APOE KO, APOEε3 and APOEε4 transgenic mice fed low fat diet (LFD). To then identify diet-responsive changes, the brain transcriptome of mice fed a LFD with that of mice fed a HFD within each genotype was compared. I also investigated the APOE genotypic changes by comparing HFD WT mice with both HFD APOEε3 and APOEε4 transgenic mice, as well as between APOEε3 and APOEε4

transgenic mice fed HFD. Although I was able to identify highly significant changes in gene expression in response to changes in APOE genotype, I did not identify any genes that passed the stringent FDR correction when comparing the effect of diet on gene expression, within each APOE genotype. This was likely due to a number of reasons, including the low power of the study, the brain region examined, and the likelihood that changes associated with diet would be more subtle. These set of experiments described below will require further studies by for example, using more mice and validating specific genes using qRT-PCR.

In the identification for diet-responsive changes, although no potential tau related kinases or phosphatases were identified, an interesting finding was the comparison of APOEε4 mice fed HFD to APOEε4 mice fed LFD that revealed differential expression of the ADRA2A gene encoding the α2A-adrenergic receptor. The α2A-adrenergic receptor mediates adrenergic suppression of insulin secretion. A polymorphism in the ADRA2A gene increases the risk of developing T2DM (Rosengren et al., 2010). This finding, replicated in two clinical studies, demonstrates a synergistic interaction between the APOEε4 gene and T2DM (Irie et al., 2008; Peila et al., 2002). Additionally, glaucoma is a progressive optic neuropathy characterised by apoptotic retinal ganglion cell (RGC) death and recent imaging research suggests that the loss of RGCs and their axons may play an important role in the visual deficit in AD patients. Interestingly, the action of α2A-adrenergic receptor agonists was shown to be neuroprotective in experimental models of glaucoma (Wheeler et al., 2001), possibly by a neuronal anti-apoptotic mechanism (Tatton et al., 2003). Moreover, α2A-adrenergic receptors were shown to regulate the dendritic growth of cortical neurons by altering the phosphorylation state of MAP2 (Song et al., 2004) and co-immunoprecipitated with the amyloid precursor-like protein 1 (APLP1), a homologue of APP in a two-hybrid screen (Weber et al., 2006). The authors of this work proposed that APLP1 regulates the trafficking of α2A-adrenergic receptors and may be a mechanism that α2A-adrenergic receptor agonists exert their protective effects. α2A-adrenergic receptors

also modulate prefrontal cortex neuronal activity related to spatial working memory in macaques and rats via the inhibition of cAMP mediated signalling (Li et al., 1999a; Ramos et al., 2006). These data together suggests that α2A-adrenergic signalling might play a protective role for AD. Our data shows the gene encoding the α2A-adrenergic receptor is increased in APOEε4 mice fed a HFD might account for a decrease of protective effects with the APOEε4 genotype. By using qRT-PCR in future experiments, the upregulation of ADRA2A can be validated in APOEε4 mice fed HFD.

Although we did not observe any APOE isoform-dependent effects on tau phosphorylation in these HFD fed mice, we went on to investigate the effects of APOE genotype on the cortical transcriptome. It was hoped this may be informative as to the possible mechanisms underlying the APOE isoform-dependent effects on tau phosphorylation observed in pioglitazone treated HFD fed mice, as presented in chapter 5. In the APOE genotypic comparison, the whole brain transcriptomic analysis of APOEε3 mice fed HFD compared to APOEε4 mice fed HFD, revealed reduced expression of microtubule associated proteins (Map7, Tubb4, Cnpase). Reduced expression of microtubule associated proteins are indicative of disruption in the microtubule dynamic network, which is likely to have a detrimental effect upon cell physiology. IPA analysis suggested microtubule related proteins were indirectly related to the following proteins Igf1, Akt, Erk1/2, p38 MAPK, JNK and calcineurin (or PP2B). These kinases and phosphatase may underlie the APOE genotypic effects observed in tau phosphorylation upon administration of pioglitazone treatment and further validation experiments by western blotting of brain lysates from pioglitazone treated APOEε3 versus APOEε4 mice would confirm this finding. The presence of Igf1 and Akt are indicative of insulin signalling, Igf1 binds insulin receptors and activates the insulin signalling pathway. However, the activation state of Akt, as measured by phosphoimmunoreactivity at the Ser473 site was not altered. Akt may also be activated via phosphorylation at an another epitope, Thr308. This epitope was not investigated in chapter 5 and would contribute to future experiments. All three MAP kinases (Erk1/2,

p38 MAPK and JNK) have been shown to phosphorylate tau (Goedert et al., 1997; Perry et al., 1999; Reynolds et al., 1997a; Reynolds et al., 1997b). *In vivo* and *in vitro* studies have shown that TZDs alter JNK and p38 MAPK activities. Rosiglitazone reduced tau phosphorylation in rats with T2DM but not in rats with T1DM, and in the human tau-transfected SHSY-5Y neuronal cell line, by reducing JNK activity (Yoon et al., 2010). In HEK-293 cells stably expressing IRS1 and in 3T3L1 adipocytes, phosphorylation of IRS1 on Ser307 and Ser612 suppressed insulin signalling and was reversed by rosiglitazone treatment by inhibiting the action of JNK and p38 MAPK (Jiang et al., 2004). Additionally, TNFα, a pro-inflammatory cytokine associated with insulin resistance induced the activity of p38 MAPK in primary brown adipocytes and upon rosiglitazone treatment, insulin signalling was restored and glucose uptake normalised (Hernandez et al., 2004). Also, the inhibition of p38 MAPK signalling by pioglitazone ameliorated microglia inflammation (Ji et al., 2010). Calcineurin, also present in the IPA network, is a calcium (Ca^{2+})-dependent phosphatase that dephosphorylates tau (Drewes et al., 1993; Gong et al., 1994). Recently both rosiglitazone and pioglitazone have been shown to inhibit different sources of Ca^{2+} influx in hippocampal neurons. Rosiglitazone reduced voltage-gated Ca^{2+} channel currents whilst pioglitazone reduced NMDA receptor-mediated currents (Pancani et al., 2009). It was suggested the actions of these TZDs are neuroprotective in regions of the brain vulnerable to AD. Interestingly, NMDA receptors are crucial to the establishment of long-term potentiation (LTP), which is intimately coupled to Ca^{2+} influx and involves calmodulin, a protein that also activates calcineurin (Tonks and Cohen, 1983; Yang et al., 1982). Taken together, one might speculate that pioglitazone may regulate Ca^{2+} signalling in neurons and improve learning and memory in the diet-induced insulin resistant APOE mice. Additionally, calcineurin might be involved with the dephosphorylation of tau (in the case for APOEε3 mice) as well as LTP. For future studies, it would be interesting to examine learning and memory in the diet-induced insulin resistant APOE mice treated with pioglitazone, to investigate whether there are apoE isoform-dependent effects, reflective of tau phosphorylation and whether they

mimic rosiglitazone clinical trials. This would show the APOE-dependent effects of TZDs on tau phosphorylation which may associate with learning and memory.

Other experiments for future studies would be to examine AD biomarkers in the mice of the current study. In the rosiglitazone clinical trial by Risner *et al*, plasma samples from treated and control patients were analysed. The following proteins corresponded to memory improvement: α-2-macroglobulin, complement factor C1 inhibitor, complement factor H and apoE (Akuffo et al., 2008). With the AD Luminex panels currently in development, these biomarkers could be examined in the plasma samples of pioglitazone treated insulin resistant APOE mice, to investigate possible correlations with the tau phosphorylation observed within the brain. Moreover, adiponectin, a peripheral marker of TZD activity has been reported to have a possible role as a CNS signalling molecule. In humans, low molecular weight adiponectin multimers have been detected in the CSF (Kusminski et al., 2007; Une et al., 2011). Adiponectin has been detected in CSF after its administration in the periphery in mice (Qi et al., 2004) and was shown to stimulated AMP-activated protein kinase (AMPK) activity in the hypothalamus of mice, increased food intake and decrease energy expenditure (Kubota et al., 2007). Signalling molecules regulated by adiponectin include AMPK, JNK, p38 MAPK, and PP2A (Kim et al., 2009b; Luo et al., 2005; Yamauchi et al., 2002b). Furthermore, adiponectin receptors have been identified in mouse cortical neurons (Thundyil et al., 2010), distributed in various cortical regions of the rat brain (Repunte-Canonigo et al., 2010) and protected hippocampal neurons against excitotoxicity (Qiu et al., 2011). This leads to the speculation that adiponectin can act on neurons and initiate downstream signalling pathways, perhaps related to AD. Future *in vitro* experiments in cultured primary cortical neurons could readily be used to examine these effects using recombinant adiponectin proteins.

In conclusion an interaction between PPARγ activation, APOE and tau phosphorylation has been identified. Diet-induced insulin resistance reduced tau phosphorylation at specific epitopes due to peripheral hyperinsulinemia, which is

independent of APOE genotype. Pioglitazone treatment reduced tau phosphorylation in an APOE isoform-dependent manner with the APOEε3 isoform being the most responsive to the actions of this drug. Further studies are required to validate the current findings and to further elucidate the mechanism. A better understanding of the relative importance of brain and peripheral insulin resistance will likely greatly improve our understanding of the disease process and also aide the rational design of therapeutics to halt its progression.

LIST OF REFERENCES

Abbott, M.A., Wells, D.G., and Fallon, J.R. (1999). The insulin receptor tyrosine kinase substrate p58/53 and the insulin receptor are components of CNS synapses. J Neurosci *19*, 7300-7308.

Abildayeva, K., Jansen, P.J., Hirsch-Reinshagen, V., Bloks, V.W., Bakker, A.H., Ramaekers, F.C., de Vente, J., Groen, A.K., Wellington, C.L., Kuipers, F.*, et al.* (2006). 24(S)-hydroxycholesterol participates in a liver X receptor-controlled pathway in astrocytes that regulates apolipoprotein E-mediated cholesterol efflux. J Biol Chem *281*, 12799-12808.

Adams, M., Reginato, M.J., Shao, D., Lazar, M.A., and Chatterjee, V.K. (1997). Transcriptional activation by peroxisome proliferator-activated receptor gamma is inhibited by phosphorylation at a consensus mitogen-activated protein kinase site. J Biol Chem *272*, 5128-5132.

Agostini, M., Schoenmakers, E., Mitchell, C., Szatmari, I., Savage, D., Smith, A., Rajanayagam, O., Semple, R., Luan, J., Bath, L.*, et al.* (2006). Non-DNA binding, dominant-negative, human PPARgamma mutations cause lipodystrophic insulin resistance. Cell Metab *4*, 303-311.

Ahn, K., Shelton, C.C., Tian, Y., Zhang, X., Gilchrist, M.L., Sisodia, S.S., and Li, Y.M. (2010). Activation and intrinsic gamma-secretase activity of presenilin 1. Proc Natl Acad Sci U S A *107*, 21435-21440.

Air, E.L., Strowski, M.Z., Benoit, S.C., Conarello, S.L., Salituro, G.M., Guan, X.M., Liu, K., Woods, S.C., and Zhang, B.B. (2002). Small molecule insulin mimetics reduce food intake and body weight and prevent development of obesity. Nat Med *8*, 179-183.

Akomolafe, A., Beiser, A., Meigs, J.B., Au, R., Green, R.C., Farrer, L.A., Wolf, P.A., and Seshadri, S. (2006). Diabetes mellitus and risk of developing Alzheimer disease: results from the Framingham Study. Arch Neurol *63*, 1551-1555.

Akuffo, E.L., Davis, J.B., Fox, S.M., Gloger, I.S., Hosford, D., Kinsey, E.E., Jones, N.A., Nock, C.M., Roses, A.D., Saunders, A.M.*, et al.* (2008). The discovery and early validation of novel plasma biomarkers in mild-to-moderate Alzheimer's disease patients responding to treatment with rosiglitazone. Biomarkers *13*, 618-636.

Alafuzoff, I., Aho, L., Helisalmi, S., Mannermaa, A., and Soininen, H. (2009). Beta-amyloid deposition in brains of subjects with diabetes. Neuropathol Appl Neurobiol *35*, 60-68.

Alonso, A., Zaidi, T., Novak, M., Grundke-Iqbal, I., and Iqbal, K. (2001a). Hyperphosphorylation induces self-assembly of tau into tangles of paired helical filaments/straight filaments. Proc Natl Acad Sci U S A *98*, 6923-6928.

Alonso, A.C., Grundke-Iqbal, I., and Iqbal, K. (1996). Alzheimer's disease hyperphosphorylated tau sequesters normal tau into tangles of filaments and disassembles microtubules. Nat Med *2*, 783-787.

Alonso, A.D., Grundke-Iqbal, I., Barra, H.S., and Iqbal, K. (1997). Abnormal phosphorylation of tau and the mechanism of Alzheimer neurofibrillary degeneration: sequestration of microtubule-associated proteins 1 and 2 and the disassembly of microtubules by the abnormal tau. Proc Natl Acad Sci U S A *94*, 298-303.

Alonso, A.D., Zaidi, T., Novak, M., Barra, H.S., Grundke-Iqbal, I., and Iqbal, K. (2001b). Interaction of tau isoforms with Alzheimer's disease abnormally hyperphosphorylated tau and in vitro phosphorylation into the disease-like protein. J Biol Chem *276*, 37967-37973.

Anderton, B.H., Betts, J., Blackstock, W.P., Brion, J.P., Chapman, S., Connell, J., Dayanandan, R., Gallo, J.M., Gibb, G., Hanger, D.P.*, et al.* (2001). Sites of phosphorylation in tau and factors affecting their regulation. Biochem Soc Symp, 73-80.

Arbones-Mainar, J.M., Johnson, L.A., Altenburg, M.K., Kim, H.S., and Maeda, N. (2010). Impaired adipogenic response to thiazolidinediones in mice expressing human apolipoproteinE4. FASEB J *24*, 3809-3818.

Arendt, T., Schindler, C., Bruckner, M.K., Eschrich, K., Bigl, V., Zedlick, D., and Marcova, L. (1997). Plastic neuronal remodeling is impaired in patients with Alzheimer's disease carrying apolipoprotein epsilon 4 allele. J Neurosci *17*, 516-529.

Arisi, I., D'Onofrio, M., Brandi, R., Felsani, A., Capsoni, S., Drovandi, G., Felici, G., Weitschek, E., Bertolazzi, P., and Cattaneo, A. (2011). Gene expression biomarkers in the brain of a mouse model for Alzheimer's disease: mining of microarray data by logic classification and feature selection. J Alzheimers Dis *24*, 721-738.

Arispe, N., Rojas, E., and Pollard, H.B. (1993). Alzheimer disease amyloid beta protein forms calcium channels in bilayer membranes: blockade by tromethamine and aluminum. Proc Natl Acad Sci U S A *90*, 567-571.

Arriagada, P.V., Growdon, J.H., Hedley-Whyte, E.T., and Hyman, B.T. (1992). Neurofibrillary tangles but not senile plaques parallel duration and severity of Alzheimer's disease. Neurology *42*, 631-639.

Arvanitakis, Z., Schneider, J.A., Wilson, R.S., Li, Y., Arnold, S.E., Wang, Z., and Bennett, D.A. (2006a). Diabetes is related to cerebral infarction but not to AD pathology in older persons. Neurology *67*, 1960-1965.

Arvanitakis, Z., Wilson, R.S., and Bennett, D.A. (2006b). Diabetes mellitus, dementia, and cognitive function in older persons. J Nutr Health Aging *10*, 287-291.

Arvanitakis, Z., Wilson, R.S., Bienias, J.L., Evans, D.A., and Bennett, D.A. (2004). Diabetes mellitus and risk of Alzheimer disease and decline in cognitive function. Arch Neurol *61*, 661-666.

Asai, M., Hattori, C., Szabo, B., Sasagawa, N., Maruyama, K., Tanuma, S., and Ishiura, S. (2003). Putative function of ADAM9, ADAM10, and ADAM17 as APP alpha-secretase. Biochem Biophys Res Commun *301*, 231-235.

Augustinack, J.C., Schneider, A., Mandelkow, E.M., and Hyman, B.T. (2002). Specific tau phosphorylation sites correlate with severity of neuronal cytopathology in Alzheimer's disease. Acta Neuropathol *103*, 26-35.

Authier, F., Posner, B.I., and Bergeron, J.J. (1996). Insulin-degrading enzyme. Clin Invest Med *19*, 149-160.

Bales, K.R., Liu, F., Wu, S., Lin, S., Koger, D., DeLong, C., Hansen, J.C., Sullivan, P.M., and Paul, S.M. (2009). Human APOE isoform-dependent effects on brain beta-amyloid levels in PDAPP transgenic mice. J Neurosci *29*, 6771-6779.

Bales, K.R., Verina, T., Cummins, D.J., Du, Y., Dodel, R.C., Saura, J., Fishman, C.E., DeLong, C.A., Piccardo, P., Petegnief, V.*, et al.* (1999). Apolipoprotein E is essential for amyloid deposition in the APP(V717F) transgenic mouse model of Alzheimer's disease. Proc Natl Acad Sci U S A *96*, 15233-15238.

Bales, K.R., Verina, T., Dodel, R.C., Du, Y., Altstiel, L., Bender, M., Hyslop, P., Johnstone, E.M., Little, S.P., Cummins, D.J.*, et al.* (1997). Lack of apolipoprotein E dramatically reduces amyloid beta-peptide deposition. Nat Genet *17*, 263-264.

Bandaru, V.V., Troncoso, J., Wheeler, D., Pletnikova, O., Wang, J., Conant, K., and Haughey, N.J. (2009). ApoE4 disrupts sterol and sphingolipid metabolism in Alzheimer's but not normal brain. Neurobiol Aging *30*, 591-599.

Banerjee, R.R., Rangwala, S.M., Shapiro, J.S., Rich, A.S., Rhoades, B., Qi, Y., Wang, J., Rajala, M.W., Pocai, A., Scherer, P.E.*, et al.* (2004). Regulation of fasted blood glucose by resistin. Science *303*, 1195-1198.

Banks, W.A., Jaspan, J.B., and Kastin, A.J. (1997). Selective, physiological transport of insulin across the blood-brain barrier: novel demonstration by species-specific radioimmunoassays. Peptides *18*, 1257-1262.

Bao, F., Arai, H., Matsushita, S., Higuchi, S., and Sasaki, H. (1996). Expression of apolipoprotein E in normal and diverse neurodegenerative disease brain. Neuroreport *7*, 1733-1739.

Barroso, I., Gurnell, M., Crowley, V.E., Agostini, M., Schwabe, J.W., Soos, M.A., Maslen, G.L., Williams, T.D., Lewis, H., Schafer, A.J.*, et al.* (1999). Dominant negative mutations in human PPARgamma associated with severe insulin resistance, diabetes mellitus and hypertension. Nature *402*, 880-883.

Baudier, J., and Cole, R.D. (1987). Phosphorylation of tau proteins to a state like that in Alzheimer's brain is catalyzed by a calcium/calmodulin-dependent kinase and modulated by phospholipids. J Biol Chem *262*, 17577-17583.

Baumann, K., Mandelkow, E.M., Biernat, J., Piwnica-Worms, H., and Mandelkow, E. (1993). Abnormal Alzheimer-like phosphorylation of tau-protein by cyclin-dependent kinases cdk2 and cdk5. FEBS Lett *336*, 417-424.

Baura, G.D., Foster, D.M., Porte, D., Jr., Kahn, S.E., Bergman, R.N., Cobelli, C., and Schwartz, M.W. (1993). Saturable transport of insulin from plasma into the central nervous system of dogs in vivo. A mechanism for regulated insulin delivery to the brain. J Clin Invest *92*, 1824-1830.

Bayer-Carter, J.L., Green, P.S., Montine, T.J., VanFossen, B., Baker, L.D., Watson, G.S., Bonner, L.M., Callaghan, M., Leverenz, J.B., Walter, B.K.*, et al.* (2011). Diet intervention and cerebrospinal fluid biomarkers in amnestic mild cognitive impairment. Arch Neurol *68*, 743-752.

Beck, B., Stricker-Krongrad, A., Burlet, A., Nicolas, J.P., and Burlet, C. (1990). Influence of diet composition on food intake and hypothalamic neuropeptide Y (NPY) in the rat. Neuropeptides *17*, 197-203.

Beffert, U., Aumont, N., Dea, D., Lussier-Cacan, S., Davignon, J., and Poirier, J. (1998). Beta-amyloid peptides increase the binding and internalization of apolipoprotein E to hippocampal neurons. J Neurochem *70*, 1458-1466.

Beffert, U., Aumont, N., Dea, D., Lussier-Cacan, S., Davignon, J., and Poirier, J. (1999). Apolipoprotein E isoform-specific reduction of extracellular amyloid in neuronal cultures. Brain Res Mol Brain Res *68*, 181-185.

Beffert, U., and Poirier, J. (1998). ApoE associated with lipid has a reduced capacity to inhibit beta-amyloid fibril formation. Neuroreport *9*, 3321-3323.

Bell, R.D., Sagare, A.P., Friedman, A.E., Bedi, G.S., Holtzman, D.M., Deane, R., and Zlokovic, B.V. (2007). Transport pathways for clearance of human Alzheimer's amyloid beta-peptide and apolipoproteins E and J in the mouse central nervous system. J Cereb Blood Flow Metab *27*, 909-918.

Bellosta, S., Nathan, B.P., Orth, M., Dong, L.M., Mahley, R.W., and Pitas, R.E. (1995). Stable expression and secretion of apolipoproteins E3 and E4 in mouse neuroblastoma cells produces differential effects on neurite outgrowth. J Biol Chem *270*, 27063-27071.

Benedict, C., Hallschmid, M., Hatke, A., Schultes, B., Fehm, H.L., Born, J., and Kern, W. (2004). Intranasal insulin improves memory in humans. Psychoneuroendocrinology *29*, 1326-1334.

Benjamini, Y., and Hochberg, Y. (1995). Controlling the False Discovery Rate: A Practical and Powerful Approach to Multiple Testing. Journal of the Royal Statistical Society Series B (Methodological) *57*, 289-300.

Bennett, B.D., Babu-Khan, S., Loeloff, R., Louis, J.C., Curran, E., Citron, M., and Vassar, R. (2000). Expression analysis of BACE2 in brain and peripheral tissues. J Biol Chem *275*, 20647-20651.

Berg, A.H., Combs, T.P., Du, X., Brownlee, M., and Scherer, P.E. (2001). The adipocyte-secreted protein Acrp30 enhances hepatic insulin action. Nat Med *7*, 947-953.

Berger, J., Bailey, P., Biswas, C., Cullinan, C.A., Doebber, T.W., Hayes, N.S., Saperstein, R., Smith, R.G., and Leibowitz, M.D. (1996). Thiazolidinediones produce a conformational change in peroxisomal proliferator-activated receptor-gamma: binding and activation correlate with antidiabetic actions in db/db mice. Endocrinology *137*, 4189-4195.

Berger, J., and Moller, D.E. (2002). The mechanisms of action of PPARs. Annu Rev Med *53*, 409-435.

Berlau, D.J., Corrada, M.M., Head, E., and Kawas, C.H. (2009). APOE epsilon2 is associated with intact cognition but increased Alzheimer pathology in the oldest old. Neurology *72*, 829-834.

Bernardi, P., Krauskopf, A., Basso, E., Petronilli, V., Blachly-Dyson, E., Di Lisa, F., and Forte, M.A. (2006). The mitochondrial permeability transition from in vitro artifact to disease target. FEBS J *273*, 2077-2099.

Bernstein, H.G., Schwarzberg, H., Reiser, M., Gunther, O., and Dorn, A. (1986). Intracerebroventricular infusion of insulin alters the behavior of rats not related to food intake. Endocrinol Exp *20*, 387-392.

Berridge, M.J. (1998). Neuronal calcium signaling. Neuron *21*, 13-26.

Bertram, L., Blacker, D., Mullin, K., Keeney, D., Jones, J., Basu, S., Yhu, S., McInnis, M.G., Go, R.C., Vekrellis, K*., et al.* (2000). Evidence for genetic linkage of Alzheimer's disease to chromosome 10q. Science *290*, 2302-2303.

Bertram, L., McQueen, M.B., Mullin, K., Blacker, D., and Tanzi, R.E. (2007). Systematic meta-analyses of Alzheimer disease genetic association studies: the AlzGene database. Nat Genet *39*, 17-23.

Bhat, R.V., Shanley, J., Correll, M.P., Fieles, W.E., Keith, R.A., Scott, C.W., and Lee, C.M. (2000). Regulation and localization of tyrosine216 phosphorylation of glycogen synthase kinase-3beta in cellular and animal models of neuronal degeneration. Proc Natl Acad Sci U S A *97*, 11074-11079.

Biere, A.L., Ostaszewski, B., Zhao, H., Gillespie, S., Younkin, S.G., and Selkoe, D.J. (1995). Co-expression of beta-amyloid precursor protein (betaAPP) and apolipoprotein E in cell culture: analysis of betaAPP processing. Neurobiol Dis *2*, 177-187.

Biessels, G.J., Staekenborg, S., Brunner, E., Brayne, C., and Scheltens, P. (2006). Risk of dementia in diabetes mellitus: a systematic review. Lancet Neurol *5*, 64-74.

Bikkavilli, R.K., and Malbon, C.C. (2009). Mitogen-activated protein kinases and Wnt/beta-catenin signaling: Molecular conversations among signaling pathways. Commun Integr Biol *2*, 46-49.

Bjorkhem, I., and Meaney, S. (2004). Brain cholesterol: long secret life behind a barrier. Arterioscler Thromb Vasc Biol *24*, 806-815.

Blair, C.K., Folsom, A.R., Knopman, D.S., Bray, M.S., Mosley, T.H., and Boerwinkle, E. (2005). APOE genotype and cognitive decline in a middle-aged cohort. Neurology *64*, 268-276.

Bolten, C.W., Blanner, P.M., McDonald, W.G., Staten, N.R., Mazzarella, R.A., Arhancet, G.B., Meier, M.F., Weiss, D.J., Sullivan, P.M., Hromockyj, A.E.*, et al.* (2007). Insulin sensitizing pharmacology of thiazolidinediones correlates with mitochondrial gene expression rather than activation of PPAR gamma. Gene Regul Syst Bio *1*, 73-82.

Bookheimer, S., and Burggren, A. (2009). APOE-4 genotype and neurophysiological vulnerability to Alzheimer's and cognitive aging. Annu Rev Clin Psychol *5*, 343-362.

Bordji, K., Becerril-Ortega, J., Nicole, O., and Buisson, A. (2010). Activation of extrasynaptic, but not synaptic, NMDA receptors modifies amyloid precursor protein expression pattern and increases amyloid-ss production. J Neurosci *30*, 15927-15942.

Bour, A., Grootendorst, J., Vogel, E., Kelche, C., Dodart, J.C., Bales, K., Moreau, P.H., Sullivan, P.M., and Mathis, C. (2008). Middle-aged human apoE4 targeted-replacement mice show retention deficits on a wide range of spatial memory tasks. Behav Brain Res *193*, 174-182.

Boyles, J.K., Pitas, R.E., Wilson, E., Mahley, R.W., and Taylor, J.M. (1985). Apolipoprotein E associated with astrocytic glia of the central nervous system and with nonmyelinating glia of the peripheral nervous system. J Clin Invest *76*, 1501-1513.

Boyles, J.K., Zoellner, C.D., Anderson, L.J., Kosik, L.M., Pitas, R.E., Weisgraber, K.H., Hui, D.Y., Mahley, R.W., Gebicke-Haerter, P.J., Ignatius, M.J.*, et al.* (1989). A role for apolipoprotein E, apolipoprotein A-I, and low density lipoprotein receptors in cholesterol transport during regeneration and remyelination of the rat sciatic nerve. J Clin Invest *83*, 1015-1031.

Braak, H., Alafuzoff, I., Arzberger, T., Kretzschmar, H., and Del Tredici, K. (2006). Staging of Alzheimer disease-associated neurofibrillary pathology using paraffin sections and immunocytochemistry. Acta Neuropathol *112*, 389-404.

Braak, H., and Braak, E. (1991). Neuropathological stageing of Alzheimer-related changes. Acta Neuropathol *82*, 239-259.

Braak, H., and Braak, E. (1995). Staging of Alzheimer's disease-related neurofibrillary changes. Neurobiol Aging *16*, 271-278; discussion 278-284.

Bradford, M.M. (1976). A rapid and sensitive method for the quantitation of microgram quantities of protein utilizing the principle of protein-dye binding. Anal Biochem *72*, 248-254.

Brant, A.M., Jess, T.J., Milligan, G., Brown, C.M., and Gould, G.W. (1993). Immunological analysis of glucose transporters expressed in different regions of the rat brain and central nervous system. Biochem Biophys Res Commun *192*, 1297-1302.

Brecht, W.J., Harris, F.M., Chang, S., Tesseur, I., Yu, G.Q., Xu, Q., Dee Fish, J., Wyss-Coray, T., Buttini, M., Mucke, L.*, et al.* (2004). Neuron-specific apolipoprotein e4 proteolysis is associated with increased tau phosphorylation in brains of transgenic mice. J Neurosci *24*, 2527-2534.

Breslow, J.L. (1996). Mouse models of atherosclerosis. Science *272*, 685-688.

Brunham, L.R., Kruit, J.K., Pape, T.D., Timmins, J.M., Reuwer, A.Q., Vasanji, Z., Marsh, B.J., Rodrigues, B., Johnson, J.D., Parks, J.S.*, et al.* (2007). Beta-cell ABCA1 influences insulin secretion, glucose homeostasis and response to thiazolidinedione treatment. Nat Med *13*, 340-347.

Brustovetsky, N., Brustovetsky, T., Purl, K.J., Capano, M., Crompton, M., and Dubinsky, J.M. (2003). Increased susceptibility of striatal mitochondria to calcium-induced permeability transition. J Neurosci *23*, 4858-4867.

Bu, G., Cam, J., and Zerbinatti, C. (2006). LRP in amyloid-beta production and metabolism. Ann N Y Acad Sci *1086*, 35-53.

Bubber, P., Haroutunian, V., Fisch, G., Blass, J.P., and Gibson, G.E. (2005). Mitochondrial abnormalities in Alzheimer brain: mechanistic implications. Ann Neurol *57*, 695-703.

Buee, L., Bussiere, T., Buee-Scherrer, V., Delacourte, A., and Hof, P.R. (2000). Tau protein isoforms, phosphorylation and role in neurodegenerative disorders. Brain Res Brain Res Rev *33*, 95-130.

Burgermeister, E., Chuderland, D., Hanoch, T., Meyer, M., Liscovitch, M., and Seger, R. (2007). Interaction with MEK causes nuclear export and downregulation of peroxisome proliferator-activated receptor gamma. Mol Cell Biol *27*, 803-817.

Busciglio, J., Pelsman, A., Wong, C., Pigino, G., Yuan, M., Mori, H., and Yankner, B.A. (2002). Altered metabolism of the amyloid beta precursor protein is associated with mitochondrial dysfunction in Down's syndrome. Neuron *33*, 677-688.

Buttini, M., Akeefe, H., Lin, C., Mahley, R.W., Pitas, R.E., Wyss-Coray, T., and Mucke, L. (2000). Dominant negative effects of apolipoprotein E4 revealed in transgenic models of neurodegenerative disease. Neuroscience *97*, 207-210.

Buttini, M., Masliah, E., Yu, G.Q., Palop, J.J., Chang, S., Bernardo, A., Lin, C., Wyss-Coray, T., Huang, Y., and Mucke, L. (2010). Cellular source of apolipoprotein E4 determines neuronal susceptibility to excitotoxic injury in transgenic mice. Am J Pathol *177*, 563-569.

Buttini, M., Orth, M., Bellosta, S., Akeefe, H., Pitas, R.E., Wyss-Coray, T., Mucke, L., and Mahley, R.W. (1999). Expression of human apolipoprotein E3 or E4 in the brains of Apoe-/- mice: isoform-specific effects on neurodegeneration. J Neurosci *19*, 4867-4880.

Buxbaum, J.D., Gandy, S.E., Cicchetti, P., Ehrlich, M.E., Czernik, A.J., Fracasso, R.P., Ramabhadran, T.V., Unterbeck, A.J., and Greengard, P. (1990). Processing of Alzheimer beta/A4 amyloid precursor protein: modulation by agents that regulate protein phosphorylation. Proc Natl Acad Sci U S A *87*, 6003-6006.

Caille, I., Allinquant, B., Dupont, E., Bouillot, C., Langer, A., Muller, U., and Prochiantz, A. (2004). Soluble form of amyloid precursor protein regulates proliferation of progenitors in the adult subventricular zone. Development *131*, 2173-2181.

Camacho, I.E., Serneels, L., Spittaels, K., Merchiers, P., Dominguez, D., and De Strooper, B. (2004). Peroxisome-proliferator-activated receptor gamma induces a clearance mechanism for the amyloid-beta peptide. J Neurosci *24*, 10908-10917.

Cao, D., Lu, H., Lewis, T.L., and Li, L. (2007). Intake of sucrose-sweetened water induces insulin resistance and exacerbates memory deficits and amyloidosis in a transgenic mouse model of Alzheimer disease. J Biol Chem *282*, 36275-36282.

Cao, X., and Sudhof, T.C. (2001). A transcriptionally [correction of transcriptively] active complex of APP with Fe65 and histone acetyltransferase Tip60. Science *293*, 115-120.

Castano, E.M., Prelli, F., Wisniewski, T., Golabek, A., Kumar, R.A., Soto, C., and Frangione, B. (1995). Fibrillogenesis in Alzheimer's disease of amyloid beta peptides and apolipoprotein E. Biochem J *306 (Pt 2)*, 599-604.

Castellano, J.M., Kim, J., Stewart, F.R., Jiang, H., Demattos, R.B., Patterson, B.W., Fagan, A.M., Morris, J.C., Mawuenyega, K.G., Cruchaga, C.*, et al.* (2011). Human apoE Isoforms Differentially Regulate Brain Amyloid-{beta} Peptide Clearance. Sci Transl Med *3*, 89ra57.

Caughey, B., and Lansbury, P.T. (2003). Protofibrils, pores, fibrils, and neurodegeneration: separating the responsible protein aggregates from the innocent bystanders. Annu Rev Neurosci *26*, 267-298.

Chang, S., ran Ma, T., Miranda, R.D., Balestra, M.E., Mahley, R.W., and Huang, Y. (2005). Lipid- and receptor-binding regions of apolipoprotein E4 fragments act in concert to cause mitochondrial dysfunction and neurotoxicity. Proc Natl Acad Sci U S A *102*, 18694-18699.

Chawla, A., Boisvert, W.A., Lee, C.H., Laffitte, B.A., Barak, Y., Joseph, S.B., Liao, D., Nagy, L., Edwards, P.A., Curtiss, L.K.*, et al.* (2001). A PPAR gamma-LXR-ABCA1 pathway in macrophages is involved in cholesterol efflux and atherogenesis. Mol Cell *7*, 161-171.

Chawla, A., Schwarz, E.J., Dimaculangan, D.D., and Lazar, M.A. (1994). Peroxisome proliferator-activated receptor (PPAR) gamma: adipose-predominant expression and induction early in adipocyte differentiation. Endocrinology *135*, 798-800.

Chen, H.K., Ji, Z.S., Dodson, S.E., Miranda, R.D., Rosenblum, C.I., Reynolds, I.J., Freedman, S.B., Weisgraber, K.H., Huang, Y., and Mahley, R.W. (2011). Apolipoprotein E4 domain interaction mediates detrimental effects on mitochondria and is a potential therapeutic target for Alzheimer disease. J Biol Chem *286*, 5215-5221.

Chen, J., Martin, B.L., and Brautigan, D.L. (1992). Regulation of protein serine-threonine phosphatase type-2A by tyrosine phosphorylation. Science *257*, 1261-1264.

Chen, L., Na, R., Gu, M., Richardson, A., and Ran, Q. (2008). Lipid peroxidation up-regulates BACE1 expression in vivo: a possible early event of amyloidogenesis in Alzheimer's disease. J Neurochem *107*, 197-207.

Chen, R.H., Ding, W.V., and McCormick, F. (2000). Wnt signaling to beta-catenin involves two interactive components. Glycogen synthase kinase-3beta inhibition and activation of protein kinase C. J Biol Chem *275*, 17894-17899.

Cheng, C.M., Tseng, V., Wang, J., Wang, D., Matyakhina, L., and Bondy, C.A. (2005). Tau is hyperphosphorylated in the insulin-like growth factor-I null brain. Endocrinology *146*, 5086-5091.

Cheng, D., Noble, J., Tang, M.X., Schupf, N., Mayeux, R., and Luchsinger, J.A. (2011). Type 2 diabetes and late-onset Alzheimer's disease. Dement Geriatr Cogn Disord *31*, 424-430.

Chien, A.J., Conrad, W.H., and Moon, R.T. (2009). A Wnt survival guide: from flies to human disease. J Invest Dermatol *129*, 1614-1627.

Chinetti, G., Lestavel, S., Bocher, V., Remaley, A.T., Neve, B., Torra, I.P., Teissier, E., Minnich, A., Jaye, M., Duverger, N., *et al.* (2001). PPAR-alpha and PPAR-gamma activators induce cholesterol removal from human macrophage foam cells through stimulation of the ABCA1 pathway. Nat Med *7*, 53-58.

Chiu, S.L., and Cline, H.T. (2010). Insulin receptor signaling in the development of neuronal structure and function. Neural Dev *5*, 7.

Choi, J.H., Banks, A.S., Estall, J.L., Kajimura, S., Bostrom, P., Laznik, D., Ruas, J.L., Chalmers, M.J., Kamenecka, T.M., Bluher, M., *et al.* (2010). Anti-diabetic drugs inhibit obesity-linked phosphorylation of PPARgamma by Cdk5. Nature *466*, 451-456.

Choi, J.H., Banks, A.S., Kamenecka, T.M., Busby, S.A., Chalmers, M.J., Kumar, N., Kuruvilla, D.S., Shin, Y., He, Y., Bruning, J.B., *et al.* (2011). Antidiabetic actions of a non-agonist PPARgamma ligand blocking Cdk5-mediated phosphorylation. Nature *477*, 477-481.

Christie, J.M., Wenthold, R.J., and Monaghan, D.T. (1999). Insulin causes a transient tyrosine phosphorylation of NR2A and NR2B NMDA receptor subunits in rat hippocampus. J Neurochem *72*, 1523-1528.

Chui, D.H., Dobo, E., Makifuchi, T., Akiyama, H., Kawakatsu, S., Petit, A., Checler, F., Araki, W., Takahashi, K., and Tabira, T. (2001). Apoptotic neurons in Alzheimer's disease frequently show intracellular Abeta42 labeling. J Alzheimers Dis *3*, 231-239.

Chui, D.H., Tanahashi, H., Ozawa, K., Ikeda, S., Checler, F., Ueda, O., Suzuki, H., Araki, W., Inoue, H., Shirotani, K., *et al.* (1999). Transgenic mice with Alzheimer presenilin 1 mutations show accelerated neurodegeneration without amyloid plaque formation. Nat Med *5*, 560-564.

Chung, S.H. (2009). Aberrant phosphorylation in the pathogenesis of Alzheimer's disease. BMB Rep *42*, 467-474.

Cleary, J.P., Walsh, D.M., Hofmeister, J.J., Shankar, G.M., Kuskowski, M.A., Selkoe, D.J., and Ashe, K.H. (2005). Natural oligomers of the amyloid-beta protein specifically disrupt cognitive function. Nat Neurosci *8*, 79-84.

Clodfelder-Miller, B.J., Zmijewska, A.A., Johnson, G.V., and Jope, R.S. (2006). Tau is hyperphosphorylated at multiple sites in mouse brain in vivo after streptozotocin-induced insulin deficiency. Diabetes *55*, 3320-3325.

Cocks, G., Wilde, J.I., Graham, S.J., Bousgouni, V., Virley, D., Lovestone, S., and Richardson, J. (2010). The thiazolidinedione pioglitazone increases cholesterol biosynthetic gene expression in primary cortical neurons by a PPARgamma-independent mechanism. J Alzheimers Dis *19*, 631-646.

Cole, A., Frame, S., and Cohen, P. (2004). Further evidence that the tyrosine phosphorylation of glycogen synthase kinase-3 (GSK3) in mammalian cells is an autophosphorylation event. Biochem J *377*, 249-255.

Cole, A.R., Causeret, F., Yadirgi, G., Hastie, C.J., McLauchlan, H., McManus, E.J., Hernandez, F., Eickholt, B.J., Nikolic, M., and Sutherland, C. (2006). Distinct priming kinases contribute to differential regulation of collapsin response mediator proteins by glycogen synthase kinase-3 in vivo. J Biol Chem *281*, 16591-16598.

Cole, G.M., and Ard, M.D. (2000). Influence of lipoproteins on microglial degradation of Alzheimer's amyloid beta-protein. Microsc Res Tech *50*, 316-324.

Cook, D., Fry, M.J., Hughes, K., Sumathipala, R., Woodgett, J.R., and Dale, T.C. (1996). Wingless inactivates glycogen synthase kinase-3 via an intracellular signalling pathway which involves a protein kinase C. EMBO J *15*, 4526-4536.

Cook, D.G., Leverenz, J.B., McMillan, P.J., Kulstad, J.J., Ericksen, S., Roth, R.A., Schellenberg, G.D., Jin, L.W., Kovacina, K.S., and Craft, S. (2003). Reduced hippocampal insulin-degrading enzyme in late-onset Alzheimer's disease is associated with the apolipoprotein E-epsilon4 allele. Am J Pathol *162*, 313-319.

Coomaraswamy, J., Kilger, E., Wolfing, H., Schafer, C., Kaeser, S.A., Wegenast-Braun, B.M., Hefendehl, J.K., Wolburg, H., Mazzella, M., Ghiso, J., *et al.* (2010). Modeling familial Danish dementia in mice supports the concept of the amyloid hypothesis of Alzheimer's disease. Proc Natl Acad Sci U S A *107*, 7969-7974.

Corder, E.H., Saunders, A.M., Pericak-Vance, M.A., and Roses, A.D. (1995). There is a pathologic relationship between ApoE-epsilon 4 and Alzheimer's disease. Arch Neurol *52*, 650-651.

Corder, E.H., Saunders, A.M., Risch, N.J., Strittmatter, W.J., Schmechel, D.E., Gaskell, P.C., Jr., Rimmler, J.B., Locke, P.A., Conneally, P.M., Schmader, K.E., *et al.* (1994). Protective effect of apolipoprotein E type 2 allele for late onset Alzheimer disease. Nat Genet *7*, 180-184.

Corder, E.H., Saunders, A.M., Strittmatter, W.J., Schmechel, D.E., Gaskell, P.C., Small, G.W., Roses, A.D., Haines, J.L., and Pericak-Vance, M.A. (1993). Gene dose of apolipoprotein E type 4 allele and the risk of Alzheimer's disease in late onset families. Science *261*, 921-923.

Courtney, E., Kornfeld, S., Janitz, K., and Janitz, M. (2010). Transcriptome profiling in neurodegenerative disease. J Neurosci Methods *193*, 189-202.

Craft, S., Asthana, S., Cook, D.G., Baker, L.D., Cherrier, M., Purganan, K., Wait, C., Petrova, A., Latendresse, S., Watson, G.S.*, et al.* (2003). Insulin dose-response effects on memory and plasma amyloid precursor protein in Alzheimer's disease: interactions with apolipoprotein E genotype. Psychoneuroendocrinology *28*, 809-822.

Craft, S., Asthana, S., Newcomer, J.W., Wilkinson, C.W., Matos, I.T., Baker, L.D., Cherrier, M., Lofgreen, C., Latendresse, S., Petrova, A.*, et al.* (1999a). Enhancement of memory in Alzheimer disease with insulin and somatostatin, but not glucose. Arch Gen Psychiatry *56*, 1135-1140.

Craft, S., Asthana, S., Schellenberg, G., Baker, L., Cherrier, M., Boyt, A.A., Martins, R.N., Raskind, M., Peskind, E., and Plymate, S. (2000). Insulin effects on glucose metabolism, memory, and plasma amyloid precursor protein in Alzheimer's disease differ according to apolipoprotein-E genotype. Ann N Y Acad Sci *903*, 222-228.

Craft, S., Asthana, S., Schellenberg, G., Cherrier, M., Baker, L.D., Newcomer, J., Plymate, S., Latendresse, S., Petrova, A., Raskind, M.*, et al.* (1999b). Insulin metabolism in Alzheimer's disease differs according to apolipoprotein E genotype and gender. Neuroendocrinology *70*, 146-152.

Craft, S., Newcomer, J., Kanne, S., Dagogo-Jack, S., Cryer, P., Sheline, Y., Luby, J., Dagogo-Jack, A., and Alderson, A. (1996). Memory improvement following induced hyperinsulinemia in Alzheimer's disease. Neurobiol Aging *17*, 123-130.

Craft, S., Peskind, E., Schwartz, M.W., Schellenberg, G.D., Raskind, M., and Porte, D., Jr. (1998). Cerebrospinal fluid and plasma insulin levels in Alzheimer's disease: relationship to severity of dementia and apolipoprotein E genotype. Neurology *50*, 164-168.

Cross, D.A., Alessi, D.R., Cohen, P., Andjelkovich, M., and Hemmings, B.A. (1995). Inhibition of glycogen synthase kinase-3 by insulin mediated by protein kinase B. Nature *378*, 785-789.

Cruz, J.C., Tseng, H.C., Goldman, J.A., Shih, H., and Tsai, L.H. (2003). Aberrant Cdk5 activation by p25 triggers pathological events leading to neurodegeneration and neurofibrillary tangles. Neuron *40*, 471-483.

Cselenyi, C.S., Jernigan, K.K., Tahinci, E., Thorne, C.A., Lee, L.A., and Lee, E. (2008). LRP6 transduces a canonical Wnt signal independently of Axin degradation by inhibiting GSK3's phosphorylation of beta-catenin. Proc Natl Acad Sci U S A *105*, 8032-8037.

Curb, J.D., Rodriguez, B.L., Abbott, R.D., Petrovitch, H., Ross, G.W., Masaki, K.H., Foley, D., Blanchette, P.L., Harris, T., Chen, R.*, et al.* (1999). Longitudinal association of vascular and Alzheimer's dementias, diabetes, and glucose tolerance. Neurology *52*, 971-975.

d'Abramo, C., Massone, S., Zingg, J.M., Pizzuti, A., Marambaud, P., Dalla Piccola, B., Azzi, A., Marinari, U.M., Pronzato, M.A., and Ricciarelli, R. (2005). Role of peroxisome proliferator-activated receptor gamma in amyloid precursor protein processing and amyloid beta-mediated cell death. Biochem J *391*, 693-698.

d'Abramo, C., Ricciarelli, R., Pronzato, M.A., and Davies, P. (2006). Troglitazone, a peroxisome proliferator-activated receptor-gamma agonist, decreases tau phosphorylation in CHOtau4R cells. J Neurochem *98*, 1068-1077.

D'Andrea, M.R., Nagele, R.G., Wang, H.Y., Peterson, P.A., and Lee, D.H. (2001). Evidence that neurones accumulating amyloid can undergo lysis to form amyloid plaques in Alzheimer's disease. Histopathology *38*, 120-134.

De Felice, F.G., Velasco, P.T., Lambert, M.P., Viola, K., Fernandez, S.J., Ferreira, S.T., and Klein, W.L. (2007). Abeta oligomers induce neuronal oxidative stress through an N-methyl-D-aspartate receptor-dependent mechanism that is blocked by the Alzheimer drug memantine. J Biol Chem *282*, 11590-11601.

de la Monte, S.M. (2009). Insulin resistance and Alzheimer's disease. BMB Rep *42*, 475-481.

Deane, R., Du Yan, S., Submamaryan, R.K., LaRue, B., Jovanovic, S., Hogg, E., Welch, D., Manness, L., Lin, C., Yu, J.*, et al.* (2003). RAGE mediates amyloid-beta peptide transport across the blood-brain barrier and accumulation in brain. Nat Med *9*, 907-913.

Deane, R., Sagare, A., Hamm, K., Parisi, M., Lane, S., Finn, M.B., Holtzman, D.M., and Zlokovic, B.V. (2008). apoE isoform-specific disruption of amyloid beta peptide clearance from mouse brain. J Clin Invest *118*, 4002-4013.

Deane, R., Wu, Z., Sagare, A., Davis, J., Du Yan, S., Hamm, K., Xu, F., Parisi, M., LaRue, B., Hu, H.W.*, et al.* (2004). LRP/amyloid beta-peptide interaction mediates differential brain efflux of Abeta isoforms. Neuron *43*, 333-344.

Deng, Y., Li, B., Liu, Y., Iqbal, K., Grundke-Iqbal, I., and Gong, C.X. (2009). Dysregulation of insulin signaling, glucose transporters, O-GlcNAcylation, and phosphorylation

of tau and neurofilaments in the brain: Implication for Alzheimer's disease. Am J Pathol *175*, 2089-2098.

Derkinderen, P., Scales, T.M., Hanger, D.P., Leung, K.Y., Byers, H.L., Ward, M.A., Lenz, C., Price, C., Bird, I.N., Perera, T.*, et al.* (2005). Tyrosine 394 is phosphorylated in Alzheimer's paired helical filament tau and in fetal tau with c-Abl as the candidate tyrosine kinase. J Neurosci *25*, 6584-6593.

Descamps, O., Bilheimer, D., and Herz, J. (1993). Insulin stimulates receptor-mediated uptake of apoE-enriched lipoproteins and activated alpha 2-macroglobulin in adipocytes. J Biol Chem *268*, 974-981.

Devaskar, S.U., Giddings, S.J., Rajakumar, P.A., Carnaghi, L.R., Menon, R.K., and Zahm, D.S. (1994). Insulin gene expression and insulin synthesis in mammalian neuronal cells. J Biol Chem *269*, 8445-8454.

Devedjian, J.C., Pujol, A., Cayla, C., George, M., Casellas, A., Paris, H., and Bosch, F. (2000). Transgenic mice overexpressing alpha2A-adrenoceptors in pancreatic beta-cells show altered regulation of glucose homeostasis. Diabetologia *43*, 899-906.

Dhavan, R., and Tsai, L.H. (2001). A decade of CDK5. Nat Rev Mol Cell Biol *2*, 749-759.

Di Luca, M., Ruts, L., Gardoni, F., Cattabeni, F., Biessels, G.J., and Gispen, W.H. (1999). NMDA receptor subunits are modified transcriptionally and post-translationally in the brain of streptozotocin-diabetic rats. Diabetologia *42*, 693-701.

Distl, R., Meske, V., and Ohm, T.G. (2001). Tangle-bearing neurons contain more free cholesterol than adjacent tangle-free neurons. Acta Neuropathol *101*, 547-554.

Doble, B.W., and Woodgett, J.R. (2003). GSK-3: tricks of the trade for a multi-tasking kinase. J Cell Sci *116*, 1175-1186.

Dodart, J.C., Bales, K.R., Johnstone, E.M., Little, S.P., and Paul, S.M. (2002). Apolipoprotein E alters the processing of the beta-amyloid precursor protein in APP(V717F) transgenic mice. Brain Res *955*, 191-199.

Dodart, J.C., Mathis, C., Bales, K.R., Paul, S.M., and Ungerer, A. (2000). Behavioral deficits in APP(V717F) transgenic mice deficient for the apolipoprotein E gene. Neuroreport *11*, 603-607.

Dominguez, D., Tournoy, J., Hartmann, D., Huth, T., Cryns, K., Deforce, S., Serneels, L., Camacho, I.E., Marjaux, E., Craessaerts, K.*, et al.* (2005). Phenotypic and biochemical analyses of BACE1- and BACE2-deficient mice. J Biol Chem *280*, 30797-30806.

Dong, F., Li, Q., Sreejayan, N., Nunn, J.M., and Ren, J. (2007). Metallothionein prevents high-fat diet induced cardiac contractile dysfunction: role of peroxisome proliferator activated receptor gamma coactivator 1alpha and mitochondrial biogenesis. Diabetes *56*, 2201-2212.

Dong, L.M., and Weisgraber, K.H. (1996). Human apolipoprotein E4 domain interaction. Arginine 61 and glutamic acid 255 interact to direct the preference for very low density lipoproteins. J Biol Chem *271*, 19053-19057.

Dong, L.M., Wilson, C., Wardell, M.R., Simmons, T., Mahley, R.W., Weisgraber, K.H., and Agard, D.A. (1994). Human apolipoprotein E. Role of arginine 61 in mediating the lipoprotein preferences of the E3 and E4 isoforms. J Biol Chem *269*, 22358-22365.

Dreses-Werringloer, U., Lambert, J.C., Vingtdeux, V., Zhao, H., Vais, H., Siebert, A., Jain, A., Koppel, J., Rovelet-Lecrux, A., Hannequin, D.*, et al.* (2008). A polymorphism in CALHM1 influences Ca2+ homeostasis, Abeta levels, and Alzheimer's disease risk. Cell *133*, 1149-1161.

Drewes, G., Mandelkow, E.M., Baumann, K., Goris, J., Merlevede, W., and Mandelkow, E. (1993). Dephosphorylation of tau protein and Alzheimer paired helical filaments by calcineurin and phosphatase-2A. FEBS Lett *336*, 425-432.

Drewes, G., Trinczek, B., Illenberger, S., Biernat, J., Schmitt-Ulms, G., Meyer, H.E., Mandelkow, E.M., and Mandelkow, E. (1995). Microtubule-associated protein/microtubule affinity-regulating kinase (p110mark). A novel protein kinase that regulates tau-microtubule interactions and dynamic instability by phosphorylation at the Alzheimer-specific site serine 262. J Biol Chem *270*, 7679-7688.

Dreyer, C., Krey, G., Keller, H., Givel, F., Helftenbein, G., and Wahli, W. (1992). Control of the peroxisomal beta-oxidation pathway by a novel family of nuclear hormone receptors. Cell *68*, 879-887.

Du, J., Chang, J., Guo, S., Zhang, Q., and Wang, Z. (2009). ApoE 4 reduces the expression of Abeta degrading enzyme IDE by activating the NMDA receptor in hippocampal neurons. Neurosci Lett *464*, 140-145.

Duckworth, W.C., Bennett, R.G., and Hamel, F.G. (1998). Insulin degradation: progress and potential. Endocr Rev *19*, 608-624.

Eckert, A., Schmitt, K., and Gotz, J. (2011). Mitochondrial dysfunction - the beginning of the end in Alzheimer's disease? Separate and synergistic modes of tau and amyloid-beta toxicity. Alzheimers Res Ther *3*, 15.

Edbauer, D., Willem, M., Lammich, S., Steiner, H., and Haass, C. (2002). Insulin-degrading enzyme rapidly removes the beta-amyloid precursor protein intracellular domain (AICD). J Biol Chem *277*, 13389-13393.

Eikelenboom, P., Bate, C., Van Gool, W.A., Hoozemans, J.J., Rozemuller, J.M., Veerhuis, R., and Williams, A. (2002). Neuroinflammation in Alzheimer's disease and prion disease. Glia *40*, 232-239.

Eldershaw, T.P., Rattigan, S., Cawthorne, M.A., Buckingham, R.E., Colquhoun, E.Q., and Clark, M.G. (1995). Treatment with the thiazolidinedione (BRL 49653) decreases insulin resistance in obese Zucker hindlimb. Horm Metab Res *27*, 169-172.

Elosua, R., Demissie, S., Cupples, L.A., Meigs, J.B., Wilson, P.W., Schaefer, E.J., Corella, D., and Ordovas, J.M. (2003). Obesity modulates the association among APOE genotype, insulin, and glucose in men. Obes Res *11*, 1502-1508.

Elshourbagy, N.A., Liao, W.S., Mahley, R.W., and Taylor, J.M. (1985). Apolipoprotein E mRNA is abundant in the brain and adrenals, as well as in the liver, and is present in other peripheral tissues of rats and marmosets. Proc Natl Acad Sci U S A *82*, 203-207.

Emilsson, L., Saetre, P., and Jazin, E. (2006). Alzheimer's disease: mRNA expression profiles of multiple patients show alterations of genes involved with calcium signaling. Neurobiol Dis *21*, 618-625.

Engel, T., Goni-Oliver, P., Lucas, J.J., Avila, J., and Hernandez, F. (2006). Chronic lithium administration to FTDP-17 tau and GSK-3beta overexpressing mice prevents tau hyperphosphorylation and neurofibrillary tangle formation, but pre-formed neurofibrillary tangles do not revert. J Neurochem *99*, 1445-1455.

Escribano, L., Simon, A.M., Gimeno, E., Cuadrado-Tejedor, M., Lopez de Maturana, R., Garcia-Osta, A., Ricobaraza, A., Perez-Mediavilla, A., Del Rio, J., and Frechilla, D. (2010). Rosiglitazone rescues memory impairment in Alzheimer's transgenic mice: mechanisms involving a reduced amyloid and tau pathology. Neuropsychopharmacology *35*, 1593-1604.

Etcheberrigaray, R., Hirashima, N., Nee, L., Prince, J., Govoni, S., Racchi, M., Tanzi, R.E., and Alkon, D.L. (1998). Calcium responses in fibroblasts from asymptomatic members of Alzheimer's disease families. Neurobiol Dis *5*, 37-45.

Evans, K.C., Berger, E.P., Cho, C.G., Weisgraber, K.H., and Lansbury, P.T., Jr. (1995). Apolipoprotein E is a kinetic but not a thermodynamic inhibitor of amyloid formation: implications for the pathogenesis and treatment of Alzheimer disease. Proc Natl Acad Sci U S A *92*, 763-767.

Fagan, A.M., Bu, G., Sun, Y., Daugherty, A., and Holtzman, D.M. (1996). Apolipoprotein E-containing high density lipoprotein promotes neurite outgrowth and is a ligand for the low density lipoprotein receptor-related protein. J Biol Chem *271*, 30121-30125.

Fagan, A.M., Holtzman, D.M., Munson, G., Mathur, T., Schneider, D., Chang, L.K., Getz, G.S., Reardon, C.A., Lukens, J., Shah, J.A.*, et al.* (1999). Unique lipoproteins secreted by primary astrocytes from wild type, apoE (-/-), and human apoE transgenic mice. J Biol Chem *274*, 30001-30007.

Fagan, A.M., Mintun, M.A., Mach, R.H., Lee, S.Y., Dence, C.S., Shah, A.R., LaRossa, G.N., Spinner, M.L., Klunk, W.E., Mathis, C.A.*, et al.* (2006). Inverse relation between in vivo amyloid imaging load and cerebrospinal fluid Abeta42 in humans. Ann Neurol *59*, 512-519.

Fagan, A.M., Watson, M., Parsadanian, M., Bales, K.R., Paul, S.M., and Holtzman, D.M. (2002). Human and murine ApoE markedly alters A beta metabolism before and after plaque formation in a mouse model of Alzheimer's disease. Neurobiol Dis *9*, 305-318.

Fagerholm, V., Gronroos, T., Marjamaki, P., Viljanen, T., Scheinin, M., and Haaparanta, M. (2004). Altered glucose homeostasis in alpha2A-adrenoceptor knockout mice. Eur J Pharmacol *505*, 243-252.

Fahrenholz, F., Gilbert, S., Kojro, E., Lammich, S., and Postina, R. (2000). Alpha-secretase activity of the disintegrin metalloprotease ADAM 10. Influences of domain structure. Ann N Y Acad Sci *920*, 215-222.

Fan, Q.W., Yu, W., Senda, T., Yanagisawa, K., and Michikawa, M. (2001). Cholesterol-dependent modulation of tau phosphorylation in cultured neurons. J Neurochem *76*, 391-400.

Farrer, L.A., Cupples, L.A., Haines, J.L., Hyman, B., Kukull, W.A., Mayeux, R., Myers, R.H., Pericak-Vance, M.A., Risch, N., and van Duijn, C.M. (1997). Effects of age, sex, and ethnicity on the association between apolipoprotein E genotype and Alzheimer disease. A meta-analysis. APOE and Alzheimer Disease Meta Analysis Consortium. JAMA *278*, 1349-1356.

Farris, W., Mansourian, S., Chang, Y., Lindsley, L., Eckman, E.A., Frosch, M.P., Eckman, C.B., Tanzi, R.E., Selkoe, D.J., and Guenette, S. (2003). Insulin-degrading enzyme

regulates the levels of insulin, amyloid beta-protein, and the beta-amyloid precursor protein intracellular domain in vivo. Proc Natl Acad Sci U S A *100*, 4162-4167.

Farris, W., Schutz, S.G., Cirrito, J.R., Shankar, G.M., Sun, X., George, A., Leissring, M.A., Walsh, D.M., Qiu, W.Q., Holtzman, D.M.*, et al.* (2007). Loss of neprilysin function promotes amyloid plaque formation and causes cerebral amyloid angiopathy. Am J Pathol *171*, 241-251.

Fassbender, K., Simons, M., Bergmann, C., Stroick, M., Lutjohann, D., Keller, P., Runz, H., Kuhl, S., Bertsch, T., von Bergmann, K.*, et al.* (2001). Simvastatin strongly reduces levels of Alzheimer's disease beta -amyloid peptides Abeta 42 and Abeta 40 in vitro and in vivo. Proc Natl Acad Sci U S A *98*, 5856-5861.

Fath, T., Eidenmuller, J., and Brandt, R. (2002). Tau-mediated cytotoxicity in a pseudohyperphosphorylation model of Alzheimer's disease. J Neurosci *22*, 9733-9741.

Ferreiro, E., Oliveira, C.R., and Pereira, C. (2004). Involvement of endoplasmic reticulum Ca2+ release through ryanodine and inositol 1,4,5-triphosphate receptors in the neurotoxic effects induced by the amyloid-beta peptide. J Neurosci Res *76*, 872-880.

Figlewicz, D.P., Szot, P., Israel, P.A., Payne, C., and Dorsa, D.M. (1993). Insulin reduces norepinephrine transporter mRNA in vivo in rat locus coeruleus. Brain Res *602*, 161-164.

Fleming, L.M., and Johnson, G.V. (1995). Modulation of the phosphorylation state of tau in situ: the roles of calcium and cyclic AMP. Biochem J *309 (Pt 1)*, 41-47.

Frame, S., and Cohen, P. (2001). GSK3 takes centre stage more than 20 years after its discovery. Biochem J *359*, 1-16.

Francis, G., Martinez, J., Liu, W., Nguyen, T., Ayer, A., Fine, J., Zochodne, D., Hanson, L.R., Frey, W.H., 2nd, and Toth, C. (2009). Intranasal insulin ameliorates experimental diabetic neuropathy. Diabetes *58*, 934-945.

Francis, G.J., Martinez, J.A., Liu, W.Q., Xu, K., Ayer, A., Fine, J., Tuor, U.I., Glazner, G., Hanson, L.R., Frey, W.H., 2nd*, et al.* (2008). Intranasal insulin prevents cognitive decline, cerebral atrophy and white matter changes in murine type I diabetic encephalopathy. Brain *131*, 3311-3334.

Frears, E.R., Stephens, D.J., Walters, C.E., Davies, H., and Austen, B.M. (1999). The role of cholesterol in the biosynthesis of beta-amyloid. Neuroreport *10*, 1699-1705.

Freude, S., Hettich, M.M., Schumann, C., Stohr, O., Koch, L., Kohler, C., Udelhoven, M., Leeser, U., Muller, M., Kubota, N.*, et al.* (2009). Neuronal IGF-1 resistance reduces Abeta accumulation and protects against premature death in a model of Alzheimer's disease. FASEB J *23*, 3315-3324.

Freude, S., Plum, L., Schnitker, J., Leeser, U., Udelhoven, M., Krone, W., Bruning, J.C., and Schubert, M. (2005). Peripheral hyperinsulinemia promotes tau phosphorylation in vivo. Diabetes *54*, 3343-3348.

Frolich, L., Blum-Degen, D., Bernstein, H.G., Engelsberger, S., Humrich, J., Laufer, S., Muschner, D., Thalheimer, A., Turk, A., Hoyer, S.*, et al.* (1998). Brain insulin and insulin receptors in aging and sporadic Alzheimer's disease. J Neural Transm *105*, 423-438.

Fryer, J.D., Simmons, K., Parsadanian, M., Bales, K.R., Paul, S.M., Sullivan, P.M., and Holtzman, D.M. (2005). Human apolipoprotein E4 alters the amyloid-beta 40:42 ratio and promotes the formation of cerebral amyloid angiopathy in an amyloid precursor protein transgenic model. J Neurosci *25*, 2803-2810.

Fujiwara, T., Wada, M., Fukuda, K., Fukami, M., Yoshioka, S., Yoshioka, T., and Horikoshi, H. (1991). Characterization of CS-045, a new oral antidiabetic agent, II. Effects on glycemic control and pancreatic islet structure at a late stage of the diabetic syndrome in C57BL/KsJ-db/db mice. Metabolism *40*, 1213-1218.

Fujiwara, T., Yoshioka, S., Yoshioka, T., Ushiyama, I., and Horikoshi, H. (1988). Characterization of new oral antidiabetic agent CS-045. Studies in KK and ob/ob mice and Zucker fatty rats. Diabetes *37*, 1549-1558.

Funfschilling, U., Saher, G., Xiao, L., Mobius, W., and Nave, K.A. (2007). Survival of adult neurons lacking cholesterol synthesis in vivo. BMC Neurosci *8*, 1.

Furukawa, K., Sopher, B.L., Rydel, R.E., Begley, J.G., Pham, D.G., Martin, G.M., Fox, M., and Mattson, M.P. (1996). Increased activity-regulating and neuroprotective efficacy of alpha-secretase-derived secreted amyloid precursor protein conferred by a C-terminal heparin-binding domain. J Neurochem *67*, 1882-1896.

Gallagher, E.J., Leroith, D., and Karnieli, E. (2010). Insulin resistance in obesity as the underlying cause for the metabolic syndrome. Mt Sinai J Med *77*, 511-523.

Galvan, V., Gorostiza, O.F., Banwait, S., Ataie, M., Logvinova, A.V., Sitaraman, S., Carlson, E., Sagi, S.A., Chevallier, N., Jin, K.*, et al.* (2006). Reversal of Alzheimer's-like

pathology and behavior in human APP transgenic mice by mutation of Asp664. Proc Natl Acad Sci U S A *103*, 7130-7135.

Gasic-Milenkovic, J., Dukic-Stefanovic, S., Deuther-Conrad, W., Gartner, U., and Munch, G. (2003). Beta-amyloid peptide potentiates inflammatory responses induced by lipopolysaccharide, interferon -gamma and 'advanced glycation endproducts' in a murine microglia cell line. Eur J Neurosci *17*, 813-821.

Gasparini, L., Gouras, G.K., Wang, R., Gross, R.S., Beal, M.F., Greengard, P., and Xu, H. (2001). Stimulation of beta-amyloid precursor protein trafficking by insulin reduces intraneuronal beta-amyloid and requires mitogen-activated protein kinase signaling. J Neurosci *21*, 2561-2570.

Geldmacher, D.S., Fritsch, T., McClendon, M.J., and Landreth, G. (2011). A randomized pilot clinical trial of the safety of pioglitazone in treatment of patients with Alzheimer disease. Arch Neurol *68*, 45-50.

Genis, I., Gordon, I., Sehayek, E., and Michaelson, D.M. (1995). Phosphorylation of tau in apolipoprotein E-deficient mice. Neurosci Lett *199*, 5-8.

George, A.J., Gordon, L., Beissbarth, T., Koukoulas, I., Holsinger, R.M., Perreau, V., Cappai, R., Tan, S.S., Masters, C.L., Scott, H.S*., et al.* (2010). A serial analysis of gene expression profile of the Alzheimer's disease Tg2576 mouse model. Neurotox Res *17*, 360-379.

Ghebremedhin, E., Schultz, C., Braak, E., and Braak, H. (1998). High frequency of apolipoprotein E epsilon4 allele in young individuals with very mild Alzheimer's disease-related neurofibrillary changes. Exp Neurol *153*, 152-155.

Ghribi, O., Herman, M.M., and Savory, J. (2003). Lithium inhibits Abeta-induced stress in endoplasmic reticulum of rabbit hippocampus but does not prevent oxidative damage and tau phosphorylation. J Neurosci Res *71*, 853-862.

Gibson, G.E., Haroutunian, V., Zhang, H., Park, L.C., Shi, Q., Lesser, M., Mohs, R.C., Sheu, R.K., and Blass, J.P. (2000). Mitochondrial damage in Alzheimer's disease varies with apolipoprotein E genotype. Ann Neurol *48*, 297-303.

Gispen, W.H., and Biessels, G.J. (2000). Cognition and synaptic plasticity in diabetes mellitus. Trends Neurosci *23*, 542-549.

Glenner, G.G., and Wong, C.W. (1984). Alzheimer's disease: initial report of the purification and characterization of a novel cerebrovascular amyloid protein. Biochem Biophys Res Commun *120*, 885-890.

Goedert, M., Hasegawa, M., Jakes, R., Lawler, S., Cuenda, A., and Cohen, P. (1997). Phosphorylation of microtubule-associated protein tau by stress-activated protein kinases. FEBS Lett *409*, 57-62.

Goedert, M., Jakes, R., Qi, Z., Wang, J.H., and Cohen, P. (1995). Protein phosphatase 2A is the major enzyme in brain that dephosphorylates tau protein phosphorylated by proline-directed protein kinases or cyclic AMP-dependent protein kinase. J Neurochem *65*, 2804-2807.

Goedert, M., Spillantini, M.G., Jakes, R., Rutherford, D., and Crowther, R.A. (1989). Multiple isoforms of human microtubule-associated protein tau: sequences and localization in neurofibrillary tangles of Alzheimer's disease. Neuron *3*, 519-526.

Gold, M., Alderton, C., Zvartau-Hind, M., Egginton, S., Saunders, A.M., Irizarry, M., Craft, S., Landreth, G., Linnamagi, U., and Sawchak, S. (2010). Rosiglitazone monotherapy in mild-to-moderate Alzheimer's disease: results from a randomized, double-blind, placebo-controlled phase III study. Dement Geriatr Cogn Disord *30*, 131-146.

Gong, C.X., Liu, F., Grundke-Iqbal, I., and Iqbal, K. (2006). Impaired brain glucose metabolism leads to Alzheimer neurofibrillary degeneration through a decrease in tau O-GlcNAcylation. J Alzheimers Dis *9*, 1-12.

Gong, C.X., Singh, T.J., Grundke-Iqbal, I., and Iqbal, K. (1993). Phosphoprotein phosphatase activities in Alzheimer disease brain. J Neurochem *61*, 921-927.

Gong, C.X., Singh, T.J., Grundke-Iqbal, I., and Iqbal, K. (1994). Alzheimer's disease abnormally phosphorylated tau is dephosphorylated by protein phosphatase-2B (calcineurin). J Neurochem *62*, 803-806.

Gong, C.X., Wang, J.Z., Iqbal, K., and Grundke-Iqbal, I. (2003). Inhibition of protein phosphatase 2A induces phosphorylation and accumulation of neurofilaments in metabolically active rat brain slices. Neurosci Lett *340*, 107-110.

Good, P.F., Perl, D.P., Bierer, L.M., and Schmeidler, J. (1992). Selective accumulation of aluminum and iron in the neurofibrillary tangles of Alzheimer's disease: a laser microprobe (LAMMA) study. Ann Neurol *31*, 286-292.

Goodman, Y., and Mattson, M.P. (1994). Secreted forms of beta-amyloid precursor protein protect hippocampal neurons against amyloid beta-peptide-induced oxidative injury. Exp Neurol *128*, 1-12.

Goto, S., Yamamoto, H., Fukunaga, K., Iwasa, T., Matsukado, Y., and Miyamoto, E. (1985). Dephosphorylation of microtubule-associated protein 2, tau factor, and tubulin by calcineurin. J Neurochem *45*, 276-283.

Gotz, J., Chen, F., van Dorpe, J., and Nitsch, R.M. (2001). Formation of neurofibrillary tangles in P301l tau transgenic mice induced by Abeta 42 fibrils. Science *293*, 1491-1495.

Gouras, G.K., Tsai, J., Naslund, J., Vincent, B., Edgar, M., Checler, F., Greenfield, J.P., Haroutunian, V., Buxbaum, J.D., Xu, H.*, et al.* (2000). Intraneuronal Abeta42 accumulation in human brain. Am J Pathol *156*, 15-20.

Grabowski, T.J., Cho, H.S., Vonsattel, J.P., Rebeck, G.W., and Greenberg, S.M. (2001). Novel amyloid precursor protein mutation in an Iowa family with dementia and severe cerebral amyloid angiopathy. Ann Neurol *49*, 697-705.

Griffin, W.S., Stanley, L.C., Ling, C., White, L., MacLeod, V., Perrot, L.J., White, C.L., 3rd, and Araoz, C. (1989). Brain interleukin 1 and S-100 immunoreactivity are elevated in Down syndrome and Alzheimer disease. Proc Natl Acad Sci U S A *86*, 7611-7615.

Grootendorst, J., Bour, A., Vogel, E., Kelche, C., Sullivan, P.M., Dodart, J.C., Bales, K., and Mathis, C. (2005). Human apoE targeted replacement mouse lines: h-apoE4 and h-apoE3 mice differ on spatial memory performance and avoidance behavior. Behav Brain Res *159*, 1-14.

Grunblatt, E., Hoyer, S., and Riederer, P. (2004). Gene expression profile in streptozotocin rat model for sporadic Alzheimer's disease. J Neural Transm *111*, 367-386.

Grunblatt, E., Salkovic-Petrisic, M., Osmanovic, J., Riederer, P., and Hoyer, S. (2007). Brain insulin system dysfunction in streptozotocin intracerebroventricularly treated rats generates hyperphosphorylated tau protein. J Neurochem *101*, 757-770.

Grundke-Iqbal, I., Iqbal, K., Tung, Y.C., Quinlan, M., Wisniewski, H.M., and Binder, L.I. (1986). Abnormal phosphorylation of the microtubule-associated protein tau (tau) in Alzheimer cytoskeletal pathology. Proc Natl Acad Sci U S A *83*, 4913-4917.

Guo, H., and Damuni, Z. (1993). Autophosphorylation-activated protein kinase phosphorylates and inactivates protein phosphatase 2A. Proc Natl Acad Sci U S A *90*, 2500-2504.

Gupta, A., Bisht, B., and Dey, C.S. (2011). Peripheral insulin-sensitizer drug metformin ameliorates neuronal insulin resistance and Alzheimer's-like changes. Neuropharmacology *60*, 910-920.

Gyure, K.A., Durham, R., Stewart, W.F., Smialek, J.E., and Troncoso, J.C. (2001). Intraneuronal abeta-amyloid precedes development of amyloid plaques in Down syndrome. Arch Pathol Lab Med *125*, 489-492.

Haag, M.D., Hofman, A., Koudstaal, P.J., Stricker, B.H., and Breteler, M.M. (2009). Statins are associated with a reduced risk of Alzheimer disease regardless of lipophilicity. The Rotterdam Study. J Neurol Neurosurg Psychiatry *80*, 13-17.

Haass, C., Hung, A.Y., Selkoe, D.J., and Teplow, D.B. (1994). Mutations associated with a locus for familial Alzheimer's disease result in alternative processing of amyloid beta-protein precursor. J Biol Chem *269*, 17741-17748.

Hallakou, S., Doare, L., Foufelle, F., Kergoat, M., Guerre-Millo, M., Berthault, M.F., Dugail, I., Morin, J., Auwerx, J., and Ferre, P. (1997). Pioglitazone induces in vivo adipocyte differentiation in the obese Zucker fa/fa rat. Diabetes *46*, 1393-1399.

Hama, E., Shirotani, K., Iwata, N., and Saido, T.C. (2004). Effects of neprilysin chimeric proteins targeted to subcellular compartments on amyloid beta peptide clearance in primary neurons. J Biol Chem *279*, 30259-30264.

Han, S.H., Einstein, G., Weisgraber, K.H., Strittmatter, W.J., Saunders, A.M., Pericak-Vance, M., Roses, A.D., and Schmechel, D.E. (1994). Apolipoprotein E is localized to the cytoplasm of human cortical neurons: a light and electron microscopic study. J Neuropathol Exp Neurol *53*, 535-544.

Hanger, D.P., and Noble, W. (2011). Functional implications of glycogen synthase kinase-3-mediated tau phosphorylation. Int J Alzheimers Dis *2011*, 352805.

Hanson, L.R., and Frey, W.H., 2nd (2008). Intranasal delivery bypasses the blood-brain barrier to target therapeutic agents to the central nervous system and treat neurodegenerative disease. BMC Neurosci *9 Suppl 3*, S5.

Hardy, J., and Allsop, D. (1991). Amyloid deposition as the central event in the aetiology of Alzheimer's disease. Trends Pharmacol Sci *12*, 383-388.

Hardy, J., and Selkoe, D.J. (2002). The amyloid hypothesis of Alzheimer's disease: progress and problems on the road to therapeutics. Science *297*, 353-356.

Harold, D., Abraham, R., Hollingworth, P., Sims, R., Gerrish, A., Hamshere, M.L., Pahwa, J.S., Moskvina, V., Dowzell, K., Williams, A.*, et al.* (2009). Genome-wide association

study identifies variants at CLU and PICALM associated with Alzheimer's disease. Nat Genet *41*, 1088-1093.

Harris, F.M., Brecht, W.J., Xu, Q., Mahley, R.W., and Huang, Y. (2004). Increased tau phosphorylation in apolipoprotein E4 transgenic mice is associated with activation of extracellular signal-regulated kinase: modulation by zinc. J Biol Chem *279*, 44795-44801.

Harris, F.M., Brecht, W.J., Xu, Q., Tesseur, I., Kekonius, L., Wyss-Coray, T., Fish, J.D., Masliah, E., Hopkins, P.C., Scearce-Levie, K*., et al.* (2003). Carboxyl-terminal-truncated apolipoprotein E4 causes Alzheimer's disease-like neurodegeneration and behavioral deficits in transgenic mice. Proc Natl Acad Sci U S A *100*, 10966-10971.

Harris, P.K., and Kletzien, R.F. (1994). Localization of a pioglitazone response element in the adipocyte fatty acid-binding protein gene. Mol Pharmacol *45*, 439-445.

Hartigan, J.A., and Johnson, G.V. (1999). Transient increases in intracellular calcium result in prolonged site-selective increases in Tau phosphorylation through a glycogen synthase kinase 3beta-dependent pathway. J Biol Chem *274*, 21395-21401.

Hashiguchi, M., Saito, T., Hisanaga, S., and Hashiguchi, T. (2002). Truncation of CDK5 activator p35 induces intensive phosphorylation of Ser202/Thr205 of human tau. J Biol Chem *277*, 44525-44530.

Hatters, D.M., Peters-Libeu, C.A., and Weisgraber, K.H. (2006). Apolipoprotein E structure: insights into function. Trends Biochem Sci *31*, 445-454.

Havrankova, J., Roth, J., and Brownstein, M. (1978). Insulin receptors are widely distributed in the central nervous system of the rat. Nature *272*, 827-829.

Hayashi, H., Campenot, R.B., Vance, D.E., and Vance, J.E. (2007). Apolipoprotein E-containing lipoproteins protect neurons from apoptosis via a signaling pathway involving low-density lipoprotein receptor-related protein-1. J Neurosci *27*, 1933-1941.

Hayashi, H., Campenot, R.B., Vance, D.E., and Vance, J.E. (2009). Protection of neurons from apoptosis by apolipoprotein E-containing lipoproteins does not require lipoprotein uptake and involves activation of phospholipase Cgamma1 and inhibition of calcineurin. J Biol Chem *284*, 29605-29613.

He, J., Vora, M., Haney, R.M., Filonov, G.S., Musselman, C.A., Burd, C.G., Kutateladze, A.G., Verkhusha, V.V., Stahelin, R.V., and Kutateladze, T.G. (2009). Membrane insertion of the FYVE domain is modulated by pH. Proteins *76*, 852-860.

He, W., Barak, Y., Hevener, A., Olson, P., Liao, D., Le, J., Nelson, M., Ong, E., Olefsky, J.M., and Evans, R.M. (2003). Adipose-specific peroxisome proliferator-activated receptor gamma knockout causes insulin resistance in fat and liver but not in muscle. Proc Natl Acad Sci U S A *100*, 15712-15717.

Heinrich, G., Ghosh, S., Deangelis, A.M., Schroeder-Gloeckler, J.M., Patel, P.R., Castaneda, T.R., Jeffers, S., Lee, A.D., Jung, D.Y., Zhang, Z*., et al.* (2010). Carcinoembryonic antigen-related cell adhesion molecule 2 controls energy balance and peripheral insulin action in mice. Gastroenterology *139*, 644-652, 652 e641.

Heitner, J., and Dickson, D. (1997). Diabetics do not have increased Alzheimer-type pathology compared with age-matched control subjects. A retrospective postmortem immunocytochemical and histofluorescent study. Neurology *49*, 1306-1311.

Heneka, M.T., Sastre, M., Dumitrescu-Ozimek, L., Hanke, A., Dewachter, I., Kuiperi, C., O'Banion, K., Klockgether, T., Van Leuven, F., and Landreth, G.E. (2005). Acute treatment with the PPARgamma agonist pioglitazone and ibuprofen reduces glial inflammation and Abeta1-42 levels in APPV717I transgenic mice. Brain *128*, 1442-1453.

Hernandez, P., Lee, G., Sjoberg, M., and Maccioni, R.B. (2009). Tau phosphorylation by cdk5 and Fyn in response to amyloid peptide Abeta (25-35): involvement of lipid rafts. J Alzheimers Dis *16*, 149-156.

Hernandez, R., Teruel, T., de Alvaro, C., and Lorenzo, M. (2004). Rosiglitazone ameliorates insulin resistance in brown adipocytes of Wistar rats by impairing TNF-alpha induction of p38 and p42/p44 mitogen-activated protein kinases. Diabetologia *47*, 1615-1624.

Himmler, A. (1989). Structure of the bovine tau gene: alternatively spliced transcripts generate a protein family. Mol Cell Biol *9*, 1389-1396.

Hirsch-Reinshagen, V., Maia, L.F., Burgess, B.L., Blain, J.F., Naus, K.E., McIsaac, S.A., Parkinson, P.F., Chan, J.Y., Tansley, G.H., Hayden, M.R*., et al.* (2005). The absence of ABCA1 decreases soluble ApoE levels but does not diminish amyloid deposition in two murine models of Alzheimer disease. J Biol Chem *280*, 43243-43256.

Ho, L., Qin, W., Pompl, P.N., Xiang, Z., Wang, J., Zhao, Z., Peng, Y., Cambareri, G., Rocher, A., Mobbs, C.V*., et al.* (2004). Diet-induced insulin resistance promotes amyloidosis in a transgenic mouse model of Alzheimer's disease. FASEB J *18*, 902-904.

Ho, R., Ortiz, D., and Shea, T.B. (2001). Amyloid-beta promotes calcium influx and neurodegeneration via stimulation of L voltage-sensitive calcium channels rather than NMDA channels in cultured neurons. J Alzheimers Dis *3*, 479-483.

Hoe, H.S., Freeman, J., and Rebeck, G.W. (2006). Apolipoprotein E decreases tau kinases and phospho-tau levels in primary neurons. Mol Neurodegener *1*, 18.

Hollingworth, P., Harold, D., Sims, R., Gerrish, A., Lambert, J.C., Carrasquillo, M.M., Abraham, R., Hamshere, M.L., Pahwa, J.S., Moskvina, V.*, et al.* (2011). Common variants at ABCA7, MS4A6A/MS4A4E, EPHA1, CD33 and CD2AP are associated with Alzheimer's disease. Nat Genet *43*, 429-435.

Holmes, C., Boche, D., Wilkinson, D., Yadegarfar, G., Hopkins, V., Bayer, A., Jones, R.W., Bullock, R., Love, S., Neal, J.W.*, et al.* (2008). Long-term effects of Abeta42 immunisation in Alzheimer's disease: follow-up of a randomised, placebo-controlled phase I trial. Lancet *372*, 216-223.

Holtzman, D.M., Bales, K.R., Tenkova, T., Fagan, A.M., Parsadanian, M., Sartorius, L.J., Mackey, B., Olney, J., McKeel, D., Wozniak, D.*, et al.* (2000a). Apolipoprotein E isoform-dependent amyloid deposition and neuritic degeneration in a mouse model of Alzheimer's disease. Proc Natl Acad Sci U S A *97*, 2892-2897.

Holtzman, D.M., Fagan, A.M., Mackey, B., Tenkova, T., Sartorius, L., Paul, S.M., Bales, K., Ashe, K.H., Irizarry, M.C., and Hyman, B.T. (2000b). Apolipoprotein E facilitates neuritic and cerebrovascular plaque formation in an Alzheimer's disease model. Ann Neurol *47*, 739-747.

Holtzman, D.M., Morris, J.C., and Goate, A.M. (2011). Alzheimer's disease: the challenge of the second century. Sci Transl Med *3*, 77sr71.

Holtzman, D.M., Pitas, R.E., Kilbridge, J., Nathan, B., Mahley, R.W., Bu, G., and Schwartz, A.L. (1995). Low density lipoprotein receptor-related protein mediates apolipoprotein E-dependent neurite outgrowth in a central nervous system-derived neuronal cell line. Proc Natl Acad Sci U S A *92*, 9480-9484.

Hong, M., Chen, D.C., Klein, P.S., and Lee, V.M. (1997). Lithium reduces tau phosphorylation by inhibition of glycogen synthase kinase-3. J Biol Chem *272*, 25326-25332.

Hong, M., and Lee, V.M. (1997). Insulin and insulin-like growth factor-1 regulate tau phosphorylation in cultured human neurons. J Biol Chem *272*, 19547-19553.

Horiuchi, K., Tajima, S., Menju, M., and Yamamoto, A. (1989). Structure and expression of mouse apolipoprotein E gene. J Biochem *106*, 98-103.

Horowitz, M.P., and Greenamyre, J.T. (2010). Mitochondrial iron metabolism and its role in neurodegeneration. J Alzheimers Dis *20 Suppl 2*, S551-568.

Hotamisligil, G.S., Shargill, N.S., and Spiegelman, B.M. (1993). Adipose expression of tumor necrosis factor-alpha: direct role in obesity-linked insulin resistance. Science *259*, 87-91.

Hoyer, S., Lee, S.K., Loffler, T., and Schliebs, R. (2000). Inhibition of the neuronal insulin receptor. An in vivo model for sporadic Alzheimer disease? Ann N Y Acad Sci *920*, 256-258.

Hsiao, K. (1998). Transgenic mice expressing Alzheimer amyloid precursor proteins. Exp Gerontol *33*, 883-889.

Hu, E., Kim, J.B., Sarraf, P., and Spiegelman, B.M. (1996a). Inhibition of adipogenesis through MAP kinase-mediated phosphorylation of PPARgamma. Science *274*, 2100-2103.

Hu, E., Liang, P., and Spiegelman, B.M. (1996b). AdipoQ is a novel adipose-specific gene dysregulated in obesity. J Biol Chem *271*, 10697-10703.

Hu, J., Ferreira, A., and Van Eldik, L.J. (1997). S100beta induces neuronal cell death through nitric oxide release from astrocytes. J Neurochem *69*, 2294-2301.

Huang, C.C., You, J.L., Lee, C.C., and Hsu, K.S. (2003). Insulin induces a novel form of postsynaptic mossy fiber long-term depression in the hippocampus. Mol Cell Neurosci *24*, 831-841.

Huang, D.Y., Weisgraber, K.H., Goedert, M., Saunders, A.M., Roses, A.D., and Strittmatter, W.J. (1995). ApoE3 binding to tau tandem repeat I is abolished by tau serine262 phosphorylation. Neurosci Lett *192*, 209-212.

Huang, S.M., Mouri, A., Kokubo, H., Nakajima, R., Suemoto, T., Higuchi, M., Staufenbiel, M., Noda, Y., Yamaguchi, H., Nabeshima, T.*, et al.* (2006). Neprilysin-sensitive synapse-associated amyloid-beta peptide oligomers impair neuronal plasticity and cognitive function. J Biol Chem *281*, 17941-17951.

Huang, Y., Liu, X.Q., Wyss-Coray, T., Brecht, W.J., Sanan, D.A., and Mahley, R.W. (2001). Apolipoprotein E fragments present in Alzheimer's disease brains induce neurofibrillary tangle-like intracellular inclusions in neurons. Proc Natl Acad Sci U S A *98*, 8838-8843.

Huber, G., Marz, W., Martin, J.R., Malherbe, P., Richards, J.G., Sueoka, N., Ohm, T., and Hoffmann, M.M. (2000). Characterization of transgenic mice expressing apolipoprotein E4(C112R) and apolipoprotein E4(L28P; C112R). Neuroscience *101*, 211-218.

Hughes, K., Nikolakaki, E., Plyte, S.E., Totty, N.F., and Woodgett, J.R. (1993). Modulation of the glycogen synthase kinase-3 family by tyrosine phosphorylation. EMBO J *12*, 803-808.

Hutton, M., Lendon, C.L., Rizzu, P., Baker, M., Froelich, S., Houlden, H., Pickering-Brown, S., Chakraverty, S., Isaacs, A., Grover, A.*, et al.* (1998). Association of missense and 5'-splice-site mutations in tau with the inherited dementia FTDP-17. Nature *393*, 702-705.

Hyman, B.T., Elvhage, T.E., and Reiter, J. (1994). Extracellular signal regulated kinases. Localization of protein and mRNA in the human hippocampal formation in Alzheimer's disease. Am J Pathol *144*, 565-572.

Ignatius, M.J., Shooter, E.M., Pitas, R.E., and Mahley, R.W. (1987). Lipoprotein uptake by neuronal growth cones in vitro. Science *236*, 959-962.

Inbar, D., Belinson, H., Rosenman, H., and Michaelson, D.M. (2010). Possible role of tau in mediating pathological effects of apoE4 in vivo prior to and following activation of the amyloid cascade. Neurodegener Dis *7*, 16-23.

Iqbal, K., and Grundke-Iqbal, I. (1991). Ubiquitination and abnormal phosphorylation of paired helical filaments in Alzheimer's disease. Mol Neurobiol *5*, 399-410.

Irie, F., Fitzpatrick, A.L., Lopez, O.L., Kuller, L.H., Peila, R., Newman, A.B., and Launer, L.J. (2008). Enhanced risk for Alzheimer disease in persons with type 2 diabetes and APOE epsilon4: the Cardiovascular Health Study Cognition Study. Arch Neurol *65*, 89-93.

Ito, E., Oka, K., Etcheberrigaray, R., Nelson, T.J., McPhie, D.L., Tofel-Grehl, B., Gibson, G.E., and Alkon, D.L. (1994). Internal Ca2+ mobilization is altered in fibroblasts from patients with Alzheimer disease. Proc Natl Acad Sci U S A *91*, 534-538.

Itoh, Y., Yamada, M., Suematsu, N., Matsushita, M., and Otomo, E. (1996). Influence of apolipoprotein E genotype on cerebral amyloid angiopathy in the elderly. Stroke *27*, 216-218.

Ittner, L.M., Ke, Y.D., Delerue, F., Bi, M., Gladbach, A., van Eersel, J., Wolfing, H., Chieng, B.C., Christie, M.J., Napier, I.A.*, et al.* (2010). Dendritic function of tau mediates amyloid-beta toxicity in Alzheimer's disease mouse models. Cell *142*, 387-397.

Iwata, N., Mizukami, H., Shirotani, K., Takaki, Y., Muramatsu, S., Lu, B., Gerard, N.P., Gerard, C., Ozawa, K., and Saido, T.C. (2004). Presynaptic localization of neprilysin contributes to efficient clearance of amyloid-beta peptide in mouse brain. J Neurosci *24*, 991-998.

Iwata, N., Tsubuki, S., Takaki, Y., Shirotani, K., Lu, B., Gerard, N.P., Gerard, C., Hama, E., Lee, H.J., and Saido, T.C. (2001). Metabolic regulation of brain Abeta by neprilysin. Science *292*, 1550-1552.

Iwata, N., Tsubuki, S., Takaki, Y., Watanabe, K., Sekiguchi, M., Hosoki, E., Kawashima-Morishima, M., Lee, H.J., Hama, E., Sekine-Aizawa, Y.*, et al.* (2000). Identification of the major Abeta1-42-degrading catabolic pathway in brain parenchyma: suppression leads to biochemical and pathological deposition. Nat Med *6*, 143-150.

Jackson, G.R., Wiedau-Pazos, M., Sang, T.K., Wagle, N., Brown, C.A., Massachi, S., and Geschwind, D.H. (2002). Human wild-type tau interacts with wingless pathway components and produces neurofibrillary pathology in Drosophila. Neuron *34*, 509-519.

Jain, R.S., and Quarfordt, S.H. (1979). The carbohydrate content of apolipoprotein E from human very low density lipoproteins. Life Sci *25*, 1315-1323.

Jansen, P.J., Lutjohann, D., Thelen, K.M., von Bergmann, K., van Leuven, F., Ramaekers, F.C., and Monique, M. (2009). Absence of ApoE upregulates murine brain ApoD and ABCA1 levels, but does not affect brain sterol levels, while human ApoE3 and human ApoE4 upregulate brain cholesterol precursor levels. J Alzheimers Dis *18*, 319-329.

Janson, J., Laedtke, T., Parisi, J.E., O'Brien, P., Petersen, R.C., and Butler, P.C. (2004). Increased risk of type 2 diabetes in Alzheimer disease. Diabetes *53*, 474-481.

Janssens, V., and Goris, J. (2001). Protein phosphatase 2A: a highly regulated family of serine/threonine phosphatases implicated in cell growth and signalling. Biochem J *353*, 417-439.

Janus, C., Pearson, J., McLaurin, J., Mathews, P.M., Jiang, Y., Schmidt, S.D., Chishti, M.A., Horne, P., Heslin, D., French, J.*, et al.* (2000). A beta peptide immunization reduces behavioural impairment and plaques in a model of Alzheimer's disease. Nature *408*, 979-982.

Jellinger, K.A. (2006). Alzheimer 100--highlights in the history of Alzheimer research. J Neural Transm *113*, 1603-1623.

Ji, H., Wang, H., Zhang, F., Li, X., Xiang, L., and Aiguo, S. (2010). PPARgamma agonist pioglitazone inhibits microglia inflammation by blocking p38 mitogen-activated protein kinase signaling pathways. Inflamm Res *59*, 921-929.

Ji, Y., Gong, Y., Gan, W., Beach, T., Holtzman, D.M., and Wisniewski, T. (2003). Apolipoprotein E isoform-specific regulation of dendritic spine morphology in apolipoprotein E transgenic mice and Alzheimer's disease patients. Neuroscience *122*, 305-315.

Ji, Z.S., Miranda, R.D., Newhouse, Y.M., Weisgraber, K.H., Huang, Y., and Mahley, R.W. (2002). Apolipoprotein E4 potentiates amyloid beta peptide-induced lysosomal leakage and apoptosis in neuronal cells. J Biol Chem *277*, 21821-21828.

Jiang, G., Dallas-Yang, Q., Biswas, S., Li, Z., and Zhang, B.B. (2004). Rosiglitazone, an agonist of peroxisome-proliferator-activated receptor gamma (PPARgamma), decreases inhibitory serine phosphorylation of IRS1 in vitro and in vivo. Biochem J *377*, 339-346.

Jiang, Q., Lee, C.Y., Mandrekar, S., Wilkinson, B., Cramer, P., Zelcer, N., Mann, K., Lamb, B., Willson, T.M., Collins, J.L.*, et al.* (2008). ApoE promotes the proteolytic degradation of Abeta. Neuron *58*, 681-693.

Jolivalt, C.G., Hurford, R., Lee, C.A., Dumaop, W., Rockenstein, E., and Masliah, E. (2010). Type 1 diabetes exaggerates features of Alzheimer's disease in APP transgenic mice. Exp Neurol *223*, 422-431.

Jolivalt, C.G., Lee, C.A., Beiswenger, K.K., Smith, J.L., Orlov, M., Torrance, M.A., and Masliah, E. (2008). Defective insulin signaling pathway and increased glycogen synthase kinase-3 activity in the brain of diabetic mice: parallels with Alzheimer's disease and correction by insulin. J Neurosci Res *86*, 3265-3274.

Julien, C., Tremblay, C., Phivilay, A., Berthiaume, L., Emond, V., Julien, P., and Calon, F. (2010). High-fat diet aggravates amyloid-beta and tau pathologies in the 3xTg-AD mouse model. Neurobiol Aging *31*, 1516-1531.

Kalaany, N.Y., Gauthier, K.C., Zavacki, A.M., Mammen, P.P., Kitazume, T., Peterson, J.A., Horton, J.D., Garry, D.J., Bianco, A.C., and Mangelsdorf, D.J. (2005). LXRs regulate the balance between fat storage and oxidation. Cell Metab *1*, 231-244.

Kallen, C.B., and Lazar, M.A. (1996). Antidiabetic thiazolidinediones inhibit leptin (ob) gene expression in 3T3-L1 adipocytes. Proc Natl Acad Sci U S A *93*, 5793-5796.

Kanemitsu, H., Tomiyama, T., and Mori, H. (2003). Human neprilysin is capable of degrading amyloid beta peptide not only in the monomeric form but also the pathological oligomeric form. Neurosci Lett *350*, 113-116.

Kang, J., Lemaire, H.G., Unterbeck, A., Salbaum, J.M., Masters, C.L., Grzeschik, K.H., Multhaup, G., Beyreuther, K., and Muller-Hill, B. (1987). The precursor of Alzheimer's disease amyloid A4 protein resembles a cell-surface receptor. Nature *325*, 733-736.

Kang, J., and Muller-Hill, B. (1990). Differential splicing of Alzheimer's disease amyloid A4 precursor RNA in rat tissues: PreA4(695) mRNA is predominantly produced in rat and human brain. Biochem Biophys Res Commun *166*, 1192-1200.

Kanoski, S.E., Zhang, Y., Zheng, W., and Davidson, T.L. (2010). The effects of a high-energy diet on hippocampal function and blood-brain barrier integrity in the rat. J Alzheimers Dis *21*, 207-219.

Kapural, M., Krizanac-Bengez, L., Barnett, G., Perl, J., Masaryk, T., Apollo, D., Rasmussen, P., Mayberg, M.R., and Janigro, D. (2002). Serum S-100beta as a possible marker of blood-brain barrier disruption. Brain Res *940*, 102-104.

Karagiannides, I., Abdou, R., Tzortzopoulou, A., Voshol, P.J., and Kypreos, K.E. (2008). Apolipoprotein E predisposes to obesity and related metabolic dysfunctions in mice. FEBS J *275*, 4796-4809.

Kaufman, L.N., Peterson, M.M., and DeGrange, L.M. (1995). Pioglitazone attenuates diet-induced hypertension in rats. Metabolism *44*, 1105-1109.

Kawarabayashi, T., Shoji, M., Younkin, L.H., Wen-Lang, L., Dickson, D.W., Murakami, T., Matsubara, E., Abe, K., Ashe, K.H., and Younkin, S.G. (2004). Dimeric amyloid beta protein rapidly accumulates in lipid rafts followed by apolipoprotein E and phosphorylated tau accumulation in the Tg2576 mouse model of Alzheimer's disease. J Neurosci *24*, 3801-3809.

Kawasaki, K., Ogiwara, N., Sugano, M., Okumura, N., and Yamauchi, K. (2009). Sialic acid moiety of apolipoprotein E and its impact on the formation of lipoprotein particles in human cerebrospinal fluid. Clin Chim Acta *402*, 61-66.

Ke, Y.D., Delerue, F., Gladbach, A., Gotz, J., and Ittner, L.M. (2009). Experimental diabetes mellitus exacerbates tau pathology in a transgenic mouse model of Alzheimer's disease. PLoS One *4*, e7917.

Kern, W., Peters, A., Fruehwald-Schultes, B., Deininger, E., Born, J., and Fehm, H.L. (2001). Improving influence of insulin on cognitive functions in humans. Neuroendocrinology *74*, 270-280.

Khachaturian, Z.S. (1989). Calcium, membranes, aging, and Alzheimer's disease. Introduction and overview. Ann N Y Acad Sci *568*, 1-4.

Kidd, M. (1963). Paired helical filaments in electron microscopy of Alzheimer's disease. Nature *197*, 192-193.

Kienlen-Campard, P., Miolet, S., Tasiaux, B., and Octave, J.N. (2002). Intracellular amyloid-beta 1-42, but not extracellular soluble amyloid-beta peptides, induces neuronal apoptosis. J Biol Chem *277*, 15666-15670.

Killick, R., Scales, G., Leroy, K., Causevic, M., Hooper, C., Irvine, E.E., Choudhury, A.I., Drinkwater, L., Kerr, F., Al-Qassab, H.*, et al.* (2009). Deletion of Irs2 reduces amyloid deposition and rescues behavioural deficits in APP transgenic mice. Biochem Biophys Res Commun *386*, 257-262.

Kim, B., Backus, C., Oh, S., Hayes, J.M., and Feldman, E.L. (2009a). Increased tau phosphorylation and cleavage in mouse models of type 1 and type 2 diabetes. Endocrinology *150*, 5294-5301.

Kim, H.S., Kim, E.M., Lee, J.P., Park, C.H., Kim, S., Seo, J.H., Chang, K.A., Yu, E., Jeong, S.J., Chong, Y.H.*, et al.* (2003). C-terminal fragments of amyloid precursor protein exert neurotoxicity by inducing glycogen synthase kinase-3beta expression. FASEB J *17*, 1951-1953.

Kim, K.Y., Baek, A., Hwang, J.E., Choi, Y.A., Jeong, J., Lee, M.S., Cho, D.H., Lim, J.S., Kim, K.I., and Yang, Y. (2009b). Adiponectin-activated AMPK stimulates dephosphorylation of AKT through protein phosphatase 2A activation. Cancer Res *69*, 4018-4026.

Kim, S.I., Yi, J.S., and Ko, Y.G. (2006). Amyloid beta oligomerization is induced by brain lipid rafts. J Cell Biochem *99*, 878-889.

Kim, W.S., Rahmanto, A.S., Kamili, A., Rye, K.A., Guillemin, G.J., Gelissen, I.C., Jessup, W., Hill, A.F., and Garner, B. (2007). Role of ABCG1 and ABCA1 in regulation of neuronal cholesterol efflux to apolipoprotein E discs and suppression of amyloid-beta peptide generation. J Biol Chem *282*, 2851-2861.

Kim, Y., Lee, Y.I., Seo, M., Kim, S.Y., Lee, J.E., Youn, H.D., Kim, Y.S., and Juhnn, Y.S. (2009c). Calcineurin dephosphorylates glycogen synthase kinase-3 beta at serine-9 in neuroblast-derived cells. J Neurochem *111*, 344-354.

Kimberly, W.T., LaVoie, M.J., Ostaszewski, B.L., Ye, W., Wolfe, M.S., and Selkoe, D.J. (2003). Gamma-secretase is a membrane protein complex comprised of presenilin, nicastrin, Aph-1, and Pen-2. Proc Natl Acad Sci U S A *100*, 6382-6387.

Kletzien, R.F., Clarke, S.D., and Ulrich, R.G. (1992). Enhancement of adipocyte differentiation by an insulin-sensitizing agent. Mol Pharmacol *41*, 393-398.

Kliewer, S.A., Umesono, K., Mangelsdorf, D.J., and Evans, R.M. (1992). Retinoid X receptor interacts with nuclear receptors in retinoic acid, thyroid hormone and vitamin D3 signalling. Nature *355*, 446-449.

Klyubin, I., Walsh, D.M., Lemere, C.A., Cullen, W.K., Shankar, G.M., Betts, V., Spooner, E.T., Jiang, L., Anwyl, R., Selkoe, D.J.*, et al.* (2005). Amyloid beta protein immunotherapy neutralizes Abeta oligomers that disrupt synaptic plasticity in vivo. Nat Med *11*, 556-561.

Knouff, C., Hinsdale, M.E., Mezdour, H., Altenburg, M.K., Watanabe, M., Quarfordt, S.H., Sullivan, P.M., and Maeda, N. (1999). Apo E structure determines VLDL clearance and atherosclerosis risk in mice. J Clin Invest *103*, 1579-1586.

Kobayashi, M., Ishiguro, K., Katoh-Fukui, Y., Yokoyama, M., and Fujita, S.C. (2003). Phosphorylation state of tau in the hippocampus of apolipoprotein E4 and E3 knock-in mice. Neuroreport *14*, 699-702.

Kohjima, M., Sun, Y., and Chan, L. (2010). Increased Food Intake Leads to Obesity and Insulin Resistance in the Tg2576 Alzheimer's Disease Mouse Model. Endocrinology.

Koistinaho, M., Lin, S., Wu, X., Esterman, M., Koger, D., Hanson, J., Higgs, R., Liu, F., Malkani, S., Bales, K.R.*, et al.* (2004). Apolipoprotein E promotes astrocyte colocalization and degradation of deposited amyloid-beta peptides. Nat Med *10*, 719-726.

Koldamova, R., Fitz, N.F., and Lefterov, I. (2010). The role of ATP-binding cassette transporter A1 in Alzheimer's disease and neurodegeneration. Biochim Biophys Acta *1801*, 824-830.

Koldamova, R., Staufenbiel, M., and Lefterov, I. (2005). Lack of ABCA1 considerably decreases brain ApoE level and increases amyloid deposition in APP23 mice. J Biol Chem *280*, 43224-43235.

Koldamova, R.P., Lefterov, I.M., Ikonomovic, M.D., Skoko, J., Lefterov, P.I., Isanski, B.A., DeKosky, S.T., and Lazo, J.S. (2003). 22R-hydroxycholesterol and 9-cis-retinoic acid induce ATP-binding cassette transporter A1 expression and cholesterol efflux in brain cells and decrease amyloid beta secretion. J Biol Chem *278*, 13244-13256.

Konstantinidou, V., Covas, M.I., Munoz-Aguayo, D., Khymenets, O., de la Torre, R., Saez, G., Tormos Mdel, C., Toledo, E., Marti, A., Ruiz-Gutierrez, V.*, et al.* (2010). In vivo nutrigenomic effects of virgin olive oil polyphenols within the frame of the Mediterranean diet: a randomized controlled trial. FASEB J *24*, 2546-2557.

Kopf, S.R., and Baratti, C.M. (1999). Effects of posttraining administration of insulin on retention of a habituation response in mice: participation of a central cholinergic mechanism. Neurobiol Learn Mem *71*, 50-61.

Kubota, N., Yano, W., Kubota, T., Yamauchi, T., Itoh, S., Kumagai, H., Kozono, H., Takamoto, I., Okamoto, S., Shiuchi, T.*, et al.* (2007). Adiponectin stimulates AMP-activated protein kinase in the hypothalamus and increases food intake. Cell Metab *6*, 55-68.

Kusminski, C.M., McTernan, P.G., Schraw, T., Kos, K., O'Hare, J.P., Ahima, R., Kumar, S., and Scherer, P.E. (2007). Adiponectin complexes in human cerebrospinal fluid: distinct complex distribution from serum. Diabetologia *50*, 634-642.

Kuusisto, J., Koivisto, K., Mykkanen, L., Helkala, E.L., Vanhanen, M., Hanninen, T., Kervinen, K., Kesaniemi, Y.A., Riekkinen, P.J., and Laakso, M. (1997). Association between features of the insulin resistance syndrome and Alzheimer's disease independently of apolipoprotein E4 phenotype: cross sectional population based study. BMJ *315*, 1045-1049.

Kyoung Pyo, H., Lovati, E., Pasinetti, G.M., and Ksiezak-Reding, H. (2004). Phosphorylation of tau at THR212 and SER214 in human neuronal and glial cultures: the role of AKT. Neuroscience *127*, 649-658.

LaDu, M.J., Falduto, M.T., Manelli, A.M., Reardon, C.A., Getz, G.S., and Frail, D.E. (1994). Isoform-specific binding of apolipoprotein E to beta-amyloid. J Biol Chem *269*, 23403-23406.

LaDu, M.J., Pederson, T.M., Frail, D.E., Reardon, C.A., Getz, G.S., and Falduto, M.T. (1995). Purification of apolipoprotein E attenuates isoform-specific binding to beta-amyloid. J Biol Chem *270*, 9039-9042.

LaFerla, F.M. (2002). Calcium dyshomeostasis and intracellular signalling in Alzheimer's disease. Nat Rev Neurosci *3*, 862-872.

LaFerla, F.M., Tinkle, B.T., Bieberich, C.J., Haudenschild, C.C., and Jay, G. (1995). The Alzheimer's A beta peptide induces neurodegeneration and apoptotic cell death in transgenic mice. Nat Genet *9*, 21-30.

Laffont, I., Takahashi, M., Shibukawa, Y., Honke, K., Shuvaev, V.V., Siest, G., Visvikis, S., and Taniguchi, N. (2002). Apolipoprotein E activates Akt pathway in neuro-2a in an isoform-specific manner. Biochem Biophys Res Commun *292*, 83-87.

Lambert, J.C., Heath, S., Even, G., Campion, D., Sleegers, K., Hiltunen, M., Combarros, O., Zelenika, D., Bullido, M.J., Tavernier, B.*, et al.* (2009). Genome-wide association study identifies variants at CLU and CR1 associated with Alzheimer's disease. Nat Genet *41*, 1094-1099.

Landen, M., Thorsell, A., Wallin, A., and Blennow, K. (1996). The apolipoprotein E allele epsilon 4 does not correlate with the number of senile plaques or neurofibrillary tangles in patients with Alzheimer's disease. J Neurol Neurosurg Psychiatry *61*, 352-356.

Lannert, H., and Hoyer, S. (1998). Intracerebroventricular administration of streptozotocin causes long-term diminutions in learning and memory abilities and in cerebral energy metabolism in adult rats. Behav Neurosci *112*, 1199-1208.

Larhammar, D., Ericsson, A., and Persson, H. (1987). Structure and expression of the rat neuropeptide Y gene. Proc Natl Acad Sci U S A *84*, 2068-2072.

Lebouvier, T., Scales, T.M., Hanger, D.P., Geahlen, R.L., Lardeux, B., Reynolds, C.H., Anderton, B.H., and Derkinderen, P. (2008). The microtubule-associated protein tau is phosphorylated by Syk. Biochim Biophys Acta *1783*, 188-192.

Lechward, K., Awotunde, O.S., Swiatek, W., and Muszynska, G. (2001). Protein phosphatase 2A: variety of forms and diversity of functions. Acta Biochim Pol *48*, 921-933.

Leduc, V., Jasmin-Belanger, S., and Poirier, J. (2010). APOE and cholesterol homeostasis in Alzheimer's disease. Trends Mol Med *16*, 469-477.

Lee, G. (2005). Tau and src family tyrosine kinases. Biochim Biophys Acta *1739*, 323-330.

Lee, G., Thangavel, R., Sharma, V.M., Litersky, J.M., Bhaskar, K., Fang, S.M., Do, L.H., Andreadis, A., Van Hoesen, G., and Ksiezak-Reding, H. (2004). Phosphorylation of tau by fyn: implications for Alzheimer's disease. J Neurosci *24*, 2304-2312.

Lee, H.K., Kumar, P., Fu, Q., Rosen, K.M., and Querfurth, H.W. (2009). The insulin/Akt signaling pathway is targeted by intracellular beta-amyloid. Mol Biol Cell *20*, 1533-1544.

Lee, J., and Stock, J. (1993). Protein phosphatase 2A catalytic subunit is methyl-esterified at its carboxyl terminus by a novel methyltransferase. J Biol Chem *268*, 19192-19195.

Lee, M.S., Kwon, Y.T., Li, M., Peng, J., Friedlander, R.M., and Tsai, L.H. (2000). Neurotoxicity induces cleavage of p35 to p25 by calpain. Nature *405*, 360-364.

Lefterov, I., Fitz, N.F., Cronican, A., Lefterov, P., Staufenbiel, M., and Koldamova, R. (2009). Memory deficits in APP23/Abca1+/- mice correlate with the level of Abeta oligomers. ASN Neuro *1*.

Lehmann, J.M., Moore, L.B., Smith-Oliver, T.A., Wilkison, W.O., Willson, T.M., and Kliewer, S.A. (1995). An antidiabetic thiazolidinedione is a high affinity ligand for peroxisome proliferator-activated receptor gamma (PPAR gamma). J Biol Chem *270*, 12953-12956.

Leibson, C.L., Rocca, W.A., Hanson, V.A., Cha, R., Kokmen, E., O'Brien, P.C., and Palumbo, P.J. (1997). Risk of dementia among persons with diabetes mellitus: a population-based cohort study. Am J Epidemiol *145*, 301-308.

Leissring, M.A., Farris, W., Chang, A.Y., Walsh, D.M., Wu, X., Sun, X., Frosch, M.P., and Selkoe, D.J. (2003). Enhanced proteolysis of beta-amyloid in APP transgenic mice prevents plaque formation, secondary pathology, and premature death. Neuron *40*, 1087-1093.

Leroy, K., Ando, K., Heraud, C., Yilmaz, Z., Authelet, M., Boeynaems, J.M., Buee, L., De Decker, R., and Brion, J.P. (2010). Lithium treatment arrests the development of neurofibrillary tangles in mutant tau transgenic mice with advanced neurofibrillary pathology. J Alzheimers Dis *19*, 705-719.

Lesne, S., Koh, M.T., Kotilinek, L., Kayed, R., Glabe, C.G., Yang, A., Gallagher, M., and Ashe, K.H. (2006). A specific amyloid-beta protein assembly in the brain impairs memory. Nature *440*, 352-357.

Lesne, S., Kotilinek, L., and Ashe, K.H. (2008). Plaque-bearing mice with reduced levels of oligomeric amyloid-beta assemblies have intact memory function. Neuroscience *151*, 745-749.

Lesort, M., and Johnson, G.V. (2000). Insulin-like growth factor-1 and insulin mediate transient site-selective increases in tau phosphorylation in primary cortical neurons. Neuroscience *99*, 305-316.

Lesort, M., Jope, R.S., and Johnson, G.V. (1999). Insulin transiently increases tau phosphorylation: involvement of glycogen synthase kinase-3beta and Fyn tyrosine kinase. J Neurochem *72*, 576-584.

Lester-Coll, N., Rivera, E.J., Soscia, S.J., Doiron, K., Wands, J.R., and de la Monte, S.M. (2006). Intracerebral streptozotocin model of type 3 diabetes: relevance to sporadic Alzheimer's disease. J Alzheimers Dis *9*, 13-33.

Lesuisse, C., Xu, G., Anderson, J., Wong, M., Jankowsky, J., Holtz, G., Gonzalez, V., Wong, P.C., Price, D.L., Tang, F.*, et al.* (2001). Hyper-expression of human apolipoprotein E4 in astroglia and neurons does not enhance amyloid deposition in transgenic mice. Hum Mol Genet *10*, 2525-2537.

Levin-Allerhand, J.A., Lominska, C.E., and Smith, J.D. (2002). Increased amyloid-levels in APPSWE transgenic mice treated chronically with a physiological high-fat high-cholesterol diet. J Nutr Health Aging *6*, 315-319.

Levy-Lahad, E., Wasco, W., Poorkaj, P., Romano, D.M., Oshima, J., Pettingell, W.H., Yu, C.E., Jondro, P.D., Schmidt, S.D., Wang, K.*, et al.* (1995). Candidate gene for the chromosome 1 familial Alzheimer's disease locus. Science *269*, 973-977.

Lew, J., Huang, Q.Q., Qi, Z., Winkfein, R.J., Aebersold, R., Hunt, T., and Wang, J.H. (1994). A brain-specific activator of cyclin-dependent kinase 5. Nature *371*, 423-426.

Lewis, J., Dickson, D.W., Lin, W.L., Chisholm, L., Corral, A., Jones, G., Yen, S.H., Sahara, N., Skipper, L., Yager, D.*, et al.* (2001). Enhanced neurofibrillary degeneration in transgenic mice expressing mutant tau and APP. Science *293*, 1487-1491.

Li, B.M., Mao, Z.M., Wang, M., and Mei, Z.T. (1999a). Alpha-2 adrenergic modulation of prefrontal cortical neuronal activity related to spatial working memory in monkeys. Neuropsychopharmacology *21*, 601-610.

Li, G., Higdon, R., Kukull, W.A., Peskind, E., Van Valen Moore, K., Tsuang, D., van Belle, G., McCormick, W., Bowen, J.D., Teri, L.*, et al.* (2004). Statin therapy and risk of dementia in the elderly: a community-based prospective cohort study. Neurology *63*, 1624-1628.

Li, Q.X., Maynard, C., Cappai, R., McLean, C.A., Cherny, R.A., Lynch, T., Culvenor, J.G., Trevaskis, J., Tanner, J.E., Bailey, K.A.*, et al.* (1999b). Intracellular accumulation of detergent-soluble amyloidogenic A beta fragment of Alzheimer's disease precursor protein in the hippocampus of aged transgenic mice. J Neurochem *72*, 2479-2487.

Li, T., Hawkes, C., Qureshi, H.Y., Kar, S., and Paudel, H.K. (2006). Cyclin-dependent protein kinase 5 primes microtubule-associated protein tau site-specifically for glycogen synthase kinase 3beta. Biochemistry *45*, 3134-3145.

Li, Y.M., Lai, M.T., Xu, M., Huang, Q., DiMuzio-Mower, J., Sardana, M.K., Shi, X.P., Yin, K.C., Shafer, J.A., and Gardell, S.J. (2000). Presenilin 1 is linked with gamma-secretase activity in the detergent solubilized state. Proc Natl Acad Sci U S A *97*, 6138-6143.

Li, Z.G., Zhang, W., and Sima, A.A. (2007). Alzheimer-like changes in rat models of spontaneous diabetes. Diabetes *56*, 1817-1824.

Liang, W.S., Dunckley, T., Beach, T.G., Grover, A., Mastroeni, D., Ramsey, K., Caselli, R.J., Kukull, W.A., McKeel, D., Morris, J.C*., et al.* (2008). Altered neuronal gene expression in brain regions differentially affected by Alzheimer's disease: a reference data set. Physiol Genomics *33*, 240-256.

Ling, Y., Morgan, K., and Kalsheker, N. (2003). Amyloid precursor protein (APP) and the biology of proteolytic processing: relevance to Alzheimer's disease. Int J Biochem Cell Biol *35*, 1505-1535.

Litersky, J.M., and Johnson, G.V. (1992). Phosphorylation by cAMP-dependent protein kinase inhibits the degradation of tau by calpain. J Biol Chem *267*, 1563-1568.

Litersky, J.M., Johnson, G.V., Jakes, R., Goedert, M., Lee, M., and Seubert, P. (1996). Tau protein is phosphorylated by cyclic AMP-dependent protein kinase and calcium/calmodulin-dependent protein kinase II within its microtubule-binding domains at Ser-262 and Ser-356. Biochem J *316 (Pt 2)*, 655-660.

Liu, F., Grundke-Iqbal, I., Iqbal, K., and Gong, C.X. (2005). Contributions of protein phosphatases PP1, PP2A, PP2B and PP5 to the regulation of tau phosphorylation. Eur J Neurosci *22*, 1942-1950.

Liu, F., Iqbal, K., Grundke-Iqbal, I., Hart, G.W., and Gong, C.X. (2004). O-GlcNAcylation regulates phosphorylation of tau: a mechanism involved in Alzheimer's disease. Proc Natl Acad Sci U S A *101*, 10804-10809.

Liu, F., Liang, Z., Shi, J., Yin, D., El-Akkad, E., Grundke-Iqbal, I., Iqbal, K., and Gong, C.X. (2006). PKA modulates GSK-3beta- and cdk5-catalyzed phosphorylation of tau in site- and kinase-specific manners. FEBS Lett *580*, 6269-6274.

Liu, F., Shi, J., Tanimukai, H., Gu, J., Grundke-Iqbal, I., Iqbal, K., and Gong, C.X. (2009a). Reduced O-GlcNAcylation links lower brain glucose metabolism and tau pathology in Alzheimer's disease. Brain *132*, 1820-1832.

Liu, L., Brown, J.C., 3rd, Webster, W.W., Morrisett, R.A., and Monaghan, D.T. (1995). Insulin potentiates N-methyl-D-aspartate receptor activity in Xenopus oocytes and rat hippocampus. Neurosci Lett *192*, 5-8.

Liu, Q., Zerbinatti, C.V., Zhang, J., Hoe, H.S., Wang, B., Cole, S.L., Herz, J., Muglia, L., and Bu, G. (2007). Amyloid precursor protein regulates brain apolipoprotein E and cholesterol metabolism through lipoprotein receptor LRP1. Neuron *56*, 66-78.

Liu, Y., Liu, F., Grundke-Iqbal, I., Iqbal, K., and Gong, C.X. (2009b). Brain glucose transporters, O-GlcNAcylation and phosphorylation of tau in diabetes and Alzheimer's disease. J Neurochem *111*, 242-249.

Liu, Y., Liu, F., Grundke-Iqbal, I., Iqbal, K., and Gong, C.X. (2011). Deficient brain insulin signalling pathway in Alzheimer's disease and diabetes. J Pathol *225*, 54-62.

Liu, Y., Liu, F., Iqbal, K., Grundke-Iqbal, I., and Gong, C.X. (2008). Decreased glucose transporters correlate to abnormal hyperphosphorylation of tau in Alzheimer disease. FEBS Lett *582*, 359-364.

Lizcano, J.M., and Alessi, D.R. (2002). The insulin signalling pathway. Curr Biol *12*, R236-238.

Ljungberg, M.C., Dayanandan, R., Asuni, A., Rupniak, T.H., Anderton, B.H., and Lovestone, S. (2002). Truncated apoE forms tangle-like structures in a neuronal cell line. Neuroreport *13*, 867-870.

Lord, A., Kalimo, H., Eckman, C., Zhang, X.Q., Lannfelt, L., and Nilsson, L.N. (2006). The Arctic Alzheimer mutation facilitates early intraneuronal Abeta aggregation and senile plaque formation in transgenic mice. Neurobiol Aging *27*, 67-77.

Lovell, M.A., Xie, C., and Markesbery, W.R. (2001). Acrolein is increased in Alzheimer's disease brain and is toxic to primary hippocampal cultures. Neurobiol Aging *22*, 187-194.

Lovestone, S., Davis, D.R., Webster, M.T., Kaech, S., Brion, J.P., Matus, A., and Anderton, B.H. (1999). Lithium reduces tau phosphorylation: effects in living cells and in neurons at therapeutic concentrations. Biol Psychiatry *45*, 995-1003.

Lowell, B.B., and Shulman, G.I. (2005). Mitochondrial dysfunction and type 2 diabetes. Science *307*, 384-387.

Lu, M., Sarruf, D.A., Talukdar, S., Sharma, S., Li, P., Bandyopadhyay, G., Nalbandian, S., Fan, W., Gayen, J.R., Mahata, S.K*., et al.* (2011). Brain PPAR-gamma promotes obesity and is required for the insulin-sensitizing effect of thiazolidinediones. Nat Med *17*, 618-622.

Lucas, J.J., Hernandez, F., Gomez-Ramos, P., Moran, M.A., Hen, R., and Avila, J. (2001). Decreased nuclear beta-catenin, tau hyperphosphorylation and neurodegeneration in GSK-3beta conditional transgenic mice. EMBO J *20*, 27-39.

Luchsinger, J.A., Tang, M.X., Shea, S., and Mayeux, R. (2004). Hyperinsulinemia and risk of Alzheimer disease. Neurology *63*, 1187-1192.

Luchsinger, J.A., Tang, M.X., Stern, Y., Shea, S., and Mayeux, R. (2001). Diabetes mellitus and risk of Alzheimer's disease and dementia with stroke in a multiethnic cohort. Am J Epidemiol *154*, 635-641.

Luciani, M.F., Denizot, F., Savary, S., Mattei, M.G., and Chimini, G. (1994). Cloning of two novel ABC transporters mapping on human chromosome 9. Genomics *21*, 150-159.

Luconi, M., Cantini, G., and Serio, M. (2010). Peroxisome proliferator-activated receptor gamma (PPARgamma): Is the genomic activity the only answer? Steroids *75*, 585-594.

Luo, D., Hou, X., Hou, L., Wang, M., Xu, S., Dong, C., and Liu, X. (2011). Effect of pioglitazone on altered expression of Abeta metabolism-associated molecules in the brain of fructose-drinking rats, a rodent model of insulin resistance. Eur J Pharmacol.

Luo, X.H., Guo, L.J., Yuan, L.Q., Xie, H., Zhou, H.D., Wu, X.P., and Liao, E.Y. (2005). Adiponectin stimulates human osteoblasts proliferation and differentiation via the MAPK signaling pathway. Exp Cell Res *309*, 99-109.

Lutjohann, D., Breuer, O., Ahlborg, G., Nennesmo, I., Siden, A., Diczfalusy, U., and Bjorkhem, I. (1996). Cholesterol homeostasis in human brain: evidence for an age-dependent flux of 24S-hydroxycholesterol from the brain into the circulation. Proc Natl Acad Sci U S A *93*, 9799-9804.

Ma, J., Yee, A., Brewer, H.B., Jr., Das, S., and Potter, H. (1994). Amyloid-associated proteins alpha 1-antichymotrypsin and apolipoprotein E promote assembly of Alzheimer beta-protein into filaments. Nature *372*, 92-94.

Maccioni, R.B., Otth, C., Concha, II, and Munoz, J.P. (2001). The protein kinase Cdk5. Structural aspects, roles in neurogenesis and involvement in Alzheimer's pathology. Eur J Biochem *268*, 1518-1527.

MacKnight, C., Rockwood, K., Awalt, E., and McDowell, I. (2002). Diabetes mellitus and the risk of dementia, Alzheimer's disease and vascular cognitive impairment in the Canadian Study of Health and Aging. Dement Geriatr Cogn Disord *14*, 77-83.

Mahley, R.W. (1988). Apolipoprotein E: cholesterol transport protein with expanding role in cell biology. Science *240*, 622-630.

Man, H.Y., Lin, J.W., Ju, W.H., Ahmadian, G., Liu, L., Becker, L.E., Sheng, M., and Wang, Y.T. (2000). Regulation of AMPA receptor-mediated synaptic transmission by clathrin-dependent receptor internalization. Neuron *25*, 649-662.

Mandelkow, E.M., Biernat, J., Drewes, G., Steiner, B., Lichtenberg-Kraag, B., Wille, H., Gustke, N., and Mandelkow, E. (1993). Microtubule-associated protein tau, paired helical filaments, and phosphorylation. Ann N Y Acad Sci *695*, 209-216.

Mandelkow, E.M., Drewes, G., Biernat, J., Gustke, N., Van Lint, J., Vandenheede, J.R., and Mandelkow, E. (1992). Glycogen synthase kinase-3 and the Alzheimer-like state of microtubule-associated protein tau. FEBS Lett *314*, 315-321.

Manelli, A.M., Bulfinch, L.C., Sullivan, P.M., and LaDu, M.J. (2007). Abeta42 neurotoxicity in primary co-cultures: effect of apoE isoform and Abeta conformation. Neurobiol Aging *28*, 1139-1147.

Manelli, A.M., Stine, W.B., Van Eldik, L.J., and LaDu, M.J. (2004). ApoE and Abeta1-42 interactions: effects of isoform and conformation on structure and function. J Mol Neurosci *23*, 235-246.

Mantyh, P.W., Ghilardi, J.R., Rogers, S., DeMaster, E., Allen, C.J., Stimson, E.R., and Maggio, J.E. (1993). Aluminum, iron, and zinc ions promote aggregation of physiological concentrations of beta-amyloid peptide. J Neurochem *61*, 1171-1174.

Marks, J.L., Porte, D., Jr., Stahl, W.L., and Baskin, D.G. (1990). Localization of insulin receptor mRNA in rat brain by in situ hybridization. Endocrinology *127*, 3234-3236.

Marr, R.A., Rockenstein, E., Mukherjee, A., Kindy, M.S., Hersh, L.B., Gage, F.H., Verma, I.M., and Masliah, E. (2003). Neprilysin gene transfer reduces human amyloid pathology in transgenic mice. J Neurosci *23*, 1992-1996.

Martin, L., Latypova, X., and Terro, F. (2011). Post-translational modifications of tau protein: implications for Alzheimer's disease. Neurochem Int *58*, 458-471.

Masliah, E., Mallory, M., Ge, N., Alford, M., Veinbergs, I., and Roses, A.D. (1995). Neurodegeneration in the central nervous system of apoE-deficient mice. Exp Neurol *136*, 107-122.

Masliah, E., Samuel, W., Veinbergs, I., Mallory, M., Mante, M., and Saitoh, T. (1997). Neurodegeneration and cognitive impairment in apoE-deficient mice is ameliorated by infusion of recombinant apoE. Brain Res *751*, 307-314.

Masters, C.L., Simms, G., Weinman, N.A., Multhaup, G., McDonald, B.L., and Beyreuther, K. (1985). Amyloid plaque core protein in Alzheimer disease and Down syndrome. Proc Natl Acad Sci U S A *82*, 4245-4249.

Mastick, C.C., and Falick, A.L. (1997). Association of N-ethylmaleimide sensitive fusion (NSF) protein and soluble NSF attachment proteins-alpha and -gamma with glucose transporter-4-containing vesicles in primary rat adipocytes. Endocrinology *138*, 2391-2397.

Matthews, D.R., Hosker, J.P., Rudenski, A.S., Naylor, B.A., Treacher, D.F., and Turner, R.C. (1985). Homeostasis model assessment: insulin resistance and beta-cell function from fasting plasma glucose and insulin concentrations in man. Diabetologia *28*, 412-419.

Mattson, M.P., Barger, S.W., Cheng, B., Lieberburg, I., Smith-Swintosky, V.L., and Rydel, R.E. (1993). beta-Amyloid precursor protein metabolites and loss of neuronal Ca2+ homeostasis in Alzheimer's disease. Trends Neurosci *16*, 409-414.

Mauch, D.H., Nagler, K., Schumacher, S., Goritz, C., Muller, E.C., Otto, A., and Pfrieger, F.W. (2001). CNS synaptogenesis promoted by glia-derived cholesterol. Science *294*, 1354-1357.

McKee, A.C., Kosik, K.S., Kennedy, M.B., and Kowall, N.W. (1990). Hippocampal neurons predisposed to neurofibrillary tangle formation are enriched in type II calcium/calmodulin-dependent protein kinase. J Neuropathol Exp Neurol *49*, 49-63.

Meir, K.S., and Leitersdorf, E. (2004). Atherosclerosis in the apolipoprotein-E-deficient mouse: a decade of progress. Arterioscler Thromb Vasc Biol *24*, 1006-1014.

Menendez-Gonzalez, M., Perez-Pinera, P., Martinez-Rivera, M., Calatayud, M.T., and Blazquez Menes, B. (2005). APP processing and the APP-KPI domain involvement in the amyloid cascade. Neurodegener Dis *2*, 277-283.

Mentlein, R., Ludwig, R., and Martensen, I. (1998). Proteolytic degradation of Alzheimer's disease amyloid beta-peptide by a metalloproteinase from microglia cells. J Neurochem *70*, 721-726.

Mi, K., Dolan, P.J., and Johnson, G.V. (2006). The low density lipoprotein receptor-related protein 6 interacts with glycogen synthase kinase 3 and attenuates activity. J Biol Chem *281*, 4787-4794.

Michikawa, M., Fan, Q.W., Isobe, I., and Yanagisawa, K. (2000). Apolipoprotein E exhibits isoform-specific promotion of lipid efflux from astrocytes and neurons in culture. J Neurochem *74*, 1008-1016.

Michikawa, M., and Yanagisawa, K. (1998). Apolipoprotein E4 induces neuronal cell death under conditions of suppressed de novo cholesterol synthesis. J Neurosci Res *54*, 58-67.

Miglio, G., Rosa, A.C., Rattazzi, L., Collino, M., Lombardi, G., and Fantozzi, R. (2009). PPARgamma stimulation promotes mitochondrial biogenesis and prevents glucose deprivation-induced neuronal cell loss. Neurochem Int *55*, 496-504.

Miller, B.C., Eckman, E.A., Sambamurti, K., Dobbs, N., Chow, K.M., Eckman, C.B., Hersh, L.B., and Thiele, D.L. (2003). Amyloid-beta peptide levels in brain are inversely correlated with insulysin activity levels in vivo. Proc Natl Acad Sci U S A *100*, 6221-6226.

Minagawa, H., Gong, J.S., Jung, C.G., Watanabe, A., Lund-Katz, S., Phillips, M.C., Saito, H., and Michikawa, M. (2009). Mechanism underlying apolipoprotein E (ApoE) isoform-dependent lipid efflux from neural cells in culture. J Neurosci Res *87*, 2498-2508.

Miyazaki, Y., Mahankali, A., Wajcberg, E., Bajaj, M., Mandarino, L.J., and DeFronzo, R.A. (2004). Effect of pioglitazone on circulating adipocytokine levels and insulin sensitivity in type 2 diabetic patients. J Clin Endocrinol Metab *89*, 4312-4319.

Morgan, D., Diamond, D.M., Gottschall, P.E., Ugen, K.E., Dickey, C., Hardy, J., Duff, K., Jantzen, P., DiCarlo, G., Wilcock, D.*, et al.* (2000). A beta peptide vaccination prevents memory loss in an animal model of Alzheimer's disease. Nature *408*, 982-985.

Mori, C., Spooner, E.T., Wisniewsk, K.E., Wisniewski, T.M., Yamaguch, H., Saido, T.C., Tolan, D.R., Selkoe, D.J., and Lemere, C.A. (2002). Intraneuronal Abeta42 accumulation in Down syndrome brain. Amyloid *9*, 88-102.

Mori, Y., Murakawa, Y., Okada, K., Horikoshi, H., Yokoyama, J., Tajima, N., and Ikeda, Y. (1999). Effect of troglitazone on body fat distribution in type 2 diabetic patients. Diabetes Care *22*, 908-912.

Moroz, N., Tong, M., Longato, L., Xu, H., and de la Monte, S.M. (2008). Limited Alzheimer-type neurodegeneration in experimental obesity and type 2 diabetes mellitus. J Alzheimers Dis *15*, 29-44.

Morris, C.M., Benjamin, R., Leake, A., McArthur, F.K., Candy, J.M., Ince, P.G., Torvik, A., Bjertness, E., and Edwardson, J.A. (1995). Effect of apolipoprotein E genotype on Alzheimer's disease neuropathology in a cohort of elderly Norwegians. Neurosci Lett *201*, 45-47.

Mrak, R.E., Sheng, J.G., and Griffin, W.S. (1996). Correlation of astrocytic S100 beta expression with dystrophic neurites in amyloid plaques of Alzheimer's disease. J Neuropathol Exp Neurol *55*, 273-279.

Mukai, F., Ishiguro, K., Sano, Y., and Fujita, S.C. (2002). Alternative splicing isoform of tau protein kinase I/glycogen synthase kinase 3beta. J Neurochem *81*, 1073-1083.

Mulder, M., Blokland, A., van den Berg, D.J., Schulten, H., Bakker, A.H., Terwel, D., Honig, W., de Kloet, E.R., Havekes, L.M., Steinbusch, H.W.*, et al.* (2001). Apolipoprotein E protects against neuropathology induced by a high-fat diet and maintains the integrity of the blood-brain barrier during aging. Lab Invest *81*, 953-960.

Nagele, R.G., D'Andrea, M.R., Anderson, W.J., and Wang, H.Y. (2002). Intracellular accumulation of beta-amyloid(1-42) in neurons is facilitated by the alpha 7 nicotinic acetylcholine receptor in Alzheimer's disease. Neuroscience *110*, 199-211.

Nagy, Z., Esiri, M.M., Jobst, K.A., Johnston, C., Litchfield, S., Sim, E., and Smith, A.D. (1995). Influence of the apolipoprotein E genotype on amyloid deposition and neurofibrillary tangle formation in Alzheimer's disease. Neuroscience *69*, 757-761.

Nakamura, T., Watanabe, A., Fujino, T., Hosono, T., and Michikawa, M. (2009). Apolipoprotein E4 (1-272) fragment is associated with mitochondrial proteins and affects mitochondrial function in neuronal cells. Mol Neurodegener *4*, 35.

Namba, Y., Tomonaga, M., Kawasaki, H., Otomo, E., and Ikeda, K. (1991). Apolipoprotein E immunoreactivity in cerebral amyloid deposits and neurofibrillary tangles in Alzheimer's disease and kuru plaque amyloid in Creutzfeldt-Jakob disease. Brain Res *541*, 163-166.

Narita, M., Bu, G., Holtzman, D.M., and Schwartz, A.L. (1997). The low-density lipoprotein receptor-related protein, a multifunctional apolipoprotein E receptor, modulates hippocampal neurite development. J Neurochem *68*, 587-595.

Nathan, B.P., Bellosta, S., Sanan, D.A., Weisgraber, K.H., Mahley, R.W., and Pitas, R.E. (1994). Differential effects of apolipoproteins E3 and E4 on neuronal growth in vitro. Science *264*, 850-852.

Nathan, B.P., Chang, K.C., Bellosta, S., Brisch, E., Ge, N., Mahley, R.W., and Pitas, R.E. (1995). The inhibitory effect of apolipoprotein E4 on neurite outgrowth is associated with microtubule depolymerization. J Biol Chem *270*, 19791-19799.

Nathan, B.P., Jiang, Y., Wong, G.K., Shen, F., Brewer, G.J., and Struble, R.G. (2002). Apolipoprotein E4 inhibits, and apolipoprotein E3 promotes neurite outgrowth in cultured adult mouse cortical neurons through the low-density lipoprotein receptor-related protein. Brain Res *928*, 96-105.

Naveilhan, P., Hassani, H., Canals, J.M., Ekstrand, A.J., Larefalk, A., Chhajlani, V., Arenas, E., Gedda, K., Svensson, L., Thoren, P.*, et al.* (1999). Normal feeding behavior, body weight and leptin response require the neuropeptide Y Y2 receptor. Nat Med *5*, 1188-1193.

Nawrocki, A.R., Rajala, M.W., Tomas, E., Pajvani, U.B., Saha, A.K., Trumbauer, M.E., Pang, Z., Chen, A.S., Ruderman, N.B., Chen, H.*, et al.* (2006). Mice lacking adiponectin show decreased hepatic insulin sensitivity and reduced responsiveness to peroxisome proliferator-activated receptor gamma agonists. J Biol Chem *281*, 2654-2660.

Ng, S.S., Mahmoudi, T., Danenberg, E., Bejaoui, I., de Lau, W., Korswagen, H.C., Schutte, M., and Clevers, H. (2009). Phosphatidylinositol 3-kinase signaling does not activate the wnt cascade. J Biol Chem *284*, 35308-35313.

Nicholson, A.M., and Ferreira, A. (2009). Increased membrane cholesterol might render mature hippocampal neurons more susceptible to beta-amyloid-induced calpain activation and tau toxicity. J Neurosci *29*, 4640-4651.

Nikolaev, A., McLaughlin, T., O'Leary, D.D., and Tessier-Lavigne, M. (2009). APP binds DR6 to trigger axon pruning and neuron death via distinct caspases. Nature *457*, 981-989.

Nilsberth, C., Westlind-Danielsson, A., Eckman, C.B., Condron, M.M., Axelman, K., Forsell, C., Stenh, C., Luthman, J., Teplow, D.B., Younkin, S.G.*, et al.* (2001). The 'Arctic' APP mutation (E693G) causes Alzheimer's disease by enhanced Abeta protofibril formation. Nat Neurosci *4*, 887-893.

Nimmrich, V., Grimm, C., Draguhn, A., Barghorn, S., Lehmann, A., Schoemaker, H., Hillen, H., Gross, G., Ebert, U., and Bruehl, C. (2008). Amyloid beta oligomers (A beta(1-42) globulomer) suppress spontaneous synaptic activity by inhibition of P/Q-type calcium currents. J Neurosci *28*, 788-797.

Nishimura, I., Yang, Y., and Lu, B. (2004). PAR-1 kinase plays an initiator role in a temporally ordered phosphorylation process that confers tau toxicity in Drosophila. Cell *116*, 671-682.

Noble, W., Olm, V., Takata, K., Casey, E., Mary, O., Meyerson, J., Gaynor, K., LaFrancois, J., Wang, L., Kondo, T.*, et al.* (2003). Cdk5 is a key factor in tau aggregation and tangle formation in vivo. Neuron *38*, 555-565.

Noble, W., Planel, E., Zehr, C., Olm, V., Meyerson, J., Suleman, F., Gaynor, K., Wang, L., LaFrancois, J., Feinstein, B.*, et al.* (2005). Inhibition of glycogen synthase kinase-3 by lithium

correlates with reduced tauopathy and degeneration in vivo. Proc Natl Acad Sci U S A *102*, 6990-6995.

Nolan, J.J., Ludvik, B., Beerdsen, P., Joyce, M., and Olefsky, J. (1994). Improvement in glucose tolerance and insulin resistance in obese subjects treated with troglitazone. N Engl J Med *331*, 1188-1193.

O'Brien, R.J., and Wong, P.C. (2011). Amyloid precursor protein processing and Alzheimer's disease. Annu Rev Neurosci *34*, 185-204.

Oakley, H., Cole, S.L., Logan, S., Maus, E., Shao, P., Craft, J., Guillozet-Bongaarts, A., Ohno, M., Disterhoft, J., Van Eldik, L.*, et al.* (2006). Intraneuronal beta-amyloid aggregates, neurodegeneration, and neuron loss in transgenic mice with five familial Alzheimer's disease mutations: potential factors in amyloid plaque formation. J Neurosci *26*, 10129-10140.

Oddo, S., Billings, L., Kesslak, J.P., Cribbs, D.H., and LaFerla, F.M. (2004). Abeta immunotherapy leads to clearance of early, but not late, hyperphosphorylated tau aggregates via the proteasome. Neuron *43*, 321-332.

Oddo, S., Caccamo, A., Shepherd, J.D., Murphy, M.P., Golde, T.E., Kayed, R., Metherate, R., Mattson, M.P., Akbari, Y., and LaFerla, F.M. (2003). Triple-transgenic model of Alzheimer's disease with plaques and tangles: intracellular Abeta and synaptic dysfunction. Neuron *39*, 409-421.

Oddo, S., Caccamo, A., Smith, I.F., Green, K.N., and LaFerla, F.M. (2006a). A dynamic relationship between intracellular and extracellular pools of Abeta. Am J Pathol *168*, 184-194.

Oddo, S., Caccamo, A., Tran, L., Lambert, M.P., Glabe, C.G., Klein, W.L., and LaFerla, F.M. (2006b). Temporal profile of amyloid-beta (Abeta) oligomerization in an in vivo model of Alzheimer disease. A link between Abeta and tau pathology. J Biol Chem *281*, 1599-1604.

Ohm, T.G., Kirca, M., Bohl, J., Scharnagl, H., Gross, W., and Marz, W. (1995). Apolipoprotein E polymorphism influences not only cerebral senile plaque load but also Alzheimer-type neurofibrillary tangle formation. Neuroscience *66*, 583-587.

Ohm, T.G., Treiber-Held, S., Distl, R., Glockner, F., Schonheit, B., Tamanai, M., and Meske, V. (2003). Cholesterol and tau protein--findings in Alzheimer's and Niemann Pick C's disease. Pharmacopsychiatry *36 Suppl 2*, S120-126.

Ohsawa, I., Takamura, C., Morimoto, T., Ishiguro, M., and Kohsaka, S. (1999). Amino-terminal region of secreted form of amyloid precursor protein stimulates proliferation of neural stem cells. Eur J Neurosci *11*, 1907-1913.

Ohyagi, Y., Asahara, H., Chui, D.H., Tsuruta, Y., Sakae, N., Miyoshi, K., Yamada, T., Kikuchi, H., Taniwaki, T., Murai, H.*, et al.* (2005). Intracellular Abeta42 activates p53 promoter: a pathway to neurodegeneration in Alzheimer's disease. FASEB J *19*, 255-257.

Okuno, A., Tamemoto, H., Tobe, K., Ueki, K., Mori, Y., Iwamoto, K., Umesono, K., Akanuma, Y., Fujiwara, T., Horikoshi, H.*, et al.* (1998). Troglitazone increases the number of small adipocytes without the change of white adipose tissue mass in obese Zucker rats. J Clin Invest *101*, 1354-1361.

Olaisen, B., Teisberg, P., and Gedde-Dahl, T., Jr. (1982). The locus for apolipoprotein E (apoE) is linked to the complement component C3 (C3) locus on chromosome 19 in man. Hum Genet *62*, 233-236.

Olichney, J.M., Hansen, L.A., Galasko, D., Saitoh, T., Hofstetter, C.R., Katzman, R., and Thal, L.J. (1996). The apolipoprotein E epsilon 4 allele is associated with increased neuritic plaques and cerebral amyloid angiopathy in Alzheimer's disease and Lewy body variant. Neurology *47*, 190-196.

Ono, K., Condron, M.M., and Teplow, D.B. (2009). Structure-neurotoxicity relationships of amyloid beta-protein oligomers. Proc Natl Acad Sci U S A *106*, 14745-14750.

Ott, A., Stolk, R.P., van Harskamp, F., Pols, H.A., Hofman, A., and Breteler, M.M. (1999). Diabetes mellitus and the risk of dementia: The Rotterdam Study. Neurology *53*, 1937-1942.

Oyama, F., Shimada, H., Oyama, R., and Ihara, Y. (1995). Apolipoprotein E genotype, Alzheimer's pathologies and related gene expression in the aged population. Brain Res Mol Brain Res *29*, 92-98.

Paik, Y.K., Chang, D.J., Reardon, C.A., Davies, G.E., Mahley, R.W., and Taylor, J.M. (1985). Nucleotide sequence and structure of the human apolipoprotein E gene. Proc Natl Acad Sci U S A *82*, 3445-3449.

Pajvani, U.B., Hawkins, M., Combs, T.P., Rajala, M.W., Doebber, T., Berger, J.P., Wagner, J.A., Wu, M., Knopps, A., Xiang, A.H.*, et al.* (2004). Complex distribution, not absolute amount of adiponectin, correlates with thiazolidinedione-mediated improvement in insulin sensitivity. J Biol Chem *279*, 12152-12162.

Pancani, T., Phelps, J.T., Searcy, J.L., Kilgore, M.W., Chen, K.C., Porter, N.M., and Thibault, O. (2009). Distinct modulation of voltage-gated and ligand-gated Ca2+ currents by PPAR-gamma agonists in cultured hippocampal neurons. J Neurochem *109*, 1800-1811.

Pardossi-Piquard, R., Petit, A., Kawarai, T., Sunyach, C., Alves da Costa, C., Vincent, B., Ring, S., D'Adamio, L., Shen, J., Muller, U.*, et al.* (2005). Presenilin-dependent transcriptional control of the Abeta-degrading enzyme neprilysin by intracellular domains of betaAPP and APLP. Neuron *46*, 541-554.

Park, C.R. (2001). Cognitive effects of insulin in the central nervous system. Neurosci Biobehav Rev *25*, 311-323.

Park, C.R., Seeley, R.J., Craft, S., and Woods, S.C. (2000). Intracerebroventricular insulin enhances memory in a passive-avoidance task. Physiol Behav *68*, 509-514.

Patel, J., Anderson, R.J., and Rappaport, E.B. (1999). Rosiglitazone monotherapy improves glycaemic control in patients with type 2 diabetes: a twelve-week, randomized, placebo-controlled study. Diabetes Obes Metab *1*, 165-172.

Pedersen, W.A., McMillan, P.J., Kulstad, J.J., Leverenz, J.B., Craft, S., and Haynatzki, G.R. (2006). Rosiglitazone attenuates learning and memory deficits in Tg2576 Alzheimer mice. Exp Neurol *199*, 265-273.

Pei, J.J., Braak, E., Braak, H., Grundke-Iqbal, I., Iqbal, K., Winblad, B., and Cowburn, R.F. (1999). Distribution of active glycogen synthase kinase 3beta (GSK-3beta) in brains staged for Alzheimer disease neurofibrillary changes. J Neuropathol Exp Neurol *58*, 1010-1019.

Pei, J.J., Grundke-Iqbal, I., Iqbal, K., Bogdanovic, N., Winblad, B., and Cowburn, R.F. (1998). Accumulation of cyclin-dependent kinase 5 (cdk5) in neurons with early stages of Alzheimer's disease neurofibrillary degeneration. Brain Res *797*, 267-277.

Pei, J.J., Tanaka, T., Tung, Y.C., Braak, E., Iqbal, K., and Grundke-Iqbal, I. (1997). Distribution, levels, and activity of glycogen synthase kinase-3 in the Alzheimer disease brain. J Neuropathol Exp Neurol *56*, 70-78.

Peila, R., Rodriguez, B.L., and Launer, L.J. (2002). Type 2 diabetes, APOE gene, and the risk for dementia and related pathologies: The Honolulu-Asia Aging Study. Diabetes *51*, 1256-1262.

Perez, M., Hernandez, F., Gomez-Ramos, A., Smith, M., Perry, G., and Avila, J. (2002). Formation of aberrant phosphotau fibrillar polymers in neural cultured cells. Eur J Biochem *269*, 1484-1489.

Perry, G., Roder, H., Nunomura, A., Takeda, A., Friedlich, A.L., Zhu, X., Raina, A.K., Holbrook, N., Siedlak, S.L., Harris, P.L.*, et al.* (1999). Activation of neuronal extracellular receptor kinase (ERK) in Alzheimer disease links oxidative stress to abnormal phosphorylation. Neuroreport *10*, 2411-2415.

Phiel, C.J., Wilson, C.A., Lee, V.M., and Klein, P.S. (2003). GSK-3alpha regulates production of Alzheimer's disease amyloid-beta peptides. Nature *423*, 435-439.

Piao, S., Lee, S.H., Kim, H., Yum, S., Stamos, J.L., Xu, Y., Lee, S.J., Lee, J., Oh, S., Han, J.K.*, et al.* (2008). Direct inhibition of GSK3beta by the phosphorylated cytoplasmic domain of LRP6 in Wnt/beta-catenin signaling. PLoS One *3*, e4046.

Piedrahita, D., Hernandez, I., Lopez-Tobon, A., Fedorov, D., Obara, B., Manjunath, B.S., Boudreau, R.L., Davidson, B., Laferla, F., Gallego-Gomez, J.C.*, et al.* (2010). Silencing of CDK5 reduces neurofibrillary tangles in transgenic alzheimer's mice. J Neurosci *30*, 13966-13976.

Piedrahita, J.A., Zhang, S.H., Hagaman, J.R., Oliver, P.M., and Maeda, N. (1992). Generation of mice carrying a mutant apolipoprotein E gene inactivated by gene targeting in embryonic stem cells. Proc Natl Acad Sci U S A *89*, 4471-4475.

Pierrot, N., Ghisdal, P., Caumont, A.S., and Octave, J.N. (2004). Intraneuronal amyloid-beta1-42 production triggered by sustained increase of cytosolic calcium concentration induces neuronal death. J Neurochem *88*, 1140-1150.

Pierrot, N., Santos, S.F., Feyt, C., Morel, M., Brion, J.P., and Octave, J.N. (2006). Calcium-mediated transient phosphorylation of tau and amyloid precursor protein followed by intraneuronal amyloid-beta accumulation. J Biol Chem *281*, 39907-39914.

Pitas, R.E., Boyles, J.K., Lee, S.H., Foss, D., and Mahley, R.W. (1987). Astrocytes synthesize apolipoprotein E and metabolize apolipoprotein E-containing lipoproteins. Biochim Biophys Acta *917*, 148-161.

Planel, E., Miyasaka, T., Launey, T., Chui, D.H., Tanemura, K., Sato, S., Murayama, O., Ishiguro, K., Tatebayashi, Y., and Takashima, A. (2004). Alterations in glucose metabolism induce hypothermia leading to tau hyperphosphorylation through differential inhibition of kinase and phosphatase activities: implications for Alzheimer's disease. J Neurosci *24*, 2401-2411.

Planel, E., Tatebayashi, Y., Miyasaka, T., Liu, L., Wang, L., Herman, M., Yu, W.H., Luchsinger, J.A., Wadzinski, B., Duff, K.E*., et al.* (2007). Insulin dysfunction induces in vivo tau hyperphosphorylation through distinct mechanisms. J Neurosci *27*, 13635-13648.

Plaschke, K., and Hoyer, S. (1993). Action of the diabetogenic drug streptozotocin on glycolytic and glycogenolytic metabolism in adult rat brain cortex and hippocampus. Int J Dev Neurosci *11*, 477-483.

Plaschke, K., Kopitz, J., Siegelin, M., Schliebs, R., Salkovic-Petrisic, M., Riederer, P., and Hoyer, S. (2010). Insulin-resistant brain state after intracerebroventricular streptozotocin injection exacerbates Alzheimer-like changes in Tg2576 AbetaPP-overexpressing mice. J Alzheimers Dis *19*, 691-704.

Plump, A.S., Smith, J.D., Hayek, T., Aalto-Setala, K., Walsh, A., Verstuyft, J.G., Rubin, E.M., and Breslow, J.L. (1992). Severe hypercholesterolemia and atherosclerosis in apolipoprotein E-deficient mice created by homologous recombination in ES cells. Cell *71*, 343-353.

Pocai, A., Morgan, K., Buettner, C., Gutierrez-Juarez, R., Obici, S., and Rossetti, L. (2005). Central leptin acutely reverses diet-induced hepatic insulin resistance. Diabetes *54*, 3182-3189.

Podlisny, M.B., Ostaszewski, B.L., Squazzo, S.L., Koo, E.H., Rydell, R.E., Teplow, D.B., and Selkoe, D.J. (1995). Aggregation of secreted amyloid beta-protein into sodium dodecyl sulfate-stable oligomers in cell culture. J Biol Chem *270*, 9564-9570.

Poirier, R., Wolfer, D.P., Welzl, H., Tracy, J., Galsworthy, M.J., Nitsch, R.M., and Mohajeri, M.H. (2006). Neuronal neprilysin overexpression is associated with attenuation of Abeta-related spatial memory deficit. Neurobiol Dis *24*, 475-483.

Polvikoski, T., Sulkava, R., Haltia, M., Kainulainen, K., Vuorio, A., Verkkoniemi, A., Niinisto, L., Halonen, P., and Kontula, K. (1995). Apolipoprotein E, dementia, and cortical deposition of beta-amyloid protein. N Engl J Med *333*, 1242-1247.

Ponce, D.P., Maturana, J.L., Cabello, P., Yefi, R., Niechi, I., Silva, E., Armisen, R., Galindo, M., Antonelli, M., and Tapia, J.C. (2011). Phosphorylation of AKT/PKB by CK2 is necessary for the AKT-dependent up-regulation of beta-catenin transcriptional activity. J Cell Physiol *226*, 1953-1959.

Pratico, D., Uryu, K., Leight, S., Trojanoswki, J.Q., and Lee, V.M. (2001). Increased lipid peroxidation precedes amyloid plaque formation in an animal model of Alzheimer amyloidosis. J Neurosci *21*, 4183-4187.

Prince, J.A., Zetterberg, H., Andreasen, N., Marcusson, J., and Blennow, K. (2004). APOE epsilon4 allele is associated with reduced cerebrospinal fluid levels of Abeta42. Neurology *62*, 2116-2118.

Qi, Y., Takahashi, N., Hileman, S.M., Patel, H.R., Berg, A.H., Pajvani, U.B., Scherer, P.E., and Ahima, R.S. (2004). Adiponectin acts in the brain to decrease body weight. Nat Med *10*, 524-529.

Qiu, G., Wan, R., Hu, J., Mattson, M.P., Spangler, E., Liu, S., Yau, S.Y., Lee, T.M., Gleichmann, M., Ingram, D.K*., et al.* (2011). Adiponectin protects rat hippocampal neurons against excitotoxicity. Age (Dordr) *33*, 155-165.

Qiu, W.Q., Walsh, D.M., Ye, Z., Vekrellis, K., Zhang, J., Podlisny, M.B., Rosner, M.R., Safavi, A., Hersh, L.B., and Selkoe, D.J. (1998). Insulin-degrading enzyme regulates extracellular levels of amyloid beta-protein by degradation. J Biol Chem *273*, 32730-32738.

Qu, Z., Jiao, Z., Sun, X., Zhao, Y., Ren, J., and Xu, G. (2011). Effects of streptozotocin-induced diabetes on tau phosphorylation in the rat brain. Brain Res *1383*, 300-306.

Querfurth, H.W., Jiang, J., Geiger, J.D., and Selkoe, D.J. (1997). Caffeine stimulates amyloid beta-peptide release from beta-amyloid precursor protein-transfected HEK293 cells. J Neurochem *69*, 1580-1591.

Querfurth, H.W., and Selkoe, D.J. (1994). Calcium ionophore increases amyloid beta peptide production by cultured cells. Biochemistry *33*, 4550-4561.

Raber, J., Wong, D., Buttini, M., Orth, M., Bellosta, S., Pitas, R.E., Mahley, R.W., and Mucke, L. (1998). Isoform-specific effects of human apolipoprotein E on brain function revealed in ApoE knockout mice: increased susceptibility of females. Proc Natl Acad Sci U S A *95*, 10914-10919.

Raffai, R.L., Dong, L.M., Farese, R.V., Jr., and Weisgraber, K.H. (2001). Introduction of human apolipoprotein E4 "domain interaction" into mouse apolipoprotein E. Proc Natl Acad Sci U S A *98*, 11587-11591.

Rall, S.C., Jr., Weisgraber, K.H., and Mahley, R.W. (1982). Human apolipoprotein E. The complete amino acid sequence. J Biol Chem *257*, 4171-4178.

Ramlo-Halsted, B.A., and Edelman, S.V. (1999). The natural history of type 2 diabetes. Implications for clinical practice. Prim Care *26*, 771-789.

Ramos, B.P., Stark, D., Verduzco, L., van Dyck, C.H., and Arnsten, A.F. (2006). Alpha2A-adrenoceptor stimulation improves prefrontal cortical regulation of behavior through inhibition of cAMP signaling in aging animals. Learn Mem *13*, 770-776.

Rapoport, M., Dawson, H.N., Binder, L.I., Vitek, M.P., and Ferreira, A. (2002). Tau is essential to beta -amyloid-induced neurotoxicity. Proc Natl Acad Sci U S A *99*, 6364-6369.

Rebeck, G.W., Reiter, J.S., Strickland, D.K., and Hyman, B.T. (1993). Apolipoprotein E in sporadic Alzheimer's disease: allelic variation and receptor interactions. Neuron *11*, 575-580.

Rees, D.A., and Alcolado, J.C. (2005). Animal models of diabetes mellitus. Diabet Med *22*, 359-370.

Reger, M.A., Watson, G.S., Frey, W.H., 2nd, Baker, L.D., Cholerton, B., Keeling, M.L., Belongia, D.A., Fishel, M.A., Plymate, S.R., Schellenberg, G.D.*, et al.* (2006). Effects of intranasal insulin on cognition in memory-impaired older adults: modulation by APOE genotype. Neurobiol Aging *27*, 451-458.

Reger, M.A., Watson, G.S., Green, P.S., Wilkinson, C.W., Baker, L.D., Cholerton, B., Fishel, M.A., Plymate, S.R., Breitner, J.C., DeGroodt, W.*, et al.* (2008). Intranasal insulin improves cognition and modulates beta-amyloid in early AD. Neurology *70*, 440-448.

Reiman, E.M., Caselli, R.J., Chen, K., Alexander, G.E., Bandy, D., and Frost, J. (2001). Declining brain activity in cognitively normal apolipoprotein E epsilon 4 heterozygotes: A foundation for using positron emission tomography to efficiently test treatments to prevent Alzheimer's disease. Proc Natl Acad Sci U S A *98*, 3334-3339.

Reiman, E.M., Chen, K., Liu, X., Bandy, D., Yu, M., Lee, W., Ayutyanont, N., Keppler, J., Reeder, S.A., Langbaum, J.B.*, et al.* (2009). Fibrillar amyloid-beta burden in cognitively normal people at 3 levels of genetic risk for Alzheimer's disease. Proc Natl Acad Sci U S A *106*, 6820-6825.

Repunte-Canonigo, V., Berton, F., Cottone, P., Reifel-Miller, A., Roberts, A.J., Morales, M., Francesconi, W., and Sanna, P.P. (2010). A potential role for adiponectin receptor 2 (AdipoR2) in the regulation of alcohol intake. Brain Res *1339*, 11-17.

Reynolds, C.H., Nebreda, A.R., Gibb, G.M., Utton, M.A., and Anderton, B.H. (1997a). Reactivating kinase/p38 phosphorylates tau protein in vitro. J Neurochem *69*, 191-198.

Reynolds, C.H., Utton, M.A., Gibb, G.M., Yates, A., and Anderton, B.H. (1997b). Stress-activated protein kinase/c-jun N-terminal kinase phosphorylates tau protein. J Neurochem *68*, 1736-1744.

Risner, M.E., Saunders, A.M., Altman, J.F., Ormandy, G.C., Craft, S., Foley, I.M., Zvartau-Hind, M.E., Hosford, D.A., and Roses, A.D. (2006). Efficacy of rosiglitazone in a genetically defined population with mild-to-moderate Alzheimer's disease. Pharmacogenomics J *6*, 246-254.

Rohan de Silva, H.A., Jen, A., Wickenden, C., Jen, L.S., Wilkinson, S.L., and Patel, A.J. (1997). Cell-specific expression of beta-amyloid precursor protein isoform mRNAs and proteins in neurons and astrocytes. Brain Res Mol Brain Res *47*, 147-156.

Ronnemaa, E., Zethelius, B., Sundelof, J., Sundstrom, J., Degerman-Gunnarsson, M., Berne, C., Lannfelt, L., and Kilander, L. (2008). Impaired insulin secretion increases the risk of Alzheimer disease. Neurology *71*, 1065-1071.

Rosen, E.D., and Spiegelman, B.M. (2001). PPARgamma : a nuclear regulator of metabolism, differentiation, and cell growth. J Biol Chem *276*, 37731-37734.

Rosengren, A.H., Jokubka, R., Tojjar, D., Granhall, C., Hansson, O., Li, D.Q., Nagaraj, V., Reinbothe, T.M., Tuncel, J., Eliasson, L.*, et al.* (2010). Overexpression of alpha2A-adrenergic receptors contributes to type 2 diabetes. Science *327*, 217-220.

Rulifson, E.J., Kim, S.K., and Nusse, R. (2002). Ablation of insulin-producing neurons in flies: growth and diabetic phenotypes. Science *296*, 1118-1120.

Ryan, K.K., Li, B., Grayson, B.E., Matter, E.K., Woods, S.C., and Seeley, R.J. (2011). A role for central nervous system PPAR-gamma in the regulation of energy balance. Nat Med *17*, 623-626.

Saeki, K., Machida, M., Kinoshita, Y., Takasawa, R., and Tanuma, S. (2011). Glycogen synthase kinase-3beta2 has lower phosphorylation activity to tau than glycogen synthase kinase-3beta1. Biol Pharm Bull *34*, 146-149.

Salkovic-Petrisic, M., Tribl, F., Schmidt, M., Hoyer, S., and Riederer, P. (2006). Alzheimer-like changes in protein kinase B and glycogen synthase kinase-3 in rat frontal cortex and hippocampus after damage to the insulin signalling pathway. J Neurochem *96*, 1005-1015.

Saltiel, A.R., and Kahn, C.R. (2001). Insulin signalling and the regulation of glucose and lipid metabolism. Nature *414*, 799-806.

Sanan, D.A., Weisgraber, K.H., Russell, S.J., Mahley, R.W., Huang, D., Saunders, A., Schmechel, D., Wisniewski, T., Frangione, B., Roses, A.D.*, et al.* (1994). Apolipoprotein E

associates with beta amyloid peptide of Alzheimer's disease to form novel monofibrils. Isoform apoE4 associates more efficiently than apoE3. J Clin Invest *94*, 860-869.

Sandouk, T., Reda, D., and Hofmann, C. (1993). Antidiabetic agent pioglitazone enhances adipocyte differentiation of 3T3-F442A cells. Am J Physiol *264*, C1600-1608.

Santacruz, K., Lewis, J., Spires, T., Paulson, J., Kotilinek, L., Ingelsson, M., Guimaraes, A., DeTure, M., Ramsden, M., McGowan, E.*, et al.* (2005). Tau suppression in a neurodegenerative mouse model improves memory function. Science *309*, 476-481.

Sasaki, N., Toki, S., Chowei, H., Saito, T., Nakano, N., Hayashi, Y., Takeuchi, M., and Makita, Z. (2001). Immunohistochemical distribution of the receptor for advanced glycation end products in neurons and astrocytes in Alzheimer's disease. Brain Res *888*, 256-262.

Sastre, M., Walter, J., and Gentleman, S.M. (2008). Interactions between APP secretases and inflammatory mediators. J Neuroinflammation *5*, 25.

Sato, T., Hanyu, H., Hirao, K., Kanetaka, H., Sakurai, H., and Iwamoto, T. (2011). Efficacy of PPAR-gamma agonist pioglitazone in mild Alzheimer disease. Neurobiol Aging *32*, 1626-1633.

Saunders, A.M., Strittmatter, W.J., Schmechel, D., George-Hyslop, P.H., Pericak-Vance, M.A., Joo, S.H., Rosi, B.L., Gusella, J.F., Crapper-MacLachlan, D.R., Alberts, M.J.*, et al.* (1993). Association of apolipoprotein E allele epsilon 4 with late-onset familial and sporadic Alzheimer's disease. Neurology *43*, 1467-1472.

Schechter, R., Holtzclaw, L., Sadiq, F., Kahn, A., and Devaskar, S. (1988). Insulin synthesis by isolated rabbit neurons. Endocrinology *123*, 505-513.

Schneider, A., Biernat, J., von Bergen, M., Mandelkow, E., and Mandelkow, E.M. (1999). Phosphorylation that detaches tau protein from microtubules (Ser262, Ser214) also protects it against aggregation into Alzheimer paired helical filaments. Biochemistry *38*, 3549-3558.

Schubert, M., Brazil, D.P., Burks, D.J., Kushner, J.A., Ye, J., Flint, C.L., Farhang-Fallah, J., Dikkes, P., Warot, X.M., Rio, C.*, et al.* (2003). Insulin receptor substrate-2 deficiency impairs brain growth and promotes tau phosphorylation. J Neurosci *23*, 7084-7092.

Schubert, M., Gautam, D., Surjo, D., Ueki, K., Baudler, S., Schubert, D., Kondo, T., Alber, J., Galldiks, N., Kustermann, E.*, et al.* (2004). Role for neuronal insulin resistance in neurodegenerative diseases. Proc Natl Acad Sci U S A *101*, 3100-3105.

Selkoe, D.J., Yamazaki, T., Citron, M., Podlisny, M.B., Koo, E.H., Teplow, D.B., and Haass, C. (1996). The role of APP processing and trafficking pathways in the formation of amyloid beta-protein. Ann N Y Acad Sci *777*, 57-64.

Selwood, S.P., Parvathy, S., Cordell, B., Ryan, H.S., Oshidari, F., Vincent, V., Yesavage, J., Lazzeroni, L.C., and Murphy, G.M., Jr. (2009). Gene expression profile of the PDAPP mouse model for Alzheimer's disease with and without Apolipoprotein E. Neurobiol Aging *30*, 574-590.

Sengupta, A., Kabat, J., Novak, M., Wu, Q., Grundke-Iqbal, I., and Iqbal, K. (1998). Phosphorylation of tau at both Thr 231 and Ser 262 is required for maximal inhibition of its binding to microtubules. Arch Biochem Biophys *357*, 299-309.

Sergeant, N., Bretteville, A., Hamdane, M., Caillet-Boudin, M.L., Grognet, P., Bombois, S., Blum, D., Delacourte, A., Pasquier, F., Vanmechelen, E.*, et al.* (2008). Biochemistry of Tau in Alzheimer's disease and related neurological disorders. Expert Rev Proteomics *5*, 207-224.

Seta, K.A., and Roth, R.A. (1997). Overexpression of insulin degrading enzyme: cellular localization and effects on insulin signaling. Biochem Biophys Res Commun *231*, 167-171.

Shankar, G.M., Bloodgood, B.L., Townsend, M., Walsh, D.M., Selkoe, D.J., and Sabatini, B.L. (2007). Natural oligomers of the Alzheimer amyloid-beta protein induce reversible synapse loss by modulating an NMDA-type glutamate receptor-dependent signaling pathway. J Neurosci *27*, 2866-2875.

Shaw, P., Lerch, J.P., Pruessner, J.C., Taylor, K.N., Rose, A.B., Greenstein, D., Clasen, L., Evans, A., Rapoport, J.L., and Giedd, J.N. (2007). Cortical morphology in children and adolescents with different apolipoprotein E gene polymorphisms: an observational study. Lancet Neurol *6*, 494-500.

Sheng, J.G., Mrak, R.E., and Griffin, W.S. (1997). Glial-neuronal interactions in Alzheimer disease: progressive association of IL-1alpha+ microglia and S100beta+ astrocytes with neurofibrillary tangle stages. J Neuropathol Exp Neurol *56*, 285-290.

Shibata, M., Yamada, S., Kumar, S.R., Calero, M., Bading, J., Frangione, B., Holtzman, D.M., Miller, C.A., Strickland, D.K., Ghiso, J.*, et al.* (2000). Clearance of Alzheimer's amyloid-ss(1-40) peptide from brain by LDL receptor-related protein-1 at the blood-brain barrier. J Clin Invest *106*, 1489-1499.

Shimizu, H., Tsuchiya, T., Sato, N., Shimomura, Y., Kobayashi, I., and Mori, M. (1998). Troglitazone reduces plasma leptin concentration but increases hunger in NIDDM patients. Diabetes Care *21*, 1470-1474.

Shonesy, B.C., Thiruchelvam, K., Parameshwaran, K., Rahman, E.A., Karuppagounder, S.S., Huggins, K.W., Pinkert, C.A., Amin, R., Dhanasekaran, M., and Suppiramaniam, V. (2011). Central insulin resistance and synaptic dysfunction in intracerebroventricular-streptozotocin injected rodents. Neurobiol Aging.

Silva, A.P., Xapelli, S., Pinheiro, P.S., Ferreira, R., Lourenco, J., Cristovao, A., Grouzmann, E., Cavadas, C., Oliveira, C.R., and Malva, J.O. (2005). Up-regulation of neuropeptide Y levels and modulation of glutamate release through neuropeptide Y receptors in the hippocampus of kainate-induced epileptic rats. J Neurochem *93*, 163-170.

Simons, M., Schwarzler, F., Lutjohann, D., von Bergmann, K., Beyreuther, K., Dichgans, J., Wormstall, H., Hartmann, T., and Schulz, J.B. (2002). Treatment with simvastatin in normocholesterolemic patients with Alzheimer's disease: A 26-week randomized, placebo-controlled, double-blind trial. Ann Neurol *52*, 346-350.

Singh, B.S., Rajakumar, P.A., Eves, E.M., Rosner, M.R., Wainer, B.H., and Devaskar, S.U. (1997). Insulin gene expression in immortalized rat hippocampal and pheochromocytoma-12 cell lines. Regul Pept *69*, 7-14.

Sinha, S., Anderson, J.P., Barbour, R., Basi, G.S., Caccavello, R., Davis, D., Doan, M., Dovey, H.F., Frigon, N., Hong, J.*, et al.* (1999). Purification and cloning of amyloid precursor protein beta-secretase from human brain. Nature *402*, 537-540.

Skovronsky, D.M., Doms, R.W., and Lee, V.M. (1998). Detection of a novel intraneuronal pool of insoluble amyloid beta protein that accumulates with time in culture. J Cell Biol *141*, 1031-1039.

Solano, D.C., Sironi, M., Bonfini, C., Solerte, S.B., Govoni, S., and Racchi, M. (2000). Insulin regulates soluble amyloid precursor protein release via phosphatidyl inositol 3 kinase-dependent pathway. FASEB J *14*, 1015-1022.

Song, Z.M., Abou-Zeid, O., and Fang, Y.Y. (2004). alpha2a adrenoceptors regulate phosphorylation of microtubule-associated protein-2 in cultured cortical neurons. Neuroscience *123*, 405-418.

Soutar, M.P., Kim, W.Y., Williamson, R., Peggie, M., Hastie, C.J., McLauchlan, H., Snider, W.D., Gordon-Weeks, P.R., and Sutherland, C. (2010). Evidence that glycogen synthase kinase-3 isoforms have distinct substrate preference in the brain. J Neurochem *115*, 974-983.

Sparks, D.L., Sabbagh, M.N., Connor, D.J., Lopez, J., Launer, L.J., Browne, P., Wasser, D., Johnson-Traver, S., Lochhead, J., and Ziolwolski, C. (2005). Atorvastatin for the treatment of mild to moderate Alzheimer disease: preliminary results. Arch Neurol *62*, 753-757.

Sparks, D.L., Scheff, S.W., Hunsaker, J.C., 3rd, Liu, H., Landers, T., and Gross, D.R. (1994). Induction of Alzheimer-like beta-amyloid immunoreactivity in the brains of rabbits with dietary cholesterol. Exp Neurol *126*, 88-94.

Spittaels, K., Van den Haute, C., Van Dorpe, J., Geerts, H., Mercken, M., Bruynseels, K., Lasrado, R., Vandezande, K., Laenen, I., Boon, T.*, et al.* (2000). Glycogen synthase kinase-3beta phosphorylates protein tau and rescues the axonopathy in the central nervous system of human four-repeat tau transgenic mice. J Biol Chem *275*, 41340-41349.

Srinivasan, K., and Ramarao, P. (2007). Animal models in type 2 diabetes research: an overview. Indian J Med Res *125*, 451-472.

Steen, E., Terry, B.M., Rivera, E.J., Cannon, J.L., Neely, T.R., Tavares, R., Xu, X.J., Wands, J.R., and de la Monte, S.M. (2005). Impaired insulin and insulin-like growth factor expression and signaling mechanisms in Alzheimer's disease--is this type 3 diabetes? J Alzheimers Dis *7*, 63-80.

Steinhilb, M.L., Dias-Santagata, D., Mulkearns, E.E., Shulman, J.M., Biernat, J., Mandelkow, E.M., and Feany, M.B. (2007). S/P and T/P phosphorylation is critical for tau neurotoxicity in Drosophila. J Neurosci Res *85*, 1271-1278.

Steppan, C.M., Bailey, S.T., Bhat, S., Brown, E.J., Banerjee, R.R., Wright, C.M., Patel, H.R., Ahima, R.S., and Lazar, M.A. (2001). The hormone resistin links obesity to diabetes. Nature *409*, 307-312.

Straus, D.S., and Glass, C.K. (2007). Anti-inflammatory actions of PPAR ligands: new insights on cellular and molecular mechanisms. Trends Immunol *28*, 551-558.

Strittmatter, W.J., Saunders, A.M., Goedert, M., Weisgraber, K.H., Dong, L.M., Jakes, R., Huang, D.Y., Pericak-Vance, M., Schmechel, D., and Roses, A.D. (1994). Isoform-specific interactions of apolipoprotein E with microtubule-associated protein tau: implications for Alzheimer disease. Proc Natl Acad Sci U S A *91*, 11183-11186.

Strittmatter, W.J., Saunders, A.M., Schmechel, D., Pericak-Vance, M., Enghild, J., Salvesen, G.S., and Roses, A.D. (1993). Apolipoprotein E: high-avidity binding to beta-amyloid and increased frequency of type 4 allele in late-onset familial Alzheimer disease. Proc Natl Acad Sci U S A *90*, 1977-1981.

Strum, J.C., Shehee, R., Virley, D., Richardson, J., Mattie, M., Selley, P., Ghosh, S., Nock, C., Saunders, A., and Roses, A. (2007). Rosiglitazone induces mitochondrial biogenesis in mouse brain. J Alzheimers Dis *11*, 45-51.

Sudoh, S., Frosch, M.P., and Wolf, B.A. (2002). Differential effects of proteases involved in intracellular degradation of amyloid beta-protein between detergent-soluble and -insoluble pools in CHO-695 cells. Biochemistry *41*, 1091-1099.

Suga, K., Saito, A., Tomiyama, T., Mori, H., and Akagawa, K. (2005). Syntaxin 5 interacts specifically with presenilin holoproteins and affects processing of betaAPP in neuronal cells. J Neurochem *94*, 425-439.

Sugano, M., Yamauchi, K., Kawasaki, K., Tozuka, M., Fujita, K., Okumura, N., and Ota, H. (2008). Sialic acid moiety of apolipoprotein E3 at Thr(194) affects its interaction with beta-amyloid(1-42) peptides. Clin Chim Acta *388*, 123-129.

Sullivan, P.M., Mezdour, H., Aratani, Y., Knouff, C., Najib, J., Reddick, R.L., Quarfordt, S.H., and Maeda, N. (1997). Targeted replacement of the mouse apolipoprotein E gene with the common human APOE3 allele enhances diet-induced hypercholesterolemia and atherosclerosis. J Biol Chem *272*, 17972-17980.

Sun, L., Liu, S.Y., Zhou, X.W., Wang, X.C., Liu, R., Wang, Q., and Wang, J.Z. (2003). Inhibition of protein phosphatase 2A- and protein phosphatase 1-induced tau hyperphosphorylation and impairment of spatial memory retention in rats. Neuroscience *118*, 1175-1182.

Sun, Y., Wu, S., Bu, G., Onifade, M.K., Patel, S.N., LaDu, M.J., Fagan, A.M., and Holtzman, D.M. (1998). Glial fibrillary acidic protein-apolipoprotein E (apoE) transgenic mice: astrocyte-specific expression and differing biological effects of astrocyte-secreted apoE3 and apoE4 lipoproteins. J Neurosci *18*, 3261-3272.

Surwit, R.S., Kuhn, C.M., Cochrane, C., McCubbin, J.A., and Feinglos, M.N. (1988). Diet-induced type II diabetes in C57BL/6J mice. Diabetes *37*, 1163-1167.

Suzuki, N., Cheung, T.T., Cai, X.D., Odaka, A., Otvos, L., Jr., Eckman, C., Golde, T.E., and Younkin, S.G. (1994). An increased percentage of long amyloid beta protein secreted by familial amyloid beta protein precursor (beta APP717) mutants. Science *264*, 1336-1340.

Szkudelski, T. (2001). The mechanism of alloxan and streptozotocin action in B cells of the rat pancreas. Physiol Res *50*, 537-546.

Taelman, V.F., Dobrowolski, R., Plouhinec, J.L., Fuentealba, L.C., Vorwald, P.P., Gumper, I., Sabatini, D.D., and De Robertis, E.M. (2010). Wnt signaling requires sequestration of glycogen synthase kinase 3 inside multivesicular endosomes. Cell *143*, 1136-1148.

Takahashi, R.H., Almeida, C.G., Kearney, P.F., Yu, F., Lin, M.T., Milner, T.A., and Gouras, G.K. (2004). Oligomerization of Alzheimer's beta-amyloid within processes and synapses of cultured neurons and brain. J Neurosci *24*, 3592-3599.

Takahashi, T., Ida, T., Sato, T., Nakashima, Y., Nakamura, Y., Tsuji, A., and Kojima, M. (2009). Production of n-octanoyl-modified ghrelin in cultured cells requires prohormone processing protease and ghrelin O-acyltransferase, as well as n-octanoic acid. J Biochem *146*, 675-682.

Takeda, S., Sato, N., Uchio-Yamada, K., Sawada, K., Kunieda, T., Takeuchi, D., Kurinami, H., Shinohara, M., Rakugi, H., and Morishita, R. (2010). Diabetes-accelerated memory dysfunction via cerebrovascular inflammation and Abeta deposition in an Alzheimer mouse model with diabetes. Proc Natl Acad Sci U S A *107*, 7036-7041.

Tanabe, C., Hotoda, N., Sasagawa, N., Sehara-Fujisawa, A., Maruyama, K., and Ishiura, S. (2007). ADAM19 is tightly associated with constitutive Alzheimer's disease APP alpha-secretase in A172 cells. Biochem Biophys Res Commun *352*, 111-117.

Tanimukai, H., Grundke-Iqbal, I., and Iqbal, K. (2005). Up-regulation of inhibitors of protein phosphatase-2A in Alzheimer's disease. Am J Pathol *166*, 1761-1771.

Tatton, W., Chen, D., Chalmers-Redman, R., Wheeler, L., Nixon, R., and Tatton, N. (2003). Hypothesis for a common basis for neuroprotection in glaucoma and Alzheimer's disease: anti-apoptosis by alpha-2-adrenergic receptor activation. Surv Ophthalmol *48 Suppl 1*, S25-37.

Terry, R.D., Masliah, E., Salmon, D.P., Butters, N., DeTeresa, R., Hill, R., Hansen, L.A., and Katzman, R. (1991). Physical basis of cognitive alterations in Alzheimer's disease: synapse loss is the major correlate of cognitive impairment. Ann Neurol *30*, 572-580.

Terwel, D., Muyllaert, D., Dewachter, I., Borghgraef, P., Croes, S., Devijver, H., and Van Leuven, F. (2008). Amyloid activates GSK-3beta to aggravate neuronal tauopathy in bigenic mice. Am J Pathol *172*, 786-798.

Tesseur, I., Van Dorpe, J., Spittaels, K., Van den Haute, C., Moechars, D., and Van Leuven, F. (2000). Expression of human apolipoprotein E4 in neurons causes hyperphosphorylation of protein tau in the brains of transgenic mice. Am J Pathol *156*, 951-964.

Thundyil, J., Tang, S.C., Okun, E., Shah, K., Karamyan, V.T., Li, Y.I., Woodruff, T.M., Taylor, S.M., Jo, D.G., Mattson, M.P.*, et al.* (2010). Evidence that adiponectin receptor 1 activation exacerbates ischemic neuronal death. Exp Transl Stroke Med *2*, 15.

Tiraboschi, P., Hansen, L.A., Masliah, E., Alford, M., Thal, L.J., and Corey-Bloom, J. (2004). Impact of APOE genotype on neuropathologic and neurochemical markers of Alzheimer disease. Neurology *62*, 1977-1983.

Tokuda, T., Calero, M., Matsubara, E., Vidal, R., Kumar, A., Permanne, B., Zlokovic, B., Smith, J.D., Ladu, M.J., Rostagno, A.*, et al.* (2000). Lipidation of apolipoprotein E influences its isoform-specific interaction with Alzheimer's amyloid beta peptides. Biochem J *348 Pt 2*, 359-365.

Tolstykh, T., Lee, J., Vafai, S., and Stock, J.B. (2000). Carboxyl methylation regulates phosphoprotein phosphatase 2A by controlling the association of regulatory B subunits. EMBO J *19*, 5682-5691.

Tonks, N.K., and Cohen, P. (1983). Calcineurin is a calcium ion-dependent, calmodulin-stimulated protein phosphatase. Biochim Biophys Acta *747*, 191-193.

Tontonoz, P., Hu, E., Graves, R.A., Budavari, A.I., and Spiegelman, B.M. (1994). mPPAR gamma 2: tissue-specific regulator of an adipocyte enhancer. Genes Dev *8*, 1224-1234.

Town, T., Zolton, J., Shaffner, R., Schnell, B., Crescentini, R., Wu, Y., Zeng, J., DelleDonne, A., Obregon, D., Tan, J.*, et al.* (2002). p35/Cdk5 pathway mediates soluble amyloid-beta peptide-induced tau phosphorylation in vitro. J Neurosci Res *69*, 362-372.

Trommer, B.L., Shah, C., Yun, S.H., Gamkrelidze, G., Pasternak, E.S., Stine, W.B., Manelli, A., Sullivan, P., Pasternak, J.F., and LaDu, M.J. (2005). ApoE isoform-specific effects on LTP: blockade by oligomeric amyloid-beta1-42. Neurobiol Dis *18*, 75-82.

Tsai, L.H., Takahashi, T., Caviness, V.S., Jr., and Harlow, E. (1993). Activity and expression pattern of cyclin-dependent kinase 5 in the embryonic mouse nervous system. Development *119*, 1029-1040.

Tsujio, I., Zaidi, T., Xu, J., Kotula, L., Grundke-Iqbal, I., and Iqbal, K. (2005). Inhibitors of protein phosphatase-2A from human brain structures, immunocytological localization and activities towards dephosphorylation of the Alzheimer type hyperphosphorylated tau. FEBS Lett *579*, 363-372.

Tugwood, J.D., Issemann, I., Anderson, R.G., Bundell, K.R., McPheat, W.L., and Green, S. (1992). The mouse peroxisome proliferator activated receptor recognizes a response element in the 5' flanking sequence of the rat acyl CoA oxidase gene. EMBO J *11*, 433-439.

Turner, R.S., Suzuki, N., Chyung, A.S., Younkin, S.G., and Lee, V.M. (1996). Amyloids beta40 and beta42 are generated intracellularly in cultured human neurons and their secretion increases with maturation. J Biol Chem *271*, 8966-8970.

Une, K., Takei, Y.A., Tomita, N., Asamura, T., Ohrui, T., Furukawa, K., and Arai, H. (2011). Adiponectin in plasma and cerebrospinal fluid in MCI and Alzheimer's disease. Eur J Neurol *18*, 1006-1009.

Uysal, K.T., Wiesbrock, S.M., Marino, M.W., and Hotamisligil, G.S. (1997). Protection from obesity-induced insulin resistance in mice lacking TNF-alpha function. Nature *389*, 610-614.

van der Heide, L.P., Kamal, A., Artola, A., Gispen, W.H., and Ramakers, G.M. (2005). Insulin modulates hippocampal activity-dependent synaptic plasticity in a N-methyl-d-aspartate receptor and phosphatidyl-inositol-3-kinase-dependent manner. J Neurochem *94*, 1158-1166.

Van Nostrand, W.E., Melchor, J.P., Cho, H.S., Greenberg, S.M., and Rebeck, G.W. (2001). Pathogenic effects of D23N Iowa mutant amyloid beta -protein. J Biol Chem *276*, 32860-32866.

Van Obberghen, E., Baron, V., Delahaye, L., Emanuelli, B., Filippa, N., Giorgetti-Peraldi, S., Lebrun, P., Mothe-Satney, I., Peraldi, P., Rocchi, S.*, et al.* (2001). Surfing the insulin signaling web. Eur J Clin Invest *31*, 966-977.

Vance, J.E., and Hayashi, H. (2010). Formation and function of apolipoprotein E-containing lipoproteins in the nervous system. Biochim Biophys Acta *1801*, 806-818.

Vassar, R., Bennett, B.D., Babu-Khan, S., Kahn, S., Mendiaz, E.A., Denis, P., Teplow, D.B., Ross, S., Amarante, P., Loeloff, R.*, et al.* (1999). Beta-secretase cleavage of Alzheimer's

amyloid precursor protein by the transmembrane aspartic protease BACE. Science *286*, 735-741.

Vekrellis, K., Ye, Z., Qiu, W.Q., Walsh, D., Hartley, D., Chesneau, V., Rosner, M.R., and Selkoe, D.J. (2000). Neurons regulate extracellular levels of amyloid beta-protein via proteolysis by insulin-degrading enzyme. J Neurosci *20*, 1657-1665.

von Rotz, R.C., Kohli, B.M., Bosset, J., Meier, M., Suzuki, T., Nitsch, R.M., and Konietzko, U. (2004). The APP intracellular domain forms nuclear multiprotein complexes and regulates the transcription of its own precursor. J Cell Sci *117*, 4435-4448.

Voskas, D., Ling, L.S., and Woodgett, J.R. (2010). Does GSK-3 provide a shortcut for PI3K activation of Wnt signalling? F1000 Biol Rep *2*, 82.

Wahrle, S., Das, P., Nyborg, A.C., McLendon, C., Shoji, M., Kawarabayashi, T., Younkin, L.H., Younkin, S.G., and Golde, T.E. (2002). Cholesterol-dependent gamma-secretase activity in buoyant cholesterol-rich membrane microdomains. Neurobiol Dis *9*, 11-23.

Wahrle, S.E., Jiang, H., Parsadanian, M., Hartman, R.E., Bales, K.R., Paul, S.M., and Holtzman, D.M. (2005). Deletion of Abca1 increases Abeta deposition in the PDAPP transgenic mouse model of Alzheimer disease. J Biol Chem *280*, 43236-43242.

Wahrle, S.E., Jiang, H., Parsadanian, M., Kim, J., Li, A., Knoten, A., Jain, S., Hirsch-Reinshagen, V., Wellington, C.L., Bales, K.R.*, et al.* (2008). Overexpression of ABCA1 reduces amyloid deposition in the PDAPP mouse model of Alzheimer disease. J Clin Invest *118*, 671-682.

Wahrle, S.E., Jiang, H., Parsadanian, M., Legleiter, J., Han, X., Fryer, J.D., Kowalewski, T., and Holtzman, D.M. (2004). ABCA1 is required for normal central nervous system ApoE levels and for lipidation of astrocyte-secreted apoE. J Biol Chem *279*, 40987-40993.

Wallum, B.J., Taborsky, G.J., Jr., Porte, D., Jr., Figlewicz, D.P., Jacobson, L., Beard, J.C., Ward, W.K., and Dorsa, D. (1987). Cerebrospinal fluid insulin levels increase during intravenous insulin infusions in man. J Clin Endocrinol Metab *64*, 190-194.

Walsh, D.M., Klyubin, I., Fadeeva, J.V., Rowan, M.J., and Selkoe, D.J. (2002). Amyloid-beta oligomers: their production, toxicity and therapeutic inhibition. Biochem Soc Trans *30*, 552-557.

Walsh, D.M., Tseng, B.P., Rydel, R.E., Podlisny, M.B., and Selkoe, D.J. (2000). The oligomerization of amyloid beta-protein begins intracellularly in cells derived from human brain. Biochemistry *39*, 10831-10839.

Wan, Q., Xiong, Z.G., Man, H.Y., Ackerley, C.A., Braunton, J., Lu, W.Y., Becker, L.E., MacDonald, J.F., and Wang, Y.T. (1997). Recruitment of functional GABA(A) receptors to postsynaptic domains by insulin. Nature *388*, 686-690.

Wang, C., Wilson, W.A., Moore, S.D., Mace, B.E., Maeda, N., Schmechel, D.E., and Sullivan, P.M. (2005). Human apoE4-targeted replacement mice display synaptic deficits in the absence of neuropathology. Neurobiol Dis *18*, 390-398.

Wang, J.Z., Grundke-Iqbal, I., and Iqbal, K. (2007). Kinases and phosphatases and tau sites involved in Alzheimer neurofibrillary degeneration. Eur J Neurosci *25*, 59-68.

Wang, J.Z., Wu, Q., Smith, A., Grundke-Iqbal, I., and Iqbal, K. (1998). Tau is phosphorylated by GSK-3 at several sites found in Alzheimer disease and its biological activity markedly inhibited only after it is prephosphorylated by A-kinase. FEBS Lett *436*, 28-34.

Wang, X., Zheng, W., Xie, J.W., Wang, T., Wang, S.L., Teng, W.P., and Wang, Z.Y. (2010). Insulin deficiency exacerbates cerebral amyloidosis and behavioral deficits in an Alzheimer transgenic mouse model. Mol Neurodegener *5*, 46.

Wang, Y.L., Frauwirth, K.A., Rangwala, S.M., Lazar, M.A., and Thompson, C.B. (2002). Thiazolidinedione activation of peroxisome proliferator-activated receptor gamma can enhance mitochondrial potential and promote cell survival. J Biol Chem *277*, 31781-31788.

Watson, G.S., Cholerton, B.A., Reger, M.A., Baker, L.D., Plymate, S.R., Asthana, S., Fishel, M.A., Kulstad, J.J., Green, P.S., Cook, D.G.*, et al.* (2005). Preserved cognition in patients with early Alzheimer disease and amnestic mild cognitive impairment during treatment with rosiglitazone: a preliminary study. Am J Geriatr Psychiatry *13*, 950-958.

Watson, G.S., and Craft, S. (2003). The role of insulin resistance in the pathogenesis of Alzheimer's disease: implications for treatment. CNS Drugs *17*, 27-45.

Weber, B., Schaper, C., Scholz, J., Bein, B., Rodde, C., and P, H.T. (2006). Interaction of the amyloid precursor like protein 1 with the alpha2A-adrenergic receptor increases agonist-mediated inhibition of adenylate cyclase. Cell Signal *18*, 1748-1757.

Webster, S., and Rogers, J. (1996). Relative efficacies of amyloid beta peptide (A beta) binding proteins in A beta aggregation. J Neurosci Res *46*, 58-66.

Weingarten, M.D., Lockwood, A.H., Hwo, S.Y., and Kirschner, M.W. (1975). A protein factor essential for microtubule assembly. Proc Natl Acad Sci U S A *72*, 1858-1862.

Weisgraber, K.H. (1990). Apolipoprotein E distribution among human plasma lipoproteins: role of the cysteine-arginine interchange at residue 112. J Lipid Res *31*, 1503-1511.

Weisgraber, K.H. (1994). Apolipoprotein E: structure-function relationships. Adv Protein Chem *45*, 249-302.

Weisgraber, K.H., Innerarity, T.L., and Mahley, R.W. (1982). Abnormal lipoprotein receptor-binding activity of the human E apoprotein due to cysteine-arginine interchange at a single site. J Biol Chem *257*, 2518-2521.

Weisgraber, K.H., Rall, S.C., Jr., and Mahley, R.W. (1981). Human E apoprotein heterogeneity. Cysteine-arginine interchanges in the amino acid sequence of the apo-E isoforms. J Biol Chem *256*, 9077-9083.

Wernette-Hammond, M.E., Lauer, S.J., Corsini, A., Walker, D., Taylor, J.M., and Rall, S.C., Jr. (1989). Glycosylation of human apolipoprotein E. The carbohydrate attachment site is threonine 194. J Biol Chem *264*, 9094-9101.

Werther, G.A., Hogg, A., Oldfield, B.J., McKinley, M.J., Figdor, R., Allen, A.M., and Mendelsohn, F.A. (1987). Localization and characterization of insulin receptors in rat brain and pituitary gland using in vitro autoradiography and computerized densitometry. Endocrinology *121*, 1562-1570.

Wertkin, A.M., Turner, R.S., Pleasure, S.J., Golde, T.E., Younkin, S.G., Trojanowski, J.Q., and Lee, V.M. (1993). Human neurons derived from a teratocarcinoma cell line express solely the 695-amino acid amyloid precursor protein and produce intracellular beta-amyloid or A4 peptides. Proc Natl Acad Sci U S A *90*, 9513-9517.

Wheeler, L.A., Gil, D.W., and WoldeMussie, E. (2001). Role of alpha-2 adrenergic receptors in neuroprotection and glaucoma. Surv Ophthalmol *45 Suppl 3*, S290-294; discussion S295-296.

Williamson, R., Scales, T., Clark, B.R., Gibb, G., Reynolds, C.H., Kellie, S., Bird, I.N., Varndell, I.M., Sheppard, P.W., Everall, I.*, et al.* (2002). Rapid tyrosine phosphorylation of neuronal proteins including tau and focal adhesion kinase in response to amyloid-beta peptide exposure: involvement of Src family protein kinases. J Neurosci *22*, 10-20.

Willson, T.M., Brown, P.J., Sternbach, D.D., and Henke, B.R. (2000). The PPARs: from orphan receptors to drug discovery. J Med Chem *43*, 527-550.

Wilson-Fritch, L., Nicoloro, S., Chouinard, M., Lazar, M.A., Chui, P.C., Leszyk, J., Straubhaar, J., Czech, M.P., and Corvera, S. (2004). Mitochondrial remodeling in adipose tissue associated with obesity and treatment with rosiglitazone. J Clin Invest *114*, 1281-1289.

Winzell, M.S., and Ahren, B. (2004). The high-fat diet-fed mouse: a model for studying mechanisms and treatment of impaired glucose tolerance and type 2 diabetes. Diabetes *53 Suppl 3*, S215-219.

Winzell, M.S., Nogueiras, R., Dieguez, C., and Ahren, B. (2004). Dual action of adiponectin on insulin secretion in insulin-resistant mice. Biochem Biophys Res Commun *321*, 154-160.

Wirths, O., Multhaup, G., Czech, C., Blanchard, V., Moussaoui, S., Tremp, G., Pradier, L., Beyreuther, K., and Bayer, T.A. (2001). Intraneuronal Abeta accumulation precedes plaque formation in beta-amyloid precursor protein and presenilin-1 double-transgenic mice. Neurosci Lett *306*, 116-120.

Wischik, C.M., Novak, M., Thogersen, H.C., Edwards, P.C., Runswick, M.J., Jakes, R., Walker, J.E., Milstein, C., Roth, M., and Klug, A. (1988). Isolation of a fragment of tau derived from the core of the paired helical filament of Alzheimer disease. Proc Natl Acad Sci U S A *85*, 4506-4510.

Wisniewski, T., Castano, E.M., Golabek, A., Vogel, T., and Frangione, B. (1994). Acceleration of Alzheimer's fibril formation by apolipoprotein E in vitro. Am J Pathol *145*, 1030-1035.

Wisniewski, T., and Frangione, B. (1992). Apolipoprotein E: a pathological chaperone protein in patients with cerebral and systemic amyloid. Neurosci Lett *135*, 235-238.

Wisniewski, T., Golabek, A., Matsubara, E., Ghiso, J., and Frangione, B. (1993). Apolipoprotein E: binding to soluble Alzheimer's beta-amyloid. Biochem Biophys Res Commun *192*, 359-365.

Wolfe, M.S., Xia, W., Ostaszewski, B.L., Diehl, T.S., Kimberly, W.T., and Selkoe, D.J. (1999). Two transmembrane aspartates in presenilin-1 required for presenilin endoproteolysis and gamma-secretase activity. Nature *398*, 513-517.

Woo, J.M., Park, S.J., Kang, H.I., Kim, B.G., Shim, S.B., Jee, S.W., Lee, S.H., Sin, J.S., Bae, C.J., Jang, M.K.*, et al.* (2010). Characterization of changes in global gene expression in the brain of neuron-specific enolase/human Tau23 transgenic mice in response to overexpression of Tau protein. Int J Mol Med *25*, 667-675.

Wood, S.J., Chan, W., and Wetzel, R. (1996). Seeding of A beta fibril formation is inhibited by all three isotypes of apolipoprotein E. Biochemistry *35*, 12623-12628.

Woodgett, J.R. (1990). Molecular cloning and expression of glycogen synthase kinase-3/factor A. EMBO J *9*, 2431-2438.

Woods, S.C., Seeley, R.J., Baskin, D.G., and Schwartz, M.W. (2003). Insulin and the blood-brain barrier. Curr Pharm Des *9*, 795-800.

Wu, G., Huang, H., Garcia Abreu, J., and He, X. (2009). Inhibition of GSK3 phosphorylation of beta-catenin via phosphorylated PPPSPXS motifs of Wnt coreceptor LRP6. PLoS One *4*, e4926.

Wu, J., Tolstykh, T., Lee, J., Boyd, K., Stock, J.B., and Broach, J.R. (2000). Carboxyl methylation of the phosphoprotein phosphatase 2A catalytic subunit promotes its functional association with regulatory subunits in vivo. EMBO J *19*, 5672-5681.

Xie, L., Helmerhorst, E., Taddei, K., Plewright, B., Van Bronswijk, W., and Martins, R. (2002). Alzheimer's beta-amyloid peptides compete for insulin binding to the insulin receptor. J Neurosci *22*, RC221.

Xu, P.T., Gilbert, J.R., Qiu, H.L., Ervin, J., Rothrock-Christian, T.R., Hulette, C., and Schmechel, D.E. (1999). Specific regional transcription of apolipoprotein E in human brain neurons. Am J Pathol *154*, 601-611.

Xu, P.T., Schmechel, D., Rothrock-Christian, T., Burkhart, D.S., Qiu, H.L., Popko, B., Sullivan, P., Maeda, N., Saunders, A.M., Roses, A.D.*, et al.* (1996). Human apolipoprotein E2, E3, and E4 isoform-specific transgenic mice: human-like pattern of glial and neuronal immunoreactivity in central nervous system not observed in wild-type mice. Neurobiol Dis *3*, 229-245.

Xu, W.L., Qiu, C.X., Wahlin, A., Winblad, B., and Fratiglioni, L. (2004). Diabetes mellitus and risk of dementia in the Kungsholmen project: a 6-year follow-up study. Neurology *63*, 1181-1186.

Yamada, T., Sasaki, H., Furuya, H., Miyata, T., Goto, I., and Sakaki, Y. (1987). Complementary DNA for the mouse homolog of the human amyloid beta protein precursor. Biochem Biophys Res Commun *149*, 665-671.

Yamauchi, K., Tozuka, M., Hidaka, H., Nakabayashi, T., Sugano, M., and Katsuyama, T. (2002a). Isoform-specific effect of apolipoprotein E on endocytosis of beta-amyloid in cultures of neuroblastoma cells. Ann Clin Lab Sci *32*, 65-74.

Yamauchi, K., Tozuka, M., Hidaka, H., Nakabayashi, T., Sugano, M., Kondo, Y., Nakagawara, A., and Katsuyama, T. (2000). Effect of apolipoprotein AII on the interaction of apolipoprotein E with beta-amyloid: some apo(E-AII) complexes inhibit the internalization of beta-amyloid in cultures of neuroblastoma cells. J Neurosci Res *62*, 608-614.

Yamauchi, T., Kamon, J., Minokoshi, Y., Ito, Y., Waki, H., Uchida, S., Yamashita, S., Noda, M., Kita, S., Ueki, K.*, et al.* (2002b). Adiponectin stimulates glucose utilization and fatty-acid oxidation by activating AMP-activated protein kinase. Nat Med *8*, 1288-1295.

Yamauchi, T., Kamon, J., Waki, H., Terauchi, Y., Kubota, N., Hara, K., Mori, Y., Ide, T., Murakami, K., Tsuboyama-Kasaoka, N.*, et al.* (2001). The fat-derived hormone adiponectin reverses insulin resistance associated with both lipoatrophy and obesity. Nat Med *7*, 941-946.

Yan, Q., Zhang, J., Liu, H., Babu-Khan, S., Vassar, R., Biere, A.L., Citron, M., and Landreth, G. (2003). Anti-inflammatory drug therapy alters beta-amyloid processing and deposition in an animal model of Alzheimer's disease. J Neurosci *23*, 7504-7509.

Yan, R., Bienkowski, M.J., Shuck, M.E., Miao, H., Tory, M.C., Pauley, A.M., Brashier, J.R., Stratman, N.C., Mathews, W.R., Buhl, A.E.*, et al.* (1999). Membrane-anchored aspartyl protease with Alzheimer's disease beta-secretase activity. Nature *402*, 533-537.

Yan, S.D., Chen, X., Fu, J., Chen, M., Zhu, H., Roher, A., Slattery, T., Zhao, L., Nagashima, M., Morser, J.*, et al.* (1996). RAGE and amyloid-beta peptide neurotoxicity in Alzheimer's disease. Nature *382*, 685-691.

Yang, A.J., Chandswangbhuvana, D., Margol, L., and Glabe, C.G. (1998). Loss of endosomal/lysosomal membrane impermeability is an early event in amyloid Abeta1-42 pathogenesis. J Neurosci Res *52*, 691-698.

Yang, D.S., Small, D.H., Seydel, U., Smith, J.D., Hallmayer, J., Gandy, S.E., and Martins, R.N. (1999). Apolipoprotein E promotes the binding and uptake of beta-amyloid into Chinese hamster ovary cells in an isoform-specific manner. Neuroscience *90*, 1217-1226.

Yang, S.D., Tallant, E.A., and Cheung, W.Y. (1982). Calcineurin is a calmodulin-dependent protein phosphatase. Biochem Biophys Res Commun *106*, 1419-1425.

Yoon, S.Y., Park, J.S., Choi, J.E., Choi, J.M., Lee, W.J., Kim, S.W., and Kim, D.H. (2010). Rosiglitazone reduces tau phosphorylation via JNK inhibition in the hippocampus of rats with type 2 diabetes and tau transfected SH-SY5Y cells. Neurobiol Dis *40*, 449-455.

Yoshimura, Y., Ichinose, T., and Yamauchi, T. (2003). Phosphorylation of tau protein to sites found in Alzheimer's disease brain is catalyzed by Ca2+/calmodulin-dependent protein kinase II as demonstrated tandem mass spectrometry. Neurosci Lett *353*, 185-188.

Yu, J.G., Javorschi, S., Hevener, A.L., Kruszynska, Y.T., Norman, R.A., Sinha, M., and Olefsky, J.M. (2002). The effect of thiazolidinediones on plasma adiponectin levels in normal, obese, and type 2 diabetic subjects. Diabetes *51*, 2968-2974.

Zannis, V.I., and Breslow, J.L. (1981). Human very low density lipoprotein apolipoprotein E isoprotein polymorphism is explained by genetic variation and posttranslational modification. Biochemistry *20*, 1033-1041.

Zannis, V.I., McPherson, J., Goldberger, G., Karathanasis, S.K., and Breslow, J.L. (1984). Synthesis, intracellular processing, and signal peptide of human apolipoprotein E. J Biol Chem *259*, 5495-5499.

Zeng, X., Huang, H., Tamai, K., Zhang, X., Harada, Y., Yokota, C., Almeida, K., Wang, J., Doble, B., Woodgett, J.*, et al.* (2008). Initiation of Wnt signaling: control of Wnt coreceptor Lrp6 phosphorylation/activation via frizzled, dishevelled and axin functions. Development *135*, 367-375.

Zerbinatti, C.V., Wahrle, S.E., Kim, H., Cam, J.A., Bales, K., Paul, S.M., Holtzman, D.M., and Bu, G. (2006). Apolipoprotein E and low density lipoprotein receptor-related protein facilitate intraneuronal Abeta42 accumulation in amyloid model mice. J Biol Chem *281*, 36180-36186.

Zhang, B., Maiti, A., Shively, S., Lakhani, F., McDonald-Jones, G., Bruce, J., Lee, E.B., Xie, S.X., Joyce, S., Li, C.*, et al.* (2005). Microtubule-binding drugs offset tau sequestration by stabilizing microtubules and reversing fast axonal transport deficits in a tauopathy model. Proc Natl Acad Sci U S A *102*, 227-231.

Zhang, D., Yang, H., Kong, X., Wang, K., Mao, X., Yan, X., Wang, Y., Liu, S., Zhang, X., Li, J.*, et al.* (2011a). Proteomics analysis reveals diabetic kidney as a ketogenic organ in type 2 diabetes. Am J Physiol Endocrinol Metab *300*, E287-295.

Zhang, S.H., Reddick, R.L., Piedrahita, J.A., and Maeda, N. (1992). Spontaneous hypercholesterolemia and arterial lesions in mice lacking apolipoprotein E. Science *258*, 468-471.

Zhang, Y., McLaughlin, R., Goodyer, C., and LeBlanc, A. (2002). Selective cytotoxicity of intracellular amyloid beta peptide1-42 through p53 and Bax in cultured primary human neurons. J Cell Biol *156*, 519-529.

Zhang, Y.W., Thompson, R., Zhang, H., and Xu, H. (2011b). APP processing in Alzheimer's disease. Mol Brain *4*, 3.

Zhang, Y.W., Wang, R., Liu, Q., Zhang, H., Liao, F.F., and Xu, H. (2007). Presenilin/gamma-secretase-dependent processing of beta-amyloid precursor protein regulates EGF receptor expression. Proc Natl Acad Sci U S A *104*, 10613-10618.

Zhao, W., Chen, H., Xu, H., Moore, E., Meiri, N., Quon, M.J., and Alkon, D.L. (1999). Brain insulin receptors and spatial memory. Correlated changes in gene expression, tyrosine phosphorylation, and signaling molecules in the hippocampus of water maze trained rats. J Biol Chem *274*, 34893-34902.

Zhao, Y., Ye, W., Boye, K.S., Holcombe, J.H., Hall, J.A., and Swindle, R. (2010). Prevalence of other diabetes-associated complications and comorbidities and its impact on health care charges among patients with diabetic neuropathy. J Diabetes Complications *24*, 9-19.

Zheng, Y.L., Amin, N.D., Hu, Y.F., Rudrabhatla, P., Shukla, V., Kanungo, J., Kesavapany, S., Grant, P., Albers, W., and Pant, H.C. (2010). A 24-residue peptide (p5), derived from p35, the Cdk5 neuronal activator, specifically inhibits Cdk5-p25 hyperactivity and tau hyperphosphorylation. J Biol Chem *285*, 34202-34212.

Zhou, J., Chen, J., and Feng, Y. (2006). Effect of truncated-ApoE4 overexpression on tau phosphorylation in cultured N2a cells. J Huazhong Univ Sci Technolog Med Sci *26*, 272-274.

Zhou, J., Wang, H., Feng, Y., and Chen, J. (2010). Increased expression of cdk5/p25 in N2a cells leads to hyperphosphorylation and impaired axonal transport of neurofilament proteins. Life Sci *86*, 532-537.

Zhu, Y., Alvares, K., Huang, Q., Rao, M.S., and Reddy, J.K. (1993). Cloning of a new member of the peroxisome proliferator-activated receptor gene family from mouse liver. J Biol Chem *268*, 26817-26820.